Singh, Geetanjali (2008) *Analysis of genetic mutations using a recombinant model of the mammalian pyruvate dehydrogenase complex.* PhD thesis.

http://theses.gla.ac.uk/214/

Analysis of genetic mutations using a recombinant model of the mammalian pyruvate dehydrogenase complex

Geetanjali Singh

Division of Biochemistry & Molecular Biology, IBLS

University
of Glasgow

A thesis submitted for the degree of

Doctor of Philosophy

Declaration

I hereby declare that the work presented in this thesis is my own, except where otherwise cited or acknowledged. No part of this thesis has been presented for any other degree.

Geetanjali Singh

January 2008

Acknowledgements

I express my deepest gratitude to my research supervisor, Professor Gordon Lindsay for his excellent supervision and guidance throughout the course of this work. His trust, generosity, honesty and professionalism all inspired me deeply. I could not have wished for a better supervisor.

I am also grateful to Dr. Olwyn Byron for accepting me as a collaborative student and for giving her valuable time, explaining finer details of AUC and enabling me to carry out various experiments and molecular graphics work.

I am very thankful to Dr. Sharon Kelly for collaborating on CD experiments and helping in analysing the data.

I am thankful to Drs. Alison Prior, Heather Lindsay and Donna McGow for helping me in various little but important things in the beginning of this research.

Many thanks to Hiba, Swetha, Mridu, Adrienne, Professor Cushley and all other people in the lab for sharing good times.

I owe special thanks to my husband, Subhash and our daughter, Suryakshi for giving a loving environment during all these years. Suryakshi, for being so very loving and understanding; and Subhash for helping me get through the difficult times, for all the love and emotional support despite being busy with his own Ph.D.

I am forever indebted to my parents for their love and blessings.

I sincerely thank everybody in University of Glasgow, who supported me in various ways in accomplishing this study.

I also acknowledge the financial funding provided by University of Glasgow and United Mitochondrial Disease Research.

ABSTRACT

The human mitochondrial pyruvate dehydrogenase complex (PDC) is a vital metabolic assembly that controls the key committed step in aerobic carbohydrate utilisation and energy production and as such is responsible for overall glucose homeostasis in man. PDC, particularly from prokaryotic sources, has been widely studied as a model system for investigating the molecular basis of cooperativity between physically and functionally linked enzymes in a metabolic pathway and the catalytic and regulatory advantages conferred by their organisation into precisely-engineered 'molecular-machines'. Defects in human PDC have been implicated in a wide variety of genetic, metabolic and autoimmune disorders. Over 200 PDC-linked mutations have been reported to date in the human population leading to clinical symptoms of various magnitudes and manifestations, mostly in the X-linked gene for the α subunit of the E1 component.

PDC is a vast molecular machine (M_r, 9-10 MDa) composed of multiple copies of 3 distinct enzymes: pyruvate dehydrogenase (E1), dihydrolipoamide acetyltransferase (E2), dihydrolipoamide dehydrogenase (E3) and an additional structural protein known as E3-binding protein (E3BP). Central to its structural, morphological and mechanistic framework is its large oligomeric 'core' comprising 60 E2 and 12 E3BP polypeptide chains, arranged as pentagonal dodecahedron, to which up to 30 $\alpha_2\beta_2$ E1 enzymes and 6-12 homodimeric E3 enzymes are tethered tightly, but non-covalently, at maximal occupancy. More recently a substitutional model of PDC has been proposed where the core is formed by 48 E2 and 12 E3BP with the 12 E3BP polypeptides replacing an equivalent number of E2s. The N-termini of the E2 enzyme(s) each contain two peripherally-extended lipoyl domains that exhibit great mobility and in effect, act as 'swinging arms' since their attached lipoic acid cofactors must visit the active sites of all the three enzymes in strict rotation during the catalytic cycle. Similarly, E3BP is a distinct E2-related polypeptide that is primarily involved in E3 integration but also displays overlapping functions with E2 as it contains a single, highly-flexible lipoyl domain that can participate in catalysis.

In this study, a model recombinant human PDC has been reconstituted from its E1, E2:E3BP and E3 components that were all overexpressed in and purified from *E. coli*

in high yield prior to assembling spontaneously into fully-active complex *in vitro*. The wild-type recombinant PDC displayed similar enzymatic activity to the native complex purified from human heart. As a prelude to examining 3 novel naturally-occurring, E2-linked mutations, the recombinant PDC model was validated initially by examining the effects of alterations in its lipoylation status on its activity and overall properties and secondly by assessing the characteristics of recombinant PDC lacking the E3BP subunit.   A possible enzymatic role for E3BP in promoting formation of an S^6, S^8-diacetylated dihydrolipoamide intermediate on E2 and E3BP was also investigated.

In the first analysis a series of mutant E2:E3BP cores were created containing all possible combinations of active and inactive lipoyl domains. These possible combinations were ++/+, -+/+, +-/+, --/+, ++/ -, -+/-, +-/- and --/-, where '+' is a lipoylated and '-' is a non lipoylated outer, inner or E3BP domain in the E2:E3BP cores. Eight recombinant PDC models were successfully reconstituted from these cores and analysed for their effects on PDC activity compared to wild-type complex. The data indicate that mutation of the outer or inner lipoyl domain of E2 by replacing the lipoylatable lysine by glutamine leads to a 25-35% decrease in activity; moreover the presence of an active or inactive lipoyl domain on E3BP had no detectable influence on PDC function. However, PDC, in which only active E3BP lipoyl domains were present, retained 15% of wild-type activity. These data confirm previous reports on the functional redundancy of lipoyl domains observed in bacterial, yeast and mammalian PDCs and suggest that the E2 lipoyl domains and the lipoyl domain of E3BP can act independently as effective substrates for E1, E2 and E3.

A parallel study on recombinant PDC lacking E3BP, was also consistent with previous studies in showing that it retained partial activity in the complete absence of this subunit. E3BP-deficient patients retain relatively high levels of PDC activity (15-20%) as compared to the 3-8% observed using stoichiometric amounts of E3 in our in *vitro* assay. However, our data also suggested that 40-50% PDC activity could be achieved in the presence of a 100-200 fold excess of E3 that may account for slightly higher activity in the patients. Interestingly, wild-type PDC activity declined by 10-30% in the presence of a large E3 excess in agreement with the idea that the E1 binding site on E2 retains a residual affinity for E3 and is able to partially displace the rate-limiting E1 enzyme when present in high amounts.

The main objective of the thesis was to apply our recombinant PDC model to conduct a detailed investigation of the molecular defects underlying three novel E2 mutations/ deletions identified at the genetic level by Dr. Garry Brown, University of Oxford in PDC-deficient patients under his care. These were two separate 'in frame' 3-bp deletions encoding glutamate-35 and valine-455 in the mature E2 protein and a phenylalanine-490 to leucine (F490L) substitution located near the active site of the enzyme. Full length copies of these mutant enzymes were generated by site-directed mutagenesis as well an outer lipoyl domain-GST construct housing the Δ35E deletion. In the case of Δ35E mutant, our data from lipoylation assays, circular dichroism, tryptophan fluorescence, non-denaturing gel electrophoresis, size exclusion chromatography and cross-linking analyses indicate that the mutant lipoyl domain is misfolded and displays a pronounced tendency to form dimers or higher order aggregates, presumably via inappropriate exposure of hydrophobic surfaces. As a result, the bulk of the E2:E3BP core does not assemble properly as evidenced by its unusual subunit composition and the presence of several abnormal species including non-specific aggregates detected by analytical ultracentrifugation. Mutant E2, E2:E3BP core and reconstituted PDC showed low activity (10-20%) as compared to wild-type controls, indicating a small proportion of active core can still form under these conditions. In this study, replacement of glu-35 by aspartate or glutamine had only minor/negligible effects on E2:E3BP core assembly and reconstituted PDC activity indicating that the size or charge of amino acid at this position is not critical for normal folding and assembly.

In the valine-455 deletion study, the patient was reported to contain no immunologically-detectable E3BP, despite the apparent absence of any mutation in the PDX1 gene. Therefore, in this study, it was hypothesised that this E2-based mutation might be responsible for preventing integration of E3BP into the E2 core assembly, thereby promoting its rapid degradation. Although, this deletion resulted in reduced E2 and PDC activity (50%), it was not found to prevent E3BP integration when the mutant core was produced at either 30 °C or 37 °C. As this patient has no detectable levels of E3BP protein despite the presence of mRNA for this component as detected by RT-PCR studies in Oxford, the precise molecular basis for this defect remains unclear at present. The patient is currently undergoing a complete medical and clinical re-evaluation.

Recombinant mutant PDC containing the F490L mutation also loses about 50% enzymatic activity as compared to the normal or wild-type PDC confirming the role of this mutation in PDC deficiency in this patient. This phenylalanine located near to the catalytic site of E2 has been found to be responsible for substrate specificity and its substitution could be directly responsible for decreased enzymatic activity in this case. No major structural changes were observed in this mutant core.

In summary, our recombinant PDC model has proved to be of considerable benefit in enabling us to gain a more informed insight into the molecular mechanisms of pathogenesis underlying these rare E2-linked mutations, particularly in the case of the ΔE35-E2 mutant. In the absence of the recombinant model, such detailed investigations would have proved impossible owing to the lack of access to human tissue from individual patients.

As a corollary to the main aim of the thesis, a preliminary attempt was made to create an equivalent recombinant OGDC model. OGDC is also a mitochondrial assembly that is involved in the TCA cycle and is increasingly implicated in the aetiology of various neurodegenerative diseases linked to oxidative stress including Alzheimer's and Parkinson's disease.

The basic organisation of the OGDC is directed by the self-assembly of 24 copies of dihydrolipoyl succinyltransferase (E2o) to form a cubic core, to which multiple copies of 2-oxoglutarate dehydrogenase (E1o) and dihydrolipoamide dehydrogenase (E3) bind non-covalently. The mammalian E2o is unusual in lacking any obvious E3 or E1o binding domain. In this study, E2o and E3 were successfully overexpressed and purified. Initially it was confirmed that E2o and E3 do not interact with each other on gel filtration although stable association of all 3 constituent enzymes occurs in the native complex. Full-length E1o was also cloned successfully although it proved impossible to achieve detectable expression in our *E. coli* BL21 host system.

Previous studies employing subunit-specific proteolysis have identified the extreme N-terminal segment of E1o as a key region involved in the maintenance of complex stability and integrity and is required for E2 and E3 binding. To investigate this region in more detail, three N-terminal E1o fragments of decreasing size were

overexpressed, one in His-tag form (193 amino acids) and two as E1o-GST fusion proteins (166 and 83 amino acids). In co-expression, purification and gel filtration studies, it was found that all these N-terminal truncates of E1o appeared capable of interacting with E2o although problems were encountered with rapid degradation and unambiguous identification in some cases. However, Western blotting revealed conclusively that even the shortest N-terminal E1o fragment (83 amino acids) was able to enter into a stable association with E2o. Owing to time constraints and difficulties with rapid degradation and/or solubility of the E1o truncates, it remains to be determined whether this N-terminal region of E1o can also interact with E2o in a post-translational fashion and whether it is directly involved in mediating E3 binding. However, this type of approach should continue to provide additional insights in the unique subunit organisation of OGDC and is an important step towards creating a recombinant model of OGDC. This will be invaluable for future studies on an important metabolic assembly that has been increasingly implicated in disorders linked to oxidative stress and neurodegeneration.

Abbreviations

Å	Angstrom
A_{280}	Absorbance at 280 nm
A_{600}	Absorbance at 600 nm
Abeta	Amyloid-beta
AD	Alzheimer's disease
Amp	Ampicillin
Approx.	Approximately
ATP	Adenosine Triphosphate
AUC	Analytical ultracentrifugation
BCOADC	Branched-chain 2-oxoacid dehydrogenase complex
CD	Circular dichroism
CoA	Coenzyme A
CV	Column volume
DHL	Dihydrolipoamide
dNTP	Deoxyribonucleotide triphosphate
DTT	Dithiothreitol
E1	Pyruvate dehydrogenase
E2	Dihydrolipoamide acetyltransferase
E1o	2-oxoglutarate dehydrogenase
E2o	Dihydrolipoyl succinyltransferase
E3	Dihydrolipoamide dehydrogenase
E3BP	E3-binding protein
EDTA	Ethylenediamine tetraacetic acid

EGFR-PTK   Epidermal growth factor receptor protein tyrosine kinase

EST   Expressed sequence tag

FAD   Flavin adenine dinucleotide

GST   Glutathione S-transferase

IPTG   Isopropyl β-D-1-thiogalactopyranoside

Kb   Kilo base

Kd   Dissociation constant

kDa   Kilo Dalton

LB   Luria Broth

LCPL   Left circularly polarized light

mA   Milliampere

mAB   Monoclonal antibodies

Min   Minutes

MODY   Maturity-onset diabetes of the young

MPTP   1-methyl 4-phenyl 1, 2, 3, 6-tetrahydropyridine

Mw   Molecular weight markers

NAD^+ Nicotinamide adenine dinucleotide

NEM   N-ethyl maleimide

NMR   Nuclear magnetic resonance

OD   Optical density

OGDC   2-oxoglutarate dehydrogenase complex

PBS   Phosphate buffered saline

PCR   Polymerase chain reaction

PD2   Patient derived hybridoma IgG

PDC	Pyruvate dehydrogenase complex
RCPL	Right circularly polarized light
rpm	Revolutions per minute
S	Svedberg
SAXS	Small angle X-ray scattering
SDS-PAGE	Sodium dodecyl sulphate polyacrylamide gel electrophoresis
SEC	Size exclusion chromatography
SV	Sedimentation velocity
TCA	Tricarboxylic acid
ThDP	Thiamine diphosphate
Tris	2-amino-2-(hydroxymethyl)-1, 3-propanol
uv	Ultraviolet
TEMED	N, N, N^{-1} N^{-1}- tetramethylethylene diamine
Ve	Elution volume
Vo	Void volume

Table of contents

List of Figures

Chapter 1

Introduction to pyruvate dehydrogenase and 2-oxoglutarate dehydrogenase complexes

1.1 Multienzyme complexes

Multienzyme complexes are organised assemblies in which the individual components function in a cooperative manner by catalysing consecutive reactions linked by common metabolic intermediates. They may provide the means to attain high local substrate concentrations, regulate competition amongst competing pathways, coordinate the activities of interdependent pathways, and/or sequester toxic and labile intermediates within cells. Two or more enzymes associating in this way allow the substrates to travel efficiently between the active sites. This process, known as 'channelling', can in certain cases be kinetically advantageous. Thus multienzyme complexes optimise the catalytic activity and ensure the regulated activity of a metabolic pathway.

The most prominent examples of multienzyme complexes are the family of stable 2-oxo acid dehydrogenase complexes, that include the pyruvate dehydrogenase (PDC), 2-oxoglutarate dehydrogenase (OGDC) and branched-chain 2-oxoacid dehydrogenase (BCOADC) complexes. PDC links glycolysis to the tricarboxylic acid (TCA) cycle and fatty acid synthesis by catalysing the oxidative decarboxylation of pyruvate with the concomitant production of acetyl-CoA and NADH. OGDC, in contrast, controls a major regulatory step in the TCA cycle and decarboxylates its substrate, 2-oxoglutarate to form succinyl-CoA (Sheu and Blass, 1999). Finally, the BCOADC oxidatively decarboxylates the branched chain 2-oxoacids derived by transamination of valine, leucine and isoleucine in addition to methionine and threonine (Jones and Yeaman, 1986) (Fig. 1.1).

The molecular understanding of the 2-oxoacid dehydrogenases began in 1950s with the isolation of lipoic acid. The years from 1960-80 involved mainly the application of standard protein-chemical and enzymatic techniques for isolation, characterisation and determination of the catalytic and regulatory functions of these complexes. This has been supplemented in recent years by the increasing application of recombinant DNA, biophysical techniques and refined structural and functional approaches. The pioneering studies on these complexes were undertaken on the microbial multienzyme complexes that have paved the way for advances and new insights into the organisation of these complexes in other species. Interestingly, there are considerable differences in the structure, function and regulation of these multienzyme complexes across plant, bacterial and animal species as elucidated by various recent studies. Human pyruvate dehydrogenase complex (PDC), the most prominent member of the mammalian 2-oxoacid dehydrogenase complex family is an excellent example of a multienzyme assembly and a major focus of research. PDC plays an important role in many metabolic disorders, one of which is congenital childhood lactic acidaemia, that is a poorly understood group of genetic diseases (Robinson and Sherwood, 1984). The most common cause of this inherited defect is a deficiency of the pyruvate dehydrogenase complex. It has also been described in patients with subacute/chronic neurodegenerative disease without significant metabolic acidosis (Dahl et al., 1992). Two clinical forms of lactic acidaemia related to PDC deficiency are recognized, neonatal and juvenile. The neonatal form is a relatively common cause of lactic acidosis in the first weeks of life and may also feature an erythematous rash. The juvenile form presents with lactic acidosis, alopecia, intermittent ataxia, seizures and erythematous rash.
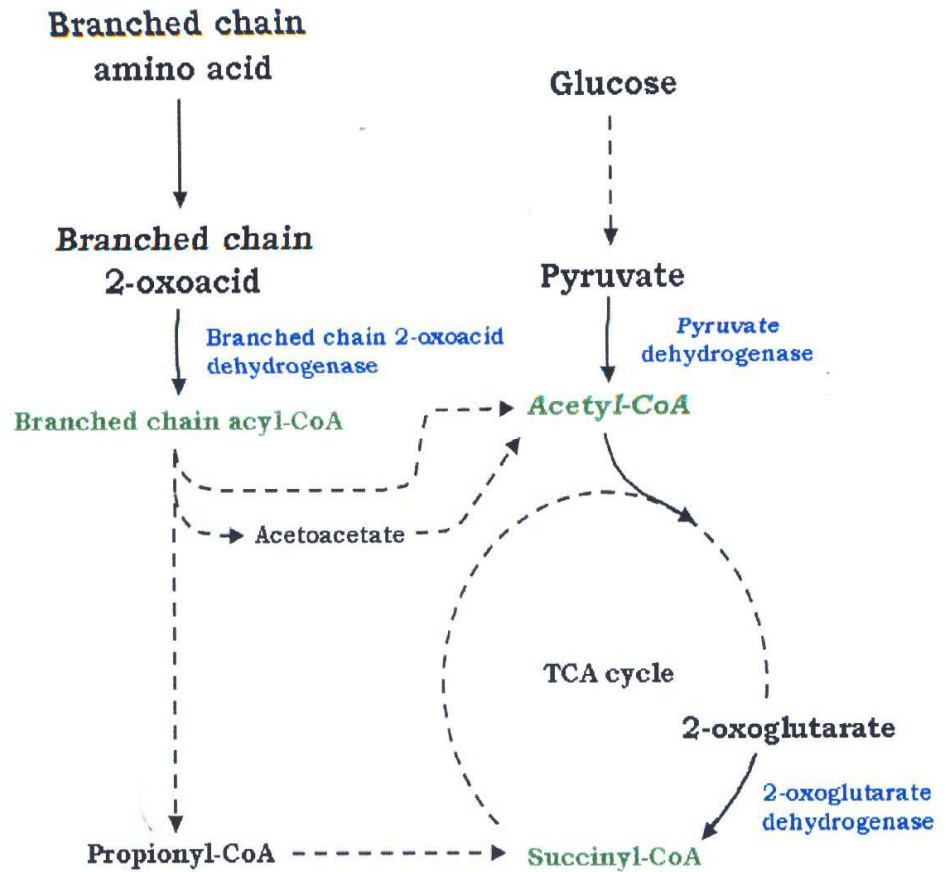
Figure 1.1: Schematic representation of involvement of 2-oxoacid dehydrogenases in cellular metabolism

Multienzyme complexes are shown in blue and their products in green.

1.2 Subunit organisation of the pyruvate dehydrogenase complex

PDC in mammalian systems is composed of multiple copies of three main enzymes - pyruvate dehydrogenase (E1), dihydrolipoamide acetyltransferase (E2) and dihydrolipoamide dehydrogenase (E3). In addition to these enzymes, there are two regulatory components, namely a tightly bound, tissue specific E1-kinase and a phospho-E1-phosphatase. Specific PDC phosphatases involved in the activation of the complex and are loosely bound to it (Teague et al., 1982). Mammalian PDC also contains an accessory protein, formerly known as protein X, now referred to as E3-binding protein (E3BP) (Behal et al., 1993).

In mammals the basic framework of the complex is provided by a central core composed primarily of E2 subunits. Sixty copies of E2 and/or E3BP are arranged in a pentagonal dodecahedron displaying 532 symmetry (Yeaman et al., 1978) (Fig. 1.2 A). However, the E2 core in the PDC of Gram negative bacteria and in all the known OGDCs and BCOADCs, exists as a 24-meric cubic structure with octahedral (432) symmetry (Fig.1.2 B). The E1 enzyme of PDC in mammals exists as an $\alpha_2\beta_2$ heterotetramer with up to thirty E1s arranged around the E2 core (Reed, 1974). E3 is a ubiquitous flavin-containing dehydrogenase and is present as a homodimer with 6-12 copies occupying the 12 pentagonal faces of the E2 core (Yeaman et al., 1978). Twelve copies of E3BP are tightly associated with E2 where, it mediates E3 binding to the complex (Gopalakrishnan et al., 1989; Lawson et al., 1991). Other studies have also suggested that one E3BP molecule binds to each of the 12 faces of the E2 core while 6-12 E3 homodimers are attached to the complex via E3BP (Sanderson et al., 1996b). Recently another model of PDC core organisation has been suggested based on sedimentation equilibrium and small angle x-ray scattering data. According to this substitution model, the core comprises 48:12 E2:E3BP instead of 60:12 to which 12 E3 are bound in 1:1 stoichiometric relationship with E3BP (Hiromasa et al., 2004).

It has been shown that E2 and E3BP must be co-expressed to promote their co-integration into a native oligomeric core. E3BP is thought to have its C-terminal region embedded in the core structure while the rest of the molecule extends outwards. Until recently, it was generally accepted that the PDC comprises at maximum occupancy 60 E2 monomers, 30 E1 heterotetramers, 12 E3BP monomers and 6-12 E3 dimers. Recent isothermal titration calorimetry studies, however, have suggested that one E3 dimer binds two E3BPs implying that each E3 is capable of forming cross bridges with the 12 E3BPs across adjacent pentagonal faces of the E2 core assembly assuming 60:12 meric E2:E3BP core organisation (Fig.1.3 A). In a similar way, it has been suggested that the E1 tetramers may also form crossbridges between pairs of E2 monomers along the 30 edges of the E2 core assembly (Fig.1.3 B). However, this study is in conflict with recent X-ray structures for the human E3 in association with E3BP where 1:1 binding of the E3BP didomain (lipoyl and E3-binding domains) and E3 has been shown (Ciszak et al., 2006).

1.3 Catalytic mechanism

PDC is responsible for controlling a key committed step in carbohydrate utilisation by catalysing the oxidative decarboxylation of pyruvate to yield acetyl CoA, CO_2 and NADH (Patel and Roche, 1990). This is a multi-step reaction involving a high degree of cooperation among the constituent enzymes of this multienzyme complex (Fig. 1.4). As no net production of carbohydrate is possible from its acetyl CoA product, PDC is the main regulator of glucose homeostasis in mammals (Sugden and Holness, 2003). E1 catalyses a two-step reaction, that is the first and the rate-limiting step in the overall catalytic mechanism. Active E1 has an absolute requirement for the cofactor thiamine diphosphate (ThDP) and Mg^{2+} ions. Pyruvate forms an adduct with the thiazole ring of ThDP and this undergoes decarboxylation to produce a 2 (1-hydroxyethylidene) ThDP intermediate that undergoes oxidation while the dithiolane ring of the lipoyl moiety on E2 becomes reductively acetylated. This reductive acetylation step supplies the acetyl group and electrons that are transferred, via E2 and E3 respectively, to CoA and NAD^+. Both of these initial partial reactions are catalysed by E1. E2 then mediates the transfer of the acetyl group from its S^8-acetyldihyrolipoamide intermediate to free CoA, thus forming acetyl

CoA. E3 reoxidises the reduced lipoyl moiety of E2 regenerating the disulphide bridge in the lipoyl group with NAD^+ acting as the final electron acceptor.

1.4 Pyruvate dehydrogenase (E1)

Mature E1 in mammalian systems exists as a heterotetramer composed of two copies each of E1α and E1β subunits (Barrera et al., 1972). The E1 component is a thiamine diphosphate dependent (ThDP) enzyme that catalyses the decarboxylation of pyruvate to CO_2 to form the intermediate compound 2(1-hydroxyethylidene) ThDP and the reductive acetylation of the lipoyl groups of the E2 as shown in Fig. 1.4. The enzymatic reaction also requires Mg^{2+}, that interacts with the pyrophosphate linkage of ThDP to facilitate binding (Walsh et al., 1976). The crystal structure of human E1 PDC has been resolved at a resolution of 1.95 Å (Ciszak et al., 2003) providing detailed insights into the catalytic mechanism and interaction between the two active sites. ThDP is found at the end of a 20 Å long hydrophobic channel that is capable of accommodating the lipoyl-lysine swinging arms. Although both active sites are chemically equivalent, their dynamic non-equivalence has been established indicating that one active-site catalyses the decarboxylation step while the other concurrently reductively acetylates E2-bound lipoamide. Similarly, access to ThDP is granted to either pyruvate or the lipoyl–lysine moiety at any given moment, resulting in flip-flop mechanism (Ciszak et al., 2003). There is a 20 Å tunnel that acts as a proton wire and is lined with acidic residues connecting the two active sites. Mutagenesis of these acidic residues greatly reduced the rate of E1-mediated decarboxylation (Frank et al., 2004). Chemical modification had previously identified cysteine-62 of the α subunit and tryptophan-135 of the β subunit (Ali et al., 1995) as being involved in the active site of mammalian E1. The amino acid sequences surrounding this tryptophan residue are conserved in E1β from several species, suggesting that this region may constitute a structurally and/or functionally essential part of the enzyme. Site-directed mutagenesis of these two residues has indicated that they are involved in coenzyme binding and could also be important for the stability of the E1 heterotetramer.
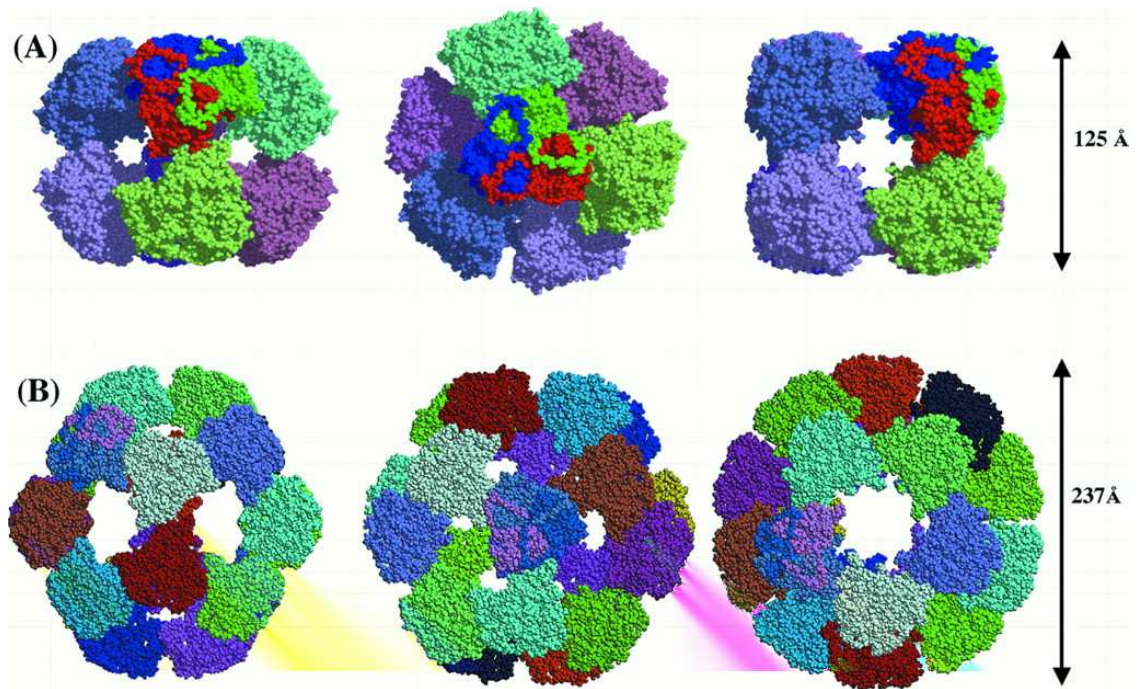
Figure 1.2: Structures of the octahedral and icosahedral E2 inner cores (acetyltransferase domains) of PDC

(A) Octahedral E2 core of the *A. vinelandii* PDC; *left to right*, twofold, threefold, and fourfold views. (B) Icosahedral core of the *B. stearothermophilus* PDC; *left to right*, twofold, threefold, and fivefold views. In both instances, the three different subunits of a single trimer are in different colours, most readily seen on the threefold views (Fussey et al., 1991).
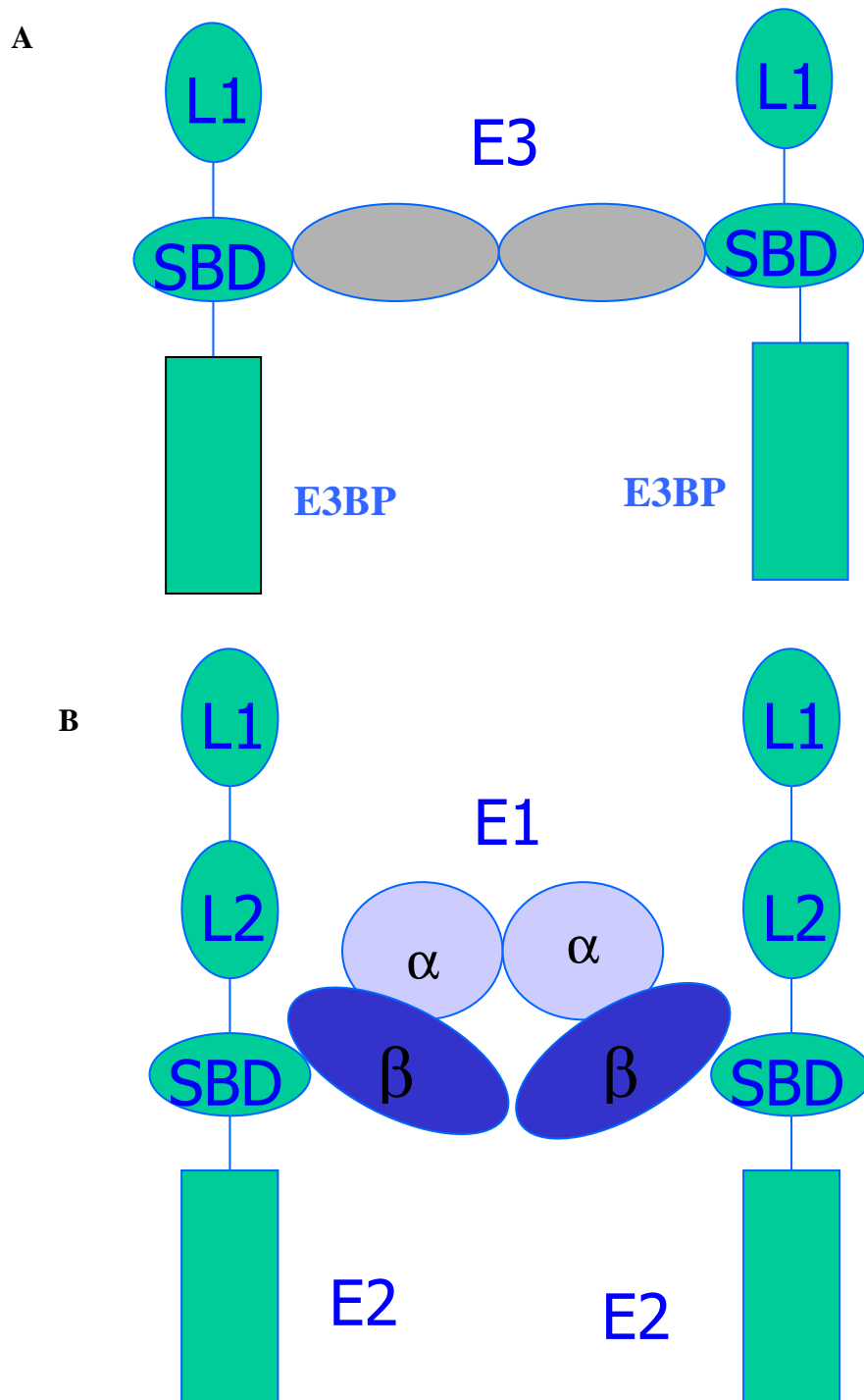
Figure1.3: Schematic representation of possible subunit organisation of E1 and E3 on the surface of the E2:E3BP core assembly

Putative crossbridges between E3 dimer and two E3BPs of PDC (A). Cross bridges between E1 tetramers and pairs of E2 monomers of PDC (B). SBD (subunit binding domain), LI & L2 (outer and inner lipoyl domains).
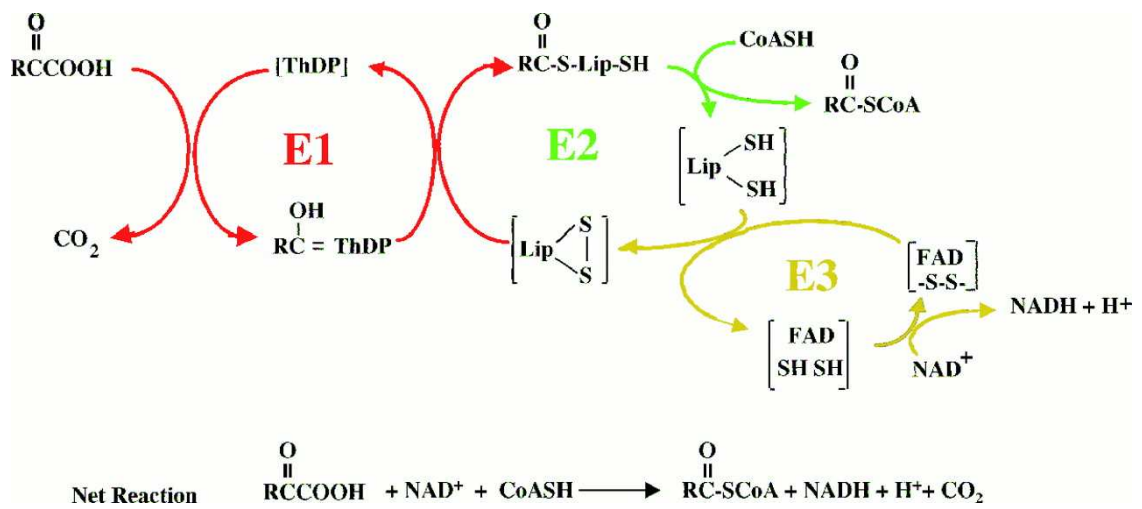
Figure 1.4: Reaction mechanism for pyruvate dehydrogenase complex

The reactions catalysed by E1 are shown in *red*, the reaction catalysed by E2 is in *green*, and that catalysed by E3 is indicated in *yellow*. R represents CH_3. Adapted from Perham (2000).

1.5 Dihydrolipoamide acetyltransferase (E2)

E2 is the central, structural and functional component of all the known PDCs as it forms a core about which the other components are tethered tightly but non-covalently. It catalyses the transfer of acetyl groups from S^8-acetyl dihydrolipoamide to CoA (Butterworth et al., 1975). The E2 subunit associates as trimers initially before assembling into a larger multimeric structure (Hendle et al., 1995). Mammalian E2-PDC has two highly conserved lipoyl domains at its N-terminus called outer and inner lipoyl domains, respectively. These are followed by a small subunit-binding domain consisting of 30-40 amino acids. At the C-terminus a large catalytic inner domain is present known as the catalytic domain that is also responsible for E2 self-assembly and integration of E3BP (Fig. 1.5). Individual domains are connected to each other by well-defined linker regions rich in alanine, proline and acidic amino acids.

1.5.1 Linker regions of E2

Linker regions of E2 comprise segments of polypeptide chains approximately 20-30 amino acids in length. These linker regions are rich in alanine and proline and charged amino acids. NMR studies have shown that these linker regions are very flexible but also have a degree of rigidity, providing the mobility needed to allow the lipoyl domains and the lipoamide prosthetic group to migrate between the catalytically active sites of the three constituent enzymes (Fussey et al., 1991). When deletions were made in the linker region that separates the lipoyl domain from the dihydrolipoamide dehydrogenase-binding domain in a genetically-modified *E. coli* E2 containing a single lipoyl domain, overall PDC activity was impaired without any effect on the reactions of the individual enzymes. Moreover, it was necessary to shorten the linker region sequence that separates the lipoyl domain from the peripheral-binding domain in the modified E2-PDC to approximately half of its original length before there was a pronounced effect on complex activity. Thus it was concluded that linker should be at least 13 amino acids long for maintenance of full activity (Miles et al., 1988).
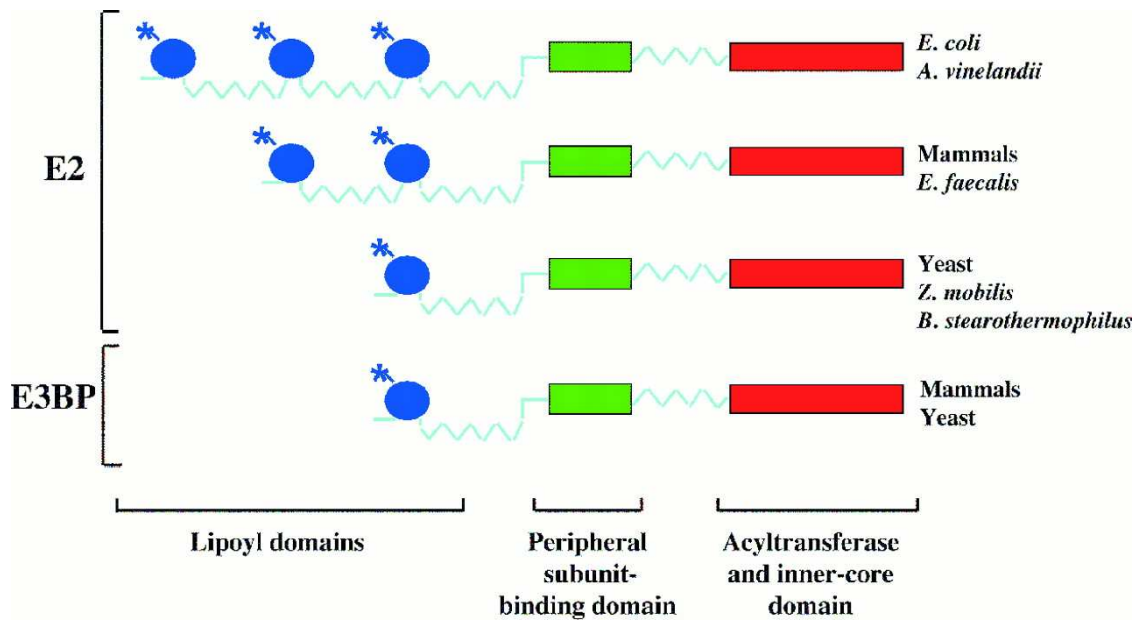
Figure 1.5: Schematic representation of the domain and linker regions of E2 and E3BP of PDC across various species

The domains are separated by long, flexible but extended linker regions of polypeptide chain (indicated in light blue). Lipoylated domains are indicated by a star. Adapted from Perham (2000).

1.5.2 The lipoyl domains of E2

The lipoyl domains play a crucial role in coupling the activities of the three enzyme components of PDC by providing 'swinging arms' that are mobile and responsible for efficient substrate product transfer among the three successive active sites (Fussey et al., 1991; Yeaman et al., 1978). A specific lysine side chain of each lipoyl domain is modified with a lipoamide prosthetic group that is essential for transportation of acetyl groups from El to E2, and reducing equivalents from E2 to E3. Lipoic acid is 6, 8-thioctic acid or 1, 2 dithiolane-3-pentanoic acid and is a sulphur containing cofactor (see section 1.5.3 for details). A correctly-folded lipoyl domain is required for the efficient attachment of its lipoyl group and recognition by its cognate lipoyl-ligase and El component. The covalent attachment of the lipoic acid cofactor to apoprotein requires two enzymes in mammals. Firstly a lipoate activating enzyme promotes the formation of lipoyl AMP (Tsunoda and Yasunobu, 1967). Then a second enzyme, lipoyl AMP:N^{ϵ}-lysine-lipoyltransferase, which depends on a structural cue rather than a specific amino acid motif, initiates lipoylation of the lysine residue (Fujiwara et al., 1994; Fujiwara et al., 1999). In contrast, in *E. coli*, lipoate-protein ligase A is responsible for cofactor attachment and catalyzes both lipoate-activating and transferring reactions (Morris et al., 1994; Zhao et al., 2003).

1.5.3 Structure of the E2 lipoyl domain

The structure of the lipoyl domain from a number of prokaryotic sources has been solved by NMR spectroscopy. However, only one structure has been solved from a mammalian source (Howard et al., 1998). The overall backbone structure of the lipoyl domain is quite similar in all species examined so far. It comprises a β-barrel-sandwich hybrid that is now known to be typical for lipoyl domains (Fig.1.6). The domain is formed by two similar and almost parallel four-stranded antiparallel β-sheets connected by loops and turns. The β-sheets each consist of three major and one minor strand, and are formed around a well-

defined core of hydrophobic residues. The lipoylatable lysine residue is located on an exposed type-1 β turn in one of the β-sheets, within a conserved DKA motif. Highly conserved aspartic acid (D) and alanine (A) residues do not appear to be important for the recognition of the lipoylatable residue lysine, as determined by site-directed mutagenesis whereas the position of the lysine residue itself appears to be critical for lipoylation. When the lysine residue was mutated to alanine or moved one residue in either direction, lipoylation was not observed as determined by mass spectrometry. This shows that lipoylating enzymes require a precise structural cue in order to initiate lipoylation. In the *B. stearothermophilus* lipoyl domain of E2, the combined results of site-directed mutagenesis and NMR spectroscopy pointed to the surface loop, close in space to the beta-turn containing the lipoyl-lysine residue, as a major determinant of the interaction of lipoyl domain with E1 (Wallis and Perham, 1994). In this study the mutant domain retained its overall three dimensional structure and ability to become lipoylated but could not be reductively acetylated by E1. Jones and co-workers (Jones et al., 2001) found that the lipoyl domain of E2 undergoes conformational changes when interacting with their homologous E1s but not heterologous E1s. Gong & co-workers (Gong et al., 2000) determined the contribution of particular amino acids of the outer lipoyl domain of human PDC in E1 recognition and found that the specificity loop involves L140, S141, and T143. Other residues that markedly reduce activity of this enzyme on mutagenesis are E162, D172, A174, and E179 located close to the lipoylatable lysine residue (K173). They also found that influential residues are spread over more than 24 Å on one side of the outer lipoyl domain, suggesting surface residues in this region contribute towards substrate recognition

At the far end of one of the sheets, the lipoyl-lysine residue is presented to the solvent in a beta-turn connecting two successive strands. The N-terminal and C-terminal ends of the folded domain meet on the exact opposite side of the domain in two adjacent beta-strands of the other sheet. Lipoyl domains display a remarkable internal symmetry that projects one β-sheet onto the other β-sheet after rotation of approximately 180° about a 2-fold rotational symmetry axis.

In *E. coli* PDC it has been shown that there are three lipoyl domains per E2 chain although only the outermost domain needs to be lipoylated for optimal activity and growth (Fussey et al., 1988). It was concluded that the reason for retaining three lipoyl domains is to extend the reach of the outermost lipoyl cofactor rather than to provide extra cofactors for catalysis.

Lipoic acid is 6, 8-thioctic acid or 1, 2 dithiolane-3-pentanoic acid and functions in transacylation, redox and transport reactions. It plays a central role in oxidative decarboxylation where it is covalently attached to a specific lysine side chain on each lipoyl domain to form a lipoamide prosthetic group. It is formed from octanoic acid via an enzymatic S insertion (Brody et al., 1997). Lipoic acid has a therapeutic role in many PDC deficiency symptoms. Clinical improvement has been achieved by oral administration of lipoic acid in a young patient (Matalon et al., 1984). In addition, lipoic acid has been reported to prevent symptoms of vitamin E deficiency (Podda et al., 1994) and to protect against cerebral ischaemia perfusion in rodents (Cao and Phillis, 1995). Ziegler and co-workers (Ziegler et al., 1997) evaluated the efficacy and safety of the oral treatment with the antioxidant lipoic acid in non-insulin dependent diabetes mellitus patients with autonomic neuropathy. Treatment with lipoic acid was well tolerated and slightly improved the patients with cardiovascular autonomic neuropathy symptoms.
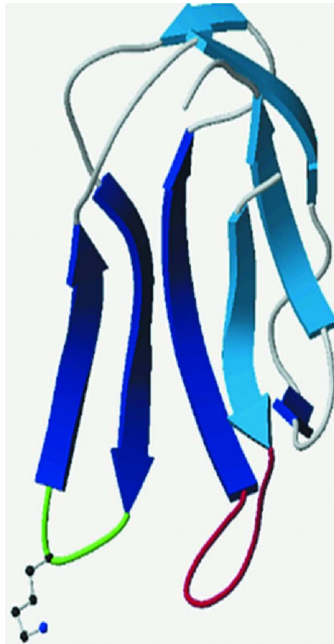
Figure 1.6: Structure of the lipoyl domain of the E2-PDC from *B. stearothermophilus*

The two sets of β-sheets are shown in *light blue* (strands 1, 3, 6, and 8) and *dark blue* (strands 2, 4, 5, and 7). The lysine residue that becomes lipoylated is in the loop between strands 4 and 5 (indicated in *green*), and the prominent surface loop between strands 1 and 2 is indicated in *red*. The orientation of the side chain of the target lysine residue is undetermined (Dardel et al., 1993).

1.5.4 Peripheral subunit binding domain of E2

The primary function of this domain in human E2 is to bind E1 primarily through the E1β subunit (Lessard and Perham, 1995), but it may also retain a residual binding affinity for E3 (McCartney et al., 1997). The three dimensional structure of this domain from *B. stearothermophilus* PDC (Kalia et al., 1993) has been resolved and shown to comprise two α helices connected by a loop. It is about 43 amino acids in length with 33 of these residues forming a structured core composed of two α helices connected by a loop that contains a short 3^{10} helix. Two highly conserved hydrophilic residues, Asp34 and Thr24 are found buried in the structure and these residues are thought to be crucial for the stability of the domain (Spector et al., 1998). Sequence comparison of this domain from a variety of organisms has shown that they share a very similar structure (Russell and Guest, 1991) and indeed is one of the most highly conserved regions of the E2 protein.

1.5.5 The C-terminal acetyltransferase domain of E2

The C-terminal domain of E2 forms the central core of PDC by associating into trimers that are located on each vertex. Eight such trimers are found in the cubic core in *A. vinelandii* (Mattevi et al., 1993b; Mattevi et al., 1992), while 20 each are found in the icosahedral core of *B. stearothermophilus* (Milne et al., 2002), yeast (Stoops et al., 1992; Stoops et al., 1997) and bovine PDC (Behal et al., 1994). The trimers are fairly loosely associated via bridges, 20 Å in length, along the two fold axes creating highly dynamic structures.

The C-terminal domain of E2 is responsible for the acetyltransferase activity of this enzyme and provides the binding sites involved in E2 self-assembly into the structural core. The active site is located in a 30 Å long channel at the C-terminal domain subunit interface and runs across trimers. A conserved sequence motif, DHRXXDG, is thought to

accommodate the histidine and aspartate necessary for catalysis (Radford et al., 1987). Two substrates for transacetylation, CoASH and the acetylated lipoyl domain have to approach the E2 active site from opposite directions (Izard et al., 1999). CoASH binds to the inside of the E2 core, while the acetylated lipoyl domain interacts with the outside (Mattevi et al., 1993b; Mattevi et al., 1993c; Mattevi et al., 1992). Structural homology has been observed between the C-terminal domain of *E. coli* E2 and several chloramphenicol acetyltransferases (CATs) (Fussey et al., 1988). The comparison of this domain with CAT also shows two highly conserved residues, a histidine and an aspartic acid, thought to be involved in the catalytic mechanism of E2. This prediction was later confirmed when the crystal structure of the cubic E2 core from *A. vinelandii* was solved to 2.6Å resolution (Mattevi et al., 1993c; Mattevi et al., 1992). CAT is also organised as a tightly-associated trimer of identical chains with a catalytic centre, containing a 30 Å long channel, found at the interface between subunits and is structurally similar to E2 from *A. vinelandii* (Leslie, 1990).

1.6 E3 binding protein (E3BP)

This subunit, also originally known as protein X, has been found only in the PDC of mammals (De Marcucci and Lindsay, 1985), *Ascaris suum* (Klingbeil et al., 1996) and yeast (Behal et al., 1989). The presence of this subunit in PDC was not recognised for many years until 1985, because it was thought to be a degradation product of E2 as it contained a covalently-attached lipoyl group that can be reductively acetylated in a similar manner to the lipoyl domain of E2. It was found to be an individual component of PDC when anti-sera raised against other components of PDC failed to elicit a reaction against E3BP and vice-versa (De Marcucci and Lindsay, 1985; Jilka et al., 1986). Peptide mapping and radiolabelling studies further confirmed E3BP as a fourth separate component of PDC (De Marcucci et al., 1986; Hodgson et al., 1986; Jilka et al., 1986; Neagle et al., 1989). The main function of this protein is to bind E3 to the core structure; hence it was renamed E3 binding protein (Lawson et al., 1991). Initially the precise role of the E3BP subunit was not known exactly because of its high affinity for the 60-meric E2 assembly from which it could only be dissociated under denaturing conditions. However, it was found that this subunit could be cleaved by selective proteolytic degradation employing arg C, releasing a

15 kDa N-terminal fragment, whereas the 35 kDa C-terminal fragment was still bound to the high molecular weight core of the complex. Arg C cleavage of E3BP was prevented by the presence of E3; moreover the proteolytically-modified E2:E3BP was no longer able to bind E3 with high affinity (Sanderson et al., 1996a).

 The human *PDX1* gene encoding E3BP was cloned in 1997 (Harris et al., 1997) and showed high similarity to that of E2-PDC. It consisted of a lipoyl domain, a subunit binding domain, a C-terminal domain and flexible linker regions (Fig. 1.5). The lipoyl domain of E3BP can be acetylated but no acetyltransferase activity or other catalytic role has been identified for E3BP. In the absence of E3BP, PDC sustains a low level of activity since the peripheral subunit-binding domain of the E2 displays residual affinity for E3 (McCartney et al., 1997). Removal of E2 lipoyl domains by collagenase treatment of the complex results in retention of 15-20% of overall PDC activity as compared to wild-type complex, suggesting that the E3BP lipoyl domain can compensate for the missing E2 lipoyl domains to some extent (Sanderson et al., 1996a).

Recent studies with low resolution structure analyses indicate that there is 2:1 binding of E3BP and E3 forming a stable complex. One lipoyl domain of this complex may be peripherally extended away from the E3 dimer, whereas the second lipoyl domain is docked into one of the E3 active sites that are located at the monomer-monomer interface in a dynamic state (Smolle et al., 2006) suggesting, as is the case for E1, that the two actively interact with their cognate substrate in a flip-flop mechanism.

Complexes deficient in E3BP have been shown to retain partial PDC activity both *in vivo* and *in vitro*. Reconstitution studies have shown that bovine PDC lacking E3BP is able to retain residual activity in the presence of a molar excess of E3. However, in the presence of stoichiometric amounts of E3, little or no activity was apparent (McCartney et al., 1997). This is thought to be due to retention of a limited ability of mammalian E2 to bind to the E3 component, allowing E3 to bind specifically but with low affinity.

This retention of residual binding activity is supported by studies on a group of patients who have no immunologically-detectable E3BP but, can still sustain PDC activity at approximately 10-20% of wild-type levels (Geoffroy et al., 1996; Marsac et al., 1997). Such patients displayed symptoms that were indistinguishable from those associated with

classical PDC deficiency. Initially it was unclear if such patients produced low amounts of E3BP that might be compatible with the maintenance of life. However subsequent analysis of E3BP deficient patients indicated that they carried large deletions within the open reading frame of E3BP cDNA (Marsac et al., 1997). These large deletions occurred as a result of point mutations at intron-exon boundaries in genomic DNA leading to aberrant splicing and loss of an entire exon (Dey et al., 2002).

1.7 Dihydrolipoamide dehydrogenase (E3)

E3 is a member of the enzyme family known as the pyridine disulphide oxidoreductases involved in the transfer of electrons between pyridine nucleotides and disulphide compounds. The other main members of this family include glutathione reductase, thioredoxin reductase and NADH peroxidase.

In PDC, E3 brings about reoxidation of the reduced lipoyl moiety on E2 and E3BP. Initially the dihydrolipoamide on E2 transfers its electrons to a reactive cysteine pair on E3, and then the electrons are passed via a tightly bound FAD cofactor before being finally transferred to NAD^+. The end result is the formation of NADH and an oxidised lipoamide moiety on E2 that is now ready for the next catalytic cycle.

In the PDC, E3 exists as a dimer of two identical subunits. Each subunit contains a redox active disulphide, a non-covalently bound FAD molecule and NAD^+ binding site. Only the dimeric form of the enzyme is active and can interact correctly with E2 (Schulze et al., 1991). The three dimensional structures of E3 from several different sources have been solved by x-ray crystallography the most recently from human (Brautigam et al., 2005).

E3 also contains two active sites, each of which is formed by the flavin ring of FAD, two cysteine residues from one monomer and a histidine residue from the second monomer (Toyoda et al., 1998). Site-directed mutagenesis of this histidine residue (His-425) in human E3 resulted in almost complete abolition of E3 activity and it was concluded that His-452, was the probable proton acceptor/donor critical to   E3 catalysis. In addition, the local environment around His-452 and Glu-457 is important in the binding of

dihydrolipoamide to the enzyme (Kim and Patel, 1992). E3 is thought to be the identical gene product serving all three 2-oxoacid dehydrogenase multienzyme complexes in mammals.

1.8 Regulation of PDC

PDC is located at a significant branch-point in metabolism channelling intermediates into the tricarboxylic acid cycle (Fig. 1.1.). Two major types of regulatory mechanism are present in PDC from higher organisms. One is the end product inhibition by NADH and acetyl CoA and the other involves covalent modification of the complex by a phosphorylation / dephosphorylation mechanism mediated by several protein kinases that are tightly bound to the complex and a specific phosphoprotein phosphatase that is more loosely associated (Behal et al., 1993) (Fig. 1.7).

Stimulation of the pyruvate dehydrogenase kinase activity by acetyl-CoA and NADH is thought to occur due to changes in acetylation and reduction states, respectively of the transacetylase lipoyl moieties (Yeaman et al., 1978). Four isoenzymes of PDC kinase namely PDK1, PDK2, PDK3 and PDK4 have been identified and characterised, PDK4 being the most recent (Rowles et al., 1996).

Initially PDC kinase (PDK) was thought to be organised as a heterodimer having an α subunit of molecular weight 48,000 and the β subunit of molecular weight 45,000 (Stepp et al., 1983). However, more recently it became apparent that there was a possibility of the individual isozymes of PDK forming homo- and heterodimers, which might differ with respect to their kinetic parameters and regulation in mammals. Indeed Boulatnikov and coworkers (Boulatnikov and Popov, 2003) have recently demonstrated heterodimerisation between PDK1 and PDK2.

The kinase is present in very small quantities and is tightly bound to the complex. PDK catalyse the phosphorylation of three serine residues present on E1 α subunit. These are Ser-264, Ser-271 and Ser-203 in human PDC. Phosphorylation at site 1 occurs independently. However, phosphorylation at site 2 (Ser-271) and site 3 (Ser–203) requires

the presence of E2 (Yeaman et al., 1978). Each of these isoenzymes exhibits tissue specific expression and acts at different preferential sites. PDK1 and 4 are mainly expressed in liver and muscle tissues, while PDK3 is present in the kidney, brain and testes. PDK2 is present in most tissues (Gudi et al., 1995). Site 1 seems to be preferentially phosphorylated by PDK2, site 2 by PDK3 while site 3 can only be phosphorylated by PDK1 (Korotchkina and Patel, 2001). PDK1-3 associate with the E2 inner lipoyl domain while PDK4 preferentially interacts with the E3BP lipoyl domain (Yeaman et al., 1978).

PDC kinase is a target protein in several drug development programmes since inhibitors of this enzyme should activate PDC, thereby increasing carbohydrate utilisation and is of particular interest in the treatment of diabetes.

Pyruvate dehydrogenase is phosphorylated and inactivated by its specific, intrinsic, cAMP-independent protein kinase, using Mg ATP as substrate (Cooper et al., 1974). Reactivation of the enzyme complex is accomplished by a Mg^{2+} and Ca^{2+} dependent phosphoprotein phosphatase, that removes the phosphoryl groups from phospho-E1. Huang and co-workers (Huang et al., 1998) showed that there are at least two isoenzymes of pyruvate dehydrogenase phosphatase (PDP), designated as PDP1 & PDP2 in mammals, that are different with respect to tissue distribution and kinetic parameters and, therefore, are likely to be different functionally. These isoenzymes have tissue specific expression with PDP1 located primarily in muscle whereas PDP2 is found in liver and adipose tissue (Huang et al., 1998). In contrast to PDK, PDP is loosely associated with PDC, although its catalytic activity is increased 7-16 fold by interaction with the E2 lipoyl domain (Chen et al., 1996).

Like PDP1, PDP2 is a Mg^{2+} dependent enzyme, but its sensitivity to Mg^{2+} ions is almost ten-fold lower than that of PDP1. In contrast to PDP1, PDP2 is not regulated by Ca^{2+} ions. Instead, it is sensitive to the polyamine spermine, which in turn has no effect on the enzymatic activity of PDP1 (Huang et al., 1998).

Another long term regulatory mechanism involves several hormones and nutritional factors that control the levels and activity of the PDC in several tissues. These factors have been studied, but to a lesser extent and probably affect the long term regulation of PDC through changes in the levels of its catalytic and regulatory components by controlling gene expression at the transcriptional and translational level (Patel and Harris, 1995).
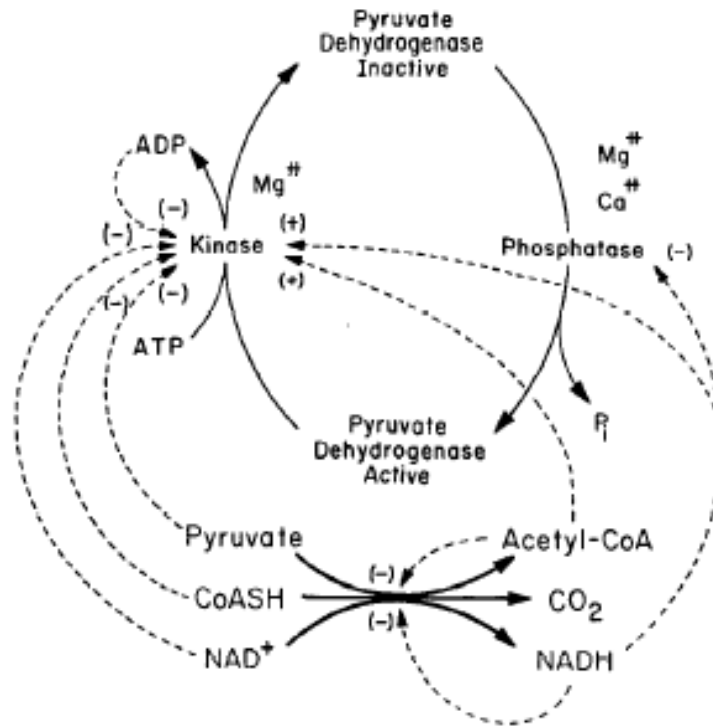
Figure 1.7: Regulatory mechanism for PDC by feedback inhibition and covalent modification via protein kinase(s) and phosphoprotein phosphatase(s)

Adapted from Behal et al. (1993).

1.9 Pyruvate dehydrogenase complex defects

As human PDC is composed of several different gene products, a genetic defect involving any one of them can lead to impairment in its function. Deficiencies of the pyruvate dehydrogenase complex are now well documented and mutations have been described in the genes *PDHA1, PDHB, DLAT, DLD, PDX1* and *PDP1* encoding the E1α, E1β, E2, E3, E3BP and PDP1 proteins, respectively (Brown, 1992; Brown et al., 2004; Lissens et al., 2000; Seyda et al., 2000).

Pyruvate dehydrogenase complex deficiency is one of the most common disorders leading to neurodegeneration associated with abnormal mitochondrial metabolism as the citric acid cycle is a major biochemical process central to energy production and maintenance of intracellular ATP levels. Malfunction of the cycle leads to abnormal lactate build-up resulting in non-specific symptoms (e.g., severe lethargy, poor feeding, tachypnea), especially during times of illness, stress, or high carbohydrate intake. Progressive neurological symptoms usually start in infancy but may be evident at birth or in later childhood. These symptoms may include developmental delay, intermittent ataxia, poor muscle tone, abnormal eye movements or seizures.

The vast majority of these lesions reported to date are caused by mutations in the coding region of the gene responsible for E1α. About 80 point, insertion and deletion mutations have been reported in the E1α subunit causing a range of symptoms of varying degrees of severity in individual patients (Chun et al., 1993). The gene for E1α is localised on the X chromosome (Szabo et al., 1990) exposing it to a greater chance of mutation. In addition, location of the E1α gene on the X chromosome is responsible for variations in the clinical symptoms of E1α mutation between males and females, specifically the potential for the occurrence of mosaicism in heterozygous females. Complete PDC E1α deficiency has not been observed in males and is presumed to be lethal at an early stage of development. By contrast, mutations that abolish E1α protein synthesis are commonly found in heterozygous female patients whose tissues are composed of two populations of cells as a consequence of X chromosome inactivation. In these females, some cells have completely normal PDC function whereas others are highly deficient (Dahl et al., 1992).

The random pattern of X inactivation in different individuals, and in different tissues in the same individual, contributes significantly to the widely divergent clinical presentations in female patients. Although the majority of these heterozygous females present with obvious PDC deficiency, a small number of females carrying an E1α subunit mutation have mild symptoms or no symptoms at all, presumably because of an X-inactivation pattern favouring expression of the normal X chromosome (Fujii et al., 1994; Matthews et al., 1994). There is a male preponderance amongst severely affected patients whereas females tend to have milder metabolic and neurological dysfunction (Brown et al., 2004). Mutations affecting the PDHB gene encoding E1β have been identified in two patients only so far. In both cases a single amino acid substitution destabilises the E1 heterotetramer (Brown et al., 2004).

Although not reported as frequently as E1 defects, abnormalities in E2, E3 and E3 binding protein have also been found producing a broad range of symptoms of varying severity (Chun et al., 1991; Dahl et al., 1992; Endo et al., 1991). Mutations in the PDX1 gene encoding E3BP have been reported in a dozen patients (Aral et al., 1997; Geoffroy et al., 1996; Ling et al., 1998; Marsac et al., 1993; Ramadan et al., 2004).

More than 20 cases of E3 deficiency have been reported due to different mutations in the DLD gene encoding the E3 enzyme, common to PDC, OGDC and BCOADC (Hong et al., 1996; Robinson et al., 1989).

Defects in the E2 component have also been detected in patients with severe lactic acidaemia (Robinson et al., 1990). However the numbers of patients encountered with defects in the E2 are relatively few.

PDC deficiency must be differentiated from other disorders causing lactic acidosis, particularly defects of the electron transport chain. Although electron transport chain defects may have similar neurological manifestations to PDC defects, they also have systemic manifestations (skeletal and cardiac myopathies) not found in inborn errors of PDC. Biochemically these two entities can be differentiated because electron transport chain defects have an abnormally elevated lactate /pyruvate ratio and impaired fatty acid oxidation (Robinson et al., 1989). Further detailed information on this topic is provided in section 4.1, Chapter 4.

Another type of disease involving PDC subunits is primary biliary cirrhosis. This is an autoimmune disease characterised by the production of anti-mitochondrial auto-antibodies (AMA) against components of PDC although the major auto-antigen is the E2 component (Fussey et al., 1988; Gershwin et al., 1987). The primary epitope appears to be the inner lipoyl domain of E2 and involves the lipoamide prosthetic group. Since this domain is conserved in E3BP, it is also another major target of the autoimmune response (Surh et al., 1989). Autoantibodies have also been reported against E2-OGDC (Fussey et al., 1988), BCOADC (Fussey et al., 1991) and the E1α protein (Fregeau et al., 1990).

Defects in ThDP-containing enzymes such as pyruvate dehydrogenase have been reported in brain and peripheral tissues from patients suffering from Alzheimer's disease (Gibson et al., 1988). A 50% decline in the activity of PDC, OGDC and cytochrome oxidase has also been shown in patients' brains suffering from Alzheimer's disease (Gibson et al., 1998). The exact molecular mechanism involved in linking PDC and OGDC to this disease is not known, however, possibilities are that free oxygen radicals and accompanying oxidative stress may cause damage to these enzymes (Shi et al., 2005). Defects in PDC may also reduce acetyl-CoA levels leading to impaired production of acetylcholine that is an important neurotransmitter in both the peripheral and central nervous systems (Szutowicz et al., 2006). Many patients suffering from systemic sclerosis, a multi-system connective tissue disorder, also produce antibodies to E1α (Fujimoto et al., 1995). Detailed enzymatic and genetic analysis of patients with such defects is very important in understanding the exact role of each component of PDC and also beneficial for clinical prenatal diagnosis, improved treatment regimens and potentially gene therapy in the future.

The diagnosis of PDC deficiency has been enhanced by the availability of specific assays for PDC and its catalytic components. Immunological and molecular biological methods have facilitated characterisation of the genetic basis of specific PDC defects. Immunoblots and RNA blot analyses using specific antibodies and cDNA probes corresponding to all the catalytic components of PDC indicate considerable heterogeneity in PDC deficiencies (Brown et al., 2004; Patel et al., 1992).

As PDC is ultimately responsible for tailoring the appropriate usage of glucose in the body to match the varying energy requirements of individual tissues on a minute-by-minute basis; therefore, PDK and its inhibitors are of great importance as therapeutics for diabetes, where glucose metabolism is impaired. Early interventions to treat PDC deficiency include

dietary manipulation and vitamin supplementation (Falk et al., 1976; Matalon et al., 1984). Ketogenic diets appear to lower blood lactate levels, but do not significantly improve neurological function in most cases. Another form of therapy includes the provision of thiamine and/or lipoic acids in an attempt to maximise residual PDC activity. Reduced lactic acidosis was observed in PDC deficient patients on treatment with dichloroacetate, which is an E1-kinase inhibitor (Berendzen et al., 2006; Stacpoole, 1989; Stacpoole et al., 2006).

Recently, a vector using recombinant adeno-associated virus (rAAV) that contained a full-length E1α green fluorescent protein (GFP) construct was used to deliver wild type E1α into mitochondria after injection of the construct *in vivo* into the central nervous system of rats and *in vitro* into human cells. Transfection of cultured fibroblasts from a male patient with E1α deficiency led to partial restoration of PDC activity, as determined by decarboxylation of ^{14}C-pyruvate. These data indicate that at least partial correction of PDC defects may be feasible by gene transfer (Stacpoole et al., 2003).

1.10 Biophysical tools in the study of PDC

PDC is a highly important multienzyme complex central to the energy metabolism of an organism. Various researchers using a combination of molecular biological, biochemical and biophysical approaches have determined the structure, function and modes of interaction of various components of PDC. For structural determination, the choice of biophysical techniques depends largely upon the physical and biochemical properties of the protein to be studied and also on the advantages and limitations of the techniques employed. For example, crystallography gives a very high resolution (up to 0.1 nm) revealing fine details of atomic structure but requires the production of high quality crystals, which is always not feasible. The crystal structure of human E1-PDC has been resolved at a resolution of 1.95 Å (Ciszak et al., 2003) and the crystal structure of human E3 (Brautigam et al., 2005) and E3BP-subunit binding domain in association with E3 has been recently resolved at 2.6 Å (Ciszak et al., 2006).

NMR is another versatile tool for structural determination of macromolecules in solution giving high resolution (0.2-0.3 nm), information about the flexibility and dynamics of specific regions of polypeptides and providing a means for mapping sites of protein-protein interaction. However, this approach requires concentrated solutions of protein and is limited to the analysis of relatively small proteins (M_r, 30 kDa or less). The structure of the inner lipoyl domain of human PDC has been resolved through NMR (Howard et al., 1998). Similarly, the three-dimensional structure of the lipoyl domain (Dardel et al., 1993) and the peripheral subunit-binding domain of dihydrolipoamide acetyltransferase from the PDC of *B. stearothermophilus* has also been solved by this approach (Kalia et al., 1993).

Small angle X-ray scattering (SAXS) is another biophysical tool that is often employed in combination with other structural and biochemical methods and is an important complementary approach to generate consistent models of biological macromolecules (Koch et al., 2003). SAXS not only provides low-resolution models of protein complexes in solution, but also in many cases delivers answers to significant functional questions. For example the structure of human E3 bound to subunit binding domain of E3BP has been resolved by SAXS and shows great asymmetry (Smolle et al., 2006). Most importantly, the method permits the study of native oligomeric protein complexes in near physiological state and the analysis of structural changes in response to variations in external conditions, thus yielding valuable information on the relationship between these structural changes and the operation of the proteins under investigation. In many cases solution structures differ significantly and are more open and extended than the equivalent crystal structures.

Determination of the three-dimensional (3D) organization of PDC is key to understanding its highly regulated, multi-functional roles and underlying molecular mechanisms. While much progress has been made in the determination of 3D structures of the constituent enzymes of microbial and yeast PDCs through X-ray crystallography, NMR spectroscopy and electron cryomicroscopy (cryo EM), 3D structural studies of the human PDC complexes have been hampered both by sample unavailability and by the increased complexity of additional regulatory components. Construction of a recombinant human PDC *in vitro* by expressing and purifying its individual enzymes in *E. coli* has been achieved in this laboratory followed by their spontaneous reconstitution into active complex. This should facilitate detailed investigation of how the multiple components of human PDC and their cofactors interact with each other in normal as well as pathological states. Various biochemical, molecular as well as common biophysical techniques such as circular dichroism, size exclusion chromatography and analytical ultracentrifugation have

been used in this study. Analytical ultracentrifugation is an extremely versatile and powerful technique for characterizing the solution-state behaviour of macromolecules. When coupled with contemporary data analysis methods, experiments performed in the analytical ultracentrifuge are capable of rigorously determining sample purity, characterizing assembly and disassembly mechanisms of biomolecular complexes, determining subunit stoichiometries and detecting and characterizing macromolecular and conformational changes.

Circular dichroism (CD) is an excellent tool for rapid determination of the secondary structure and folding properties of proteins that have been obtained using recombinant techniques or purified from tissues. The most widely used applications of protein circular dichroism are to determine whether an expressed, purified protein is folded correctly or if mutations affect its conformation or stability. CD is defined as the differential absorbance of left circularly polarized light (LCPL) and right circularly polarized light (RCPL): CD = Abs (LCPL) – Abs (RCPL). Ellipticity is the unit of circular dichroism and is defined as the tangent of the ratio of the minor to major elliptical axis. To be "CD active", a molecule must be structurally asymmetric and exhibit absorbance in the uv region. Asymmetry can result from chiral molecules such as the peptide backbone of proteins, a non-chiral molecule covalently attached to a chiral molecule (aromatic amino acid side chains), or a non-chiral molecule in an asymmetric environment (e.g. a chromophore bound to a protein). Increased relative absorption of left polarized light results in a positive CD signal, while a negative signal is the result of right polarized light being more highly absorbed. Proteins are CD active (all amino acids except glycine contain a chiral carbon), and the resulting CD signals are sensitive to protein secondary and tertiary structure.

Three common secondary structure motifs (alpha helix, beta sheet, and random coil) exhibit distinctive CD spectra in the far-ultraviolet region (170-260 nm). Alpha-helical proteins have negative peaks at 222 nm and 208 nm and a positive peak at 193 nm. Proteins with well-defined, antiparallel β-pleated sheets (β-helices) have a trough at 218 nm and a peak at 195 nm, whereas disordered proteins have very low ellipticity above 210 nm and negative bands near 195 nm (Greenfield and Fasman, 1969; Holzwarth and Doty, 1965; Venyaminov et al., 1993). Secondary structure determination by CD is reported to achieve accuracies of 0.97 for helices, 0.75 for beta sheet, 0.50 for turns and 0.89 for other structure types (Manavalan and Johnson, 1987).

Using CD spectra, the secondary structure of proteins can be estimated using a variety of computer algorithms. The near ultraviolet region (320-260 nm) provides a fingerprint of the tertiary structure of proteins. Asymmetric environments of aromatic amino acids, that are sensitive to protein conformation in the local environment, provide the basis of the near-uv CD signal (Greenfield, 1975).

Tryptophan fluorescence is another approach widely used in protein studies to determine structural changes in proteins. The major goal in the application of this tool is to interpret the fluorescence properties in terms of structural parameters and to predict the structural changes in the protein. Since the wavelength and intensity of tryptophan fluorescence emission spectra is sensitive to the surrounding environment therefore, it is regularly employed to monitor perturbation of the local tertiary structure.

1.11 The 2-oxoglutarate dehydrogenase complex (OGDC)

This mitochondrial enzyme assembly catalyses the oxidative decarboxylation of 2-oxoglutarate to succinyl CoA. E1o also utilizes thiamine diphosphate (ThDP) as a cofactor. The ThDP is tightly but non-covalently bound to E1, which catalyses the oxidative decarboxylation of 2-oxoglutarate and subsequent binding of the resultant succinyl moiety to a sulphur residue of E2 bound lipoic acid with concomitant regeneration of the ThDP. The core enzyme E2 catalyses succinyl group transfer to coenzyme A producing succinyl-CoA. A multiple random coupling mechanism has been proposed for the E2 lipoyl domain in OGDC from *E. coli* (Hackert et al., 1983). E3 catalyses the two electron transfer of reducing equivalents from E2 to produce NADH and H^+.

The basic organisation of this complex is also believed to be similar to PDC with 24 copies of dihydrolipoyl succinyltransferase (E2o) forming a cubic core structure displaying octahedral symmetry to which 12 copies of 2-oxoglutarate dehydrogenase (E1o) bind non-covalently (Yeaman et al., 1978). An estimated 6 copies of dihydrolipoamide dehydrogenase (E3) are attached non-covalently to the six faces of this complex. In mammalian OGDC, some early studies suggested that E1o appears to bind more tightly to the E2o core than E3 (Yeaman et al., 1978). More recent reports indicate that single copies

of E1o and E3 form a high-affinity subcomplex, with the homodimers binding to the E2o core through the N-terminal region of E1o (McCartney et al., 1998).

OGDC plays an important role in the regulation of 2-oxoglutarate concentration which is a key citric acid cycle intermediate and a common substrate for several enzymes. Regulation of OGDC is subject to feedback inhibition with its end products, NADH and succinyl CoA inhibiting the E1o component directly (Lawlis and Roche, 1981). Changes in both Ca^{2+} and Mg^{2+} concentrations can also control OGDC activity and along with ThDP are required for maximal enzyme activity (Panov and Scarpa, 1996). Agonists that increase cytosolic free Ca^{2+} levels have been shown to stimulate metabolic flux through the 2-oxoglutarate dehydrogenase complex. Another study indicated that physiological concentrations of inorganic Pi may exert significant activation of OGDC that could further be potentiated by Mg^{2+} (Chinopoulos et al., 1999). A number of inhibitors reduce the activity of this complex including several reactive oxygen species and lipid peroxidation products such as 4-hydroxy-2-nonenal (Andersson et al., 1998; Chinopoulos et al., 1999; Humphries and Szweda, 1998; Park et al., 1999). Hydrogen peroxide interacts with nitric oxide (NO) to form peroxynitrite a reactive nitrogen species that is also reported to be an effective inhibitor of OGDC (Park et al., 1999). Hydroxynonenal and perhaps hydrogen peroxide may reduce the activity of OGDC relatively selectively compared to other mitochondrial components of energy metabolism (Lucas and Szweda, 1999). Methotrexate and some other environmental toxins can also inhibit OGDC function (Caetano et al., 1997).

1.12 Dihydrolipoamide succinyltransferase (E2o)

The core protein, E2o is encoded by the DLST gene that in humans is located on chromosome 14q24.3. The human DLST gene and a pseudogene were first characterised in 1994 (Nakano et al., 1994). The sequence of the human gene showed minor variations from those of previously published cDNAs (Ali et al., 1994; Nakano et al., 1993). Determination of the entire sequence of the dihydrolipoamide succinyltransferase gene of human OGDC revealed a complete absence of any obvious nucleotide sequence corresponding to the E3-binding and/or E1-binding domain. It has been suggested that the

exon coding for the E3-binding and/or E1-binding domain may have been lost from the gene during evolution (Nakano et al., 1994). Thus human dihydrolipoamide succinyltransferase possesses a unique structure consisting of only two domains in contrast to the dihydrolipoamide acyltransferases of the other 2-oxoacid dehydrogenase complexes.

1.13 2-oxoglutarate dehydrogenase (E1o)

E1o in humans is coded by the OGDH gene located on chromosome at position 7p13-p14 and the gene was initially characterised in 1998 by Koike (Koike, 1998). Although, thiamine diphosphate is a cofactor for this enzyme, its deficiency did not lower the levels of the mRNA for this component in several tissue culture systems (Pekovich et al., 1998). In the octahedral complex of OGDC, E1o exists as an α_2 homodimer whereas E1 of PDC is a heterotetramer. Studies on mammalian OGDC employing specific proteolysis and N-terminal sequence analysis, have identified a proteolytically sensitive region at the extreme N- terminus of the E1o component with significant sequence similarity to the E3BP and E2 components of mammalian PDC (Rice et al., 1992). These similarities suggested that E1o may perform some functions normally devolved to E2 in PDC and BCOADC. Gel permeation of the E1o/E3 fraction of OGDC, under associative conditions, has demonstrated that these two enzymes interact with high affinity to form a stable subcomplex with an apparent M_r consistent with a 1:1 stoichiometry. These studies provide the first direct biochemical evidence that uniquely, in mammalian OGDC, its constituent $E1_O$ enzyme is responsible for binding the E3 component to the multi-enzyme complex (McCartney et al., 1998), a function similar to protein E3BP in PDC. Moreover, subsequent immunological analysis indicated that antiserum to E1o recognised antigenic epitopes in E3BP of PDC, whereas anti-E3BP-specific serum was also able to weakly recognise E1o (McCartney et al., 1998).

1.14 Dihydrolipoamide dehydrogenase (E3)

Human dihydrolipoamide dehydrogenase (E3) is an enzymatic component common to the mitochondrial 2-oxoacid dehydrogenase and glycine decarboxylase complexes and has been described earlier in section 1.7 in this chapter. It is encoded by the DLD gene which was first characterised in 1993 (Feigenbaum and Robinson, 1993).

Site-directed mutagenesis of human E3 has shown that lysine-54 is necessary for the protein-FAD interaction and for the catalytic activity of this enzyme whereas, glutamate–192 is involved in maintaining the appropriate orientation of lysine-54 during catalysis (Liu et al., 1999). The amount of E3 found in mitochondria typically exceeds the amount required for the maximal activation of OGDC, PDC and BCOADC. This finding has led to speculation that E3 may also have roles in the transfer of electrons between substrates within mitochondria including ascorbic acid (Xu and Wells, 1996).

1.15 Role of OGDC in disease

OGDC deficiencies have been associated with several neurodegenerative disorders including Alzheimer's disease and Parkinson's disease. It is also linked to primary biliary cirrhosis, characterised by the presence of anti-mitochondrial antibodies against the subunits of the 2-oxoacid dehydrogenase complexes including E2o (Kaplan and Lundsgaarde, 1996). However, deficiency of OGDC is more characteristically associated with neurological syndromes. This association is not surprising because of the acute dependence of the integrity of the nervous system on oxidative metabolism. The neurological syndromes linked to OGDC deficiency vary from fatal disease of the neonates to chronic disease of the elderly. Infantile lactic acidosis with severe mental retardation is the characteristic symptom of OGDC deficiency (Hong et al., 1996; Munnich et al., 1982;

Robinson et al., 1989; Shaag et al., 1999). Many symptoms of OGDC deficiency are a result of deficiency of E3, with accompanying deficiencies in PDC as well as BCOADC (Hong et al., 1996; Munnich et al., 1982; Robinson et al., 1989). The affected patients can be homozygous for mutations in DLD or can be compounded heterozygotes, inheriting different defective DLD genes from each of their parents (Robinson et al., 1989). Psychomotor retardation in early childhood has been associated with somewhat milder deficiency of OGDC (Bonnefont et al., 1992; Guffon et al., 1993). Intermittent psychomotor symptoms occur in Ashkenazi Jews who generally have mild E3 deficiency (Shaag et al., 1999). For example, a group of these children have intermittent attention deficit disorder with mild ataxia, incoordination and hypotonic weakness linked to a single G229C mutation in the DLD gene.

Friedreich's ataxia (Wong et al., 1999) is another condition associated with OGDC deficiency (Sheu and Blass, 1999). This condition was named after the German physician Nicholas Friedreich, who first described the condition in the 1860s. These patients develop ataxia and signs of damage to the long tracts of the spinal cord, with significant clinical manifestations typically beginning in adolescence or early adult life (Sheu and Blass, 1999). The primary genetic defect is in the FRDA gene (Wong et al., 1999). FRDA encodes the protein frataxin that is involved in free radical metabolism within mitochondria. The Friedrich mutations can lead to inactivation of a number of key mitochondrial enzymes including aconitase (Rotig et al., 1997). E3 deficiency has been confirmed in the brain of Friedreich's ataxia patients (Mastrogiacomo et al., 1996).

Loss of mitochondrial enzyme activities including PDC and OGDC has been found in spinocerebellar ataxia also (Sheu and Blass, 1999; Sorbi et al., 1989). These ataxias involve varying combinations of signs and symptoms associated with dysfunction of the spinal cord and cerebellum and sometimes other parts of the brain. The precise gene product involved differs among the various types of spinocerebellar ataxias characterised so far (Pandolfo and Montermini, 1998).

Another important association of OGDC is with Parkinson's disease, a common disease of later life that impairs secondary motor function and often impairs intelligence as well. The best known defect in energy metabolism is in complex 1 of the electron transport chain, that may be caused in some Parkinson's disease patients by a defect in mitochondrial DNA (Schapira et al., 1998). Deficiency of OGDC has been found in Japanese patients with Parkinson's disease, based on immunocytochemical studies (Mizuno et al., 1994). A

genetic abnormality in the DLST gene, encoding E2o has also been reported in Japanese patients suffering from Parkinson's disease (Kobayashi et al., 1998). The Parkinson's syndrome can be induced by poisoning with the compound MPTP (1-methyl 4-phenyl 1, 2, 3, 6-tetrahydropyridine), a chemical that is related to the opioid analgesic drugs. This chemical is converted in mitochondria to MPP^+. MPP^+ inhibits complex 1 of the electron transport chain but also inhibits OGDC. The reported activity of OGDC in human brain is about 10% of that of complex 1, suggesting that MPTP inhibition of OGDC might be functionally more important than inhibition of the electron transport chain per se (Sheu and Blass, 1999).

Alzheimer's disease (AD) accounts for over 80% of dementias in older people (Nolan et al., 1998). The classical pathological lesions visible under the light microscope are amyloid plaques and neurofibrillary tangles (Geddes et al., 1997). Among the characteristic biochemical lesions are oxidative stress and deficiency of OGDC (Butterworth and Besnard, 1990; Gibson et al., 1988; Mastrogiacomo et al., 1996; Terwel et al., 1998). At least two mechanisms may contribute to the reduction of OGDC activity in AD. A genetic component is implied by the finding that OGDC deficiency persists in cultured skin fibroblasts from many but not all patients with AD (Sheu and Blass, 1999). However, a plausible pathogenic mutation has not been defined as yet. Secondary damage to OGDC also appears to occur in AD due to other mutations and particularly as a result of oxidative stress. OGDC is particularly susceptible to oxidative stress (Sheu and Blass, 1999) which appears to be an important part of AD process and may be the main contributor to the reduction of OGDC activity in this disease. Thus genetic and non genetic mechanisms are not mutually exclusive and indeed polymorphisms (or mutations) in a gene encoding an OGDC component may sensitise OGDC to damage by free radicals.

Human apolipoprotein E (APOE), a major component of lipoproteins, plays a central role in the metabolism and redistribution of lipids such as cholesterol and dysfunctional forms of APOE are associated with increased risk for AD (Corder et al., 1993; Farrer et al., 1997; Saunders et al., 1993; Strittmatter et al., 1993). Indeed, evidence indicates that DLST and a dysfunctional isoform of APOE, APOE4 may interact in the causation of AD (Sheu and Blass, 1999). In molecular genetics studies, the association of DLST with AD was found to be significant only in patients who were also positive for APOE4. The presence of this isoform has been proposed to be deleterious as a result of increased production of free radical evident from significantly enhanced lipid oxidation in brain cortex (Ramassamy et al., 1999) and such mechanisms can also affect OGDC.

Amyloid aggregates of the amyloid-beta (Abeta) peptide are implicated in the pathology of AD. Anti-Abeta monoclonal antibodies (mAbs) have been shown to reduce amyloid plaques *in vitro* and in animal studies. Consequently, passive immunization is being considered for treating AD and anti-Abeta mAbs are now in phase II trials (Gardberg et al., 2007).

OGDC defects have also been found associated with diabetes. Maturity-onset diabetes of the young (MODY) is a rare form of juvenile diabetes mellitus that presents with hyperglycaemia in the absence of ketosis. Mutations in the gene encoding hepatocyte nuclear factor-1α (HNF1α) are the cause of MODY3. Induction of HNF1-P291fsinsC the most common HNF1α mutation, is generated by a mutational hotspot in exon 4 occurring in unrelated families. This frameshift mutation, resulting from insertion of a C in a poly(C) tract centred around codon 290, encodes a truncated protein of 315 amino acids. This mutation has been reported to significantly inhibit expression of mitochondrial E1o mRNA and protein with a corresponding decrease in OGDC catalytic activity (Wang et al., 2000).

1.16 Aims of this thesis

The main aim of this thesis is to develop a recombinant model of human PDC for studying genetic mutations found in the human population. To achieve this, a recombinant model of PDC is created by overexpressing and purifying its various constituent enzymes before assembling into a fully-active complex. Initially reconstituted PDC is evaluated for its functional abilities by using various biochemical and molecular biology approaches to study the effects of known mutations in PDC on lipoylation status and role of E3BP. Once the usefulness and validity of this novel model system is established as described in Chapter 3, this model is used to study the role of three recently-discovered mutations in the E2 enzyme of PDC encountered in indvidual patients. Two of these mutations are unusual 'in frame' three base pair deletions and the third one is a substitution of an amino acid located in the proximity of the active site. Structure function relationships are studied by mimicking the natural mutations in a PDC recombinant model. These mutations and subsequent analysis of their effects on PDC assembly and enzymatic functions are described in Chapter 4.

This study is designed not only to generate new information on the precise consequences of the mutations at a molecular level and of their underlying consequences leading to the appearance of clinical symptoms, but also to establish the utility of this recombinant PDC model as a vehicle for conducting more comprehensive studies of this kind in future. Analysis of such mutant PDCs carrying the appropriate single amino acid substitutions/ deletions within the E2 and E3BP core polypeptides should provide important new insights into the PDC structure, assembly, mode of action and regulation and will be of potential clinical value for the future.

A minor ancillary aim of this thesis also involves preliminary study of subunit interaction/organisation of components OGDC as described in Chapter 5, with a view to mapping the domain organization of E1o more precisely, in particular those regions involved in maintaining critical subunit contacts. This will provide more information on the structural organisation of OGDC and will be a step towards creating a recombinant model of OGDC that is increasingly implicated in various metabolic, genetic and autoimmune disorders.

Chapter 2

Materials and Methods

2.1 Biological materials

2.1.1 Bacterial strains

E. coli strain*s* BL21 (DE3), BL21 (DE3) Star, BL21 (DE3) plysS as well as Top 10 and DH5α were purchased from Invitrogen.

2.1.2 Bacterial media

Luria Broth (LB) was prepared by dissolving 10 g Bacto–tryptone, 5 g Bacto-yeast-extract and 10 g NaCl per litre of distilled H_2O, pH 7.5. LB plates were made by adding 7.5 g of micro agar to 500 ml LB. All media were autoclaved before use. Wherever it was necessary, broth and LB plates were supplemented with ampicillin at 50 µg/ml, kanamycin at 30 µg/ml and chloramphenicol at 34 µg/ml.

2.1.3 Mutagenic primers

The following mutagenic primers were ordered from Sigma Genosys. The mutations created are shown in colour.

Primers for lysine-46 to glutamine mutation in E2-PDC

K46Q forward

5'-GAG ATA GAA ACT GAC CAG GCC ACT ATA GGT TTT TG-3'

K46Q reverse

5'-CAA AAA CCT ATA GTG GCC TGG TCA GTT TCT ATC TC-3'

Primers for lysine-175 to glutamine mutation in E2-PDC

K175Q forward

5'-GAG GTT GAA ACT GAT CAG GCC ACT GTT GGA TTT GAG-3'

K175Q reverse

5'-CTC AAA TCC AAC AGT GGC CTG ATC AGT TTC AAC CTC-3'

Primers for lysine-44 to glutamine mutation in E3BP-PDC

K44Q forward

5'-GAA ATT GAG ACT GAC CAG GCT GTG GTT ACC-3'

K44Q reverse

3'-GGT AAC CAC AGC CTG GTC AGT CTC AAT TTC-5'

Primers for glutamate-35 deletion in E2-PDC

ΔE35 E2 forward

5'-GAG GGG GAC AAA ATC AAT GGT GAC CTA ATT GCA GAG-3'

ΔE35 E2 reverse

5'-CTC TGC AAT TAG GTC ACC ATT GAT TTT GTC CCC CTC-3'

Primers for glutamate-35 to glutamine mutation in E2-PDC

E35Q E2 forward

5'-GAG GGG GAC AAA ATC AAT CAG GGT GAC CTA ATT GCA GAG-3'

E35Q E2 reverse

5'-CTC TGC AAT TAG GTC ACC CTG ATT GAT TTT GTC CCC CTC-3'

Primers for glutamate -35 to aspartate mutation in E2-PDC

E35D E2 forward

5'-GGG GGA CAA AAT CAA TGG TGA CCT AAT TGC AGA G-3'

E35D E2 reverse

5'-CTC TGC AAT TAG GTC ACC ATC ATT GAT TTT GTC CCC-3'

Primers for phenylalanine- 490 to leucine mutation in E2-PDC

P490L E2 forward

5'-GGA ATT AAG AAT TTA TCT GCT ATT ATT AAC CCA CC-3'

P490L E2 reverse

5'-GGT GGG TTA ATA ATA GCA GAT AAA TTC TTA ATT CC-3'

Primers for valine-455 deletion in E2-PDC

ΔV455 E2 forward

5'-GAA ACC ATT GCT AAT GAT GTT TCT TTA GCA ACC AAA GCA AG-3'

ΔV455 E2 reverse

5'-CTT GCT TTG GTT GCT AAA GAA ACA TCA TTA GCA ATG GTT TCC-3'

2.1.4 Oligonucleotide primers

The following oligonucleotide primers were ordered from MWG-Biotech AG. The restriction sites created are shown in colour.

Primers for E1-OGDC construct

OGDE1(Nde1) forward

5'-GCT CAT ATG AGA CCA TTG ACG GCT TCC CAG-3'

OGDE1(Xho1) reverse

5'-AGG CTC GAG CTA CGA GAA GTT CTT GAA GAC G-3'

Primers for N-terminal E1 (166amino acid) GST fusion construct

E1BamH1 forward

5'-CAT TTT CAG GAT CCA GAC CAG CAG CAG CTA GG- 3'

E1500EcoR1 reverse

5'-GCA CTG GAA TTC TCA GAA AGT GGT GGT GGG CAA G-3'

Primers for N-terminal E1 (83 amino acids) GST fusion construct

E1BamH1 forward

5'-CAT TTT CAG GAT CCA GAC CAG CAG CAG CTA GG- 3'

E1250EcoR1 reverse

5'-GAC CAG GAA TTC TCA ATG GGC CAC AGC AGC AGC CAG-3'

All PCR primers were designed to obtain a balanced G:C composition, compatible melting temperatures and contain a GC clamp at the 3' termini. They were screened for internal secondary structures e.g. hairpin loops or possible dimerisation using software available at the Sigma Genosys website (http://orders.sigma-genosys.eu.com/).

2.1.5 Chemicals and standard materials

Ampicillin, kanamycin, chloramphenicol, rubidium chloride, L-glutathione reduced, N-ethylmaleimide (NEM), lipoic acid, lipoamide, L-cysteine, NADPH, NADH, NAD$^+$, CoA, thiamine diphosphate, trypsin, phosphotransacetylase, acetyl phosphate, pepstatin, leupeptin, aprotinin, Ponceau S dye, ethidium bromide and glutaraldehyde were purchased from Sigma.

QIAquick Gel Extraction kit, Penta His-HRP kit and Ni-NTA Agarose were purchased from Qiagen. Quick Ligation Kit was purchased from New England Biolabs. Wizard SV DNA Minipreps Kit, restriction enzymes, *Taq* polymerase, dNTP and 10 kb DNA ladders were from Promega. Quick Change Site-directed Mutagenesis Kits were from Stratagene.

HiPrep 16/60 Sephacryl S-300 High Resolution and Glutathione Sepharose 4B columns, nitrocellulose membrane (ECL Hybond), ECL Western blotting detection reagents, low molecular weight SDS Marker Kits, thrombin, zinc chloride and PD10 columns were

purchased from Amersham. 20 MC metal chelate resin was purchased from Applied Biosystems, USA. Dialysis cassettes of various cut off sizes were obtained from Pierce (USA).

Precast 4-12% Bis-Tris gels and MES SDS Buffer were purchased from Invitrogen. Protease inhibitor EDTA-free and Complete Protease Inhibitor Mini tablets were purchased from Roche. Imidazole was from VWR. Centricon filters with cut off sizes 5, 30, 60 and 100 kDa and N, N, N^{-1} N^{-1}- tetramethylethylene diamine (TEMED) were from Fisher. Acrylamide 30% (w/v) was from Thistle Scientific. Bradford reagent was from BioRad. Bacto-tryptone, Bacto yeast extract, DTT, and IPTG were from Melford Laboratories Ltd. Coomassie Blue dye was obtained from Fluka and sodium borohydride from Aldrich. Monoclonal antibody PD2 (patient derived hybridoma IgG) was a kind gift from Professor Freda Stevenson, University of Southampton.

2.2 Molecular biology methods

2.2.1 Polymerase chain reaction

Polymerase chain reactions were carried out in a PTC 100 ^{TM} thermocycler (Genetic Research Instrumentation). A typical single 100 µl reaction mixture using the Promega PCR kit consisted of the following ingredients-

10x PCR buffer	10.0 µl
dNTP mixture	16.0 µl
5' primer	5.0 µl
3' primer	5.0 µl
Platinum$^{®}$*Taq* DNA polymerase	0.5 µl (2.5 units)
DNA template	50 ng
Sterile water	to a final volume of 100 µl

Platinum® *Taq* DNA Polymerase High Fidelity is an enzyme mixture composed of recombinant *Taq* DNA polymerase, Pyrococcus species derived thermostable polymerase, and Platinum® *Taq* Antibody. Pyrococcus species polymerase possesses a proofreading ability by virtue of its 3' to 5' exonuclease activity. Mixture of the proofreading enzyme with *Taq* DNA polymerase increases fidelity approximately six times over that of *Taq* DNA polymerase alone. Additionally, because a proofreading enzyme is present in the mixture, amplification of simple and complex DNA templates over a large range of target sizes is possible. Targets 12-20 kb can be amplified with some optimization.

One of the most critical factors for successful amplification of DNA is the magnesium ion concentration. Too much $MgCl_2$ will cause high levels of non-specific amplification, whereas too little will inhibit the reaction. Therefore, in this protocol 1.5 mM $MgCl_2$ was used as the final concentration for the *Taq* DNA polymerase. Template was denatured for 5 min at 94 °C prior to the initial cycle. A typical cycling temperature profile was: denaturing at 94 °C for 45 s, annealing at 60 °C for 45 s and extension at 72 °C for 1 min for 25-30 cycles. A 10 min extension at 72 °C was given at the end of each cycle. Annealing temperatures were critical and required experimental optimisation. Low temperature annealing increases non-specific amplification; high temperatures inhibit annealing but may increase specificity. Typical annealing reactions were performed in the range of 55 °C to 65 °C. PCR products were viewed by agarose gel electrophoresis using 1% (w/v) agarose.

2.2.2 Agarose gel electrophoresis

The appropriate amount of agarose was dissolved in 1X TAE (40 mM Tris, 1mM EDTA, 40 mM glacial acetic acid, pH 7.5) for pouring agarose gel slabs. DNA samples for analysis were diluted fivefold by the addition of loading buffer (0.25% (w/v) bromophenol blue, 0.25% (v/v) xylene cyanol FF, 15% (w/v) Ficoll), before being loaded on the agarose gel. These were run at 100 V/250 mA for 40 min to 1 h until the dye front was about 1 cm from the bottom of the gel. Gels were then stained with a small volume of ethidium bromide before being viewed under a UV transilluminator.

2.2.3 Extraction of DNA from agarose gel

DNA was purified from agarose gels using the QIAquick Gel Extraction kit. The DNA was run on the gel and excised using a sterile scalpel blade. The excised agarose containing the DNA was solubilised at 50 ^{o}C in the appropriate buffer and 100% (v/v) isopropanol. This solubilised mixture was applied to a spin column and centrifuged for 1 min to allow the DNA to bind to the column. The column was washed with 750 µl of Wash Buffer containing 80% (v/v) ethanol. Residual ethanol was removed by centrifuging the column for 2 min before eluting the DNA in 50 µl of Buffer EB (10 mM Tris-HCl, pH 8.5). The quantity and quality of DNA was analysed by agarose gel electrophoresis.

2.2.4 Restriction digestion

Restriction digestions were performed either as a step prior to cloning for preparing vector and insert or for diagnostic purposes. Restriction enzymes and buffers from Promega were used as per manufacturer's instructions. Digestions were usually performed at 37 ^{o}C for 60 min and analysed by agarose gel electrophoresis.

2.2.5 Ligation

Vector was cut with appropriate restriction enzymes, treated with calf intestinal phosphatase and gel purified. The insert was ligated into the vectors at a 3:1 insert : vector ratio using the Quick Ligation Kit. The Quick Ligation Kit enables ligation of cohesive end or blunt end DNA fragments in 5 min at room temperature (25 °C). Products were

transformed into chemically competent *E. coli* DH5α cells and grown overnight on LB-ampicillin plates at 37 °C.

2.2.6 Ethanol precipitation of DNA

Before sending DNA for sequencing, ethanol precipitation was carried out. A solution of 3 M sodium acetate (50 μl) was added to about 50 μl DNA suspension and left on ice for 30 min in an Eppendorf tube. Thereafter, it was centrifuged at 13,000 rpm for 15 min. The supernatant was discarded and 250 μl of ice cold 70% (v/v) ethanol was added before centrifuging it again for 15 min. After again discarding the supernatant, tubes were left to air dry for 20-30 min.

2.2.7 DNA sequencing

Ethanol precipitated DNA samples were sent for sequencing, which was carried out by MWG Biotech. The sequencing results were read and analysed by Gene-Jockey software.

2.2.8 Production of competent cells

Competent cells were made using the rubidium chloride method. The appropriate *E. coli* strains were streaked on a LB-agar plate and grown overnight at 37 ^{o}C. A single colony was picked and cultured overnight in 5 ml LB. This 5 ml culture was subcultured into 100 ml LB and grown at 37 ^{o}C with continuous shaking until an optical density at 550 nm of 0.50 was obtained. The culture was chilled on ice for 5 min and then spun at 2000 -3000

rpm in an Allegra^{Tm} 6R centrifuge at 4 ^{o}C in 50 ml sterile Falcon tubes. The supernatant was poured off and each pellet was resuspended gently by pipetting in 20 ml buffer 1 (30 mM potassium acetate pH 5.8, 100 mM rubidium chloride, 10 mM calcium chloride, 50 mM manganese chloride and 15% (v/v) glycerol). The solution was re-spun in the same manner as before and the supernatant discarded. The pellet was resuspended in 2 ml buffer 2 (10 mM MOPS, pH 6.5, 75 mM calcium chloride, 10 mM rubidium chloride and 15% (v/v) glycerol) by gentle pipetting and chilled on ice for 15 min before storing in 200 μl aliquots. Competent cells were stored at -80 ^{o}C until required.

2.2.9 Transformation of competent bacteria

Competent cells were thawed on ice. To 50 μl of competent bacteria, 1 μl DNA (about 0.1-50 ng) was added. The bacterial cells were chilled on ice for 15 min. Cells were then heat shocked for 90 s at 45 ^{o}C and then returned to ice for 2 min. To these cells, 450 μl LB media was added and this bacterial cell suspension was incubated at 37 ^{o}C for 45 min with continuous shaking. About 200 μl of suspension was plated on a LB plate containing the appropriate antibiotic and incubated overnight at 37 ^{o}C.

2.2.10 Purification of DNA from bacterial cultures (Miniprep)

DNA was purified using the Wizard SV DNA Miniprep kit. The kit was used as per manufacturer's instructions. A single colony grown on a LB plate was picked and cultured in 5 ml LB medium containing the same antibiotic. The culture was incubated at 37 ^{o}C overnight with continuous shaking and cells pelleted by centrifuging at 10,000 rpm for 5 min in an Allegra^{Tm} 6R centrifuge. The pellet was re-suspended in 250 μl Cell Re-suspension solution (50 mM Tris-HCl, pH 7.8, 10 mM EDTA, 100 μg /ml RNAse A). Cells were lysed by the addition of 250 μl of Cell Lysis Solution (0.2 M NaOH, 1% (w/v) SDS) and incubated for 5 min in the presence of 250 μg alkaline protease to inactivate any

endonucleases released during cell lysis. Cell Neutralising Buffer 350 µl (4.09 M GdmCl, 0.759 M potassium acetate, 2.12 M acetic acid) was added and the mixture was centrifuged at 10,000 rpm for 10 min in a Sanyo Microcentaur benchtop centrifuge to pellet the cell debris. The supernatant was poured into a spin column and centrifuged briefly to allow the DNA to bind to the membrane of the spin column. The column was washed twice with Column Wash Solution (60 mM potassium acetate, 10 mM Tris-HCl, pH 7.8, 60% (v/v) ethanol) prior to elution of the DNA with 100 µl nuclease free water. The quality of the DNA was analysed by agarose gel electrophoresis.

2.2.11 Site-directed mutagenesis

The QuikChange Site-directed mutagenesis kit was employed to make point mutations using *PfuTurbo*DNA polymerase. The DNA template in which mutations were to be created, was prepared by the standard Miniprep protocol. For the PCR reaction, the mixture consisted of 5 µl 10x reaction buffer, 50 ng double stranded DNA template, 125 ng each of forward and reverse primers, 1 µl of dNTP mix and double distilled water to make a final volume of 50 µl. Cycling parameters were as follows: initial denaturing at 95 °C for 1 min, followed by 12-18 cycles involving 95 °C for 1 min, annealing at 50-60 °C for 1 min and extension at 65 °C for 1-2 minutes/kb of plasmid length. PCR was carried out in a PTC 100 ^{TM} Programmable Thermal Controller. Following temperature cycling, the product was treated with 10 U/µl *Dpn* I. The *Dpn* I endonuclease is specific for methylated and hemimethylated DNA and is used to digest the parental DNA template and to select for mutation-containing, newly-synthesized DNA. DNA isolated from almost all *E. coli* strains is dam methylated and therefore susceptible to *Dpn* I digestion. Dam methylation is the addition of a methyl group to adenine in the sequence 5'-GATC-3' in newly-synthesized DNA. The nicked vector DNA containing the desired mutations was then transformed into XL1-Blue supercompetent cells. Cells were heat pulsed for 45 s at 42 °C followed by returning to ice for 2 min. LB media (0.5 ml) was added to the transformation reaction and incubated at 37 °C for 1 h with shaking at 225-250 rpm. About 100-200 µl incubated reaction mixture was plated on LB plates containing ampicillin. Plates were incubated at 37 °C for 16 h. Colonies were picked and grown in LB media

containing ampicillin overnight at 37 °C. Next day, plasmids were purified from these cultures and sent for sequence analysis to enable detection of the desired mutation.

2.3 Protein methods

2.3.1 Large-scale protein induction

A single colony was picked and added to 15 ml of LB medium containing the appropriate antibiotic. Cells were grown at 37 °C overnight with continuous shaking. At this stage, 500 ml LB supplemented with antibiotic was inoculated with 10-15 ml overnight culture and grown at 37 °C with constant shaking until an A_{600} of 0.5 was reached. For small-scale induction 100 ml LB was inoculated with 1-5 ml overnight culture. The cultures were induced by the addition of 1 mM IPTG. For overexpression of E2-PDC, E3BP or OGDC proteins, 0.1 mM lipoic acid was also added to the medium. Individual cultures were shaken at 200-220 rpm at various temperatures ranging from 16-37 °C for different lengths of times as required. Samples (1 ml) were taken at regular time intervals to check for overexpression. These were pelleted by centrifugation and the pellets resuspended in Laemmli sample buffer (10 µl per 0.1 A_{600} unit) and viewed by SDS-PAGE as described in section 2.3.4. Cells were harvested by centrifugation at 10,000 rpm for 10-15 min at 4°C in a JA14 rotor in a Beckman J2-21 centrifuge and pellets stored at –20 °C.

2.3.2 French press treatment

E. coli pellets from 500 ml cultures were mixed with 20 ml of appropriate binding buffer (50 mM KH_2PO_4, 1M NaCl, 0.5 mM Imidazole, pH 8) or PBS (170 mM NaCl, 3 mM KCl, 10 mM Na_2HPO_4, 1 mM KH_2PO_4, pH 7.2). Protease inhibitor cocktail tablets were added at this point. Cells were disrupted by 3-4 passes through a French pressure cell at 950 psi.

The disrupted cells were spun at 10,000 rpm at 4 °C for 10 min and the supernatant containing soluble protein was kept for protein purification.

2.3.3 Checking the solubility of recombinant proteins

Overexpression cultures (50 ml) were centrifuged at 3,000 rpm for 15 min at 4 °C. The supernatant was discarded and pellets re-suspended in 3 ml binding buffer prior to French press treatment. An aliquot (100 μl) was kept aside for SDS-PAGE for analysing whole cell extracts. An aliquot (100 μl) of the disrupted cell extract was centrifuged at 4 °C at 13,000 rpm in a Sanyo Microcentaur benchtop centrifuge and the supernatant was saved while the pellet was re-suspended and washed with PBS buffer 3 times; each time the supernatant was discarded and replaced with fresh PBS buffer. Finally the pellet was suspended in binding buffer (100 μl) and the suspension saved for a pellet sample. An equal volume of Laemmli sample buffer was mixed with the whole cell extract, supernatant fraction and pellet suspension and the solubility of the recombinant protein reviewed by SDS-PAGE.

2.3.4 Sodium dodecyl sulphate polyacrylamide gel electrophoresis (SDS-PAGE)

Sodium dodecyl sulphate (SDS) is an anionic detergent that denatures proteins and confers a net negative charge. In denaturing SDS-PAGE, separation of proteins is based not on the intrinsic electrical charge of the polypeptide but on molecular weight. The following buffers were prepared for making SDS gels: -

SDS-PAGE buffers

Resolving gel :   8-15% (w/v) acrylamide,

0.5 M Tris-HCl buffer, pH 8.8

0.1% (w/v) SDS

0.1% (w/v) ammonium persulphate

0.1% (v/v) N,N,N^{-1} N^{-1}- tetramethylethylene diamine (TEMED)

Stacking gel :   5.4% (w/v) acrylamide

0.06 M Tris-HCl buffer, pH 6.8

0.1% (w/v) SDS

0.1% (w/v) ammonium persulphate

0.1 % (v/v) TEMED

SDS buffer   0.025 mM Tris-HCl buffer, pH 8.3

0.2 M glycine

1% (w/v) SDS

Laemmli sample buffer   2% (w/v) SDS

10% (w/v) sucrose

62.5 mM Tris-HCl, pH 6.8

Pyronin Y dye (trace).

Samples for SDS-PAGE were suspended in 10 μl Laemmli sample buffer and DTT (150 mM final concentration) was added prior to boiling for 5 min to ensure that all proteins were denatured. The denatured protein samples were loaded either onto precast 4-12% Bis-Tris gels using ready-made MES SDS buffer (1M MES, 1M Tris base, 69.3 mM SDS, 20.5 mM EDTA, free acid, pH 7.5) and run at a constant current of 125 mA per gel. Alternatively, the gels were made with a 4% stacking gel and 10-15% resolving gel, the composition of which is described above. SDS buffer (as above) was employed as running buffer at a constant current of 125 mA per gel. Proteins were stained with 0.1% (w/v) Coomassie Brilliant blue dye dissolved in 50% (v/v) methanol, 10% (v/v) acetic acid for 30 min with shaking. Protein bands were visualised by destaining the gels in 10% (v/v) methanol and 10% (v/v) acetic acid overnight.

2.3.5 Non denaturing gel electrophoresis

Non denaturing or native gels were prepared to separate proteins based on their size and charge. A native gel comprised both a stacking gel and a resolving gel. For preparing these gels, separating buffer (1.5 M Tris-HCl, pH 8.8) and stacking buffer (0.05 M Tris, pH 6.8) were prepared initially.

For a 6% resolving gel, 2 ml 30% (w/v) acrylamide, 2.5 ml separating buffer, 2 ml distilled water, 50 μl 10% (w/v) ammonium sulphate and 8 μl TEMED were mixed together. The mixture was poured into a glass plate sandwich and allowed to polymerise. A space (approx 0.5 cm) on the top of the sandwich was left for the stacking gel but was first filled

with dH$_2$O. For preparing the 5% stacking gel, 2.3 ml water, 0.67 ml 30% (w/v) acrylamide, 1 ml stacking buffer, 30 μl of 10% (w/v) ammonium persulphate and 7 μl TEMED were mixed. When the resolving gel was fully polymerised, the water on its top was discarded and stacking gel mixture was poured onto it. A comb was inserted into this mixture to make wells for protein samples. Stacking gel was allowed to polymerise and the comb was removed when polymerisation was complete. After securing the gel in the electrophoresis tank, electrophoresis buffer (25 mM Tris, 192 mM glycine; pH 8.8) was poured into the chamber. Protein samples (10-20 μl) were first suspended in sample buffer (312.5 mM Tris-HCl, pH 6.8, 50% (v/v) glycerol, 0.05% (w/v) bromophenol blue and 1.4 ml water) before loading into wells. Unused wells were also filled with sample buffer. Electrophoresis was carried out at 100-200 volts at constant current until the dye front migrated to the bottom of the gel. The gels were removed and viewed after staining with Coomassie Brilliant blue dye.

2.3.6 Purification of His-tagged proteins

Buffers for purification of His-tagged proteins by affinity chromatography-

Stripping buffer   50 mM EDTA, 1M NaCl

Zinc Loading buffer   0.1 M ZnCl$_2$, pH 4.5

Salt Wash buffer   0.5 M NaCl

Buffer A   50 mM KH$_2$PO$_4$, 1 M NaCl, 0.5 mM imidazole; pH 8

Buffer B   50 mM KH$_2$KPO$_4$, 1M NaCl, 500 mM imidazole; pH 6

All buffers were filtered through Whatman filters of pore size 2 μm using a vacuum pump and stored at 4 $^{\circ}$C. Distilled water was also filtered. His-tagged proteins were purified using metal chelate affinity chromatography on a BioCAD Sprint workstation (Applied Biosystems, USA). A 20 MC column (Applied Biosystems) was washed initially with 5 column volume (CV) of stripping buffer to remove any remaining metal ions from

previous use. This was followed by a wash with 5 CV of dH$_2$O. Zinc ions were loaded on to the column matrix by passing 30 CV of Zinc Loading buffer prior to a wash with 5 CV of dH$_2$O. Unbound zinc ions were removed with a 5 CV wash of Salt Wash buffer and the column was equilibrated with 5 CV of buffer B followed by 10 CV of buffer A. Samples were injected in 5 ml aliquots and washed through with 3 CV of buffer A. After the final injection, the column was washed with 9 CV of buffer A. Finally, the His-tagged protein was eluted from the column employing a 0-100% gradient of buffer B and the eluate collected in 2 ml fractions.

2.3.7 Ni-NTA affinity purification

The E1 enzyme of PDC was purified using nickel nitrilo-triacetic acid (Ni-NTA) resin. The following buffers were prepared for Ni-NTA affinity purification.

E1 Lysis buffer

50 mM KH$_2$PO$_4$, pH 7.

 0.2 mM MgCl$_2$

0.2 mM thiamine diphosphate

5 mM β-mercaptoethanol

E1 Buffer A

50 mM KH$_2$PO$_4$, pH 7.5

100 mM KCl

0.2 mM MgCl$_2$

0.2 mM thiamine diphosphate

E1 Imidazole Wash buffer

50 mM KH_2PO_4, pH 7.5

100 mM KCl

0.2 mM $MgCl_2$

0.2 mM thiamine diphosphate

50 mM imidazole

E1 Buffer B

50 mM KH_2PO_4, pH 7.5

100 mM KCl

0.2 mM $MgCl_2$

0.2 mM thiamine diphosphate

500 mM imidazole

Four pellets, each from a 500 ml culture, were suspended in 25 ml E1 Lysis buffer containing four tablets of Complete protease inhibitor cocktail (EDTA-free) and disrupted by French press treatment (section 2.3.2). The lysate was spun for 20 min at 10,000 rpm in a Beckman J2-21 centrifuge using a JA-17 rotor and the supernatant collected in a fresh tube. Ni-NTA resin (1 ml) contained in ethanol was added to a second Falcon tube and left to settle. The resin supernatant was sucked out with a pipette and the resin washed with E1 Buffer A. Washed resin was then mixed with the lysate supernatant with gentle rotation for 1 h at room temperature. The supernatant and resin mix was poured into an empty PD-10 column. The resin was washed with 200 ml E1 Buffer A and then with 50 ml of E1 Imidazole Wash buffer. The protein was eluted with 1 ml E1 buffer B in three separate 1 ml elutions. Aliquots of eluted fractions were checked for purity by analysing on SDS-PAGE.

2.3.8 Dialysis of proteins

In order to exchange buffers, proteins were dialysed in 4-5 l of the buffer of choice overnight at 4 ^{o}C. Dialysis was usually conducted according to manufacturer's instructions in dialysis cassettes.

2.3.9 Concentration of proteins

Proteins were concentrated by centrifuging the samples in a Centricon concentrator with a specific molecular weight 'cut off' depending on the protein under investigation. Samples were centrifuged at a speed of 3000 rpm in an Allegra ^{Tm} 6R centrifuge for various times until the desired volume was achieved.

2.3.10 Determination of protein concentration

Dividing the measured absorbance of a protein solution by the calculated or known molar extinction coefficient (ε) yields the molar concentration of the protein. The absorbance of various proteins was measured using an Ultospec 4300 Pro uv/visible spectrophotometer, whereas, the molar extinction coefficient was determined by analysing the known sequence of the protein in PROTPRAM (http://expasy.org/tools/protparam.html). The extinction coefficient for the 60: 12 meric E2:E3BP was calculated as 217,590 M^{-1} cm^{-1} at 280 nm. The extinction coefficient for the outer lipoyl domain protein was determined as 50,450 M^{-1} cm^{-1} at 280 nm, while the extinction coefficient for the E3 dimer was calculated as 22600 M^{-1} cm^{-1}, exploiting FAD absorbance at 450 nm. Similarly, for E1 an extinction coefficient

at 280 nm was determined as 140,000 M^{-1} cm^{-1}. The concentration (in mg/ml) was calculated by multiplying the molar concentration by the respective molecular weight of the protein.

2.3.11 Measuring protein concentration using the Bradford assay

Bio-Rad assays were also performed to determine protein concentration on occasions and to ensure equal loading of wild-type and mutant versions of the same protein. The dye Coomassie Brilliant Blue G-250 is converted from red to blue upon protein binding followed by an increase in absorption at 595 nm. A standard curve was plotted using known concentrations of IgG versus A_{595} values of IgG bound to this dye. The concentrations of unknown protein bound to dye were thereafter calculated using this standard curve. A Shimadzu UV-2101 PC UV-VIS scanning spectrophotometer was used for these determinations.

2.3.12 Size exclusion chromatography

Size exclusion chromatography was performed using a HiPrep 16/60 Sephacryl S-300 High Resolution column (bed volume 120 ml) attached to a BioCAD 700E workstation. The column was equilibrated with 2 CV of gel filtration buffer (50 mM potassium phosphate, 150 mM NaCl; pH 7.5) at a flow rate of 0.5 ml/minute. A concentrated protein sample (1 ml) was loaded onto the column and absorbance was monitored at 280 nm. Peak fractions were collected and analysed by SDS-PAGE. An estimate of the molecular mass of protein was carried out from a standard curve generated by plotting the ratio of elution volume to void volume (Ve/Vo) versus $\log_{10}$ molecular mass of a range of standard proteins of known sizes (Fig. 4.16 A; Chapter 4).

2.3.13 Purification of glutathione S-transferase (GST) tagged proteins

The following buffers were prepared for the purification of GST tagged proteins:-

PBS buffer - 170 mM NaCl, 3 mM KCl, 10 mM Na_2HPO_4, 1 mM KH_2PO_4, pH 7.2

Glutathione elution buffer - 50 mM Tris-HCl buffer, pH 8.0, 10 mM reduced

glutathione.

GST-fusion proteins were produced in 500 ml LB cultures for 3-5 h and the *E. coli* pelleted by centrifugation. The bacterial pellet from 250 ml culture medium was resuspended in 10 ml PBS buffer. One tablet of Protease inhibitor (EDTA free) was added to 10 ml suspension followed by disruption using French press treatment. The crude extract was centrifuged at 10,000 rpm at 4 ^{o}C in a Beckman J2-21 centrifuge using a JA17 rotor. The soluble supernatant fraction was used for further purification. A glutathione Sepharose 4B column with bed volume 5 ml, attached to BioCAD Sprint workstation was washed with 5 CV of PBS. The supernatant was passed through the column followed by 5 CV washes of PBS. The bound protein was eluted in glutathione buffer and collected in 2 ml fractions. The fractions were concentrated and visualised by SDS–PAGE after staining with Coomassie Brilliant blue.

2.3.14 Removal of GST tag

Purified GST-tagged proteins were dialysed against either PBS or 50 mM Tris buffer, pH 7.5. Thrombin was added at 100 U/ mg protein and incubated with gentle shaking either at room temperature or at 37 °C for 4-16 h. Cleavage of the GST-tag was viewed by taking samples at 2 h time intervals and visualising by SDS-PAGE.

2.3.15 Western Blotting

Proteins were separated by SDS-PAGE and electrophoretically transferred onto nitrocellulose membrane (ECL Hybond, Amersham) at 425 mA for 45 min in the presence of transfer buffer (25 mM Tris-HCl buffer, pH 7.2, 192 mM glycine, 0.02% (w/v) SDS, 20% (v/v) methanol). The nitrocellulose membrane was briefly checked for the presence of transferred proteins by staining with Ponceau S solution. This was followed by shaking for 1 min and washing with dH_2O. Excess binding sites were blocked by immersing the nitrocellulose membrane in blocking solution (20 mM Tris-HCl buffer, pH 7.2, 15 mM NaCl, 5% (w/v) milk powder, 0.25% (v/v) Tween-20) for 1 h at room temperature with constant shaking. The membrane was washed twice with wash solution (20 mM Tris-HCl buffer, pH 7.2, 15 mM NaCl, 1% (w/v) milk powder, 1% (v/v) Tween-20), each for 10 min. After these washes, the membrane was incubated in primary antibody solution (20 mM Tris-HCl buffer, pH 7.2, 15 mM NaCl, 5% (w/v) milk powder, 0.25% (v/v) Tween-20 and a 1:2500 dilution of primary antibody) at room temperature for 1 h. Excess primary antibody was removed by 4 changes of wash solution and membrane was again incubated at room temperature in secondary antibody solution (20 mM Tris-HCl buffer, pH 7.2, 15 mM NaCl, 5% (w/v) milk powder, 0.25 (v/v) Tween-20 and a 1:1000 dilution of secondary antibody conjugated with horseradish peroxidase). In the case of anti-His tag antibody, the primary antibody was already conjugated with horseradish peroxidase; therefore no secondary antibody was required.

The membrane was then washed for 15 min with wash solution followed by a 30 min wash in high salt solution (20 mM Tris-HCl buffer, pH 7.2; 150 mM NaCl). Detection of immune complex was carried out according to the manufacturer's instructions employing the ECL Western blotting reagents.

2.3.16 Dihydrolipoamide acetyltransferase (E2) assay

E2 activity was measured by monitoring the formation of acetyldihydrolipoamide at 232 nm (Yang et al., 1997).

The following stock buffers and chemicals were prepared for dihydrolipoamide acetyltransferase assay:

1 M Tris-HCl, pH 7.4

100 mM acetyl phosphate

1 mM CoA

1 mM Dihydrolipoamide

Preparation of dihydrolipoamide (DHL): For preparing dihydrolipoamide**,** lipoamide (DL-6,8-thioctic acid amide) (1 g) was dissolved in 25 ml 80% (v/v) methanol and cooled on ice. Sodium borohydride (1 g) was dissolved in 5 ml distilled H_2O and also cooled on ice before adding to the lipoamide solution while stirring on ice. At this stage the mixture was removed from ice, stirred for a further 20 min at room temperature and the pH adjusted to 2.0 with 0.25 M HCl. DHL was extracted from the solution by mixing thoroughly with 50 ml chloroform. The mixture was allowed to settle into two phases; the bottom organic phase was decanted into another flask and the chloroform extraction process was repeated 4 times. Chloroform was removed by evaporation using a rotary evaporator. The resulting precipitate was dissolved in a 2.5: 1.0 ratio of toluene and heptane and heated to ensure complete re-suspension. The mixture was dried until a small volume was left using a rotary evaporator. This was further dried until a white precipitate of DHL formed. The precipitate was stored at -20 ^{o}C. The quality of the DHL was checked by assaying E3 activity with increasing amounts of DHL, dissolved in 100% ethanol at a concentration of 20 mg/ml (100 mM) until no further increase in the activity was recorded.

The assay was performed at 30 $^{\circ}$C in a total reaction volume of 1 ml in a quartz cuvette containing 30 mM Tris-HCl, pH 7.4, 1 mM DHL, 1 mM acetyl phosphate, 20 μM CoA and 2U phosphotransacetylase. A baseline was established before E2 samples were added. The change in absorbance was measured over 45 s using a Shimadzu UV-2101 UV-VIS scanning spectrophotometer and recorded as ΔA_{232} min^{-1}. E2 activity is expressed as change in absorbance/min since the extinction coefficient of the immediate product, 8-acetyldihydrolipoamide has not been determined accurately.

2.3.17 PDC assay

Enzymatic activity of PDC was determined by monitoring production of NADH at 340 nm (Brown and Perham, 1976). For enzymatic assays of recombinant and native PDC, the following solutions were prepared:-

Solution A

3 mM NAD$^{+,}$

2 mM MgCl$_2$. 6H$_2$O,

0.2 mM ThDP

All the above ingredients were dissolved in approx. 5 ml of 1 M KPi buffer, pH 7.6. After dissolving, 70 ml of water was added. The pH of the solution was adjusted to 7.6 with KOH and the volume was finally adjusted to 100 ml with dH$_2$O.

Solution B

0.13 M Cysteine   HCl

6.8 mM CoASH (tri-lithium salt)

The above ingredients were dissolved in 20 ml dH$_2$O.

Solution C

Pyruvate (100 mM) was dissolved in dH_2O.

For enzymatic assay of PDC, 670 µl of solution A and 14 µl of solution B were added to plastic cuvette at 30 °C. To this 14 µl of solution C was added immediately prior to adding 10-50 µl purified PDC. The solution was mixed rapidly and the change in absorbance at 340 nm ($\Delta A_{340\,nm}$) was monitored over the first 90 s.

2.3.18 Structure prediction by Swiss modelling

A preliminary structure of the E2 outer lipoyl domain and its mutant version was determined based on sequence homology to other resolved protein structures in the Protein DATA Bank using SWISS MODEL (Schwede et al., 2003). Then a model of the domain was generated using RASMOL 2.6.

2.3.19 Analytical Centrifugation

2.3.19.1 Calculation of buffer densities and viscosities

Buffer densities and viscosities were calculated from the buffer composition using the computer program SEDNTERP (Laue et al., 1992).

2.3.19.2 Sedimentation velocity

Sample optical density was in the range of 0.1 to 1. Protein samples (380 µl) each present in gel filtration buffer (50 mM potassium phosphate, 150 mM NaCl, pH 7.5) were loaded into 12 mm path length, charcoal-filled, epon double sector centrepieces. A high speed of 20k rpm was used to cause rapid sedimentation of solute towards the bottom of the cell.

This high speed produces a depletion of solute near the meniscus and formation of a sharp boundary between the depleted region and the uniform concentration of sedimenting solute (the plateau) (Fig. 2.1). The rate of movement of this boundary was measured leading to the determination of sedimentation coefficients that depend directly on the mass of the particles and inversely on the frictional coefficients, which is in turn a measure of effective size. A series of scans was collected using interference optics. The data were analysed using the computer program SEDFIT (Schuck, 2000; Schuck et al., 2002) and sedimentation coefficients determined.

2.3.20 Circular dichroism (CD)

Circular dichroism spectroscopy measures differences in the absorption of left-handed polarized light versus right-handed polarized light which arise due to structural asymmetry. For CD studies, proteins were dialysed against 50 mM K_2HPO_4 buffer, pH 7.5. Circular dichroism experiments were performed at room temperature on a Jasco J-810 spectropolarimeter scanning the spectra in the far and near uv regions. All circular dichroism experiments were performed in collaboration with Dr. S. Kelly IBLS, University of Glasgow.

2.2.21 Tryptophan fluorescence

Tryptophan fluorescence is widely used as a tool to monitor changes in protein structure and to make inferences regarding local structure and dynamics. Protein samples in 50 mM K_2HPO_4 buffer, pH 7.5 were excited at 295 nm and fluorescence emission spectra were recorded at 320-350 nm in a Perkin Elmer LS 50B spectrophotometer. All tryptophan fluorescence experiments were carried out in collaboration with Dr. S. Kelly IBLS, University of Glasgow.
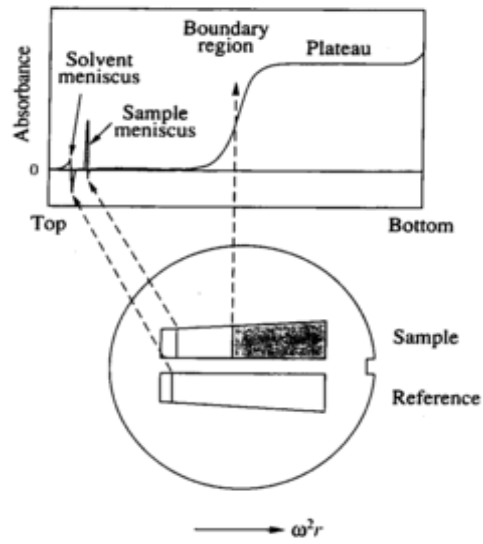
Figure 2.1: Schematic representation of sedimentation of solute in a sedimentation velocity experiment

Chapter 3

Production and assessment of a recombinant human PDC model system

3.1 Introduction

The pyruvate dehydrogenase complex (PDC) is a nuclear-encoded, mitochondrial multienzyme assembly that provides the primary link between glycolysis and the TCA cycle by catalysing the irreversible conversion of pyruvate to acetyl-CoA. Human PDC is composed of multiple copies of three distinct enzymes E1, E2 and E3 and another structural protein termed E3BP. Inborn errors of PDC were initially described about 35 years ago and are the most common cause of congenital lactic acidosis.

Over 200 naturally-occurring mutations in this complex have been identified in the human population at the genetic level. More than 90% of the cases of PDC deficiency involve defects in the E1 enzyme. There have been a small number of deficiencies involving E2 and E3. In addition, there have been reports of both E3BP and E1 phosphatase defects (Patel et al., 1992). Clinical presentation of these mutations is highly variable ranging from mild lactic acidosis and muscular weakness to severe developmental and neurodegenerative conditions. In most of the cases, mutational analysis is not sufficient to

explain the clinical heterogeneity of the PDC deficiency. The clinical investigation of specific enzymatic and regulatory defects in PDC is limited largely because the main clinical symptom namely, lactic acidosis, is common to many other mitochondrial disorders. Analysing mutations using human tissues also poses many challenges; lack of access to tissues from individual patients being the main problem owing to the practical and ethical issues involved.

Analysis of these pathological mutations becomes even more important as no systematic therapeutic approaches are available for treating PDC deficiency. Alternative strategies have been utilized to treat the major symptoms but unfortunately, none of the approaches have been tested in a systematic fashion and there is no clear evidence of any universally effective therapy. Early interventions included vitamin supplementation and dietary manipulation such as ketogenic diets to provide an alternative source of acetyl–CoA. These therapies do lower the blood lactate, but do not dramatically improve neurological function. With the characterisation of PDC deficiency at a molecular level, its pathophysiology should become clearer and it should also be possible to evaluate different therapeutic approaches more effectively.

The aim of this study was to produce a recombinant model PDC by overexpressing its constituent enzymes in *E. coli* followed by purification and reconstitution *in vitro.* This could then be used subsequently to conduct detailed analysis of naturally occurring mutations of particular interest in human PDC. For assembly of recombinant PDC, all the human clones of PDC subunits were already available in the laboratory. Each of the individual enzymes i.e. E1, E2:E3BP and E3 were also His-tagged permitting rapid metal-based affinity chromatography, leading to high yields and routine rapid purification of fully-active enzymes. As the His-tag is a small peptide it normally does not affect the folding and function of proteins. Protease cleavage is, therefore, usually not necessary before reconstitution, although it is an option with most modern vectors that normally have a specific protease cleavage site engineered into the plasmid. Moreover, this system allows anchorage of the protein to resins that have a high binding capacity and also permits the study of interactions between proteins in which one of the potential partners is not tagged.

Another major aim of this study was to test the validity and effectiveness of the recombinant PDC model to conduct in depth analyses of genetic defects in PDC encountered in the human population. Once this ability could be verified successfully, it was anticipated that it would be possible to carry out comprehensive evaluation of the

underlying molecular basis of PDC malfunction in specific cases of interest. This would be invaluable in relating patient symptoms to the effects of specific mutations and in developing improved therapies and treatment protocols in future for recently detected mutations. Thus, reconstituted recombinant PDC should provide us with an ideal biological tool to mimic many natural mutations and correlate their effects on function/assembly with patient symptoms.

Before the advent of recombinant DNA technology, it was necessary to rely entirely on extraction of proteins and enzymes from natural sources, which was often laborious and time consuming. It was usually impossible to procure mutant protein samples in the case of genetic diseases owing to lack of access to patient tissue. Use of the recombinant model to study these defects overcomes many of these challenges and is a non invasive and efficient method for obtaining mutant enzymes for further analysis. Human growth hormone, human insulin, follicle stimulating hormone are some of the human recombinants that have replaced the original enzymes harvested from animal and human tissues. In addition, there are others like erythropoietin granulocyte colony stimulating hormone, alpha-glactosidase and alpha-L-iduronidase that are readily available only in recombinant form. Development of a functional recombinant PDC, a massive molecular machine, that is implicated in various genetic, metabolic and autoimmune diseases like PDC deficiency, diabetes, Alzheimer's disease and primary biliary cirrhosis represents the largest recombinant multienzyme system produced to date in *E. coli*.

Although genetic defects in PDC are considered to be rare, their frequency of occurrence is difficult to estimate owing to the diverse and non-specific pattern of clinical presentation. In particular the most common manifestation, the presence of metabolic lactic acidosis to varying degrees can be attributed to a wide range of metabolic disorders and is a sign of mitochondrial dysfunction in general. It is now clear that its frequency has been underestimated in the past and more patients are being diagnosed with PDC deficiencies than ever before. In this study, the effects of 3 rare, recently-discovered mutations in the E2 enzyme on overall complex function and assembly are investigated with a view to obtain a more detailed understanding of its catalytic mechanism, regulation and mode of assembly (see Chapter 4).

Before carrying out such an investigation and to gain experience in developing and handling this reconstituted PDC model system, it was important to test the ability of the recombinant model in terms of mimicking such mutations. Therefore, it was decided initially to test the overall properties of reconstituted wild-type and mutant PDCs carrying all possible combinations of active and inactive lipoyl domains and also PDC totally lacking the E3BP subunit. This chapter describes reconstitution of recombinant PDC from overexpressed and purified E2:E3BP, E1 and E3 and various experiments performed to test the validity of this recombinant PDC model. Initially wild-type recombinant PDC and PDC lacking E3BP were reconstituted and the effects of adding increased amounts of E3 on the overall complex activity were investigated. Mutant PDCs lacking the full complement of active lipoyl domains were also generated and a comprehensive evaluation carried out on the effect of reduced lipoylation on overall complex activity. In the last section, recombinant wild-type PDC and PDC lacking E3BP have been used to determine a possible role for E3BP subunit in the so-called diacetylation reaction that is a unique characteristic of mammalian and yeast PDCs. These experiments not only validated the usefulness of the recombinant PDC model for subsequent analysis of natural mutations but also generated interesting additional data on structure-function relationships at the molecular level.

3.2 Post-translational mixing of E2 and E3BP

Initial experiments revealed that successful production of functional E2:E3BP core required co-expression of E2 and E3BP. Thus these two components that are tightly integrated into the 'core' assembly do not co-associate if mixed post-translationally. In this study, E2 in pET-11b (without His-tag) and E3BP in pET-28b (with His-tag) were expressed separately in *E. coli* BL21 (DE3) Star cells at 30 ℃ for 5 h. After individual expression, bacterial pellets were disrupted by French press treatment (see section 2.3.2) and mixed together. The mixed supernatant of both cultures was subjected to zinc chelate chromatography (see section 2.3.6). It was observed that only His-tagged E3BP could be purified and E2 failed to associate with it post-translationally (Fig. 3.1) and came out in the 'flow through' (data not shown). This was in contrast to a similar purification (see section 3.3) in which co-transformed E2 and E3BP in the same bacterial host cells were found to

co-integrate successfully into a purified oligomeric E2:E3BP assembly. In addition, it was found that protein E3BP that has a marked tendency to precipitate when purified alone did not precipitate in the latter case, presumably as a direct result of its integration into the oligomeric E2 core.

3. 3 Overexpression of E2 and E3BP

E. coli BL21 (DE3) Star cells were transformed with two separate plasmids, pET-11b and pET-28b housing E2 and E3BP respectively to obtain a functional 60-meric:12-meric E2:E3BP core, using double antibiotic selection with ampicillin and kanamycin. Successful overexpression was achieved (Fig. 3.2) after induction with 1 mM isopropyl β-thiogalactopyranoside (IPTG). Overexpressions were originally carried out in *E. coli* BL21 (DE3), BL21 (DE3) plysS, and BL21 (DE3) Star strains as described in Methods section 2.3.1 and the latter found to be the most effective. In this expression system, only E3BP contained a His-tag and its expression was limiting to 'core' assembly so that only assembled E2:E3BP 'core' was purified with E2 being present by virtue of its stable association with His-tagged E3BP. E3BP has been shown to be tightly associated with the E2 core assembly and in contrast to E1 and E3, cannot be dissociated even by treatment with high salt or high pH. Chaotrophic agents such as *p*-hydroxymercuriphenylsulfonate or 5 M urea are required to dissociate E3BP from the E2 core (De Marcucci and Lindsay, 1985); however, such treatment also promotes general dissociation of the core assembly
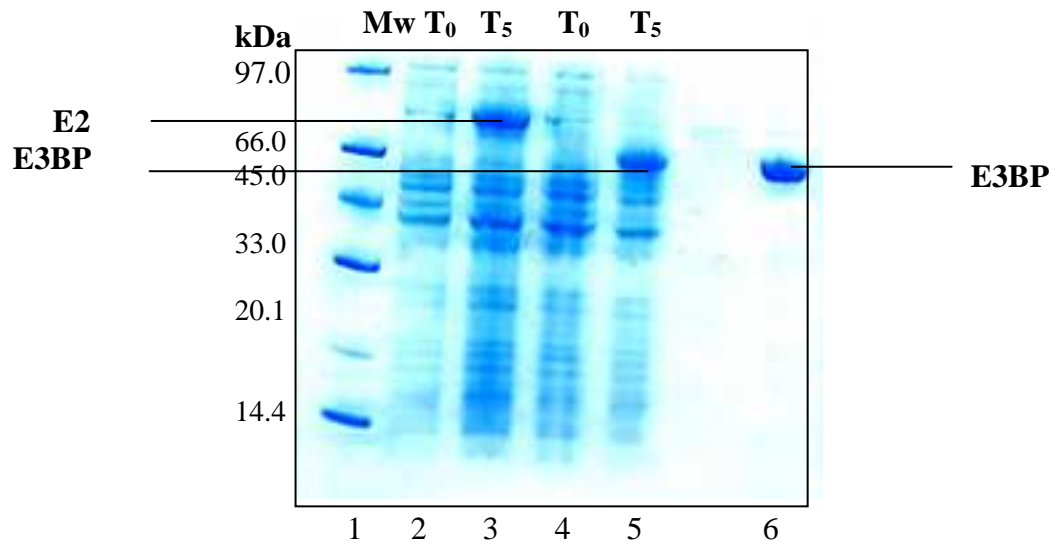
Figure 3.1: E2 and E3BP do not integrate into a core on post-translational mixing

E2 and E3BP were separately overexpressed at 30 ºC for 5 h (lanes 3 and 5, respectively). SDS-PAGE analysis on a 4-12% Bis-Tris gel shows that only His-tagged E3BP was purified on zinc chelate chromatography (lane 6), indicating that on post-translational mixing the two subunits do not associate to form a native core assembly. Molecular weight markers (Mw) are in lane 1.

.
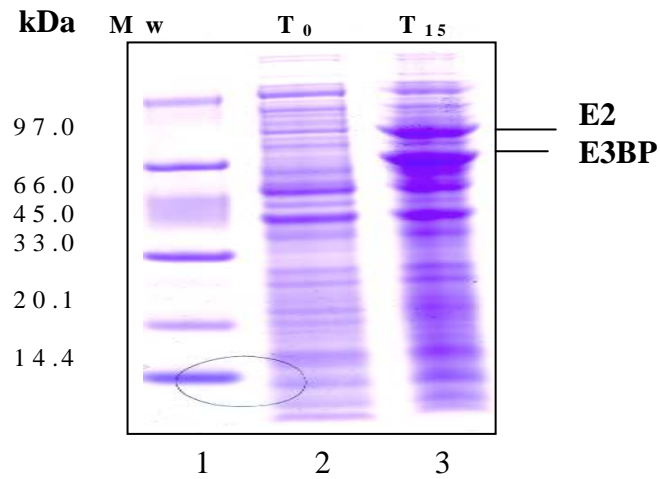
Figure 3.2: Overexpression of E2:E3BP core

SDS-PAGE analysis on a 4-12% Bis-Tris gel showing overexpression of wild-type E2:E3BP core at 15 ºC in *E. coli* BL21 (DE3) Star cells at zero time (T_0) and 15 h post induction (T_{15}). Molecular weight markers (Mw) are in lane 1.

3.4 Purification of E2:E3BP

E2:E3BP core assembly was purified by zinc chelate chromatography as described in Methods section 2.3.6. In this system only E3BP was His-tagged and E2 was co-purified owing to its stable interaction with E3BP. After initial isolation, the core was further purified by gel filtration in GFC buffer (50 mM KH_2PO_4, 150 mM NaCl, pH 7.5) using a Sephacryl HiPrep S-300 High Resolution column attached to a BioCAD 700E workstation. The high M_r core was stored at -20 °C in 50% (v/v) glycerol until further use. Interestingly, it was observed that excess E3BP produced from this plasmid that was not integrated into core could be separated by gel filtration (Fig. 3.3 A). The integrated core eluted at the void volume as expected, but excess E3BP eluted later with an elution volume corresponding to a M_r value of 100,000 consistent with its presence as a dimeric species (Fig. 3.3 A & B).

3.5 Lipoylation of E2:E3BP core

Interestingly, the essential covalent modification of human E2 and E3BP lipoyl domains, namely insertion of the lipoic acid co-factor, can be achieved in *E. coli*. This is accomplished through the action of its endogenous bacterial lipoyl ligase. The two peripherally located lipoyl domains of E2 (present in tandem repeat at its N-terminus) and the single lipoyl domain of E3BP (also with a similar N-terminal location), both require the covalent attachment of the lipoic acid moiety to a specific lysine residue within these domains that is situated at the exposed tip of a type 1 β-turn. Complete lipoylation was ensured by addition of exogenous lipoic acid (0.1 mM) to the medium during induction of heterologous protein synthesis and checked by employing PD2 (patient derived hybridoma IgG) monoclonal antibody that recognises only the lipoylated forms of E2 and E3BP exclusively (Thomson et al., 1998). Successful lipoylation of E2:E3BP core was found to be occurring on Western blotting with PD2 antibody (Fig. 3.4) confirming that the heterologous human lipoyl domain is recognised by the bacterial lipoylation machinery. Initially it was thought that *E. coli* lipoyl ligase was capable of recognising a specific DKA

motif present on the lipoyl domains of E2 and E3BP. Later, however, it was demonstrated that it was primarily a precise structural cue that was recognised by the lipoylating machinery of the cell as opposed to a conserved sequence motif (Wallis and Perham, 1994).

3.6 Solubility of E2:E3BP core

Checking the solubility of recombinantly produced oligomeric cores prior to purification is an important step in their characterisation as the presence of soluble protein generally suggests that they are capable of folding into their native or near native state in the bacterial host and in addition that the N-terminal His-tag has not adversely affected folding or expression. Bacterial cells containing overexpressed E2:E3BP core were disrupted by French press treatment to permit the release of soluble protein into the supernatant fraction and insoluble cellular debris was removed by centrifugation. To achieve optimal solubility and production of the E2:E3BP core, it was initially overexpressed at different temperatures after induction with IPTG. In one set, expression was induced at 30 °C for 4-5 h with 1 mM IPTG and in a second set at 37 °C for 3 h. In the third set, overexpression was induced with 1 mM IPTG at 22 °C for 5-6 h while a similar induction was also carried at 15 ºC overnight for 18 h with 0.5 mM IPTG. All the overexpressions were studied using *E. coli* BL21 (DE3) Star cells. Although, E2:E3BP could be expressed successfully at all temperatures, on solubility checking, it was found to be most soluble when expressed at 15 °C (Fig. 3.5). Therefore, E2:E3BP core was overexpressed at this temperature in subsequent experiments in *E. coli* BL21 (DE3) Star cells.

A

B
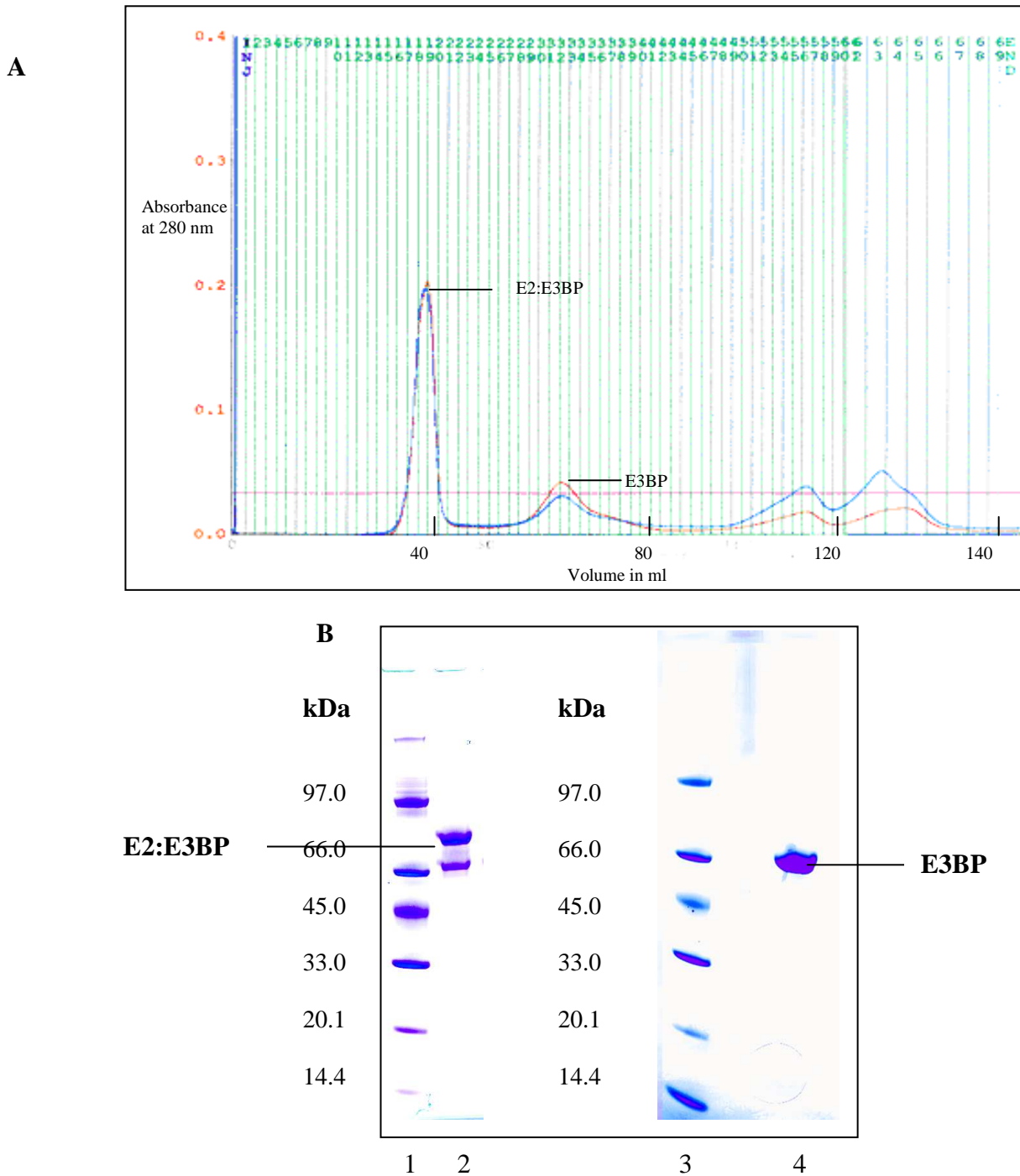
Figure 3.3: His-tag purification and gel filtration of E2:E3BP core

(A) His-tagged E2:E3BP core, purified by zinc chelate chromatography was gel filtered through a Sephacryl HiPrep S-300 High Resolution column attached to a BioCAD 700E workstation. (B) On SDS-PAGE analysis, the peak eluting at the void volume corresponded to E2:E3BP core (lane 2) and the second peak to excess E3BP (lane 4) not bound to the core. Molecular weight markers (Mw) are in lanes 1 and 3.
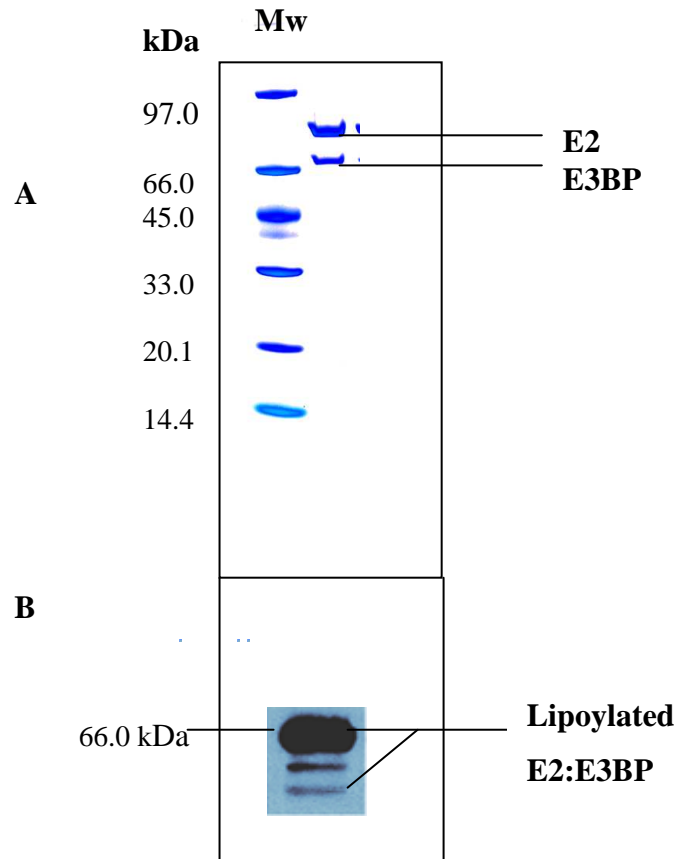
Figure 3.4: Western blot analysis of the wild-type E2:E3BP core with PD2 antibody

Panel A shows SDS-PAGE analysis of E2:E3BP core prior to Western blot analysis (panel B) with PD2 antibody. The blot shows that the core was lipoylated as PD2 antibody recognises only lipoylated subunits of PDC (Thomson et al., 1998).
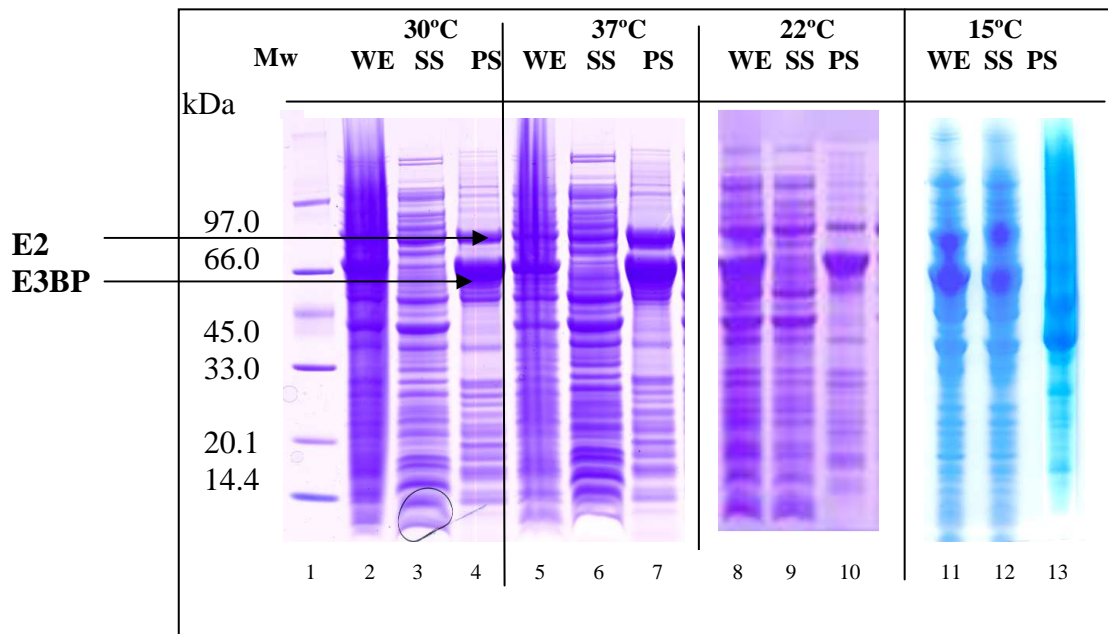
Figure 3.5: Solubility checking of wild-type E2:E3BP core overexpressed at various temperatures

E2:E3BP core was overexpressed at 15 °C, 22 °C, 30 °C and 37 °C in *E. coli* BL21 (DE3) Star cells. SDS-PAGE analysis on a 4-12% Bis-Tris gel shows that at 30 °C, 37 °C and 22 °C, E2:E3BP was largely insoluble and present mainly in the pellet samples (PS) (lanes 4, 7 and 10 respectively) and not in supernatant samples (SS) (lanes 3, 6 and 9 respectively). When expressed at 15 ºC overnight, the core assembly was soluble and present in the supernatant sample (SS) (lane 12) and not in the pellet sample (PS) (lane 13). Whole cell extracts (WE) in lanes 2, 5, 8 and 11, respectively. Molecular weight markers (Mw) are in lane 1.

3.7 Overexpression of E3

E. coli BL21 (DE3) plysS cells were transformed with E3 cDNA housed in the pET-14b vector. Overexpression was induced by the addition of 0.1mM IPTG at 22 °C and viewed by SDS-PAGE analysis (Fig. 3.6). E3 was overexpressed at this temperature in all experiments unless stated otherwise.

3.8 Overexpression of E1

Co-expression of the α and ß subunits of E1 was first successfully achieved in the laboratory by co-transformation of *E. coli* with two separate plasmids, pET- 28b for E1α and pET-141b for E1ß using double antibiotic selection with ampicillin and kanamycin. However, difficulties were experienced in reconstituting active, soluble hetero-tetrameric human E1, although high levels of expression of both subunits were readily attained. This problem was finally overcome by Dr. Alison Prior, who subcloned the genes for both E1α and E1 ß from pET-28b and pET-11b respectively into a modified pQE-9 vector system to permit their co-expression from a single plasmid in *E. coli* M15 cells. These cells contain a kanamycin-resistant plasmid, pREP4 which encodes the *lac* repressor encoded by the *lacI* gene. The levels of expression in this vector system were relatively low, but were sufficient to produce 2-3 mg of E1 protein on a routine basis (Fig. 3.7) from 2-3 l of culture. Overexpression was induced by 1 mM IPTG at 18 ºC overnight.
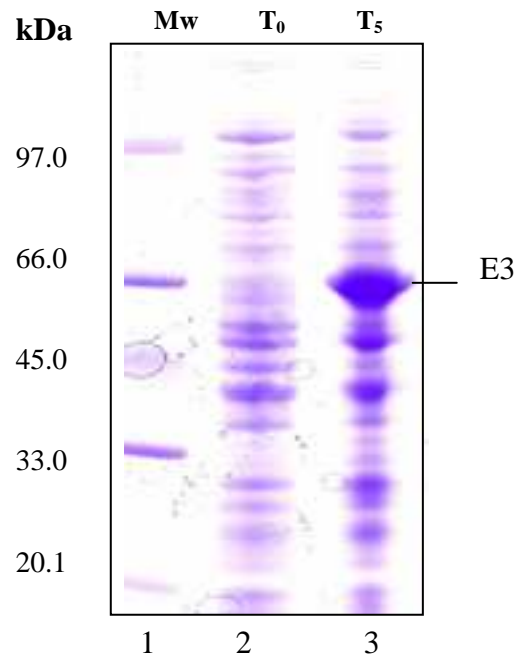
Figure 3.6: Overexpression of E3

Overexpression of the E3 enzyme was carried out in *E. coli* BL21 (DE3) plysS cells at 22 °C. SDS-PAGE analysis on a 4-12% Bis-Tris gel shows expression levels at zero time (T_0) and after 5 h of induction (T_5). Molecular weight markers (Mw) are in lane 1.
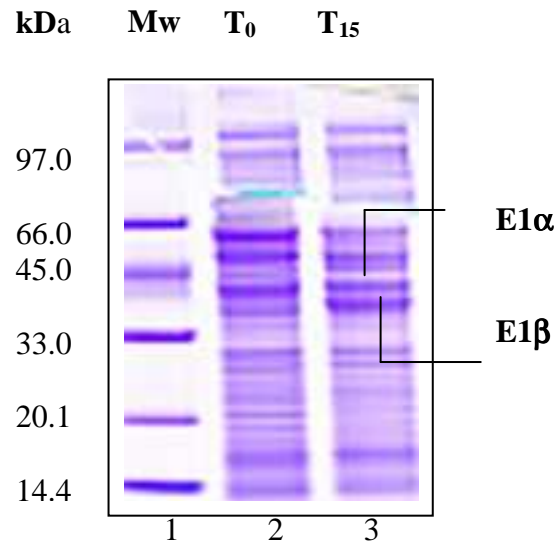
Figure 3.7 Overexpression of co-transformed E1α and E1β subunits

E1α and E1 β were co-expressed in *E. coli* M15 cells at 18 °C overnight. SDS-PAGE analysis on a 12% Bis-Tris gel shows samples at zero time (T_0) and 15 h after induction (T_{15}). Molecular weight markers (Mw) are in lane 1.

3.9 E3 purification

E3 was purified by zinc chelate chromatography (see section 2.3.6). Purified fractions were gel filtered using GFC buffer (50 mM KH_2PO_4, pH 7.5, 150 mM NaCl) prior to SDS-PAGE analysis for checking the purity of pooled fractions (Fig. 3.8). The enzyme was stored at 4 ºC until required.

3.10 E1 purification

E1 was purified by the protocol described in the Methods section 2.3.7. Attempts to dialyse purified E1 resulted in precipitation of the enzyme. Therefore, purified fractions were concentrated in a Centricon concentrator with a 'cut off' size of 100 kDa with addition of excess Buffer A (50 mM KH_2PO_4 , 1 M NaCl, 0.5 mM imidazole, pH 8), to lower the concentration of imidazole. SDS-PAGE analysis was performed to check its purity (Fig. 3.8). Purified enzyme was stored at -20 ºC in 50 % (v/v) glycerol.

3.11 Reconstitution of recombinant PDC

For reconstituting recombinant PDC from its constituent enzymes, the concentration of each purified enzyme was measured using its extinction co-efficient (see Methods section 2.3.10). Then enzymes were mixed together in stoichiometric amounts i.e. for each μmole of E2:E3BP core, 12 μmole E3 and 30 μmole E1 were added at room temperature. After mixing the individual components, reconstituted PDC was immediately assayed.

Recombinant PDC was found to assemble spontaneously from its constituent enzymes within a 2 min preincubation period when they were mixed in the equivalent ratios to those found in the native complex. PDC activity was measured using standard spectrophotometric assay techniques (see Methods section 2.3.17) in which NADH production was monitored spectrophotometrically at 340 nm in the presence of pyruvate as substrate. Reconstituted recombinant PDC appeared to be fully active and displayed a similar specific activity (3.5-4 μmol NADH min^{-1} mg protein^{-1}) to reported values for the native, wild-type complex isolated from human heart (Palmer et al., 1993).
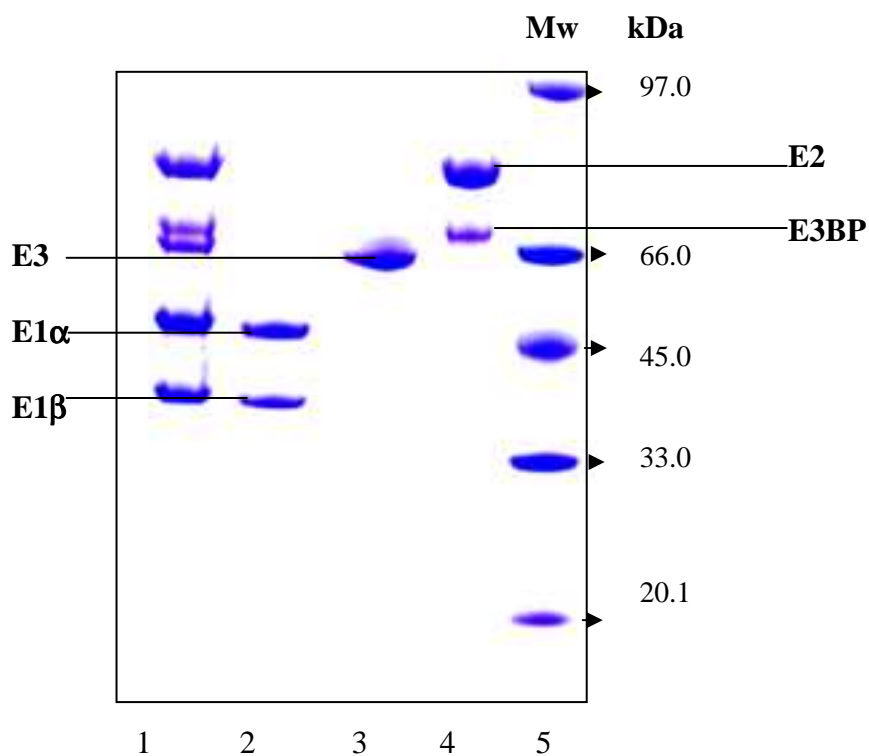
Figure 3.8: Reconstitution of PDC from individual components

SDS-PAGE analysis on a 4-12% Bis-Tris gel shows PDC (lane 1) reconstituted from stoichiometric amounts of purified E1 (lane 2), E3 (lane 3) and E2:E3BP (lane 4). Molecular weight markers (Mw) are in lane 5.

3.12 Effect of increasing amounts of E3 on wild-type PDC activity

Recombinant human PDC assembled spontaneously from its constituent enzymes within a 2 min preincubation period when they were mixed in the equivalent ratio as the native complex i.e. in stoichiometric amounts. This reconstituted recombinant human PDC appeared to be fully active and displayed a similar specific activity to PDC purified from human tissue. These initial studies confirmed that the individual components of PDC retain their capability to interact with each other in the recombinant model and mimic the functional abilities of the native complex. Recombinant PDC was reconstituted as described in section 3.11 of this Chapter. Enzymatic assay of wild-type recombinant PDC in the presence of excess amounts of purified E3 (up to 200-fold) was performed using the spectrophotometric method described in Methods section 2.3.17. With the addition of increasing amounts of E3, there was a slight but significant decline (20-25%) in overall PDC activity as shown in Fig. 3.9. The decline in activity is probably caused by displacement of the rate-limiting E1 enzyme from its binding site on E2 by excess E3 confirming earlier observations (McCartney et al., 1997) that E3 displays a residual affinity for E2.

3.13 Effect of increasing amounts of E3 on the activity of PDC lacking E3BP

Recombinant PDC was reconstituted by adding stoichiometric amounts of E1 and E3 to recombinant E2 core produced in the absence E3BP. Activity assays were performed in the same way as for native PDC. Recombinant PDC lacking E3BP displayed little activity (3-8%) with stoichiometric amounts of E1 and E3. However, overall activity rose gradually with increasing E3 with activity levels reaching approx. 50% of wild-type values with a

200-fold excess of this component (Fig. 3.9). These results were in agreement with previous studies on the native bovine complex (McCartney et al., 1997) and again suggested that the partial activity of PDC detected in the total absence of E3BP stems from the ability of E3 to interact with the E1 binding site on E2 with low affinity.
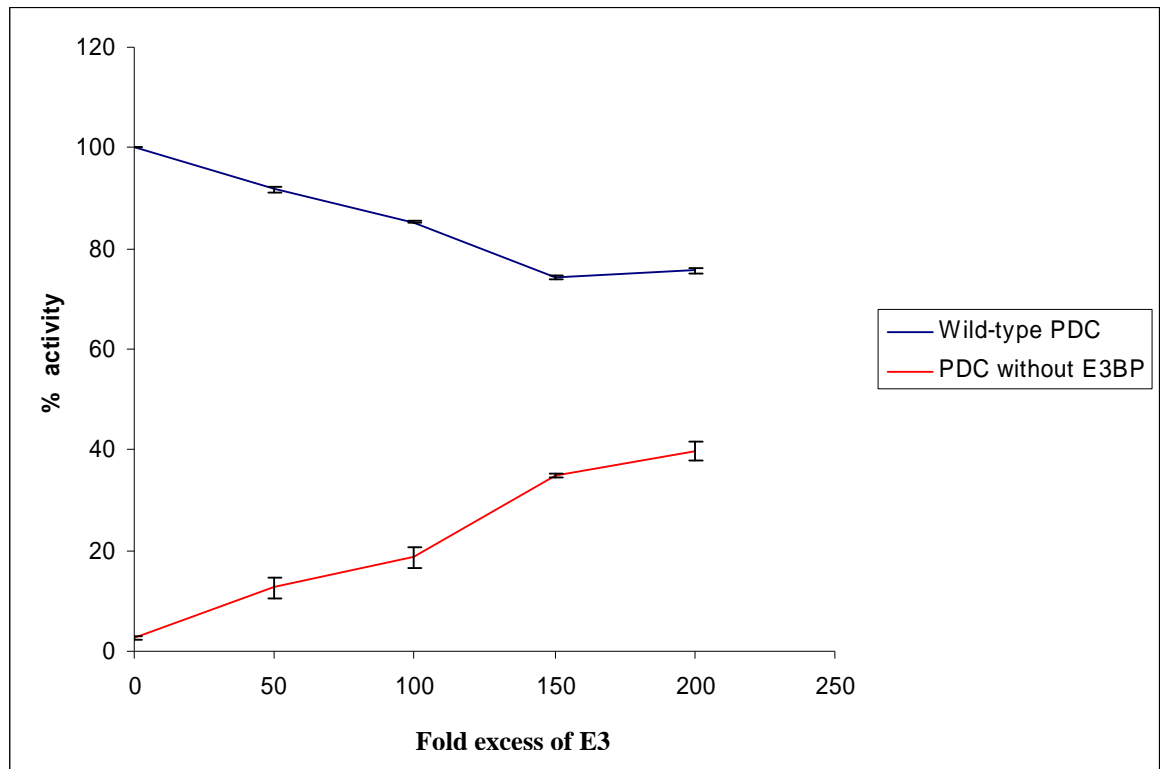
Figure 3.9: Effect of increasing amounts of E3 on the activity of recombinant wild-type PDC and recombinant PDC devoid of E3BP

A decline in the activity of native PDC is observed with increasing amounts of added E3 (blue) whereas there is a marked increase in the activity of recombinant PDC (without E3BP) with increasing amounts of E3 (red). Added E3 ranges from stoichiometric amounts to a 200-fold excess.

3.14 Effect of differing combinations of active and inactive lipoyl domains in E2:E3BP core on overall PDC activity

The lipoyl group is attached in amide linkage to the N^6-amino group of a lysine residue located on an exposed type-1 β turn within lipoyl domains. It is a highly specific post-translational modification carried out by an ATP-dependent lipoate protein ligase (Morris et al., 1994). A major advantage of producing recombinant human E2 components of PDC, in *E. coli* is that the bacterial ligase is capable of inserting exogenous lipoic acid onto the key lysine of a variety of heterologous lipoyl domains. The apodomains can be lipoylated *in vitro* also with partially purified *E. coli* lipoate protein ligase (Quinn et al., 1993). This ligase is also responsible for the octanoylation of lipoyl domains in the absence of lipoic acid or when there is excessive production of apodomains (Ali et al., 1990; Dardel et al., 1990; Quinn et al., 1993). While overexpressing wild-type and mutant E2 and E2:E3BP cores, exogenous lipoic acid was added to ensure complete lipoylation. The effects of loss of lipoylation of recombinant E2 and E3BP lipoyl domains and its effect on overall activity was assessed in this study.

A series of mutant E2:E3BP cores was created lacking the full complement of active lipoyl domains. In these mutant cores, lipoylation was prevented by selectively altering the lipoylatable lysine to glutamine in individual domains, thereby preventing co-factor insertion. As discussed earlier also, the lipoyl domains play a crucial role in coupling the activities of the three enzyme components of PDC by providing 'swinging arms' that are mobile and responsible for substrate transfer among the three successive active sites (Fussey et al., 1991; Yeaman et al., 1978). Thus, eight distinct 'cores' containing all possible combinations and numbers of active/ inactive E2/E3BP lipoyl domains namely ++/+, ++/-, +-/+, +-/-, -+/+, -+/-, --/+ and --/- were constructed using site-directed mutagenesis. A schematic representation of these cores is depicted in Fig. 3.10.
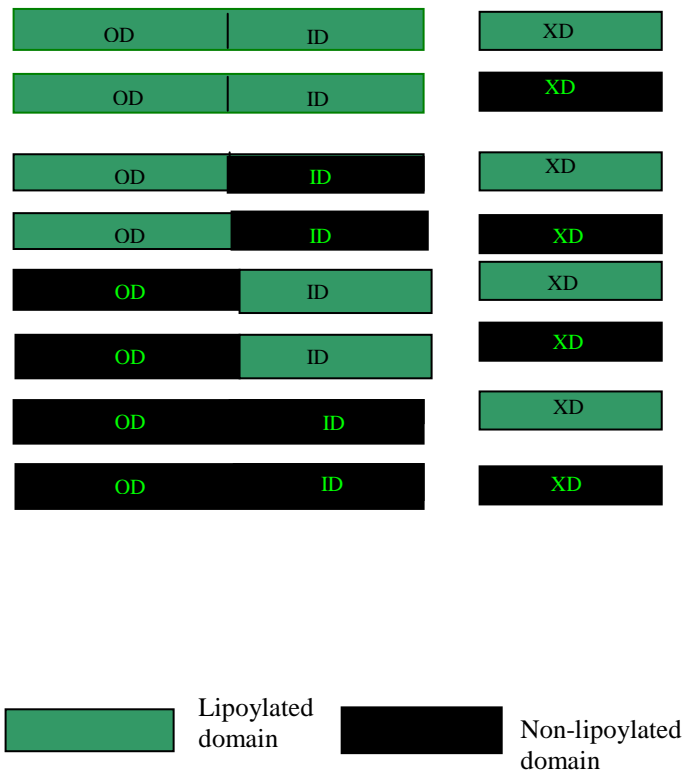
Figure 3.10: Schematic representation of eight wild-type and mutant constructs of E2:E3BP cores

Representation shows either lipoylated (green) or non-lipoylated domain (black); E2 outer lipoyl domain (OD), E2 inner lipoyl domain (ID) and E3BP lipoyl domain (XD) in eight E2:E3BP cores generated to determine the effect of lipoylation status on overall complex activity.

The '+' represents wild-type lipoylated domain in E2:E3BP core, whereas, '-'is a mutant lipoyl domain created in the core by lysine to glutamine replacement employing site-directed mutagenesis (Methods section 2.2.11). The appropriate mutants were created by A. S. Stephanou, University of Glasgow, by designing and using mutagenic primers described in Materials and Methods, section 2.1.3. In all the constructs, wild-type, K46Q, K175Q and K46Q:K175Q E2 were contained in the pET-11b vector exhibiting ampicillin resistance whereas wild-type and K44Q E3BP were housed in pET-28b displaying kanamycin resistance. After checking for the correct mutations by DNA sequencing, wild-type and mutant E2 and E3BP constructs were co-transformed into *E. coli* BL21 (DE3) Star cells in eight different combinations as shown in Fig. 3.10. Co-transformed cells were induced to overexpress at 30 ºC in LB medium with 1 mM IPTG and with the addition of 0.1 mM lipoic acid. Wild-type and mutant cores were isolated by zinc chelate chromatography as described in Methods section 2.3.6 and subsequently gel filtered as described in Methods section 2.3.12. SDS-PAGE analysis was conducted to check their purity (Fig. 3.11).

Western blot analysis of these eight wild-type and mutant 'cores' with PD2 antibody revealed varying degrees of lipoylation in which the wild-type core displayed a strong E2 signal whereas cores with either a single active inner or outer lipoyl domain displayed less cross-reactivity. Mutant E2 core with both inner and outer lipoyl domains inactive exhibited no signal with E2. Active E3BP lipoyl domain in mutant and wild-type cores also gave a signal, although weak as compared to lipoylated E2 domains. Complete loss of signal indicating no lipoylation was observed when all the lipoyl domains were rendered inactive in E2 as well as E3BP (Fig. 3.11).
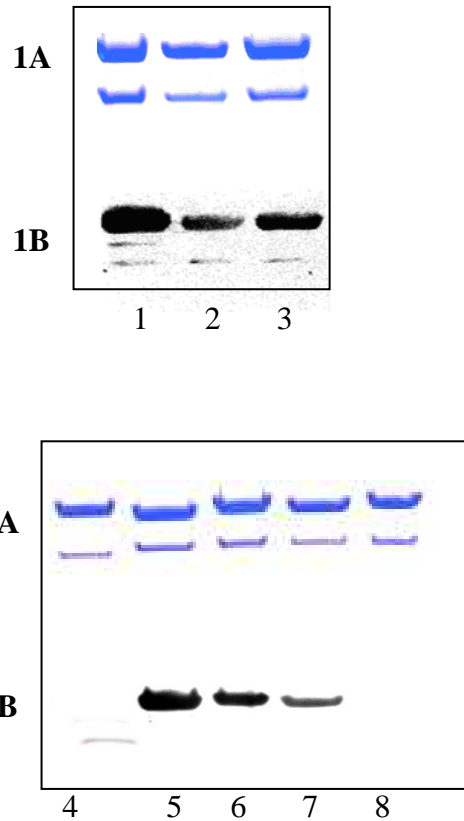
Figure 3.11: SDS-PAGE and Western blot analysis of wild-type and mutant E2:E3BP cores by PD2 antibody

SDS-PAGE (1A) and Western blot analysis with PD2 antibody (1B) of ++/+, -+/+ and +-/+ E2:E3BP cores in lanes 1, 2 and 3 respectively. SDS-PAGE (2A) and Western blot analysis with PD2 antibody (2B) of --/+, ++/-, -+/-, +-/- and --/- E2:E3BP cores in lanes 4, 5, 6, 7 and 8 respectively. The '+' represents wild-type lipoylated domain in E2:E3BP core, whereas, '-' is a mutant non-lipoylated domain.

To investigate the effect of the differing combinations of active and inactive lipoyl domains on overall PDC activity, eight sets of recombinant PDCs were reconstituted from the various wild-type and mutant cores by adding stoichiometric amounts of E1 and E3 employing the protocol described in section 3.11. Equal amounts of wild-type and mutant PDCs were assayed in duplicate as described in Methods 2.3.17 and the activity compared to the wild-type PDC as control (100% activity). Mutant PDCs were found to sustain high levels of activity (65-75%) with approx. half of their full complement of lipoyl domains (only inner or outer lipoyl domain active on E2). Moreover, the presence or absence of a functional lipoyl domain on E3BP had no additional significant effect on activity with E2s possessing either one or two active lipoyl domains (Fig. 3.12). Interestingly, however, PDC with only E3BP-linked active lipoyl domain retained approx. 15% of wild-type activity while total loss of activity required non-lipoylation of all 3 domains.
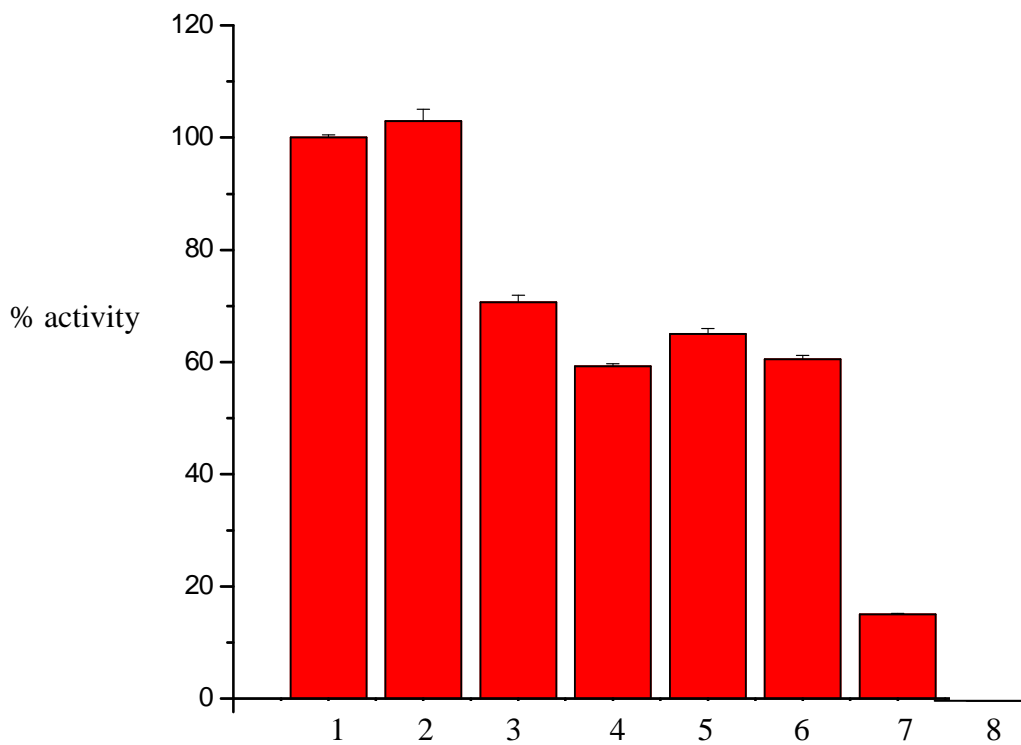
Figure 3.12: Effect of differing combinations of active and inactive lipoyl domains on recombinant PDC activity

Histogram corresponds to enzymatic activity of recombinant PDCs with the following types of E2:E3BP cores: 1 ++/+, 2 ++/-, 3 +-/+, 4 +-/-, 5 -+/+, 6 -+/-, 7 --/+ and 8 --/-. The '+' represents wild-type lipoylated domain in E2:E3BP core whereas, '-' is a mutant non-lipoylated domain. Samples were assayed in duplicate and error bars indicate extent of variation between duplicates.

3.15 Discussion

Recombinant PDC could be successfully reconstituted from purified E2:E3BP, E1 and E3. Its enzymatic function was fully restored indicating that all the enzymes were correctly folded. It displayed a specific activity (3.5-4 µmol NADH min $^{-1}$ mg protein^{-1}) similar to PDC purified from human heart (Palmer et al., 1993). Interaction between the three components was further tested in an assay where increasing amounts of E3 were added to the recombinant PDC. With the addition of increasing E3, overall complex activity was found to decrease gradually, presumably due to partial displacement of the E1 enzyme by excess E3. This result was consistent with surface plasmon resonance measurements performed by Dr. Susan Richards in our laboratory (unpublished data). In this study the affinity of E3BP for E3 was found to be approx. 100-fold higher (Kd value of 5.31 x 10^{-9} M) than for the equivalent E2-E3 interaction (Kd value 3.39 x 10^{-7} M) confirming that the E1 binding site on E2 retains a residual affinity for E3. This residual affinity for E3 has also been reported previously (McCartney et al., 1997). Interestingly, it is reminiscent of the situation in *B. stearothermophilus* PDC, where E1 and E3 must compete for a single binding site on E2 and are capable of displacing each other (Lessard et al., 1996).

When increased amounts of E3 were added to recombinant PDC lacking the E3BP subunit and overall complex activity monitored, it was found that the activity gradually rose to approx. 50% of wild-type activity levels in the presence of a 100-200 fold E3 excess. These data are also compatible with the presence of a low affinity binding site for E3 on the E2 core assembly that is able to partially substitute for the E3BP-located subunit binding domain in the absence of the latter subunit.

All these findings are also in agreement with the previous surprising identification (in collaboration with French colleagues) of PDC deficient patients with metabolic lactic acidosis who totally lack E3BP. These patients possess a partially active PDC (10-20% of wild-type) as compared to the control group (Geoffroy et al., 1996; Marsac et al., 1997) again indicating that even *in vivo* the E2 subunit provides a weak secondary E3 binding site. However in this genetic defect, E3 is not stably integrated into the mutant complex

which functions much less efficiently under these conditions. In summary, these studies highlighted the partial functional redundancy of the E3BP subunits, while also demonstrating that E2 and E3BP display both overlapping and distinct functions. Analysis of E3BP deficient PDC, both *in vitro* and *in vivo*, has contributed to a better understanding of the role of E3BP subunit and has provided a rational basis for conducting prenatal diagnosis for possible E3BP deficiency in affected families (Marsac et al., 1993).

The effect of differing combinations of active and inactive lipoyl domains of E2:E3BP core on lipoylation status was also studied using a series of 8 mutant PDCs. On Western blotting with PD2 antibody, it was seen that mAb cross-reactivity was at a maximum when all the lipoyl domains were fully functional and gradually declined with the loss of lipoylatable domains on E2 and E3BP. Overall complex activity also declined gradually with the loss of functional lipoyl domains. However, inactivation of inner or outer lipoyl domains on E2 caused minor reduction in overall complex activity indicating considerable redundancy at this level. Thus reducing the complement of lipoyl domains by approx. 50% led to a 25-35% loss of activity. Moreover, introduction of E3BP with a non-functional lipoyl domain had no further significant effect on activity in comparison to wild-type PDC or in the case of mutants carrying an inactive outer or inner lipoyl domain on E2. Finally, PDC in which only the 12 lipoyl domains of E3BP were lipoylated also retained partial activity (15%) and only complete loss of lipoylation led to complete inhibition.

This study represents the first systematic investigation of the effects of alterations in the lipoylation status of the E2:E3BP core on mammalian PDC complex activity. The enzymatic activity results were found to be consistent with the lipoylation status as determined by Western blotting. The observation that recombinant PDC displayed 15% activity with only E3BP containing active lipoyl domains (12 out of a possible 132/108) is in agreement with the results of Rahmtullah and co-workers (Rahmatullah et al., 1990) and Sanderson and co-workers (Sanderson et al., 1996a) where 10-15 % activity is retained with the proteolytical removal of lipoyl domains of E2 on collagenase treatment. This suggested that E3BP-linked domains can substitute to some extent for the lipoyl domains of E2 in overall complex catalysis. These data also demonstrated considerable functional redundancy at this level that is genetically advantageous as null mutations producing totally inactive PDC would be expected to be embryonically lethal. Interestingly, this study is the first in mammalian PDC in which the correctly folded E2 and E3BP domains have been retained in a non-functional state. Previous studies have employed genetically engineered or proteolytically modified E2:E3BP core assemblies, where the entire domain

is absent, potentially allowing greater flexibility and improved access to catalytic sites for the remaining active domains. Our data, however, tend to confirm and extend these earlier studies and indicate that inner and outer lipoyl domains of E2 or the single E3BP lipoyl domain are all effective substrates for E1, E2 and E3 and that there is no obvious preferential recognition of individual domains by these enzymes. In addition, the presence of a full complement of domains in which a high proportion is inactive does not produce any apparent steric hindrance effects.

3.16 Study on involvement of E3BP in diacetylation

In PDC, acetyl group transfer occurs after the initial decarboxylation step, which is catalysed by E1 with the production of CO_2 and an enzyme-bound hydroxyethylidene thiamine diphosphate derivative. There is then E1-mediated reductive acetylation of the lipoamide cofactor attached to E2 and /or E3BP leading to formation of a S^8-acetyl intermediate. Subsequently acetyl groups migrate between the S^6 and S^8 positions (Koike and Koike, 1976). In the final step, E3 re-oxidises E2 and E3BP linked lipoamide cofactors followed by reduction of NAD^+.

It is a unique property of mammalian PDC to be able to generate a S^6, S^8 diacetyl–dihydrolipoamide intermediate on addition of either pyruvate in the absence of CoASH or NADH and acetyl CoA. Treatment of PDC with pyruvate or NADH and acetyl CoA leads to rapid initial generation of a S^8–acetyldihydrolipoamide intermediate and exchange of acetyl groups between S^6 and S^8 sulphur atoms on the dithiolane ring. The formation of the S^6, S^8 diacetyl–dihydrolipoamide intermediate by mammalian PDC was initially detected by ^{13}C-NMR spectroscopy (O'Connor et al., 1982).

This property does not require the presence of E2 lipoyl domains as the capacity of E3BP lipoamide thiols to undergo the diacetylation reaction is shown to be unaffected by the removal of E2 lipoyl domains in collagenase-modified PDC complex (which causes selective removal of lipoyl domains of E2). This was shown by studies on ^{14}C–acetylation in bovine heart PDC, where the single lipoyl domain of E3BP was shown to be capable of diacetylation (Sanderson et al., 1996b). Moreover, collagenase-treated PDC possessed

residual activity (about 15%), indicating that protein-E3BP-linked lipoamide groups could substitute for the lipoyl domains of E2 in overall complex catalysis.

Interestingly, the ability to catalyse diacetylation is absent in the bacterial PDC complex and so is the E3BP subunit. However, it has been demonstrated in bovine and S. *cerevisiae* PDC complexes, where the E3BP polypeptide has been well characterised (Hodgson et al., 1986). The equivalent phenomenon is also absent in the OGDC complex where transfer of a succinyl group occurs and a single S^6 or S^8 succinyl-dihydrolipoamide intermediate is formed. Therefore, it was suspected that formation of the diacetyl dihydrolipoamide intermediate could be uniquely mediated through E3BP. This reaction might be of physiological relevance to permit PDC to act as a reservoir for acetyl groups and electrons under conditions of excess acetyl CoA and NADH production, e.g. on high fat diets or in abnormal states such as starvation and diabetes. In these conditions, each molecule of PDC could bind a maximum of 264 acetyl groups (assuming a 60E2:12E3BP core) and an equivalent number of electrons, thereby providing a safe buffer against production of ketone bodies and regulate the formation of NADH. If indeed E3BP is involved uniquely in diacetylation, then it could be of great physiological importance. The cell lines of patients deficient in E3BP were of considerable interest in this regard (Marsac et al., 1993). In this study, reconstituted recombinant PDC provided an important tool to study this potential enzymatic and physiological role of E3BP as no specific catalytic function for E3BP has been revealed to date.

It has been shown that the E2 component of *E. coli* PDC can be inactivated selectively by maleimides in the presence of pyruvate or NADH (Brown and Perham, 1976; Danson and Perham, 1976). The E2-bound lipoyl moieties become reductively acetylated or reduced and the corresponding intermediates react with NEM when there are free thiol groups present leading to inactivation of the complex. Hodgson et al. (1986) also showed that the presence of NADH or pyruvate promoted incorporation of NEM into E2 as well as E3BP components.

On the addition of NADH and acetyl CoA to PDC, however, it has been shown that the complex is rapidly protected once again from inhibition by NEM. Hodgson et al. (1986) also demonstrated that the group incorporating NEM in E3BP was in all respects similar to the lipoyl groups on the E2 subunit.

The extent of protection against NEM inhibition, was found to be greater as the time of preincubation was increased (Cate et al., 1980) and formation of a S^6, S^8 diacetyl–dihydrolipoamide intermediate under these conditions was identified.

To elucidate whether addition of a second acetyl group to the S-acetyldihydrolipoamide intermediate is a unique catalytic function of E3BP, a recombinant PDC was reconstituted from purified E1, E2, a molar excess of E3 and devoid of E3BP. As discussed earlier, reconstituted PDC complex in the absence of E3BP shows limited activity (3-8%) as E3 is not stably integrated into the complex in these conditions. Native bovine PDC extracted as per the protocol described by De Marcucci and co-workers (De Marcucci et al., 1988) was used as a control in this experiment.

Four conditions were tested using recombinant PDC (without E3BP) and native PDC (Fig. 3.13). In the first reaction, native as well as recombinant PDC (devoid of E3BP) were incubated with 0.2 mM NADH and 1 mM NEM. In the second reaction instead of NADH, 0.2 mM NAD^+ was added followed by addition of 1 mM NEM. In the third reaction, native as well as recombinant PDC (devoid of E3BP) were incubated with 0.2 mM NADH and 0.4 mM AcCoA followed by incubation with 1 mM NEM. In the fourth reaction, both the complexes were treated with NAD, AcCoA and NEM as before. In all the reaction mixtures, 50 mM DTT was added to quench excess NEM. After 10 min NEM treatment, activity assays of all the individual complexes (100 µl) were performed as described in Methods section 2.3.17.
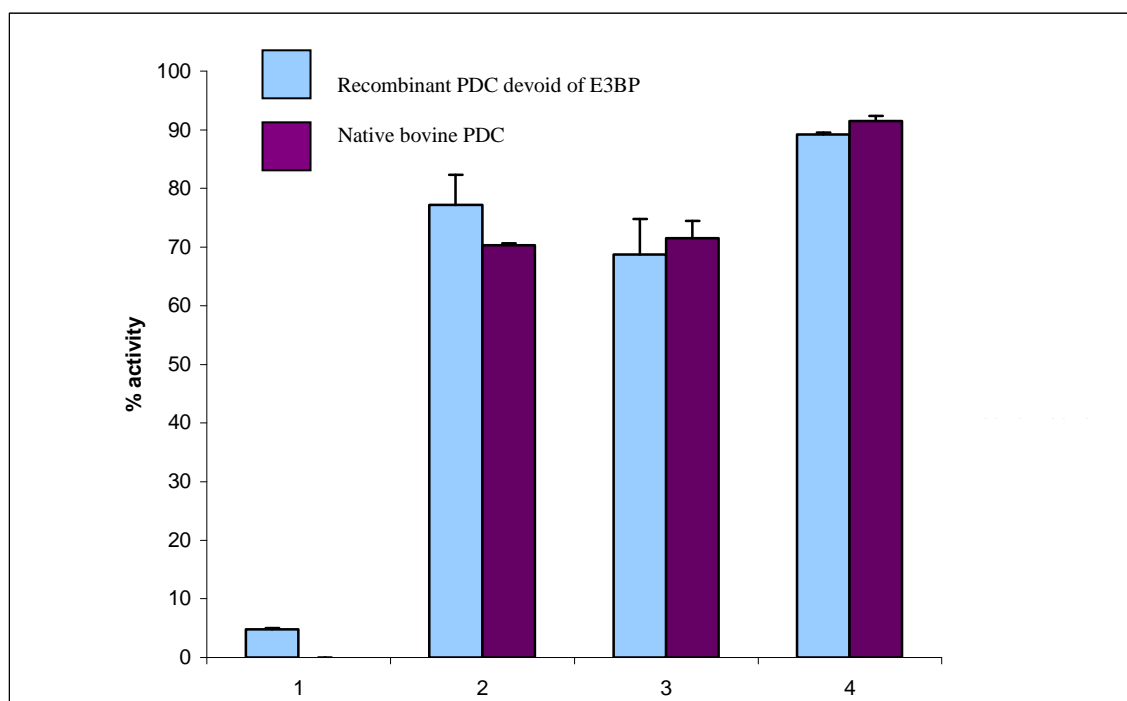
Figure 3.13: Recombinant PDC devoid of E3BP is protected from inhibition by NEM due to formation of diacetylated dihydrolipoamide groups

Native bovine PDC and recombinant PDC reconstituted from stoichiometric amounts of E2, E1 and a 200-fold excess of E3, were individually incubated with following chemicals for the stated times and conditions before the enzymatic assays were carried out .

1 PDC + 0.2 mM NADH (10 min) + 1 mM NEM (10 min) + 50 mM DTT (10 min).

2 PDC + 0.2 mM NAD$^+$ (10 min) + 1 mM NEM (10 min) + 50 mM DTT (10 min).

3 PDC + 0.2 mM NADH (10 min) + 0.4 mM AcCoA (10 min) + 1 mM NEM (10 min) + 50 mM DTT (10 min).

4 PDC + 0.2 mM NAD$^+$ (10 min) + 0.4 mM AcCoA (10 min) +1 mM NEM (10 min) + 50 mM DTT (10 min).

Bars represent percentage activity of native (purple) and recombinant (blue) PDC complexes in above four conditions. Samples were assayed in duplicate and error bars indicate extent of variation between duplicates. Native PDC (100 μg) and recombinant PDC (200 μg) were employed for each analysis to account for the large molar excess of E3 in the recombinant PDC. Activity of native bovine PDC was taken as 100% control.

3.17 Results and discussion on diacetylation of E3BP

In the first reaction, native and recombinant PDC were monitored and incubated with NEM in the presence NADH; the activities were found to be inhibited in both the complexes (Fig. 3.13). This was in agreement with the previous studies (Brown and Perham, 1976; Danson and Perham, 1976) where NADH was shown to cause reduction of lipoamide groups on E2 and E3BP, facilitating incorporation of NEM and thus inhibiting overall PDC function.

When the same reaction was carried out in the presence of NAD^+, instead of NADH, reduction of lipoamide groups did not take place as anticipated and no loss of activity was observed in both PDC complexes (Fig. 3.13). Similar results have been reported in earlier studies with bovine PDC (Hodgson et al., 1986).

In the third reaction, on the addition of acetyl CoA in combination with NADH to both these PDC cores, incubation with NEM did not cause inhibition of the activities of either complex. One explanation for this restored activity of PDC has been given by Hodgson et al. (1986). Preincubation of PDC with NADH and AcCoA leads to formation of a S^6, S^8 – diacetyl-dihydrolipoamide intermediate that is not amenable to modification by NEM and the activity of the complex is retained. The presence of this activity in the recombinant complex lacking the E3BP subunit, demonstrates that E3BP is not uniquely involved in diacetylation. Similar results were obtained in the fourth reaction, where instead of NADH, NAD^+ was added as a control. It was seen earlier that with the addition of NEM in the presence of NAD^+, PDC activity was maintained as anticipated. These reactions demonstrate that the recombinant model of PDC can be used to determine potential physiological roles of individual components.

The tight association of protein E3BP with E2 core prevents the detailed analysis of its functional involvement in the complex. Specific deletion of the region encoding subunit binding domain of E3BP in *S. cervisiae* PDC showed loss of high-affinity binding of E3 and concomitant loss of overall activity (Lawson et al., 1991). Moreover, collagenase

treatment of native PDC complex provided information about the substitutional catalytical role of E3BP linked lipoamide groups for E2 lipoyl domains (Rahmatullah et al., 1990). Earlier [14]C- acetylation studies in bovine heart PDC showed that lipoyl domains of E3BP are capable of E2 type reactions including diacetylation (Hodgson et al., 1986). Production of a versatile recombinant PDC model is another step towards understanding the structural and functional roles of E3BP under normal and disease conditions.

In this study, a potential role of E3BP in promoting diacetylation of E2 enzyme was investigated. This phenomenon could be responsible for giving PDC a unique role as a metabolic 'reservoir' harbouring excess electrons and acetyl groups under abnormal physiological conditions. However, the diacetylation phenomenon was still found to occur in recombinant PDC devoid of E3BP. As this process appears to be exclusive to yeast and mammalian PDCs, it is presumably a characteristic property of the eukaryotic E2 enzyme.

Chapter 4

Analysis of naturally occurring mutations in human PDC

4.1 Introduction

This chapter focuses on the investigation and analysis of three recently-discovered mutations in the 60-meric E2 enzyme of PDC that lead to clinical manifestation of PDC deficiency by unknown mechanisms. Clinical presentation and progression of this disorder is highly variable. An abnormal lactate build-up results in non-specific symptoms (e.g., severe lethargy, poor feeding, tachypnea), especially during times of illness, stress, or high carbohydrate intake. A number of acquired conditions including infections, severe catabolic states, tissue anoxia, dehydration and poisoning can give rise to hyperlactic acidaemia. All these causes should be ruled out before considering inborn errors of PDC metabolism. When the lactate / pyruvate ratio is normal or low, PDC deficiency is highly probable (Poggi-Travert et al., 1996).

The definitive diagnosis of PDC deficiency is usually established by enzyme assay in patients' cells or tissues commonly by measuring $^{14}CO_2$ production from ^{14}C-labelled pyruvate with subsequent confirmation of the basic defect by Western blotting with antibodies against subunits of the complex and /or by direct cDNA or genomic sequencing (Eschbach et al., 1987; Old and De Vivo, 1989; Otero et al., 1998). Detection of mutations

in the E1α gene using reverse transcription of total RNA, polymerase chain reaction amplification of the coding region of the gene and single-strand conformation polymorphism (SSCP) analyses have been found to be rapid and efficient approaches in the detection of gene defects (Matsuda et al., 1995). SSCP is the electrophoretic separation of single-stranded nucleic acids based on subtle differences in sequence (often a single base pair) which results in a different secondary structure and a measurable difference in mobility through a gel.

The mutations in this study were discovered for the first time at the Oxford Medical School by Dr. Garry Brown and his colleagues, where the patients are currently under clinical investigation. The mutations were detected by employing patients' white blood cells to derive mRNA to prepare the relevant cDNA as a template for subsequent DNA sequencing. Two of these mutations are homozygous unusual 'in-frame' 3 base pair deletions in E2. One mutation is in the outer lipoyl domain of E2 leading to the deletion of glutamate 35 whereas the second mutation causes the loss of valine at position 455 that is located in the C-terminal domain. The third mutation leads to substitution of leucine for a phenylalanine at position 490 near the active site of E2. The main objective of this study was to evaluate the potential of our model recombinant PDC system for analysing newly-discovered genetic defects of this type. This evaluation should not only test the usefulness of this recombinant PDC model, but also lead to a detailed understanding of the precise basis of the molecular defects underlying the malfunctioning of the PDC complex in these patients. Another important aim was to correlate the findings with the severity of the clinical phenotype, methods of treatment and disease prognosis. These mutations could be producing a clinical phenotype by affecting a variety of properties of PDC including enzymatic function, enzyme-enzyme cooperativity, cofactor insertion, protein folding and complex assembly or stability. A description of the results achieved on detailed analysis of these three mutations is presented in this chapter.

4.2 Valine- 455 deletion in the E2 enzyme of PDC

This case study was characterised by deletion of a highly conserved valine at position 455 in the catalytic region of the E2 enzyme. A patient presented at Oxford Medical School with clinical symptoms corresponding to PDC deficiency. On clinical investigation, no detectable levels of E3BP were found. E2 levels were also found to be reduced, although this could represent partial loss of an epitope leading to loss of E2 recognition by the anti-E2 monoclonal antibody. A detailed analysis of E3BP DNA was carried out for the presence of any mutation; however, genomic and cDNA for E3BP was found to be free of mutations. This led to further analysis of E2 genomic DNA with the discovery of the absence of a 3 base pair sequence encoding a highly conserved valine at position 455. Interestingly, the patient was found to be heterozygous for this mutation at the genomic level; however, at the cDNA level only the mutant transcript was detected and the genetic basis for the absence of mRNA corresponding to the normal allele is still under investigation (unpublished data). As this deletion is in the C-terminal region, it had the potential to disrupt E2 core assembly or its interaction with E3BP. In previous studies also, mutations in one enzyme subunit have been found to promote concomitant loss of its binding partner. Thus, in the E1 enzyme of PDC, amino acids at positions 88, 263 and 382-387 were found to be essential for the linking of the alpha subunit with the beta subunit and for the activity of the holoenzyme (Marsac et al., 1997). In this study, these mutations in the gene for E1α caused depletion in the levels of not only E1α, but also of E1β.

E3BP does not normally have an independent existence and it was postulated that the E2-located valine deletion may affect integration of E3BP into the native core assembly. Therefore, examining whether or not the absence of E3BP protein was a secondary phenomenon induced by the E2-linked valine 455 deletion was the main focus of this study.

4.2.1 Creating the ΔV455 mutation in the E2 enzyme by site-directed mutagenesis

To mimic this mutation, standard site-directed mutagenesis was performed as discussed in Methods (section 2.2.11) using full length E2 cDNA housed in pET-14b as well as a non His-tagged version housed in pET-11b for co-expression with E3BP (housed in pET-28b). Mutagenic primers as described in Materials & Methods section 2.1.3 were used in both constructs. The insertion of the correct mutation was checked by DNA sequencing.

4.2.2 Overexpression and purification of the ΔV455 E2 enzyme

E2-pET-14b was transformed into *E. coli* BL21 (DE3) Star cells and overexpressed at 30 ºC for 4-5 h. Overexpression was checked by SDS-PAGE analysis (Fig. 4.1). Mutant E2 was purified in the same way as the wild-type using zinc metal chelate chromatography and gel filtration. Purified fractions were analysed by SDS-PAGE (Fig. 4.2). Purified mutant enzyme was subsequently used for comparing its acetyltransferase activity with wild-type E2 as described in section 4.2.4.

4.2.3 Checking assembly of the ΔV455 E2:E3BP core by overexpression and purification

The purification protocol for the co-expressed E2:E3BP 'core' relies on capturing E2 only when it is tightly bound to His-tagged E3BP so if E3BP failed to integrate correctly, the mutant E2 subunit will either be completely absent in purified E3BP preparations or present in reduced amounts. A failed association of mutant E2 and E3BP was predicted as a possible outcome resulting from this mutation. Clinical evaluation had also indicated the

absence of E3BP, possibly due to non integration, leading to its subsequent rapid degradation.

To test this hypothesis, wild-type and ΔV455 E2 pET-11b constructs were co-transformed respectively, with the E3BP pET-28b construct. Both wild-type and mutant E2:E3BP cores were overexpressed and purified in the same way as previously described for the wild-type E2:E3BP core (Chapter 3, sections 3.3 & 3.4) The mutant core was also found to be associating properly and the subunit composition of wild-type and mutant cores appeared very similar as judged by SDS-PAGE analysis (Fig. 4.3). The same experiment was repeated by overexpressing wild-type and mutant cores at 37 ºC i.e. normal body temperature to determine whether the mutation was temperature sensitive. However, similar results were obtained compared to the experiment carried out at 30 ºC (data not shown).
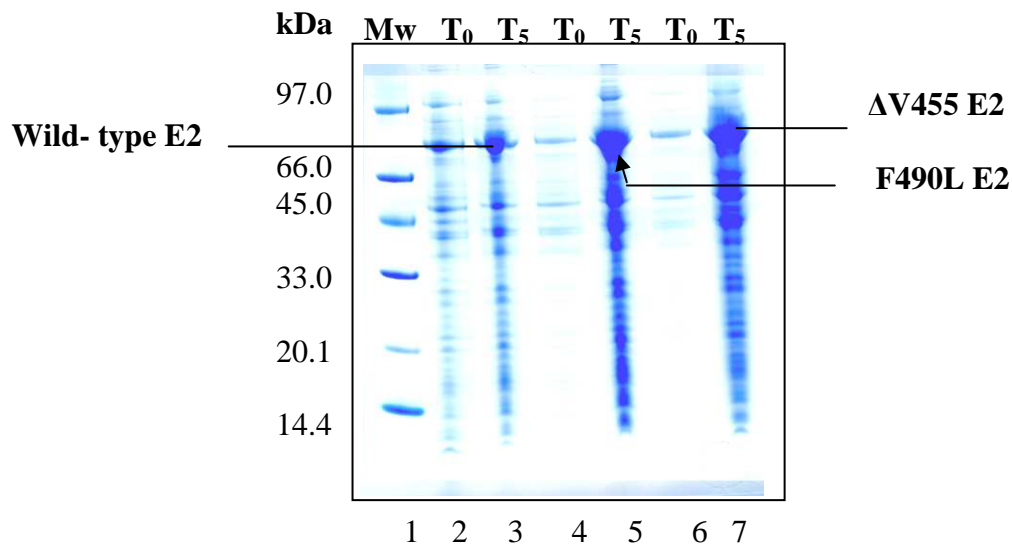
Figure 4.1 Overexpression of wild-type, ΔV455 and F490L E2 enzymes

SDS-PAGE analysis of overexpression of wild-type (lane 3), F490L (lane 5) and ΔV455 (lane 7) recombinant E2 enzymes on a 4-12% Bis-Tris gel. The overexpressions were carried out in *E. coli* BL21 (DE3) Star cells at 30 ºC for 4-5 h and are shown at zero time (T_0) and 5 h after induction (T_5). Molecular weight markers (Mw) are in lane 1. See section 4.3.2 for further analysis of the F490L mutation.

Mw
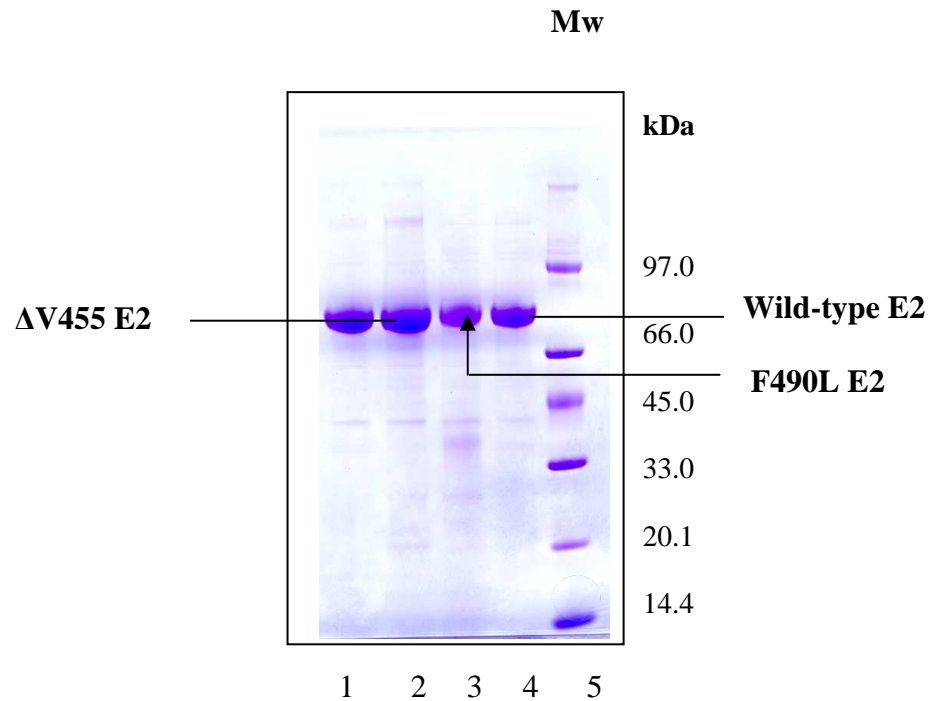
Figure 4.2: Purification of wild-type, ΔV455 and F490L E2 enzymes

SDS-PAGE analysis of purified ΔV455 (lanes 1 & 2), F490L (lane 3) and wild-type (lane 4) E2 enzymes on a 4-12% Bis-Tris gel. Wild-type and mutant enzymes were purified by zinc chelate chromatography. Molecular weight markers (Mw) are in lane 5.

A

B
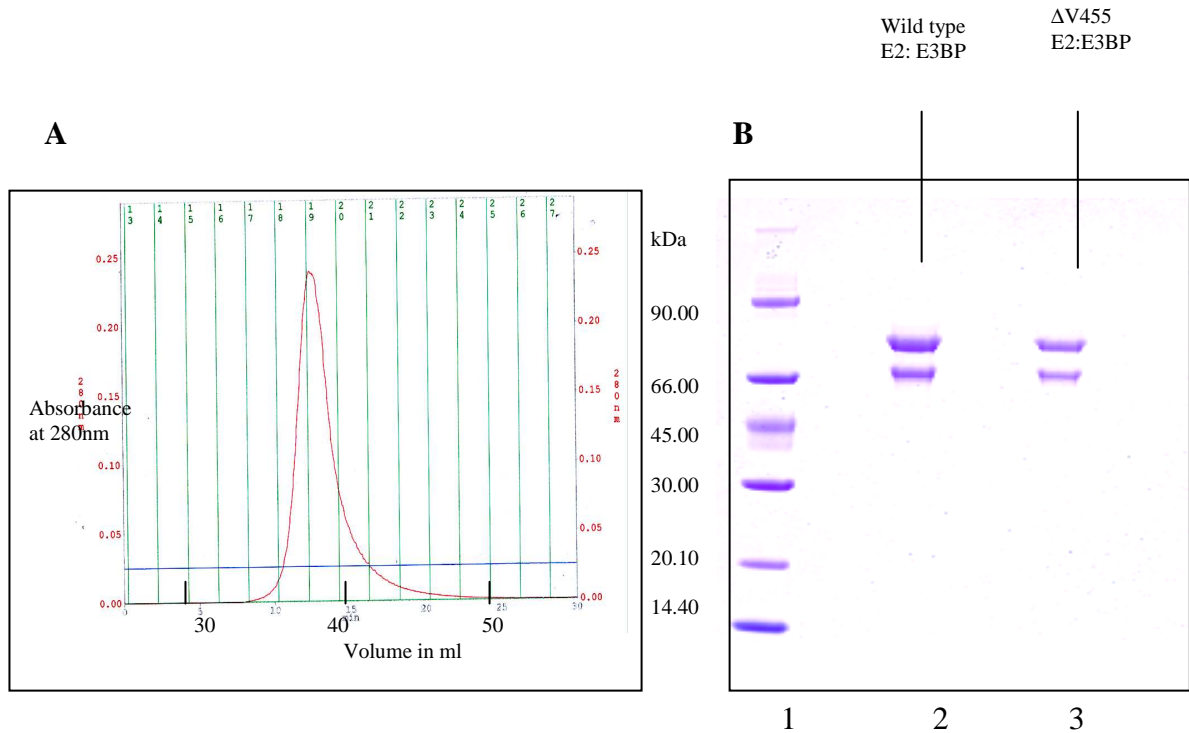
Figure 4.3: Integration of E3BP with E2 in ΔV455 and wild-type E2:E3BP cores

(A) Gel filtration profile of the ΔV455 E2:E3BP core showing a single peak eluting at the void volume. Prior to gel filtration on a HiPrep 16/60 Sephacryl S-300 High Resolution column attached to a BioCAD 700E workstation, the His-tagged E2:E3BP core was purified by zinc metal chelate chromatography.

(B) SDS-PAGE analysis of gel filtered wild-type and ΔV455 E2: E3BP cores on a 4-12% Bis-Tris gel shows that E3BP is integrated into the ΔV455 E2 core (lane 3) and was comparable to wild-type E2:E3BP core (lane 2). Molecular weight markers (Mw) are in lane 1.

4.2.4 Enzymatic activities of the ΔV455 E2 enzyme, E2:E3BP core and reconstituted PDC

The acetyltransferase activities of the wild-type and ΔV455 E2 recombinant enzymes were determined according to the protocol described in Methods section 2.3.16. The enzymatic activity of the mutant E2 was approx. 50% of wild-type, taken as 100% control (Fig. 4.4 A). Similarly, the acetyltransferase activities of recombinant wild-type and mutant E2:E3BP cores were determined to check whether the presence of E3BP led to retention of normal activity. However, the activity of the mutant core was again found to be low as compared to the wild-type E2:E3BP core (Fig. 4.4 B). In the next step, wild-type and recombinant PDCs were reconstituted from purified recombinant PDC components and enzymatic activities determined as described in Methods section 2.3.17. The overall activity of the mutant complex was also reduced to approx. 50% as compared to wild-type complex (Fig. 4.4 C). All enzymatic assays were performed in duplicate and equal amounts of enzymes used in each experiment.

4.2.5 Western blot analysis of the wild-type and ΔV455 E2: E3BP cores

Purified wild-type and ΔV455 E2:E3BP recombinant cores were subjected to Bradford assays and equal amounts were used to perform Western blotting with a monoclonal antibody (PD2) that recognises only lipoylated components of PDC.

The ability of the ΔV455 E2:E3BP core to undergo lipoylation was not lost and was comparable to wild-type core as determined by Western blotting (Fig. 4.5).
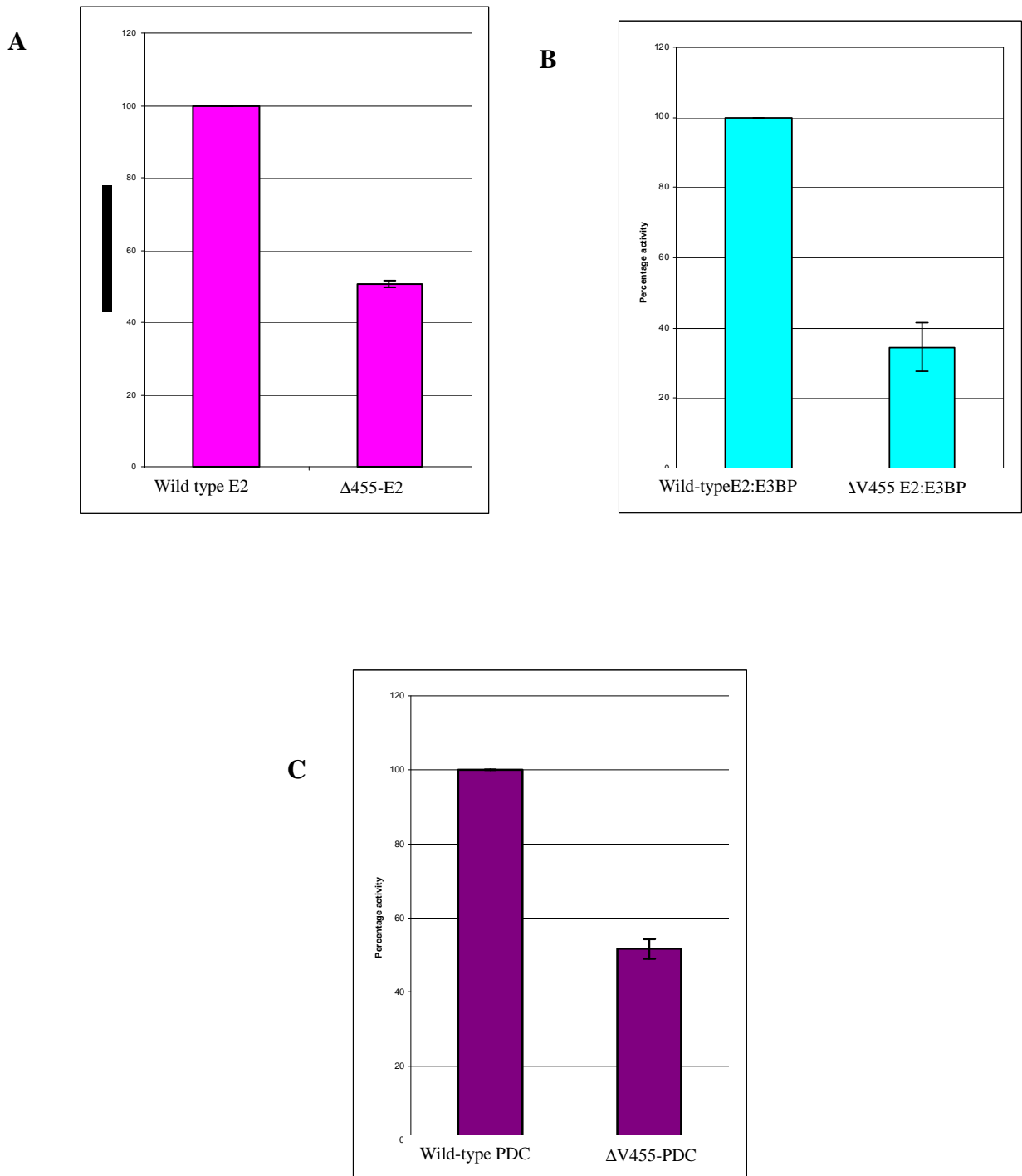
Figure 4.4: Comparison of enzymatic activities of the wild-type and ΔV455 E2 recombinant enzymes, E2:E3BP cores and PDCs

Panels A & B show the reduced acetyltransferase activities of the mutant E2 and E2:E3BP cores a as compared to the wild-type E2 and the core. In panel C, wild-type and mutant PDCs were reconstituted from individual components and enzymatic activities compared. The activity of the mutant PDC is reduced as compared to the wild-type. All samples were assayed in duplicate and error bars shown where necessary.

A   **Mw**

B
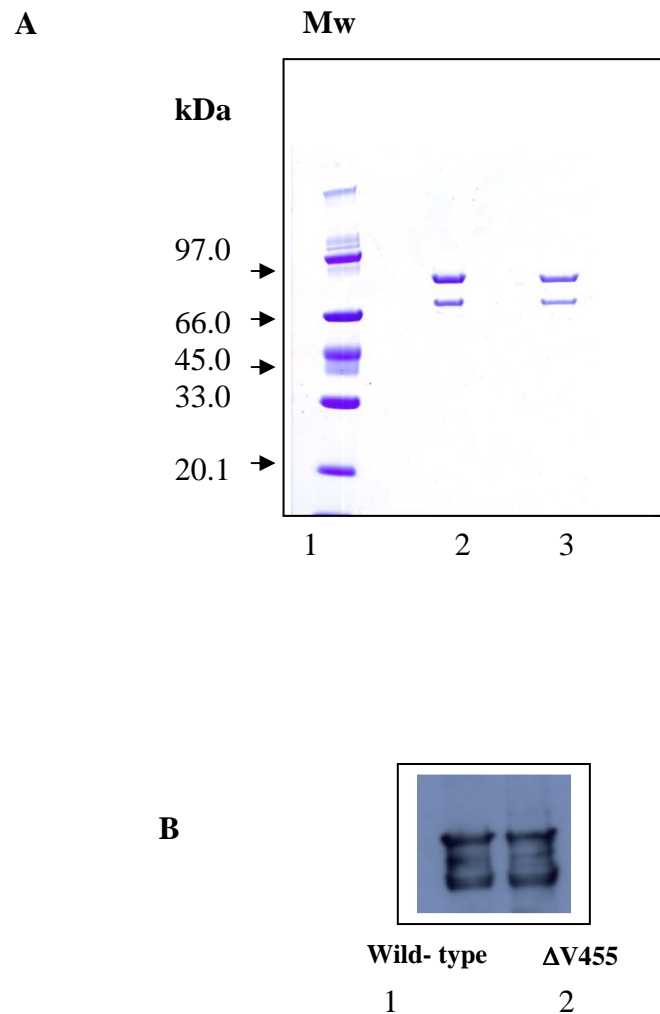
Wild- type   ΔV455
1   2

Figure 4.5: Western blot analysis of wild-type and ΔV455 E2:E3BP cores

(A) SDS-PAGE analysis of wild- type (lane 2) and ΔV455 E2:E3BP (lane 3) cores on a 4-12% Bis-Tris gel. Equal amounts of protein were loaded prior to Western blotting. Molecular weight markers (Mw) are in lane 1.

(B) Western blot analysis of wild-type and ΔV455 E2:E3BP cores with PD2 antibody shows that mutant core (panel B, lane 2) was also lipoylated and lipoylation was comparable to wild-type E2:E3BP core (panel B, lane 1).

4.2.6 Far uv and fluorescence emission spectra of the wild-type and ΔV455 E2:E3BP cores

Purified and gel filtered recombinant wild-type and ΔV455 E2:E3BP cores, dialysed in 50 mM KH_2PO_4 buffer, were subjected to far uv spectrophotometry in the 190 to 260 nm range as described in Methods section 2.3.20. At these wavelengths the chromophore is the peptide bond. Alpha-helix, beta-sheet and random coil structures each give rise to a characteristic shape and magnitude of CD spectrum. The CD profile shown in Fig. 4.6 suggested that there was no major change in the structure of the mutant core as its overall line-shape is the same as for wild-type. It was not possible to determine the alpha helix and beta sheet content as the data were not of good quality below 200 nm.

A potential change in structure was also studied using intrinsic tryptophan fluorescence as described in Methods section 2.3.21. No shift in the wavelength of the fluorescence emission spectrum was observed in the mutant core and the result was comparable to wild-type E2:E3BP (Fig. 4.7).
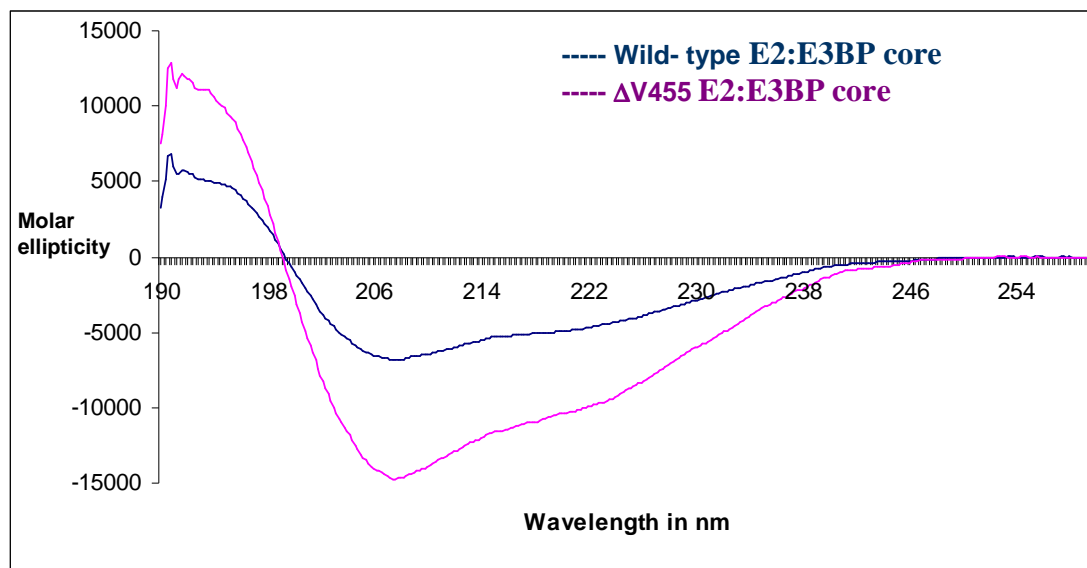
Figure 4.6: Far uv CD spectra of wild-type and ΔV455 E2:E3BP cores

Wild-type and ΔV455 E2:E3BP cores were subjected to circular dichroism analysis and spectra recorded in the far uv region (190-260 nm). The CD signal was measured as molar ellipticity in degrees cm^2 dmol^{-1} (Y-axis) as a function of wavelength (X-axis).
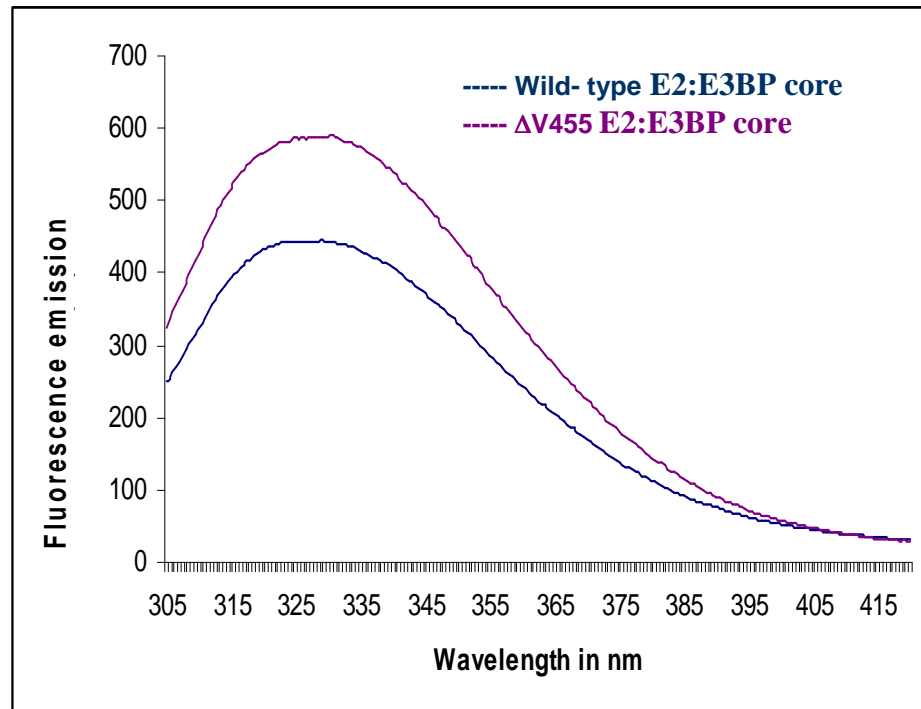
Figure 4.7: Fluorescence emission spectra of the wild-type and ΔV455 E2:E3BP cores

Wild-type and ΔV455 E2:E3BP cores were excited with uv light of wavelength 295 nm. Fluorescence emission (in arbitrary units) was recorded over a range of 310-420 nm. Maximum emission of fluorescence occurred at 330 nm for wild-type as well as for the ΔV455 E2:E3BP core.

4.2.7 Comparison of sedimentation coefficients of the wild-type and ΔV455 E2: E3BP cores

Sedimentation velocity is an analytical ultracentrifugation method that measures the rate at which molecules move in response to centrifugal force. This sedimentation rate provides information about both the molecular mass and the shape of molecules. Sedimentation velocity experiments were performed as described in Methods section 2.3.19.2 to obtain more information on the assembly of the ΔV455 E2:E3BP core as compared to the wild-type core. For sedimentation velocity experiments, wild-type and mutant E2:E3BP cores were co-expressed, purified (see sections 3.3 & 3.4), gel filtered (Methods section 2.3.12) and SDS-PAGE analysis performed to check the purity of the cores. No proteolysis or degradation was evident from SDS-PAGE analysis (Fig. 4.8 E). The sample concentrations were 3.33, 1.07 and 1.00 μM for the wild-type and 3.17, 3.45 and 0.88 μM for the mutant. Samples (380 μl) were loaded into 12 mm double sector centrepieces and data recorded at 4 ℃ at a rotor speed of 20,000 rpm using interference optics. A series of 360 scans, 60 s apart was taken for each sample. Sedimentation coefficients were determined using SEDFIT (Schuck, 2000). The weight average $s_{4,w}$ values were corrected to $s_{20,w.}$ The weight average sedimentation coefficient, $s_{20,w}$ for the wild-type core was determined as 30.61 ± 0.36 S (Fig. 4.8 A). The reported value of human E2:E3BP core is 32 S (Hiromasa et al., 2004). Behal et. al. (1994) reported sedimentation coefficients of 30 and 32 S for native E2:E3BP core at $A_{280} = 0.25$ and 0.5 respectively. They also observed sedimentation coefficient heterogeneity with increasing concentration. The weight average sedimentation coefficient, $S_{20,w}$ for the mutant cores was determined as 28.89 ± 0.0 S (Fig. 4.8 C), slightly lower than for its wild-type equivalent. The mutant core also appeared to be more heterogenous than the wild-type indicating that there might be a degree of perturbation in its structure. However, this difference could also be caused by sample variability as only one sample preparation was analysed due to time constraints. More rigorous analysis of several mutant preparations would be necessary to confirm a significant difference.

A

B

c

D

E

ΔV455 E2: E3BP
Wild-type E2: E3BP
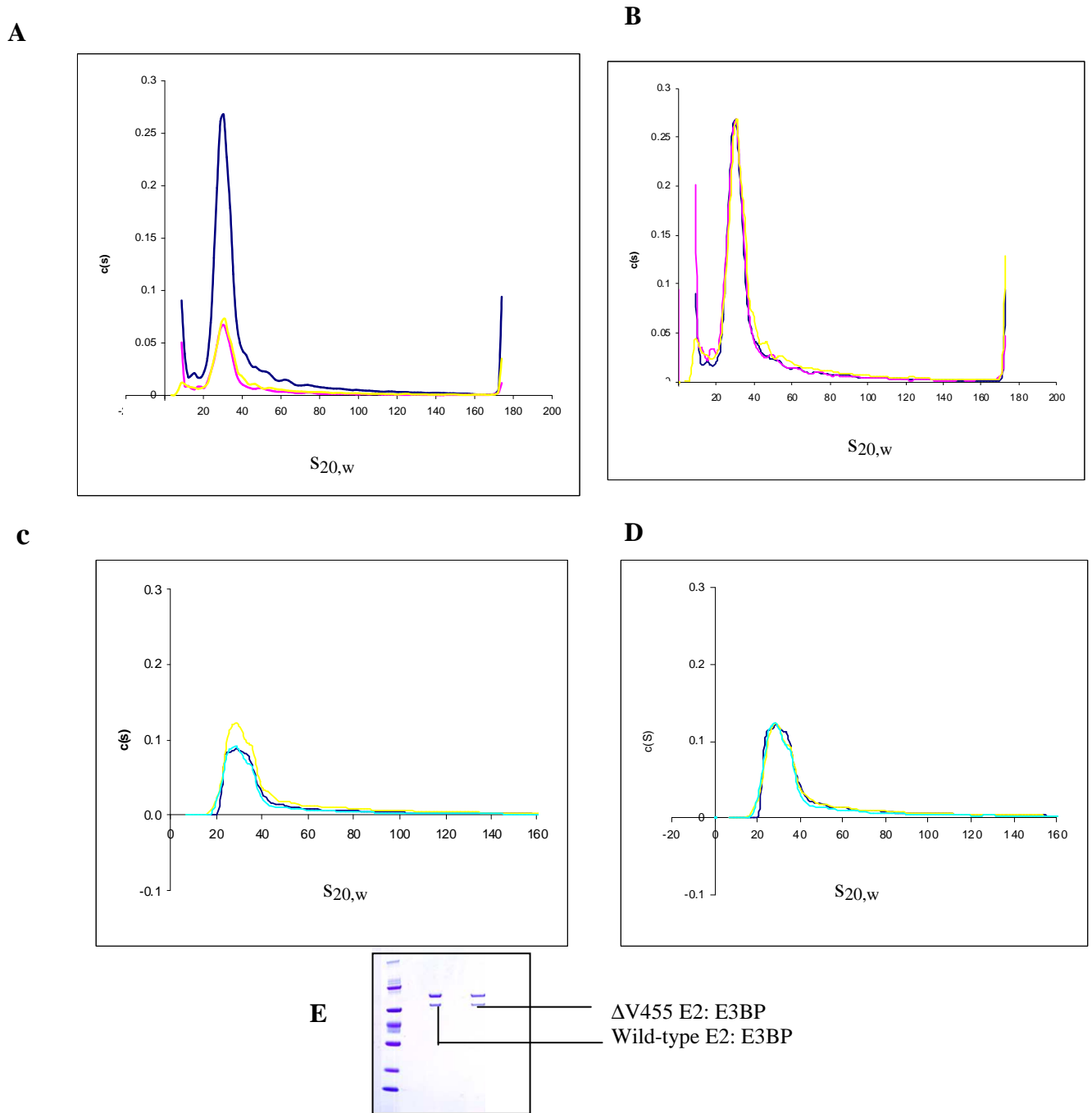
Figure 4.8: Comparison of the sedimentation velocity analyses of the wild-type and ΔV450 E2: E3BP cores

c(s) distribution from SV interference data for 3.33 μM (——) , 1.07 μM (——) and 1.00 μM (——) wild-type E2:E3BP core (Fig. A) and distribution of the same after maximising c(s) to the peak observed at 30.40 S (Fig. B). c(s) distribution from SV interference data for 3.17 μM(——), 3.45 μM (——) and 0.88 μM (——) ΔV450 E2:E3BP core (Fig. C) and c(s) distribution of the same after maximising c(s) to the peak observed at 28.89 S (Fig. D). SDS-PAGE analysis of the wild-type and mutant cores used in SV experiment (Fig. E).

4.2.8 Discussion of the effects of valine-455 deletion on the E2 enzyme of PDC

Our PDC model was employed here to study the influence of a specific valine deletion (val 455) in the catalytic region of the E2 enzyme. This deletion was encountered in a patient with no detectable E3BP and reduced levels of E2. Therefore, it was anticipated that this deletion could be disrupting the formation of the E2:E3BP core with the subsequent degradation of E3BP. Such disruption has also been observed in patients with a defect in the E1α component leading to severe concomitant depletion of E1β (Saijo et al., 1996) presumably induced by an impaired ability to form heterotetrameric E1. However, no large scale disruption was detected in the recombinant mutant core and integration of E3BP appeared normal at both 30 ℃ and 37 ℃ (Fig. 4.3). Moreover, lipoylation of the E2:E3BP domains was not affected as predicted since this mutation is located in the C-terminal domain away from N-terminal lipoyl domains (Fig. 4.5). No major changes in secondary or tertiary structure were detected as determined by far uv spectrophotometry and fluorescence emission spectroscopy (Fig. 4.6 & Fig. 4.7) also suggesting that there was no gross perturbation of the E2:E3BP core assembly. A degree of heterogeneity of sedimentation coefficient was observed as compared to wild-type core (Fig. 4.8) although there was insufficient time to investigate the reproducibility of this phenomenon.

However, this mutation did result in an overall reduction of PDC activity. The loss of activity was found in the mutant E2 enzyme, E2:E3BP core and at PDC level also (Figs. 4.4 A, B & C). This could be due to partial disruption of the catalytic function of the E2 enzyme. Indeed the deleted valine 455 is in the C-terminal region that houses the acetyltransferase active site. Resolution of the structure of the E2 of *A. vinelandii* showed two highly conserved residues-a histidine and an aspartic acid implicated in catalysis (Mattevi et al., 1993c). A third important residue His-610 in *A. vinelandii* E2 PDC was also confirmed to play a catalytic role (Mattevi et al., 1993a). A conserved sequence motif, DHRXXDG, is thought to accommodate the histidine and aspartate necessary for catalysis (Radford et al., 1987). The valine residue deletion currently under investigation, is located 76 amino acids before the conserved sequence motif in human E2.

Defects in the E2 enzyme of PDC were reported for the first time by (Robinson et al., 1990) with clinical symptoms comprising reduced PDC activity and lactic acidaemia. Only two other mutations in E2 have been recently reported (Brown et al., 2004).

In this analysis, it was seen that a stable E2:E3BP core was forming as assessed by AUC (Fig. 4.8). Possible structural alterations in the E2:E3BP core were evident from the heterogeneity of the peak of the mutant as compared to the wild-type core on sedimentation analysis. However, no major changes were detectable by far uv CD spectrophotometry and tryptophan fluorescence. In addition, there was significant loss of mutant PDC activity as compared to the wild-type PDC (Fig. 4.4 C). Substantial residual activity was retained in the mutant recombinant complex which was comparable to the patient's PDC activity as measured by CO_2 release assay (unpublished data, personal communication, G. Brown). As the E2 enzyme is the structural and functional centre of the PDC, its complete disruption is unlikely since it is required to sustain foetal development.

Our data in this case could not readily be reconciled with the patient's situation, because this mutation seemed to cause disruption of E2:E3BP core with reduced amounts of E2 and complete absence of E3BP in the patient. Interestingly, the genomic DNA analysis carried out by Dr. Garry Brown and colleagues detected no abnormality in E3BP genomic DNA. Moreover, the patient appears to produce mRNA exclusively from the mutant E2 allele. A complete re-evaluation of the patient's enzymatic, immunological and genetic status with regard to PDC deficiency is currently in progress.

Another similar type of case has been reported recently, where a patient displayed a clinical phenotype consistent with PDC deficiency (Dahl et al., 1992). Cultured skin fibroblasts from this patient demonstrated 55% reduction in PDC activity and markedly decreased immunoreactivity for the E1β. Surprisingly there were no pathological mutations in *PDHA* and *PDHB* genes coding for E1α and E1β subunits, respectively. However, PDC activity could be restored in cells from this patient and normal levels of E1β detected following treatment with MG132, a specific proteasomal inhibitor and with tryphostin 23, a specific inhibitor of epidermal growth factor receptor protein tyrosine kinase (EGFR-PTK). This study proposed that high basal levels of EGFR-PTK activity led to ubiquitination of cellular proteins. However, in this study it was unclear that why only E1β protein was prone to this process in the absence of any mutations and how mitochondrial proteins gained access to proteasomes located in the cytosolic and nuclear compartments.

In our study, the reduced levels of E2 and loss of E3BP in the patient could be due to enhanced degradation where E2 harbours a potentially pathological mutation and as a result E3BP may also remain unbound to E2 leading to their reduced levels. No such degradation could be observed employing our recombinant PDC model produced in *E. coli* where there is no equivalent proteasomal machinery and no translocation or processing of precursor polypeptides is required; hence, the defective mature protein may also assemble to form a core structure under these conditions.

Indeed the data in this study suggest that although there may be some minor structural changes in the E2:E3BP core and there is an overall reduction in enzymatic activity the core has not failed to assemble in *E. coli*. However, this may not be the case in human cells where mutant or partially–misfolded proteins may be more readily recognised and degraded leading to a more obvious phenotype.

4.3 Phenylalanine–490 to leucine mutation

This case study was characterised by substitution of phenylalanine- 490 by leucine in the catalytic region of the E2 enzyme. A male patient born to first cousins presented at Oxford Medical School with clinical symptoms mainly of episodic dystonia, but also with significant developmental delay. Development was normal until 11 months of age but, after that there were episodes of arching of the body, stiffening of the limbs with flexion of wrists, eye-rolling and distress. Developmental progress slowed down, paroxysmal dystonia continued and at the age of eight years the patient was wheelchair bound. Dystonia, either as a main clinical feature or in combination with other neurological manifestations, is increasingly being recognized in patients with PDC deficiency (Brown et al., 2004; Lissens et al., 1996). The lactate concentration in both blood and cerebro-spinal fluid in the patient was normal. Neuropathology of PDC deficient patients has been found to be quite variable. In this patient, localised neuroradiological findings revealed circumscribed lesions restricted to the globus pallidus bilaterally. However, this finding and other clinical symptoms were also not distinctive and consistent with features of PDC deficiency. Therefore, diagnosis alone on clinical symptoms and biochemical tests was not enough and prompted more detailed investigations.

Various other conditions were ruled out before this mutation was diagnosed by using the patient's mRNA to prepare the relevant cDNA as a template for subsequent DNA sequencing by Dr. Garry Brown and his colleagues. They further found an approx. 50% decline in PDC activity in crude fibroblast extracts by the radiolabelled CO_2 release assay. This assay is not particularly accurate as the extent of inhibition is difficult to assess precisely since normal (wild-type) levels of PDC activity vary over a 2-fold range in individual patients. Moreover, from this assay alone, it was not clear whether the decline in activity was caused by loss of E2 activity per se or as an indirect effect caused by disruption in E2 interaction with E3BP or alterations in the core assembly. Therefore, the focus of this study was to determine if this represented a straightforward case of reduced enzymatic activity of E2 resulting from alterations in a residue that may be involved in the catalytic mechanism. Changes in structure and assembly of the E2:E3BP core were also assessed in the following experiments.

4.3.1 Creating the F490L mutation in the E2 enzyme by site-directed mutagenesis

To mimic this mutation, site-directed mutagenesis was performed by preparing and using appropriate primers described in Materials & Methods section 2.1.3. Standard site-directed mutagenesis was performed as discussed in Methods section 2.2.11 using full length E2 cDNA housed in pET-14b and also in pET-11b for co-expression with E3BP in pET- 28b. The presence of the correct mutation was checked by DNA sequencing.

4.3.2 Overexpression and purification of the F490L E2 enzyme

E2 pET-14b was transformed into *E. coli* BL21 (DE3) Star cells and overexpressed at 30 ºC for 4-5 h. Overexpressions were analysed by SDS-PAGE (Fig. 4.1). Mutant E2 enzyme was purified in the same way as wild-type using zinc chelate chromatography and gel filtration. To check the purity of the proteins, SDS-PAGE analysis of purified fractions was performed (Fig. 4.2). Purified mutant enzyme was subsequently used for comparing acetyltransferase activity with the wild-type E2 as described in section 4.3.4.

4.3.3 Checking integration of the F490L E2:E3BP core by overexpression and purification

F490L E2-pET-11b was co-expressed with the E3BP pET-28b construct at 15 ºC. Mutated and wild-type E2:E3BP cores were purified in the same way as wild-type core described in Chapter 3, section 3.4. The core was not found to be disrupted by the presence of the F490L mutation, as was evident from zinc chelate chromatography and gel filtration. In this case also, E2 was found to interact stably with E3BP and the integrated core could be purified owing to the presence of the N-terminal His-tag on E3BP (Fig. 4.9).

kDa Mw

97.0 ──────────── **F490L E2:E3BP**

66.0 ──────────── **Wild-type E2:E3BP**
45.0

33.0

20.1
14.4
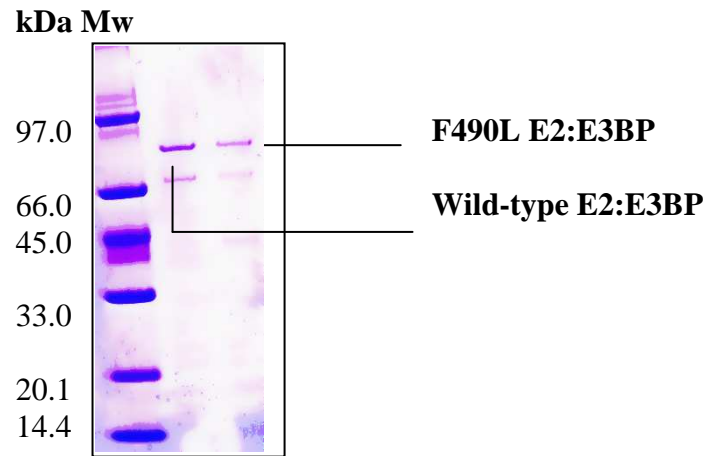
Figure 4.9: Integration of E3BP with E2 in F490L mutation

SDS-PAGE analysis of purified wild-type and F490L E2:E3BP cores on a 4-12% Bis-Tris gel. The presence of E2 in the F490L core shows that E3BP is integrated into E2 (lane 3) and was comparable to wild-type E2:E3BP core (lane 2). Molecular weight markers (Mw) are in lane 1.

4.3.4 Enzymatic activities of the F490L E2 enzyme, E2:E3BP core and PDC

The acetyltransferase activities of the recombinant wild-type and F490L E2 enzymes were determined using the protocol described in Methods section 2.3.16. The activity of the mutant E2 was found to be approx. 50% of native E2 taken as 100% control (Fig. 4.10 A). Similarly, the acetyltransferase activity of the wild-type and F490L E2:E3BP cores were determined using the same protocol. The activity of the mutant core was also found to be low as compared to wild-type E2:E3BP core (Fig. 4.10 B). Wild-type and mutant PDCs were reconstituted as per the protocol described in Chapter 3 (see section 3.10). Enzymatic activity was determined as described in the Methods section (2.3.17). The overall activity of the F490L PDC was found to be reduced by approx. 30% as compared to wild-type complex (Fig. 4.10 C).

A

B

C
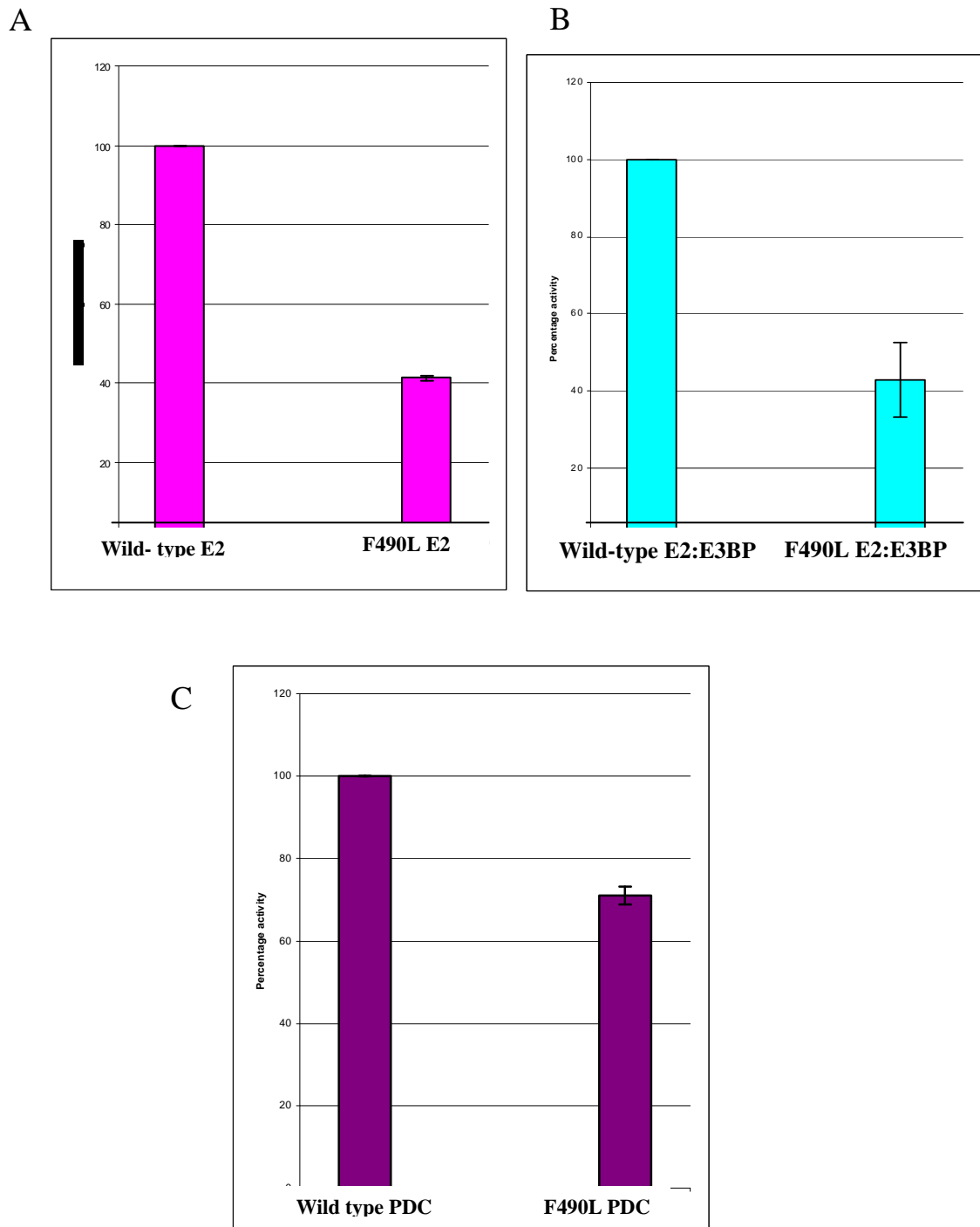
Figure 4.10: Comparison of the enzymatic activities of recombinant wild-type and F490L E2 enzyme, E2:E3BP core and PDC

Panels A & B show the reduced acetyltransferase activities of the mutant E2 and E2:E3BP cores are as compared to the wild-type E2 and core. In Panel C, wild-type and mutant PDC were reconstituted from individual components and enzymatic activities compared. Activity of the mutant PDC is also reduced compared to wild-type. All samples were assayed in duplicate and error bars shown where necessary.

4.3.5 Far uv and fluorescence emission spectra of the wild-type and F490L E2:E3BP cores

The secondary structure of the mutant core was estimated using far uv spectrophotometry in the far uv spectral region (190-250 nm) as described in Methods section 2.3.20. The data were not of good quality in the 190-200 nm region (not shown) and therefore percentage of alpha helices and beta sheets could not be estimated. However, the line shapes of the spectra in the 200-280 nm region were similar overall for the mutant as well as wild–type core. This indicated that there were no major changes in the secondary structure of the mutant core as compared with the wild-type core (Fig. 4.11).

Change in structure was also studied using tryptophan fluorescence as described in Methods section 2.3.21. However, no shift in the spectral emission peak (330 nm) was observed between the mutant and the wild-type E2:E3BP cores (Fig. 4.12). This suggested that there was no perturbation of the local environment in the region occupied by the six tryptophan residues located in the E2:E3BP core.
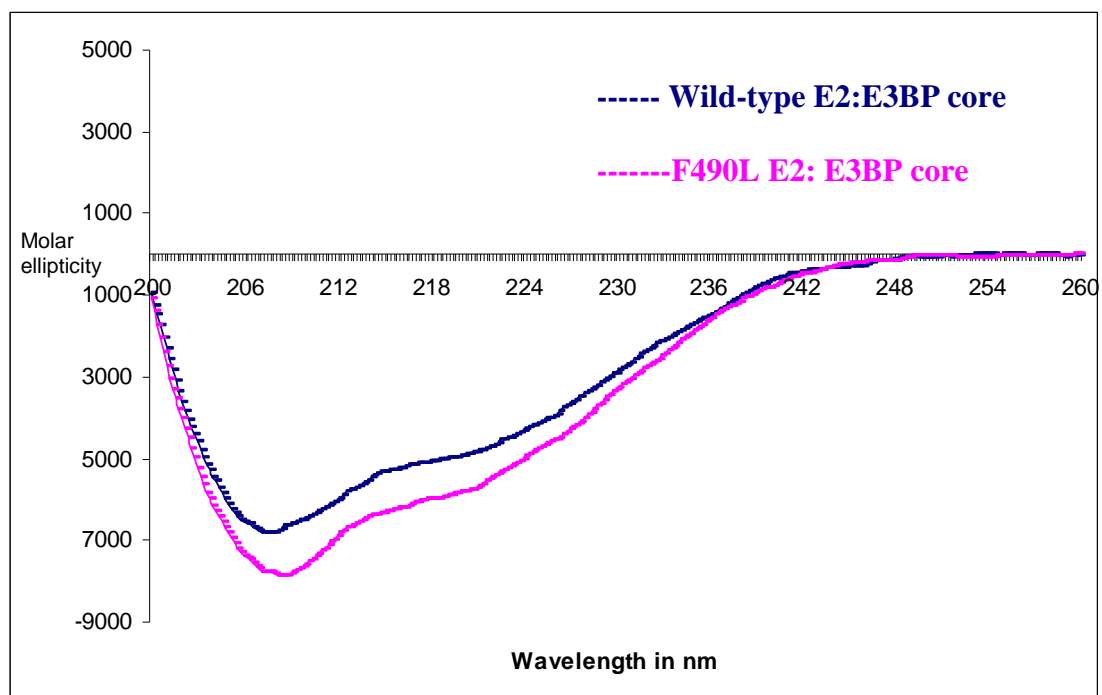
Figure 4.11: Far uv CD spectra of the wild-type and F490L E2:E3BP core

Wild-type and F490L E2:E3BP cores were subjected to circular dichroism and spectra recorded in the far uv region (190-260 nm). The CD signal was measured as molar ellipticity in degrees cm^2 dmol^{-1} (Y- axis) plotted as a function of wavelength (X -axis).
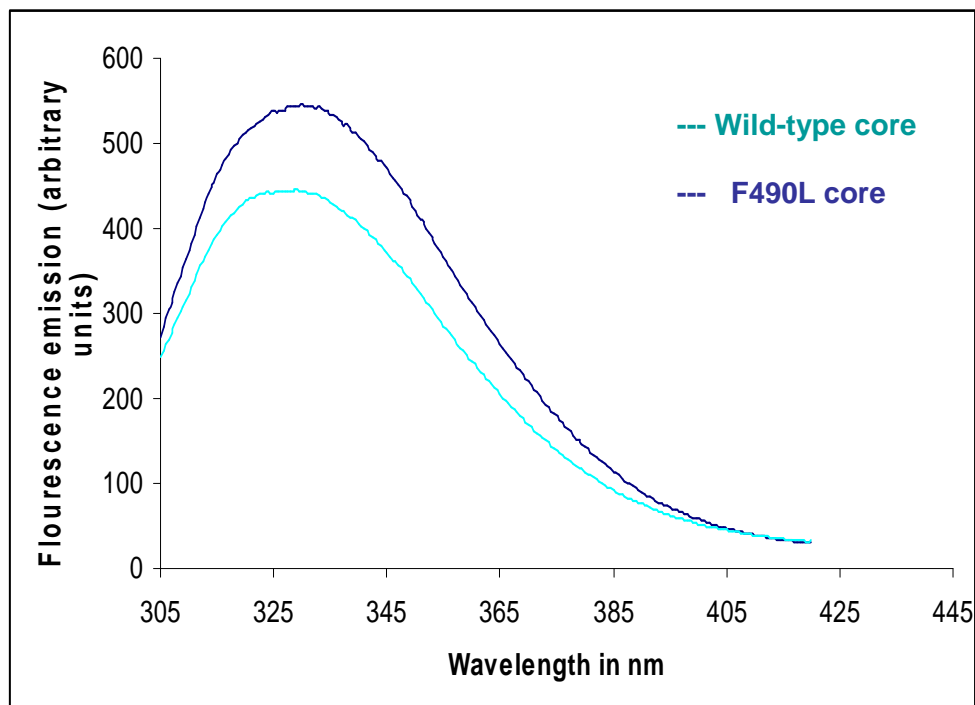
Figure 4.12: Fluorescence emission spectra of wild-type and F490L E2:E3BP cores

Wild-type and F490L E2:E3BP cores were excited with uv light of wavelength 295 nm. Emission of fluorescence was recorded over a range of 310-420 nm. The figure shows that the maximum emission of fluorescence occurred at 330 nm wavelength for wild-type and F490L E2:E3BP cores.

4.3.6 Discussion of phenylalanine–490 to leucine mutation

This mutation was found to cause reduced PDC activity and various clinical symptoms in a patient (Brown et al., 2004). Our data provided an explanation for the functional consequences of this deletion. The E2:E3BP core appeared to be integrating stably as evidenced from zinc chelate chromatography, gel filtration (Fig. 4.9), circular dichroism (Fig. 4.11) and tryptophan fluorescence studies (Fig. 4.12). However, there was loss of enzymatic activity in mutant E2, E2:E3BP core and recombinant PDC (Figs. 4.10 A, B & C). Earlier also, this mutation was shown to be responsible for reduced PDC activity by functional complementation in which activity was restored by transfecting normal E2 cDNA into patient's fibroblasts (Brown et al., 2004). However, in that study full activity could not be restored. Demonstration of loss of acetyltransferase activity using a recombinant model of PDC not only substantiated the functional complementation study but also provided more definitive diagnosis. The recombinant mutant PDC in this study lost about 50% enzymatic activity as compared to the normal or wild-type PDC. Thus, this mutation appears to be the reason for the loss of PDC activity in the patient also.

This mutated phenylalanine residue is highly conserved across various eukaryotic and prokaryotic species and is reported to be responsible for substrate specificity in E2 (Mattevi et al., 1993b) thus replacement of the phenylalanine by the smaller leucine residue could potentially affect acetyltransferase activity. In the corresponding position in the E2 enzyme of BCOADC, this position is occupied by serine, and it is proposed that the larger phenylalanine limits access to the active site to the smaller acetyl group substrate of E2-PDC (Mattevi et al., 1993c). Another plausible explanation could be that the catalytic activity is affected as this mutation is located 42 amino acids from the conserved motif, DHRXXXDG that is important for E2 catalytic activity and could potentially perturb the local environment in this active site region. Substantial residual enzymatic activity was retained, however, in agreement with PDC activity measurements on patient fibroblasts employing the CO_2 release assay. Thus it is apparent that this mutation does not cause large-scale changes in the assembly of the 'core' that might have caused more severe loss of PDC function. In general all of these data are consistent with the F490L mutation having a direct affect on E2 activity and the underlying catalytic mechanism.

4.4 Glutamate 35 deletion in the E2 enzyme

In this section the role of the glutamate 35 deletion in the outer lipoyl domain of the E2 enzyme in a young patient was investigated. The patient was a male born at term to first cousins. He was in a good mental condition and the main clinical features were ataxia and dystonia, which developed at an early stage. He was introduced to a ketogenic diet that significantly resolved the symptoms. However, residual problems in fine-motor coordination still persisted at the age of 11 years. As ataxia and dystonia are increasingly being noted in PDC deficient patients, this led to a check for any abnormalities in genes encoding PDC subunits leading to discovery of this mutation.

On sequencing cDNA derived from patient's white blood cells, a highly conserved 3 base pair sequence encoding glutamate 35 in the outer lipoyl domain of the E2 enzyme was found to be missing. The involvement of this deletion in promoting reduced PDC activity was determined by functional complementation by expressing normal E2 in the patient's fibroblasts. However, many questions remained unanswered as to how this mutation could lead to PDC deficiency since it affected only one lipoyl domain out of three in the E2:E3BP core. In previous studies, the presence of all E2-linked lipoyl domains were not found to be necessary for maximal *E. coli* PDC activity *in vitro* (Fussey et al., 1988). However, isogenic *E. coli* strains with three active lipoyl domains outgrew those with just one or two indicating that the loss of lipoyl domains does reduce PDC efficiency *in vivo* (Fussey et al., 1988). In this case study, however, there was about 70% reduction in PDC activity, as determined by CO_2 release assay. This drastic loss of activity could not be readily accounted for solely by potential loss of lipoylation in the outer lipoyl domain since, there are an additional 72 inner and E3BP lipoyl domains in PDC, that should be unaffected. Our own data in this thesis in Chapter 3 (see section 3.14, Fig. 3.12) also suggest that loss of lipoylation of the outer domain in E2-PDC only causes 25-30% loss of enzymatic activity. Therefore, the main aim of this study was to determine how this mutation induced such a substantial decline in overall PDC activity.

4.4.1 Creating the E35D, E35Q and ΔE35 mutants of the outer lipoyl domain

To study the role of this mutation, a 3 base pair 'in frame' deletion encoding glutamate 35 in a GST outer lipoyl domain fusion construct (already available in laboratory) was created by site-directed mutagenesis using primers described in Materials & Methods section 2.1.3.

Two other mutants of the lipoyl domain fused with GST were also created. In one construct, glutamate-35 was substituted by an aspartate (E35D) and in the other with a glutamine (E35Q) again by employing the relevant primers (Materials and Methods, section 2.1.3). These mutants were created to study the possible influence of charge and size of amino acid at this position when comparing with the ΔE35 mutant of the outer lipoyl domain. All mutations were checked by DNA sequencing as described in Methods section 2.2.7.

4.4.2 Overexpression and purification of the wild-type, E35D, E35Q and ΔE35 lipoyl domains

Wild-type, ΔE35, E35D, E35Q outer lipoyl domains and non-lipoylated K173Q inner lipoyl domain constructs in pGEX-2T were transformed into *E. coli* BL21 (DE3) cells, respectively. Transformed cells were grown and protein expression induced with IPTG at 30 ºC for 4-5 h after cultures attained an A_{600} of 0.5. All the fusion proteins were found to be overexpressed in soluble form as analysed by SDS-PAGE. Recombinant lipoyl domain GST fusion proteins were purified by glutathione Sepharose 4B chromatography as described in Methods section 2.3.13 and analysed by SDS-PAGE (Fig. 4.13 A).

4.4.3 Western blot analysis of wild-type, E35D, E35Q and ΔE35 lipoyl domains

Western blotting of wild-type, ΔE35, E35D, E35Q outer lipoyl domain and K173Q inner lipoyl domain fusion proteins was performed using a monoclonal antibody (PD2) that recognises lipoylated components of PDC using a protocol described in Methods section 2.3.15. On Western blotting it was found that the ΔE35 lipoyl domain was not lipoylated when compared to the wild-type and the result was comparable to the non-lipoylatable mutant inner lipoyl domain (K173Q). The other two mutants of the outer lipoyl domain, E35D and E35Q, created to investigate the effect of change in charge and size on the folding and lipoylation status of this domain were found to be fully lipoylated (Fig. 4.13 B).

4.4.4 Non denaturing gel electrophoresis of the wild-type, E35D, E35Q and ΔE35 lipoyl domains

The GST tags of wild-type, ΔE35, E35D and E35Q outer lipoyl domains were removed with thrombin by the protocol described in Methods section 2.3.14. Interestingly, it was noted that tags could be removed from the ΔE35 outer lipoyl domain in a short time interval (2 h), whereas for the wild-type and other two mutants it took about 8-10 h. After the removal of the GST tags, the proteins were first analysed by SDS-PAGE for checking of purity. Thereafter, they were analysed on a 6% native gel (Methods section 2.3.5). The ΔE35 outer lipoyl domain was found to exhibit a markedly decreased mobility on the native gel as compared to the wild-type and the other mutants (Fig. 4.14) indicating either a major change in charge, conformation or aggregation state or a combination of these factors.
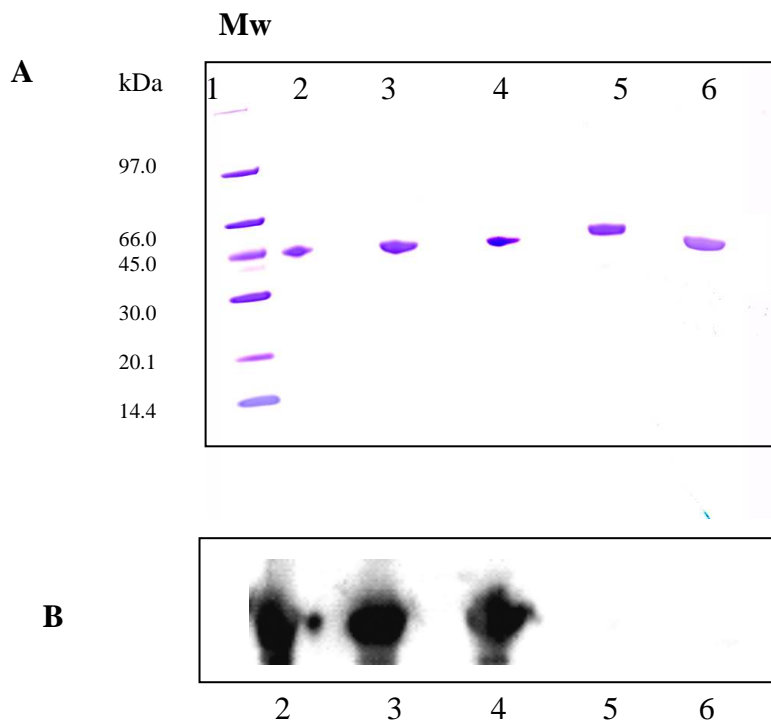
Figure 4.13: SDS-PAGE and Western blot analysis of the wild-type, E35D, E35Q, ΔE35 outer lipoyl domains and K173Q inner lipoyl domain

(A) SDS-PAGE analysis of purified wild-type (lane 2), E35D (lane 3), E35Q (lane 4), ΔE35 (lane 5) outer lipoyl domain GST fusion proteins and K173Q inner lipoyl domain GST fusion protein (lane 6) resolved on a 4-12% Bis-Tris gel. Wild-type and mutant fusion proteins were purified by glutathione Sepharose 4B chromatography. Molecular weight markers (Mw) are in lane 1.

(B) Western blot analysis of wild-type (lane 2), E35D (lane 3) E35Q (lane 4), ΔE35 (lane 5) outer lipoyl domain GST fusion proteins and K173Q inner lipoyl domain GST fusion protein (lane 6) with PD2 antibody. The ΔE35 outer lipoyl domain is not detected (lane 5) and is comparable to the negative control, K173Q inner lipoyl domain (lane 6).

4.4.5 Structural prediction for the wild-type and ΔE35 outer lipoyl domains

A possible structural change in the ΔE35 lipoyl domain was suspected on the basis of ease of removal of its GST tag by thrombin, Western blotting and native gel electrophoresis. Therefore, it was decided to ascertain if any change in the structure of the mutant domain was predicted on the basis of Swiss modelling (see section 2.3.18). The structure of the outer human lipoyl domain has not been solved either by NMR or by X-ray crystallography; therefore both the structures were created based on sequence homology. The potential structure for the mutant lipoyl domain was found to be similar to the wild-type lipoyl domain (Fig. 4.15 A & B). Overall its conformation appeared to be very similar to the lipoyl domain of *B. stearothermophilus* which consists of two 4-stranded antiparallel β sheets in the form of a flattened β-barrel with the lipoylatable lysine residue located on an exposed type-1 β turn in one of the β sheets (Dardel et al., 1993) (Fig. 4.15 C).
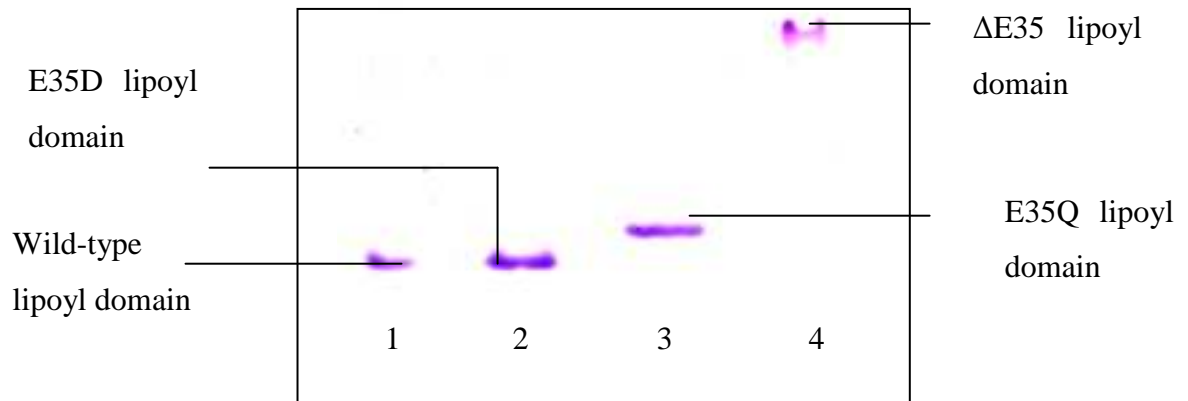
Figure 4.14: Non denaturing gel electrophoresis of the wild-type, E35D, E35Q and ΔE35 lipoyl domains

Native gel analysis on a 6% polyacrylamide gel shows that the ΔE35 outer lipoyl domain (lane 4) is either aggregated or has a major change in charge and/or shape as compared to wild-type (lane 1), E35D (lane 2) and E35Q (lane 3) outer lipoyl domains.

A

B

Glutamate-
35

Lipoylatable
lysine

C
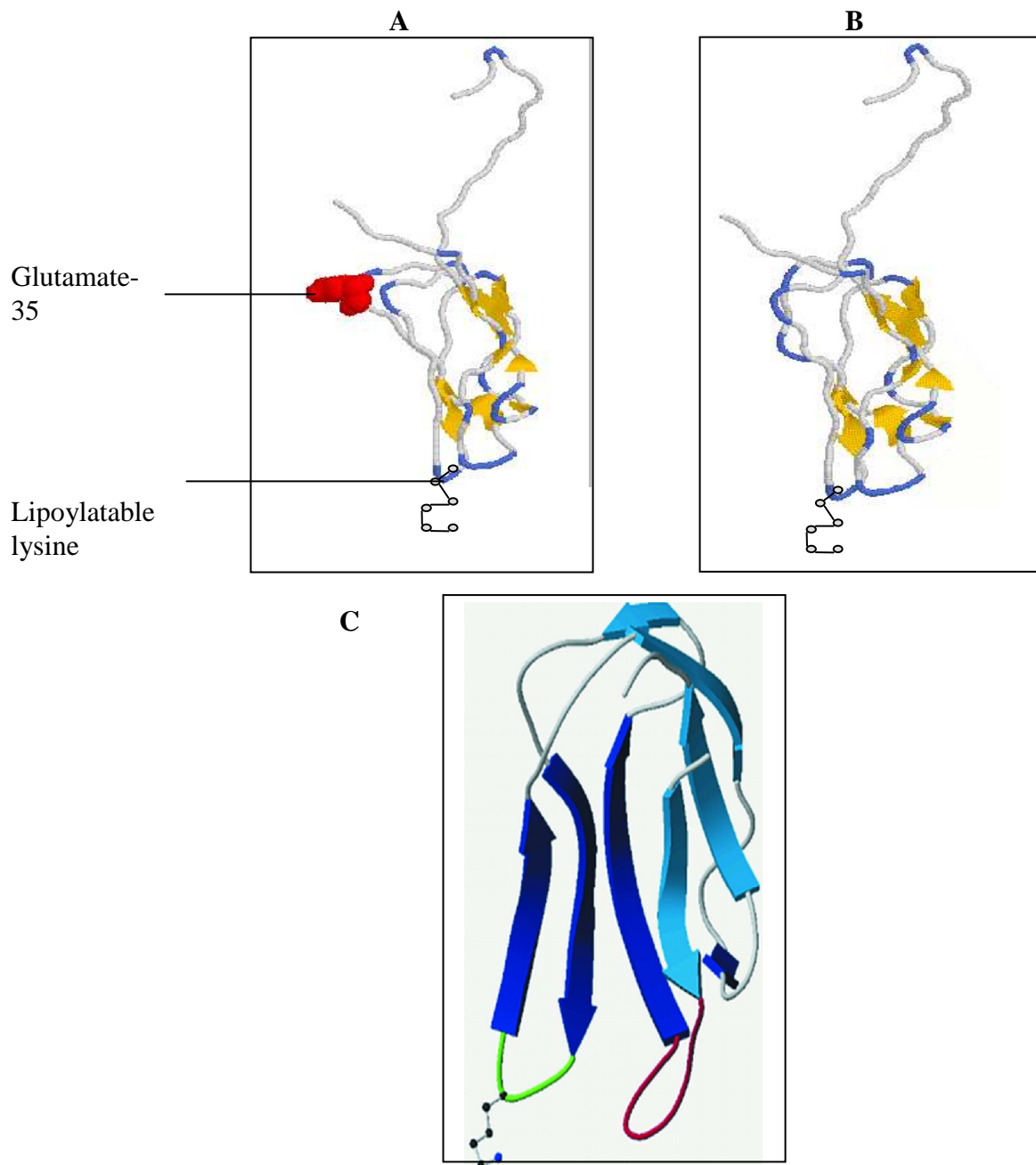
Figure 4.15: Structure prediction of the wild-type and ΔE35 lipoyl domain using Swiss modelling

The structure of the wild-type (A) and ΔE35 (B) outer lipoyl domains as predicted by Swiss modelling (Schwede et al., 2003) was not found to be significantly altered and was similar to the structure of the lipoyl domain of *B. stearothermophilus* E2-PDC. (C) Adapted from Dardel et al. (1993).

4.4.6 Molecular weight determination of the wild-type, E35D, E35Q and ΔE35 lipoyl domains by size exclusion chromatography

Size exclusion chromatography (SEC) separates proteins based on their size, shape or their hydrodynamic volume. SEC allows the separation of folded and unfolded forms, as the folded polypeptide elutes much later due to its more compact structure. The purified wild-type, ΔE35 and E35D outer lipoyl domains were passed through a HiPrep 16/60 Sephacryl S-300 High Resolution column attached to a BioCAD 700E workstation as described in Methods section 2.3.12 and elution profiles compared. Similarly, the wild-type and ΔE35 lipoyl domain GST fusion proteins were also subjected to gel filtration chromatography on the same column for comparative purposes.

It was observed that the wild-type and E35D outer lipoyl domains eluted at the same elution volume whereas the ΔE35 outer lipoyl domain appeared at an earlier stage in the elution profile (Fig. 4.16 B). Ratio of elution volume to void volume Ve/Vo was calculated for each protein and was found to be 2.21 for the wild-type and for the E35D outer lipoyl domains, whereas for the ΔE35 lipoyl domain, this ratio was 1.98. Similarly, the main peak for the ΔE35 lipoyl domain GST fusion protein was also observed at an earlier stage and displayed a Ve/Vo of 1.52 whereas for the wild-type-GST construct, this value was 1.68 (Fig. 4.16 C).

The molecular masses of these proteins were calculated employing a calibration curve generated by plotting logarithm of molecular weights of known proteins on the Y-axis and Ve/Vo on the X-axis (Fig. 4.16 A). It was found that the molecular weight of the ΔE35 outer lipoyl domain was twice that of wild-type lipoyl domain. Thus, the predicted molecular mass of this domain was 20.7 kDa; however, the observed molecular mass as determined from the standard curve (Fig. 4.16 A) was 45 kDa. A similar trend was observed when the molecular mass of the wild-type and mutant domains fused with GST were compared. The predicted molecular mass of the GST fusion mutant was 90 kDa; however, the observed molecular mass using the standard curve was 180 kDa. In both cases, the ΔE35 lipoyl domain was present as a dimeric species whilst also displaying an increased tendency to form aggregates of higher order and showing a substantial peak at the void volume in the case of the lipoyl domain GST fusion protein (Fig. 4.16 B & C).

A

B

C
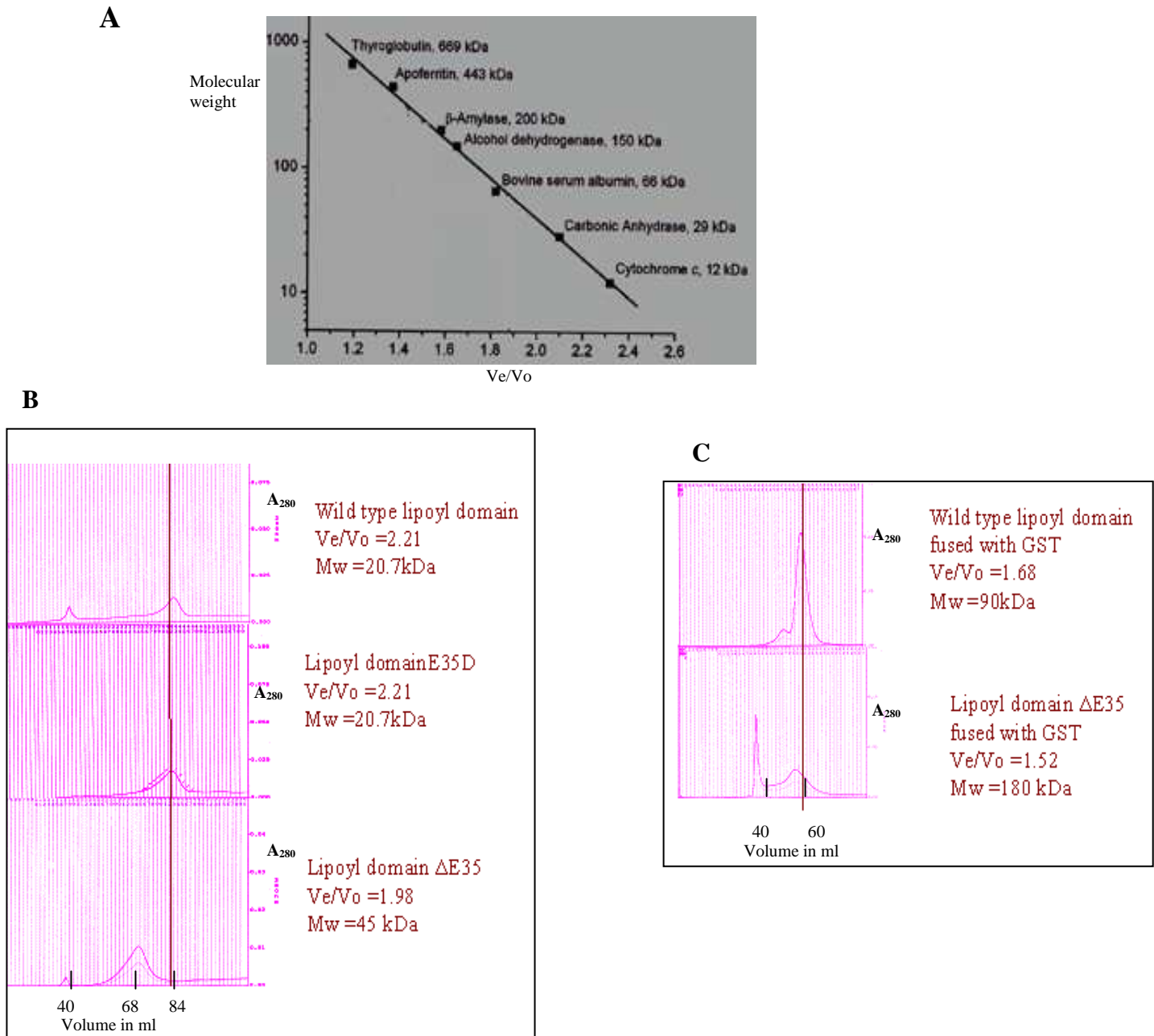
Figure 4.16: Molecular mass determination of the wild-type, E35D, E35Q and ΔE35 lipoyl domains by size exclusion chromatography

(A) Standard curve generated by plotting the logarithm of molecular weights of known proteins on the Y-axis and ratio of elution to void volume Ve/Vo on the X-axis. Ve/Vo of the test samples were determined by resolving on a HiPrep 16/60 Sephacryl S-300 High Resolution column attached to BioCAD 700E workstation. (B) Gel filtration elution profiles and Ve/Vo ratios of the wild-type, E35D, ΔE35 lipoyl domains (C) Gel filtration elution profiles and Ve/Vo ratios of the wild-type and ΔE35 lipoyl domain GST fusion proteins.

4.4.7 Cross linking of the wild-type and ΔE35 lipoyl domains by glutaraldehyde treatment

If two proteins physically interact with each other forming dimers or oligomers of higher order, then they can be covalently cross-linked chemically. Chemical cross linking offers a direct method of identifying both transient and stable interactions. This technique involves the formation of covalent bonds between two interacting proteins by using bifunctional reagents containing reactive end groups that link to functional groups such as primary amines and thiol groups of amino acid residues. Homo-bifunctional reagents, specifically reacting with primary amine groups (*i.e.* ε-amino groups of lysine residues) have been used extensively as they are soluble in aqueous solvents and can form stable inter- and intra-subunit covalent bonds. Glutaraldehyde is a popular homo-bifunctional reagent, which is extensively used for cross linking. SDS polyacrylamide gels of oligomeric proteins, for instance dimeric proteins, after treatment with glutaraldehyde will show cross linked dimers where inter-subunit cross linking has occurred. In this experiment, purified wild-type and ΔE35 outer lipoyl domains were treated with 2% (v/v) glutaraldehyde respectively for 30 min at room temperature. Thereafter, SDS-PAGE analysis of the treated samples was carried out employing the routine protocol outlined in Methods section 2.3.4. It was found that the wild-type lipoyl domain migrated at its normal molecular mass (20 kDa) even after glutaraldehyde treatment whereas the ΔE35 outer lipoyl domain migrated more slowly corresponding to a molecular mass of approx. 45 kDa, consistent with its existence as a homodimer prior to cross linkage (Fig. 4.17).
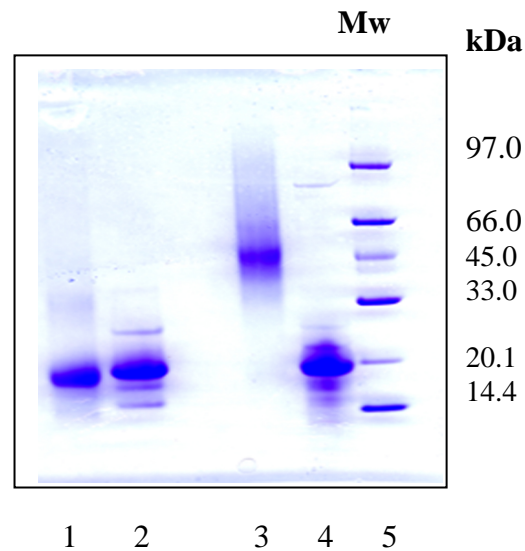
Figure 4.17: SDS-PAGE analysis of the wild-type and ΔE35 lipoyl domains cross-linked with glutaraldehyde

The Bis-Tris (4-12%) SDS gel was stained with Coomassie blue and shows that the ΔE35 lipoyl domain present as a dimer after treatment with 2% glutaraldehyde (lane 3), whereas the wild-type outer lipoyl domain treated in same way is monomeric (lane 1). Wild-type and ΔE35 lipoyl domains without glutaraldehyde treatment are in lanes 2 and 4, respectively. Molecular weight markers (Mw) are in lane 5.

4.4.8 Analysis of the far uv spectra of the wild-type, E35D, E35Q and ΔE35 lipoyl domains by circular dichroism

Secondary structure can be estimated by CD spectroscopy in the far-uv spectral region (190-250 nm). Samples of the wild-type, ΔE35, E35D and E35Q outer lipoyl domains, all free of their GST tags, were prepared as discussed in Methods section 2.3.20. Domains were examined for possible changes in secondary structure using CD spectroscopy in the far uv region. The CD spectrum of the ΔE35 outer lipoyl domain was quite distinct when compared with the wild-type and other mutants (Fig. 4.18). Secondary structures were estimated using the CDSSTR algorithm which is available from the online DICHROWEB server hosted by the Birkbeck college (http://www.cryst.bbk.ac.uk). From the spectral data, the algorithm estimated that the wild-type and mutants E35D and E35E consisted of predominantly beta sheet structure (approx. 45%), whereas, the ΔE35 outer lipoyl domain consisted mainly of random coil.

4.4.9 Near uv spectra of the wild-type E35D, E35Q and ΔE35 lipoyl domains by circular dichroism

The CD spectrum of a polypeptide in the near-uv spectral region (250-350 nm) can be sensitive to certain aspects of tertiary structure. Over this wavelength range the major chromophores are the aromatic amino acids and disulphide bonds, that can give rise to individual spectral contributions and the CD signals produced can be a sensitive probe for detecting alterations in the overall tertiary structure of the protein. Signals in the region from 250-270 nm are attributable to phenylalanine residues, signals from 270-290 nm to tyrosine and those from 280-300 nm to tryptophan. Disulphide bonds give rise to broad weak signals throughout the near-uv spectrum. Samples of the wild-type, ΔE35, E35D and E35Q outer lipoyl domain were prepared as mentioned in Methods section 2.3.20. Near uv CD spectra in this region indicated that in the wild-type, E35D and E35Q outer lipoyl

domains, the aromatic amino acids such as tyrosine were in a rigid environment giving rise to well-defined troughs in this region. In contrast, in the ΔE35 outer lipoyl domain, this rigid environment was lost as indicated by the disappearance of the characteristic troughs centred around 278 nm, 286 nm and 292 nm (Fig. 4.19).

4.4.10 Fluorescence emission spectra of the wild-type, E35D, E35Q and ΔE35 outer lipoyl domains

Fluorescence emission spectra of the wild-type, E35D, E35Q and ΔE35 outer lipoyl domains were generated and analysed by exciting the individual samples at 295 nm as described in Methods section 2.3.21. The fluorescence emission spectra were recorded at 320-350 nm. Maximum emission occurred at 330 nm for the wild-type, E35D and E35E outer lipoyl domains whereas maximum emission for the ΔE35 lipoyl domain shifted to 345 nm (Fig. 4.20). This indicated that the single buried tryptophan residue in the ΔE35 lipoyl domain was exposed to the external aqueous phase and this domain appeared to be largely unfolded as compared to the wild-type and other mutants.
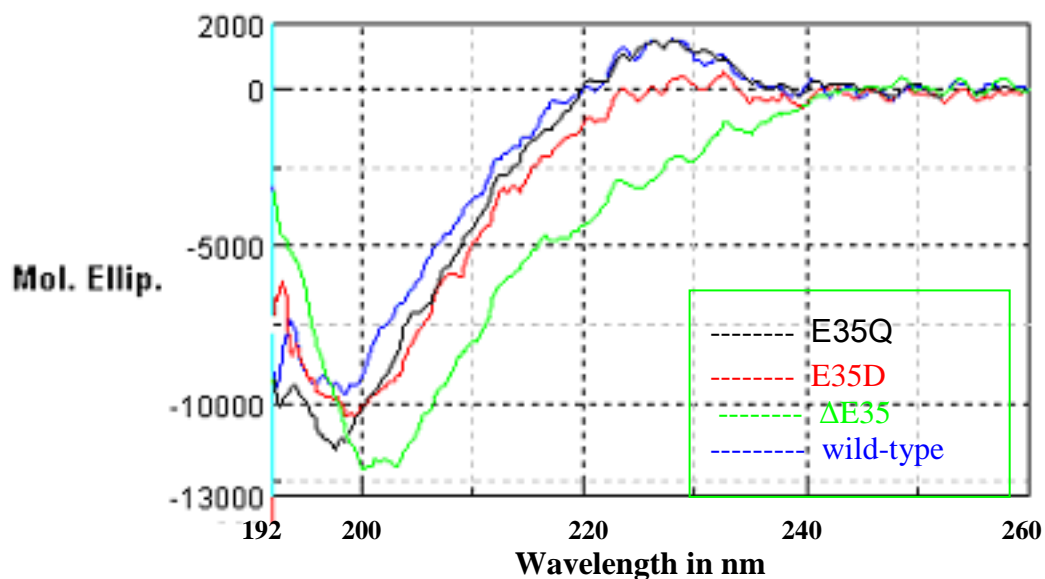
Figure 4.18: Far uv CD spectra for the wild-type, E35D, E35Q and ΔE35 lipoyl domains

The wild-type, E35Q, E35D and ΔE35 outer lipoyl domains were subjected to circular dichroism and spectra recorded in the far uv region (190-260 nm). The CD signal was measured as molar ellipticity in degrees cm^2 $dmol^{-1}$ (Y-axis) plotted as a function of wavelength (X-axis).
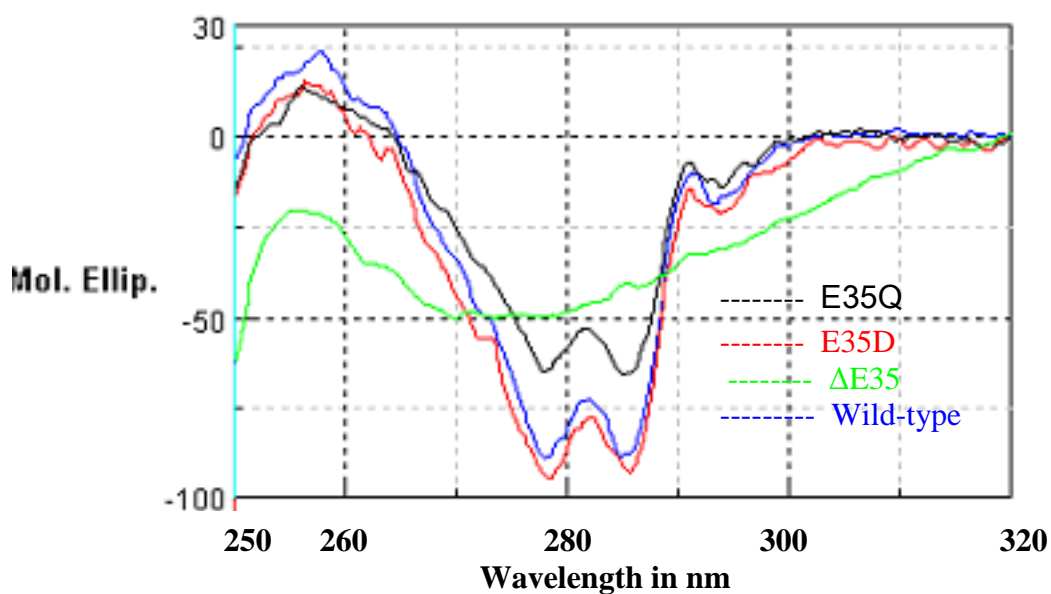
Figure 4.19: Near uv CD spectra for the wild-type, E35D, E35Q and ΔE35 lipoyl domains

The wild-type, E35Q, E35D and ΔE35 outer lipoyl domains were subjected to circular dichroism and spectra recorded in the near uv region (250-320 nm). The CD signal was measured as molar ellipticity in degrees cm^2 $dmol^{-1}$ (Y-axis) as a function of wavelength (X- axis).
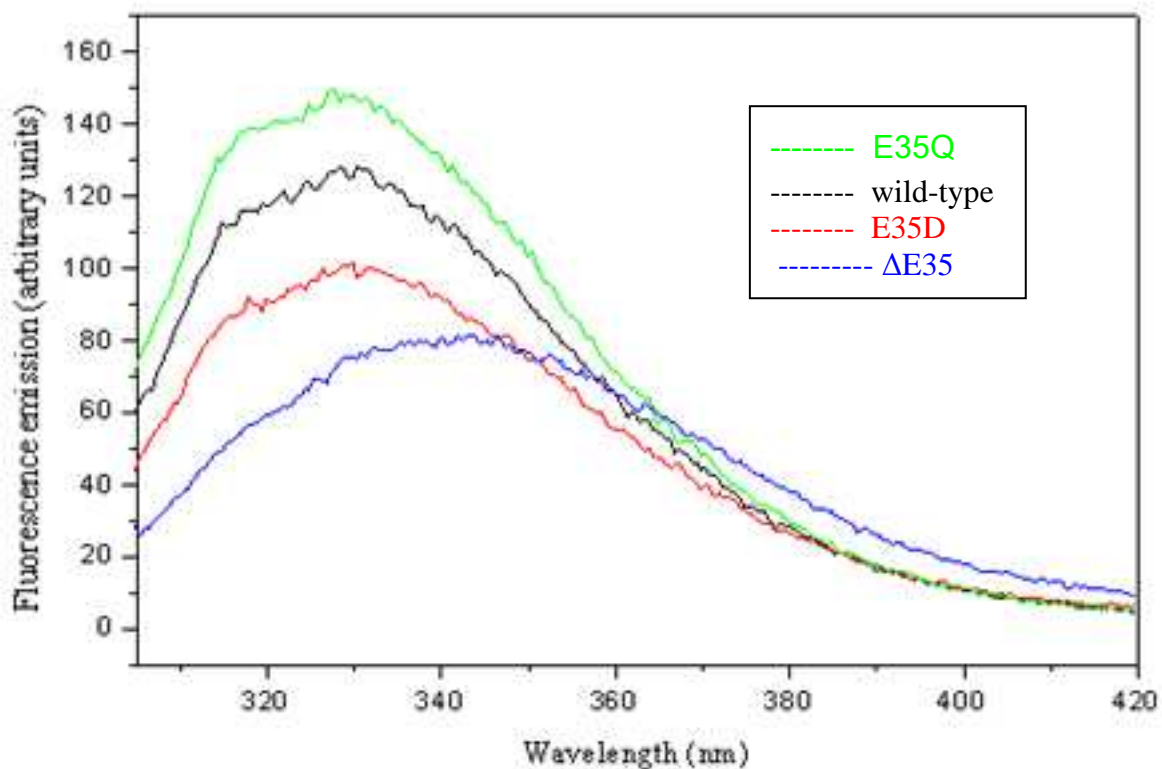
Figure 4.20: Fluorescence emission spectra of the wild-type, ΔE35, E35D and E35Q outer lipoyl domains

The wild-type, ΔE35, E35D and E35Q outer lipoyl domains were excited with uv light of wavelength 295 nm. Emission of fluorescence was recorded over the wavelength range 310-420 nm. The data show that maximum emission of fluorescence occurs at 330 nm for the wild-type, E35D and E35Q lipoyl domains, whereas for the ΔE35 outer lipoyl domain, the peak of fluorescence emission shifts to 345 nm.

4.4.11 Creating the ΔE35, E35D and E35Q mutants of full length E2

The glutamate-35 mutation was created in full length E2 cDNAs housed in pET-14b and pET-11b vectors respectively by site-directed mutagenesis using appropriate primers (Materials & Methods section 2.1.3). In the same way, E35D and E35Q mutants of E2 in pET-14b and pET-11b were also created for detailed analysis of these mutations. The primers specified in Materials & Methods (section 2.1.3) were used for creating E35D and E35Q E2 mutants. On DNA sequencing, the correct mutations were found to be incorporated into all the mutant constructs. Six mutant constructs of E2 namely: ΔE35 pET-14b, ΔE35 pET-11b, E35D pET-14b, E35D pET-11b, E35Q pET-14b and E35Q pET-11b were generated in this manner. The pET-14b constructs were required to study the effects of the glutamate 35 deletion on E2 activity whereas, the pET-11b constructs of E2 facilitated co-expression with E3BP in pET-28b to obtain mutant E2:E3BP cores described in Section 4.4.14, enabling us to study the effects of this mutation on the E2:E3BP core and overall PDC activity.

4.4.12 Overexpression and purification of the wild-type, ΔE35, E35D and E35Q E2 enzymes

To overexpress wild-type, ΔE35, E35D and E35Q E2 enzymes, pET-14b constructs housing the relevant cDNAs were transformed into *E. coli* BL21 (DE3) cells. Overexpressions were carried out at 30 ºC for 5-6 h and visualised by SDS-PAGE (Fig. 4.21). The N-terminally His-tagged proteins were purified by zinc chelate chromatography and viewed by SDS-PAGE (Fig. 4.22).
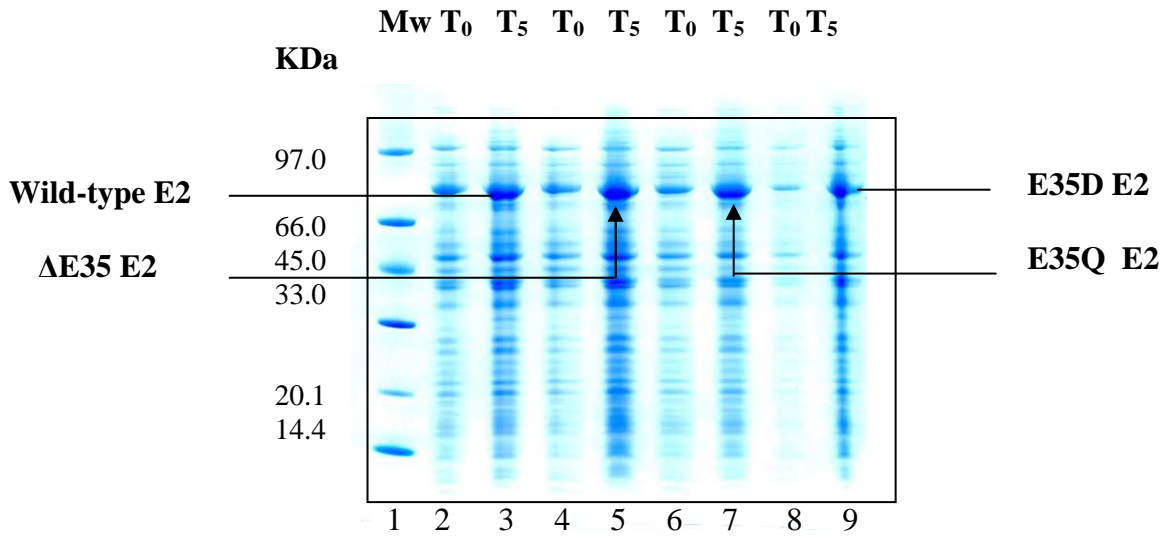
Figure 4.21: Overexpression of the wild-type, ΔE35, E35D and E35Q E2 enzymes

SDS-PAGE analysis of overexpression of the wild-type (lane 3), ΔE35 (lane 5), E35D (lane 7) and E35Q (lane 9) recombinant E2 enzymes on a 4-12% Bis-Tris gel. The overexpressions were carried out in *E. coli* BL21 (DE3) cells at 30 ºC for 4-5 h and are shown at zero time (T_0) and 5 h after induction (T_5). Molecular weight markers (Mw) are in lane 1.
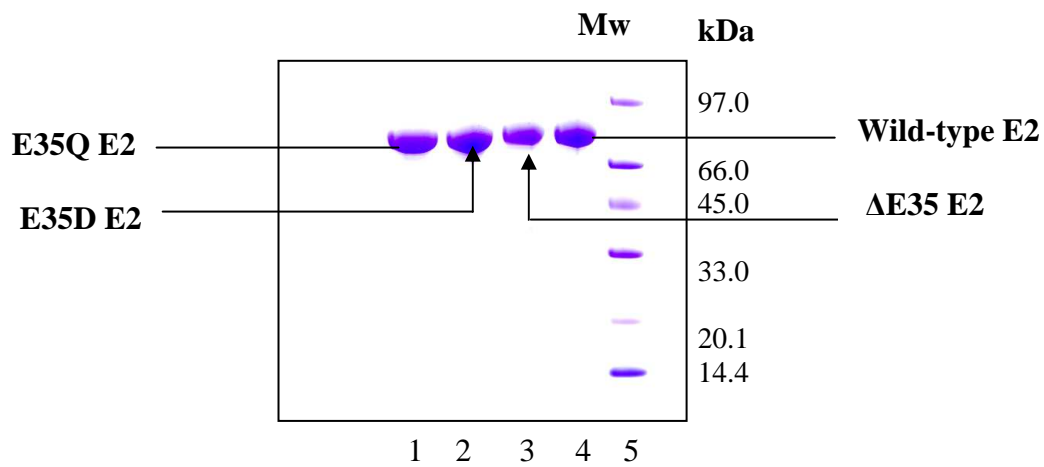
Figure 4.22: SDS-PAGE analysis of purified wild-type, ΔE35, E35D and E35Q E2 enzymes

SDS-PAGE analysis of the purified wild-type (lane 4), ΔE35 (lane 3), E35D (lane 2) and E35Q (lane1) recombinant E2 enzymes on a 4-12% Bis-Tris gel. Wild-type and mutant enzymes were purified by zinc chelate chromatography. Molecular weight markers (Mw) are in lane 5.

4.4.13 Enzymatic activity of wild-type and ΔE35, E35D and E35Q mutants of E2

The acetyltransferase activities of the purified wild-type, ΔE35, E35D and E35Q E2 enzymes were compared spectrophotometrically following the protocol described in Methods section 2.3.16. Equal amounts of wild-type and mutant E2 enzymes were used to determine acetyltransferase activity by initially performing Bradford assays (see section 2.3.11). Further SDS-PAGE analysis of these enzymes was carried out to ensure that equal amounts were assayed for acetyltransferase activity. All activity assays were performed in duplicate with wild-type control and the E35D mutant displaying 100% activity. In comparison, the E35Q E2 mutant displayed approx. 80%, whereas ΔE35 E2 displayed only approx. 20% activity (Fig. 4.23). These results were found to be reproducible with 3 different preparations of recombinant wild-type and mutant E2s.
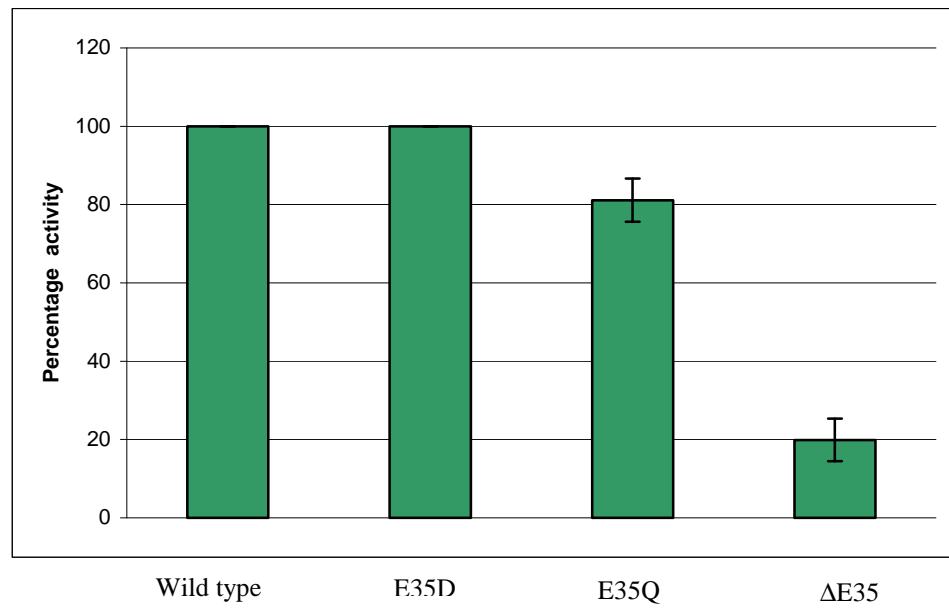
Figure 4.23: Comparison of acetyltransferase activity of the wild-**type, ΔE35, E35D and E35Q E2 enzymes**

Percentage enzymatic activities of wild-type and mutant E2 enzymes are shown. Error bars indicate extent of variation between duplicates.

4.4.14 Co-transformation and overexpression of the wild-type, ΔE35, E35D and E35Q E2:E3BP cores

Wild-type E2 cDNA in pET-11b and E3BP cDNA in pET-28b were co-transformed into *E. coli* BL21 (DE3) Star cells and single colonies employed for overexpression studies. Overexpression yielded the most soluble E2:E3BP core at 15 ºC (Chapter 3, Fig. 3.5). The ΔE35, E35D and E35Q E2:E3BP cores were successfully overexpressed in the same manner. Lipoic acid (0.1 mM) was added to each before induction with 1 mM IPTG. The solubility of the ΔE35 E2:E3BP core was also checked at 37 ºC, 30 ºC, 22 ºC and 15 ºC, and was found to be maximal at 15 ºC (Fig. 4.24). Therefore, in subsequent experiments, wild-type and mutant E2:E3BP cores were all overexpressed at 15 ºC overnight.

4.4.15 Purification of the wild-type and ΔE35, E35D and E35Q E2:E3BP cores

The E2:E3BP cores contained only N-terminally His-tagged E3BP and consequently their purification relied on the formation of a stable E2:E3BP core assembly in which E3BP co-integrated with its E2 partner. Mutant cores could be purified successfully by metal chelate chromatography in a similar manner as described for the wild-type core in Chapter 3 (see section 3.4). The purified wild-type and mutant cores were also subjected to gel filtration on a HiPrep 16/60 Sephacryl S-300 High Resolution column attached to a BioCAD 700E workstation before viewing by SDS-PAGE (Fig. 4.25). On SDS-PAGE analysis, the ΔE35 core was found to contain reduced levels of E2 and a high proportion of E3BP as compared to the wild-type core. Several preparations of this mutant core analysed by routine SDS-PAGE consistently displayed this feature, which was the first indication of abnormal assembly.
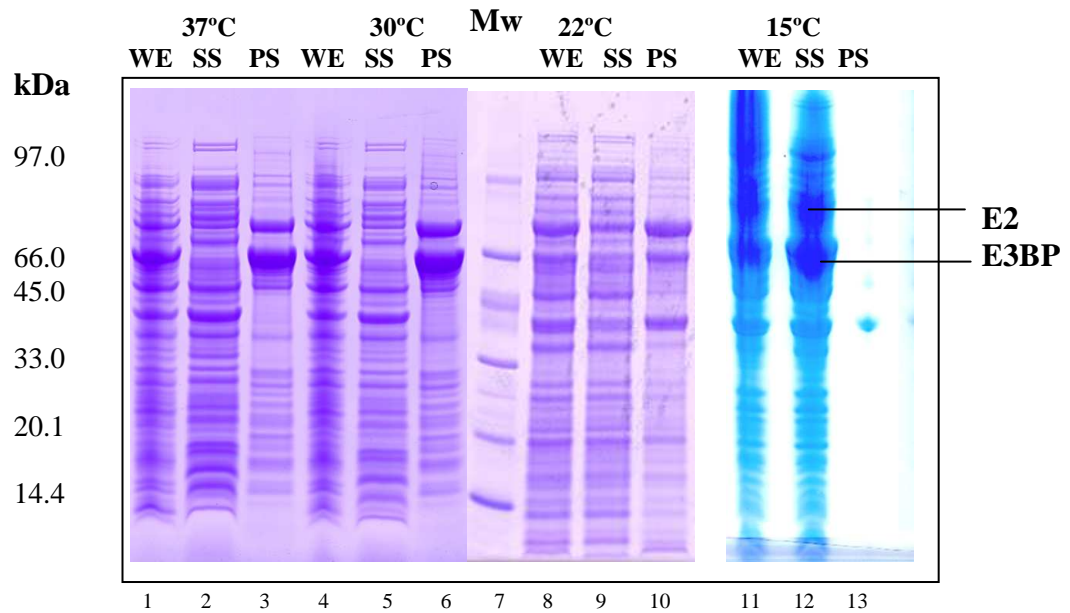
Figure 4.24: Solubility check of ΔE35 E2:E3BP core overexpressed at various temperatures

The ΔE35 E2:E3BP core was overexpressed at 15 ℃, 22 ℃, 30 ℃ and 37 ℃ in *E. coli* BL21 (DE3) Star cells. SDS-PAGE analysis on a 4-12% Bis-Tris gel shows that at 37 ℃, 30 ℃ and 22 ℃, mutant E2:E3BP was largely insoluble and present in the pellet fraction (PS)(lanes 3, 6 and 10 respectively). When overexpressed at 15 ℃ overnight, this protein was present in the soluble supernatant (SS) (lane 12). Whole cell extracts (WE) in lanes 1, 4, 8 and 11, respectively. Molecular weight markers (Mw) are in lane 7.
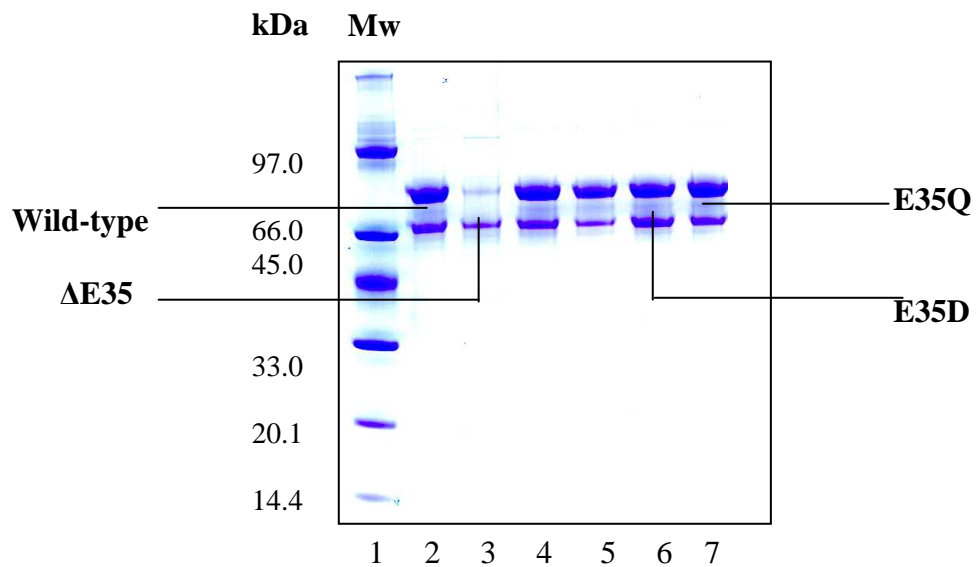
 Figure 4.25: SDS-PAGE of the purified wild-type, ΔE35, E35D and E35Q E2:E3BP cores

SDS-PAGE analysis of the purified wild-type (lane 2), ΔE35 (lane 3), E35D (lane 6) and E35Q (lane 7) recombinant E2:E3BP cores on a 4-12% Bis-Tris gel. Wild-type and mutant enzymes were purified by zinc chelate chromatography and gel filtration. Gel also shows ΔV455 and F490L E2:E3BP cores in lanes 4 and 5, respectively. Molecular weight markers (Mw) are in lane 1.

4.4.16 Enzymatic activity of the wild-type, ΔE35, E35D and E35Q E2:E3BP cores

Purified wild-type, ΔE35, E35D and E35Q E2:E3BP cores (see section 4.4.13) were checked for protein levels by performing Bradford assays as described in Methods section 2.3.11. SDS-PAGE analysis was also carried out to ensure that equal amounts of wild and mutant cores were assayed for acetyltransferase activity. Assays were conducted to compare wild-type (taken as a 100% control) with the mutant cores, in the same manner as for the wild-type and mutant E2 enzymes (see section 4.4.13). In the previous E2 assay, it was seen that ΔE35 E2 showed very low activity (80% reduction). The purpose of employing E2 cores containing E3BP was to establish if the presence of E3BP had any influence on ΔE35 E2 activity. As previously however, the E35D core displayed 100% activity, the E35Q core displayed approx. 80% whereas the ΔE35 core assembly displayed only 20% of the control activity levels, in agreement with the values obtained employing the wild-type and mutant E2 enzymes. Thus the pattern of results on assembled native and mutant E2:E3BP cores was similar to those obtained for the equivalent set of purified E2 samples.

4.4.17 Comparison of overall PDC activity in recombinant preparations of reconstituted wild-type, ΔE35, E35D and E35Q core assemblies

Wild-type, ΔE35, E35D and E35Q E2:E3BP cores were reconstituted into wild-type and mutant PDCs by adding stoichiometric amounts of E1 and E3 respectively (see Chapter 3, section 3.11). Enzymatic assays were performed in duplicate with freshly prepared wild-type and mutant PDCs as per the protocol described in Methods section 2.3.17. Wild-type PDC was taken as control with 100% activity. In comparison, the E35D PDC displayed 80%, E35Q PDC 75%, whereas the ΔE35 PDC displayed consistently low activity of about 10 -12 % (Fig. 4.27).
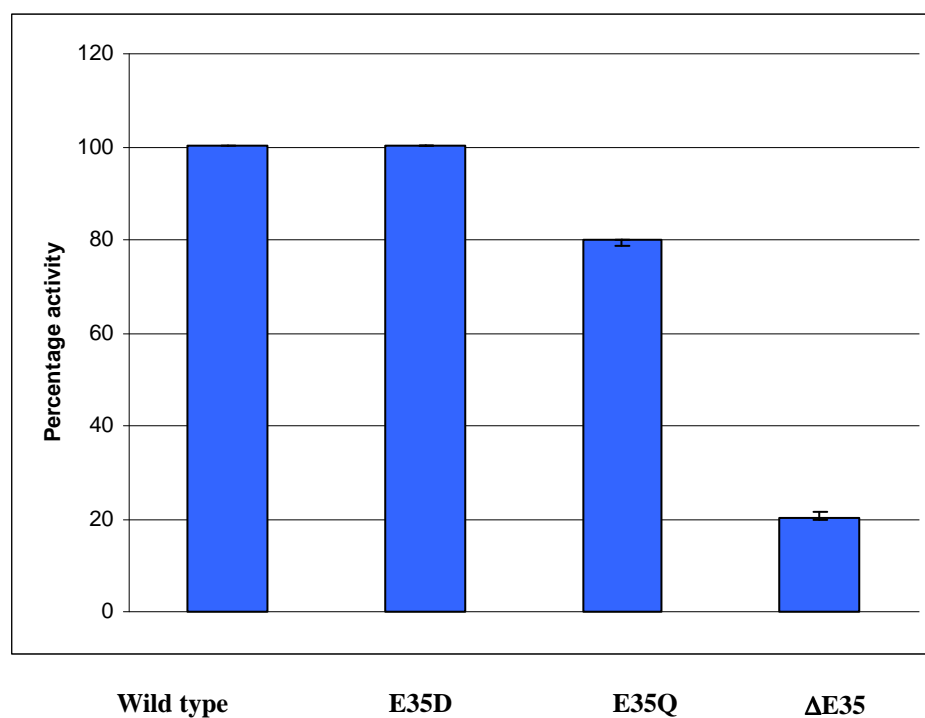
Fig 4.26: Comparison of enzymatic activity of wild-type, ΔE35, E35D and E35Q E2:E3BP cores

Percentage enzymatic activities of mutant E2:E3BP cores relative to the wild-type as 100% control are shown. Samples were assayed in duplicate and error bars are shown where necessary and indicate extent of variation between duplicates.
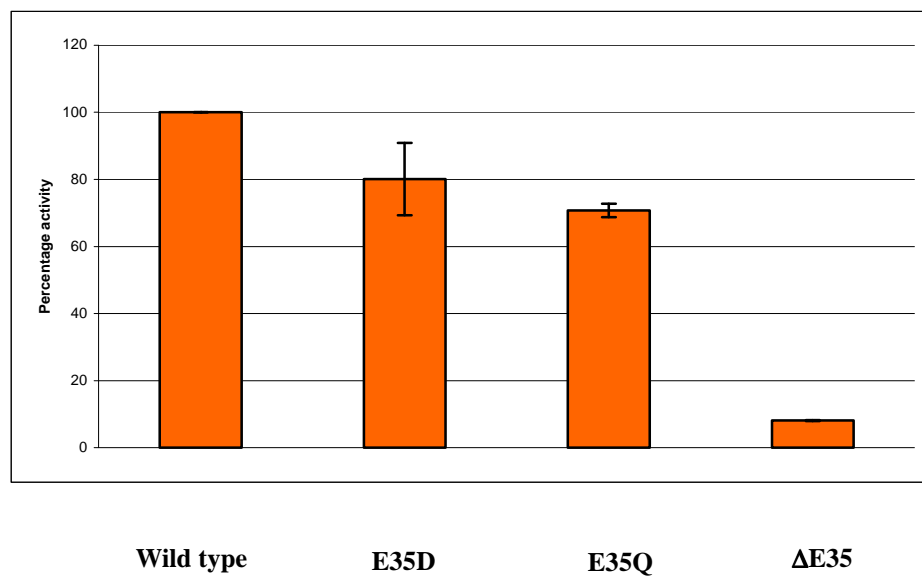
Figure 4.27: Comparison of recombinant PDC activities reconstituted with the wild-type, ΔE35, E35D and E35Q E2:E3BP cores

Enzymatic activities of the wild-type and mutant PDCs reconstituted from individual components are shown with respect to wild-type complex as control. Samples were assayed in duplicate and error bars shown where necessary indicating the extent of variation between duplicates.

4.4.18 Far UV spectra of the wild-type, ΔE35, E35D and E35Q E2: E3BP cores by circular dichroism

The wild-type and mutant cores were subjected to CD in the region of 190-250 nm and spectra recorded as described in Methods section 2.3.20.

The data were not of high quality in the 190-200 nm region and therefore, quantitative estimation of α helix and β sheet content was not attempted. However, differences were observed in the spectra of the ΔE35 mutant core as compared to the wild type and other mutant cores, where a well defined peak at 206 nm is absent in the ΔE35 core (Fig. 4.28).

4.4.19 Fluorescence emission spectra of the wild-type, ΔE35, E35D and E35Q E2:E3BP cores

Fluorescence emission spectra of the wild-type, ΔE35, E35D and E35Q; E2:E3BP cores were also compared as described in the Methods section 2.3.21. It was found that maximum fluorescence emission spectrum of ΔE35 E2:E3BP core shifted from 330 nm to 343 nm, as compared to the spectra of the wild-type and other mutant cores, which emitted maximally at 330 nm (Fig. 4.29). Since the single E2 polypeptide contains 4 tryptophans and E3BP polypeptide contains 2, this suggests large scale perturbation of the core assembly in which several tryptophans are exposed to the aqueous environment.
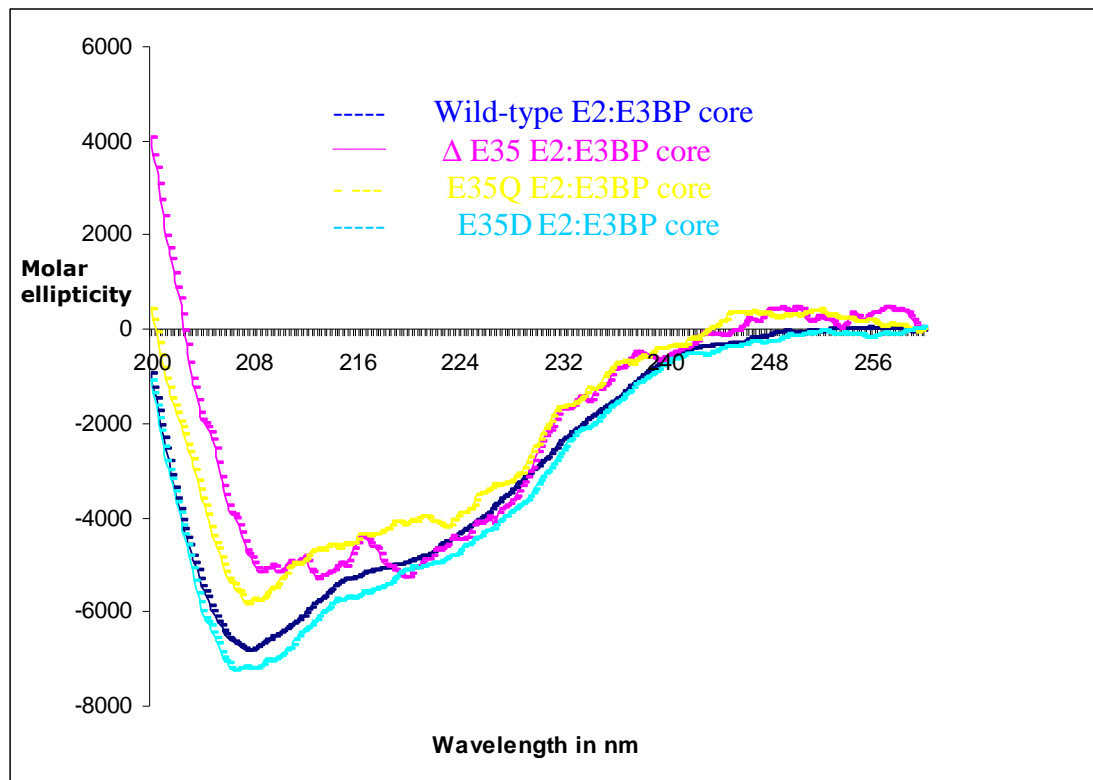
Figure 4.28: Far uv CD spectra of the wild-type, E35Q, E35D and ΔE35 E2:E3BP cores

Wild-type, E35Q, E35D, and ΔE35 E2:E3BP cores were subjected to circular dichroism and spectra recorded in the far uv region (190-260 nm). The CD signal was measured as ellipticity in degrees cm^2 $dmol^{-1}$ (Y-axis) plotted as a function of wavelength (X-axis).
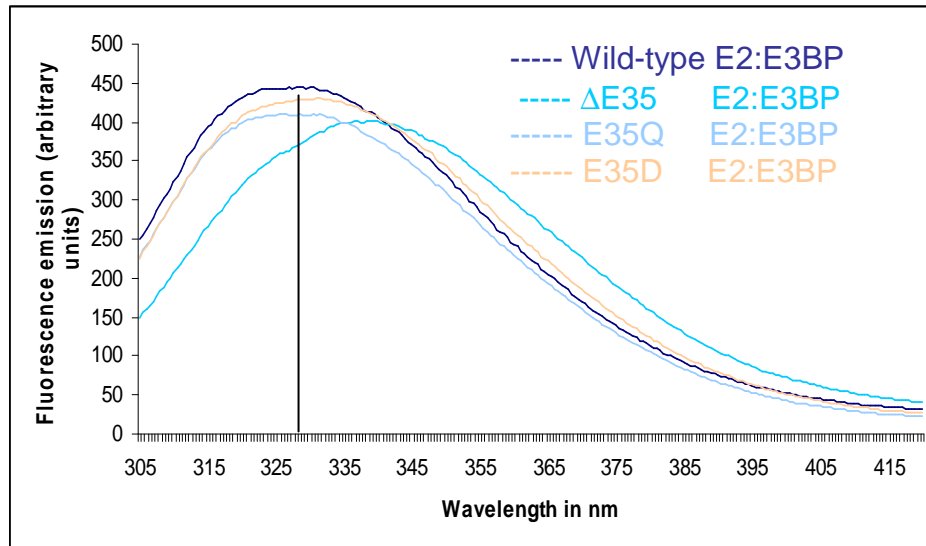
Figure 4.29: Fluorescence emission spectra of wild type, E35Q, E35D, ΔE35 E2:E3BP cores

Wild-type, E35D, E35Q, ΔE35 E2:E3BP cores were excited with uv light of wavelength 295 nm. Emission of fluorescence was recorded over a range of 310-420 nm. Figure shows that the maximal emission of fluorescence occurred at 326 nm for the wild-type, E35D and E35Q cores, whereas for the ΔE35 core, maximal fluorescence emission shifted to 343 nm.

4.4.20 Comparison of sedimentation behaviour of the wild-type and ΔE35 E2:E3BP cores

Major disruption of the ΔE35 E2:E3BP core was anticipated as observed from circular dichroism and intrinsic tryptophan fluorescence studies. Therefore, sedimentation velocity experiments were conducted in order to provide further insights into the nature of the mutant core assembly. These experiments were performed as described in the Methods section 2.3.19.2 and the sedimentation behaviour of the ΔE35 E2:E3BP core was compared to the wild-type core. Wild-type and mutant cores were co-expressed, purified (see sections 3.3 & 3.4), gel filtered (see the Methods section 2.3.12) and SDS-PAGE analysis conducted for checking the purity of the cores. No proteolysis or degradation was evident from SDS-PAGE analysis (Fig. 2.30 E).

The sample concentrations analysed were 3.33, 1.07 and 1.00 μM for the wild-type and 2.06, 1.72, 1.07, 2.60, 2.26 and 0.50 μM for the mutant. Samples (380 μl) were loaded into 12 mm double sector centrepieces and data recorded at 4 ℃ at a rotor speed of 20000 rpm using interference optics. A series of 360 scans, 60 s apart was taken for each sample. Sedimentation coefficients were determined using SEDFIT (Schuck, 2000). The weight average $s_{4,w}$ values were corrected to $s_{20,w}$. The weight average sedimentation coefficient, $s_{20,w}$ for the wild-type cores was determined as 30.61±0.36 S, whereas sedimentation coefficient for the mutant core displayed a great degree of heterogeneity (8-40 S). A small amount of the mutant core showed a sedimentation coefficient comparable to wild-type core, but the vast majority was present as sedimenting species of lower M_r value. This result was anticipated, in view of previous CD spectroscopy, fluorescence tryptophan and enzymatic assays that indicated the probability of major disruption in its assembly. A range of sedimentation coefficients (30-32 S) for normal E2:E3BP core and 8 S for unassembled trimers of E2 produced upon treatment of the core by chaotrophic agents have been reported (Behal et al., 1994). These 8 S species associated non-cooperatively to give additional assembly intermediates exhibiting sedimentation coefficients of 10-32 S. In this case also, the lower sedimenting species (Fig. 2.30 C) could be trimers of E2, which have failed to assemble into a proper core as a result of this mutation.
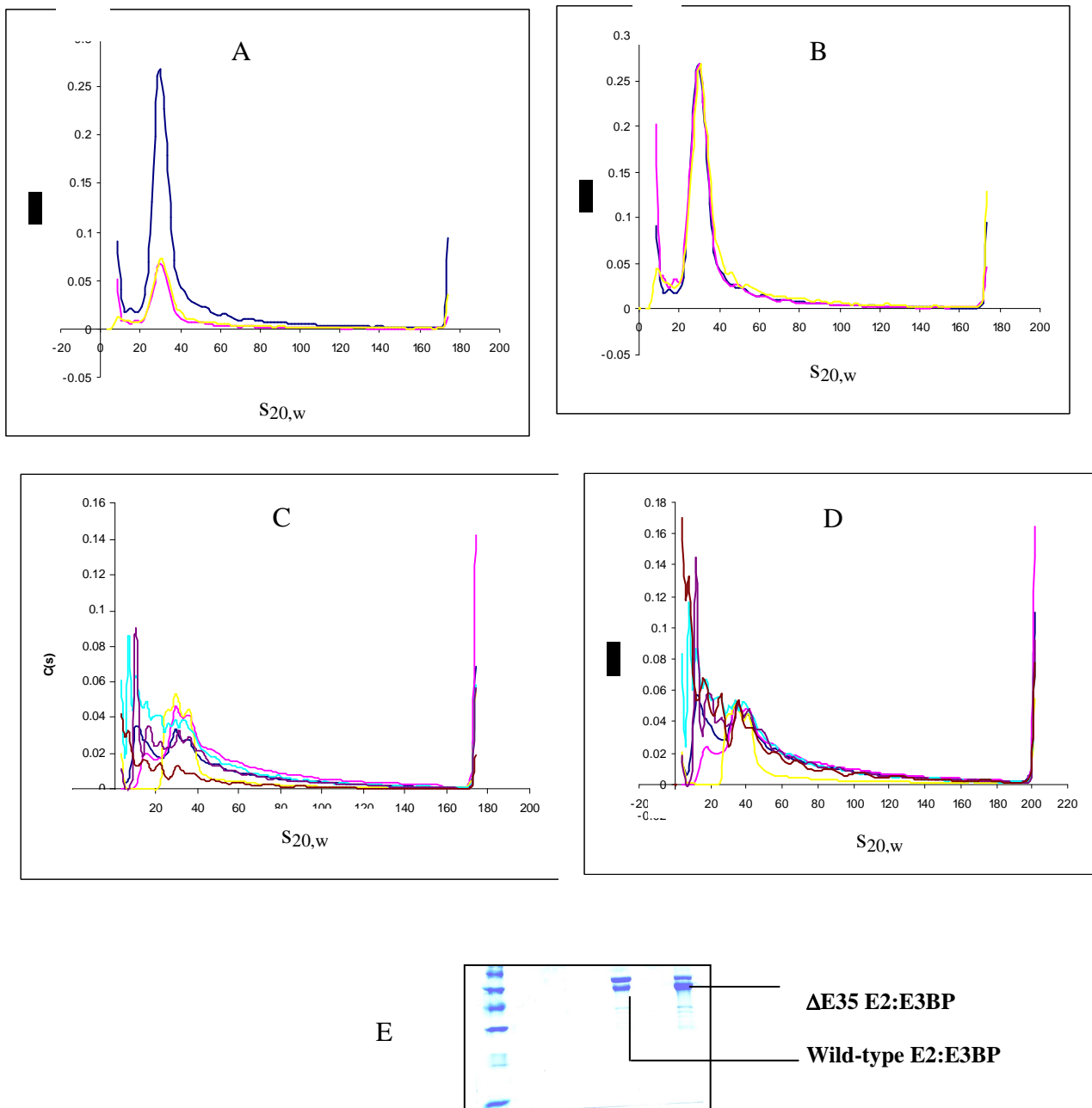
Fig. 2.30: Comparison of the sedimentation velocity analyses of wild-type and ΔE35 E2:E3BP cores

c(s) distribution from SV interference data collected for 3.33 μM (——), 1.07 μM (——) and 1.00 μM (——) wild-type E2:E3BP core (Fig. A) and maximising c(s) to the peak observed at 30.40 S (Fig. B). c(s) distribution from SV interference data collected for 2.06 μM (——), 1.72 μM (——), 1.07 μM (——), 2.60 μM (——), 2.26 μM (——) and 0.50 μM (——) ΔE35 E2:E3BP core (Fig. C) and maximising c(s) to the peak observed at 34 S (Fig. D). SDS-PAGE analysis of the wild-type and mutant cores used in this SV experiment (Fig. E).

4.4.21 Discussion of Glutamate 35 deletion

In this chapter the glutamate 35 deletion in the lipoyl domain of the E2 enzyme of PDC, encountered in a clinical case has been analysed in detail employing our model recombinant PDC. None of the mutations (ΔE35, ΔV455 and P490L), discussed in this Chapter have been identified in 50 dihydrolipoamide acetyltransferase (DLAT) alleles analysed to date, nor were they found in any DLAT cDNA or genomic sequences in the human EST (expressed sequence tag) and genomic DNA databases (Brown et al., 2004). In fact, no other mutations have been reported so far in the lipoyl domains of E2 of PDC. This may be due to the fact that such mutations might be prevalent, but do not produce a significant phenotype leading to failure of detection in the absence of a real necessity to diagnose them at genetic level. The non severity of the phenotype could also be attributable to functional redundancy owing to the presence of multiple lipoyl domains on E2 and E3BP that is also genetically advantageous. As a result the affected person may be carrying the mutation leading to slightly decreased PDC activity, but without producing any major health problems. In contrast, mutations in the E1α and E3 components produce mild to severe, but more detectable phenotypes.

The glutamate deletion was an interesting mutation in the sense that loss of lipoylation per se would not be expected to cause such severe clinical symptoms in the patient. Nevertheless it was important to demonstrate that the mutation was indeed the cause of the PDC deficiency and also to investigate the molecular basis of disruption of normal complex function in this case.

The precise role of the mutation was studied at three levels- at the lipoyl domain, at the E2 enzyme and at the PDC level. In all cases, two more mutants were investigated in parallel, namely E35D and E35Q, in order to better understand the role of the deleted glutamate 35. These mutants enabled us to establish whether a change in charge or size of amino acid was the over-riding factor for structural perturbation or the actual presence of the glutamate residue was more important. At the lipoyl domain level, it was seen that the ΔE35 lipoyl domain was non-lipoylated as compared to the wild-type and the other two

mutant domains. A monoclonal antibody (PD2) was employed for Western blotting, that recognises only the lipoylated components of PDC (Thomson et al., 1998). Lipoylation or insertion of lipoic acid on a particular lysine is a very specific phenomenon, occurring only if a precise structural cue is present (Wallis and Perham, 1994) and is indicative of the presence of correctly folded lipoyl domain. In the the case of glutamate 35 deletion, this structural cue appears to have been lost. This result was the first indication that this deletion caused a change in the structure of the lipoyl domain. The other two mutant domains, however, were still found to be lipoylated (Fig. 4.13) showing that glutamate-35 is an important and specific residue in this region required for the correct folding of the lipoyl domain or the maintenance of its structural stability. This result also confirmed that not only the DKA motif at the site of lipoylation is important, but that residues located some distance away from the site (12 residues to the N-terminal side in this case) are also essential for recognition.

The relative ease with which GST tags could be cleaved from the ΔE35 lipoyl domain as compared to the wild-type and other mutant domains also indicated that the ΔE35 mutant provided less steric hindrance to proteolytic attack by thrombin, suggesting that it was not properly folded. Major alterations were again observed when this domain was run on a non-denaturing gel indicating either a gross change in charge or oligomerisation state (Fig. 4.14). Striking differences were also observed in intrinsic tryptophan fluorescence indicating that ΔE35 lipoyl domain was not folded properly and that its single tryptophan was exposed to solvent.

The aromatic amino acids tryptophan, tyrosine and phenylalanine are all capable of contributing to the intrinsic fluorescence of proteins. When all three residues are present in a protein, pure emission from tryptophan can be obtained by photoselective excitation at wavelengths above 295 nm (Eftink, 1991). Although tyrosine and phenylalanine are natural fluorophores, tryptophan is the most extensively used amino acid for fluorescence analysis of proteins. In a protein containing all three fluorescent amino acids, observation of tyrosine and phenylalanine fluorescence is often complicated by interference from tryptophan caused by resonance energy transfer (Eftink, 1991). The application of tyrosine and phenylalanine fluorescence is therefore mostly limited to tryptophan-free proteins; however, a recent study reports an exception to this (Ruan et al., 2002). More importantly, tyrosine fluorescence is insensitive to environmental factors such as polarity (Ross, 1992). Fluorescence of phenylalanine is weak and seldom used in protein studies. Hence, the term 'natural protein fluorescence' is almost always associated with tryptophan fluorescence.

Tryptophan residues serve as intrinsic, site-specific fluorescent probes for protein structure and dynamics. The well documented sensitivity of tryptophan fluorescence to environmental factors such as polarity makes it a valuable tool in studies of this type by providing specific and sensitive information on protein structure and its interactions (Eftink, 1991). As a result of the exposure of a buried tryptophan, the maximum emission spectrum shifts 10 to 20 nm to longer wavelengths as compared to the spectra of the same protein in which tryptophan is still buried. This phenomenon was seen in the glutamate deleted lipoyl domain as well as the mutant E2:E3BP core (Fig. 4.20 & Fig. 4.29). However, in the lipoyl domain only a single tryptophan residue accounts for total fluorescence emission. In contrast, in the E2:E3BP core, there are 4 tryptophan residues in the single polypeptide chains of E2, one in the outer lipoyl domain, one in the extreme N-terminal region and two in the catalytic domain. Moreover, there are two tryptophans in the E3BP polypeptide, one each in the lipoyl domain and C-terminal catalytic domain. All these tryptophans contribute to the net fluorescence emission spectrum for the E2:E3BP core. Interestingly, in the mutant core the spectral shift to longer wavelength as compared to the wild type core, is contributed by a number of tryptophan residues indicating that there are major structural changes. The lipoyl domains of *A. vinelandii* OGDC and *B. stearothermophilus* PDC also have a single tryptophan residue occupying the centre of the hydrophobic core consisting of a number of residues (Berg et al., 1996; Dardel et al., 1993) and is key to stability of this domain by holding the beta sheets together.

Loss of secondary and tertiary structure in the ΔE35 lipoyl domain was visible by far uv spectrophotometry, where it appeared as a random coil compared to more structured beta sheets in the wild-type and other two mutants. In near uv spectrophotometry, signals arising from aromatic amino acids in a rigid environment were also lost in this particular mutant as compared to the wild type and other mutants. From all these observations, it was evident that ΔE35 lipoyl domain had undergone a major structural change because of this single deletion. This change in structure could not be revealed through structural modelling based on known lipoy domain structures (Fig. 4.15) indicating the limitations of such computer generated structures to mimic structural changes resulting from point mutations.

It was further observed that the ΔE35 lipoyl domain had a pronounced tendency to form dimers and also aggregates of higher order as viewed by gel filtration (Fig. 4.16). Folding of newly-synthesized proteins *in vivo* is believed to be facilitated by the cooperative interaction of a defined group of proteins known as molecular chaperones. Proteins in a non-native state are normally protected from aggregation by these chaperones. The first

events in the formation of proteins are the most critical. Starting at the ribosome, nascent polypeptides undergo complex folding processes that can be endangered by aggregation reactions. Proteins with organellar destinations such as mitochondria require correct targeting to the translocation machineries located in the organellar membranes and prevention from premature folding. In the case of mitochondrial precursors, maintenance of an 'unfolded' state is a prerequisite for permitting efficient translocation. The high precision and speed of these processes is ensured by a cystosolic system consisting of molecular chaperones, folding catalysts and targeting factors (Bukau et al., 1996). Folding and assembly of mitochondrial protein complexes takes place only as they emerge into the mitochondrial matrix.

Misfolded, denatured or damaged proteins present in a non-native state may expose 'sticky' hydrophobic regions or patches that are highly prone to aggregation (Bukau et al., 1996). Many neurodegenerative diseases are caused by genetic mutations that can lead to accumulation of aggregated toxic proteins in neuronal inclusions and plaques (Taylor et al., 2002). Our data indicate that the ΔE35 domain is misfolded exposing 'sticky' hydrophobic surfaces leading to formation of aggregates, mostly dimers but also higher order aggregates on occasions. Initially in this study, it was thought that the 'stickiness' of the lipoyl domain led to immobility of the lipoyl 'swinging arms' and hence reduction of PDC activity. However, subsequent data revealed an 80% reduction in E2 activity. This E2 assay is not dependent on the lipoyl domain or subunit binding domain regions of E2 so this marked reduction in E2 activity suggested that this N-terminal mutation was affecting assembly of the C-terminal domain, perhaps because of premature and inappropriate interactions of the N-termini. This prompted analysis of the core assembly using AUC, revealing that the correct core assembly was not forming in the presence of the glutamate mutation. Based on these observations a schematic model is proposed (see Chapter 6, Fig. 6.1) indicating how this mutation might affect normal trimer formation and/or subsequent steps in E2:E3BP core formation.

The effect of this mutation on acetyltransferase activity was studied in the E2 enzyme and E2:E3BP core. Intrinsic acetyltransferase activities of the ΔE35 enzyme and E2:E3BP core were found to be reduced by around 80% or more. The overall activity of reconstituted PDC complex with the glutamate mutation was also determined and compared to wild-type recombinant PDC using the standard spectrophotometric assay that monitors formation of NADH at 340 nm. The activity of mutant PDC was again found to be very low (approx. 10-15%) as compared to the wild-type.

This loss of activity could not be attributed solely due to loss of lipoylation in the outer lipoyl domains of the enzyme and in the core. Although lipoylation of PDC is crucial for catalysis, the inner lipoyl domains in the E2 enzyme and E3BP lipoyl domains in the core were still lipoylated (data not shown). In studies employing *E. coli* PDC, where only one lipoyl domain was functional out of three lipoyl domains in tandem repeat, the activity of the complex was comparable to wild-type complex (Allen et al., 1989). Our own data (Chapter 3, section 3.14) also showed that the loss of one lipoylatable lysine in the complex caused only a 25-35% decline in complex activity. However, the overall complex activity due to the ΔE35 mutation was found to extremely low, in the range 10-15% of the wild-type control. This drastic decline in enzymatic activity can be explained in terms of improper E2:E3BP core formation. The loss of core structure in the event of glutamate mutation is evident from tryptophan fluorescence and far uv spectrophotometry. However, more rigorous evidence comes from analytical ultracentrifugation, where the sedimentation coefficient of the ΔE35 E2:E3BP core is not only lower than the wild-type core, but also indicates the presence of several molecular species (Fig. 4.30). The premature aggregation of 'sticky' lipoyl domains may lead to the formation of mostly abnormal, less compact or low molecular weight core with abnormal subunit composition rather than the normal high molecular weight 60:12 meric E2:E3BP core. However, in the sedimentation velocity experiment, it was also found that a small amount of normal sized core was present that could account for the 10-20% residual activity and was in agreement with the patient's PDC activity as determined by CO_2 release assay.

The low activity in the patient's PDC could also be explained partly by E1 and E3 enzyme binding to a large population of inactive cores and therefore be catalytically ineffective. E1 catalysed reductive acetylation of a lipoyl group depends on the 3D structure of lipoyl domain (Dardel et al., 1993). Some isoforms of PDC kinase, particularly isoform 4, appear to bind more strongly to the outer lipoyl domain of the mammalian enzyme (Tuganova et al., 2002; Yeaman et al., 1978). In this study the structure of outer lipoyl domain has also found to be lost (Fig. 4.19 & Fig. 4.20) which might impair the attachment of this kinase *in vivo* leading to further dysregulation of the complex.

These experimental data showed that glutamate 35 mutation is crucial for the structural integrity of the complex and has different consequences from the earlier mutation investigated in Chapter 3 in which the single lipoylatable lysine is replaced by glutamine.

The two mutants (E35D & E35Q), studied simultaneously were not found to be equivalent to the deletion mutant. The aspartate substitution was similar in all respects to the wild-type in terms of structure and function, whereas very slight structural and functional changes were shown by the glutamine mutant. Thus, alterations in the size and charge of amino acids at this position have only minor effects on core assembly and function whereas the omission of the glutamate-35 indicates its importance for the folding, assembly and integrity of the entire E2:E3BP core. These data provide a detailed explanation for the unexpected severity of the effect of the glutamate 35 deletion in the outer lipoyl domain of E2, accounting for the unusual nature of the PDC deficiency in this patient.

Chapter 5

A preliminary investigation of the subunit organisation of the recombinant 2-oxoglutarate dehydrogenase (OGDC)

5.1 Introduction

The 2-oxoglutarate dehydrogenase (OGDC), along with the pyruvate dehydrogenase (PDC) and branched chain 2-oxoacid dehydrogenase complex (BCOADC), collectively constitute the family of 2-oxoacid dehydrogenase multi-enzyme complexes. They are important in controlling carbon flux from carbohydrate precursors and a select group of amino acids into and around the tricarboxylic acid cycle. Located in the mitochondrial matrix, the mammalian complexes catalyze the irreversible oxidative decarboxylation of their respective 2-oxoacid substrates yielding the appropriate acyl CoA derivatives, NADH and CO_2. Central to this catalysis is the consecutive action of their three catalytic components, each present in multiple copies : a substrate-specific 2-oxoacid dehydrogenase

(E1), a distinct dihydrolipoamide acyltransferase (E2) and a common dihydrolipoamide dehydrogenase (E3) (Behal et al., 1993; Patel and Harris, 1995).

The OGDC appears to be much more conserved in evolution than the PDC; both *E. coli* and pig heart complexes exhibit similar quaternary structures (Koike and Koike, 1982; Tanaka et al., 1972; Yeaman et al., 1978), and unlike eukaryotic PDC or BCOADC, mammalian OGDC is not regulated by phosphorylation and dephosphorylation (Koike and Koike, 1982).

OGDC is an important mitochondrial multienzyme complex that has been increasingly associated with a number of neurological disorders. It catalyzes a critical step in the Krebs cycle that is also important in the metabolism of the excitotoxic neurotransmitter, glutamate. In human brain, the activity of OGDC is lower than that of any other enzyme of energy metabolism, including phosphofructokinase, aconitase and the electron transport complexes (Sheu and Blass, 1999). Thus deficiencies of OGDC are likely to impair brain energy metabolism and therefore brain function, leading to the manifestation of neurological symptoms. The severity of the neurological symptoms varies according to the nature of the deficiency. Several disorders implicating OGDC defects have been recognized including infantile lactic acidosis, psychomotor retardation in childhood, intermittent neuropsychiatric disease with ataxia and other motor manifestations, Friedreich's and other spinocerebellar ataxias, Parkinson's disease and Alzheimer's disease (AD) (Butterworth and Besnard, 1990; Gibson et al., 1988; Mastrogiacomo et al., 1996; Terwel et al., 1998).

The persistence of abnormalities in the OGDC and particularly in its E2o component in familial AD fibroblasts indicates that abnormalities of this complex are an intrinsic part of the AD process (Sheu and Blass, 1999). OGDC is not uniformly distributed in human brain, and the neurons that appear selectively vulnerable in human temporal cortex in AD are enriched in OGDC. A statistically significant negative correlation was observed between OGDC activity and neurofibrillary tangle count in AD parietal cortex (Mastrogiacomo et al., 1993). However, reduced levels of OGDC are a feature of some, but not all patients with AD (Kish, 1997). Reproducible reductions occur in the PDC, OGDC and cytochrome oxidase activities in AD brain and evidence suggests that OGDC deficiencies may be genetic in some cases whereas evidence that the other two enzyme systems have a genetic component is lacking (Gibson et al., 1998).

In recent studies, OGDC has been found to be a primary site of ROS production in normally functioning mitochondria (Starkov et al., 2004). This complex is also one of several major autoantigens in primary biliary cirrhosis. Loss of OGDC activity is observed in thiamine deficiency and it was recently demonstrated that the response of brain OGDC activity, mRNA levels and immunoreactivity of its E1o, E2o and E3 components to thiamine deficiency is region and time dependent. Loss of OGDC activity in brain cortex is probably related to post-translational modification rather than a loss of protein whereas, in the sub-medial thalamic nucleus, transcriptional and post-translational modifications may account for diminished activity (Shi et al., 2007).

Less information is available on the subunit organization and the mode of interaction of constituent enzymes of OGDC as compared to PDC and BCOADC. The constituent enzymes of OGDC are assembled in a tight but non-covalent fashion around a 24-meric E2o core, exhibiting octahedral symmetry. In prokaryotes, in combination with its catalytic role, the oligomeric E2o core is responsible for tethering and orientating both the E1o and E3 enzymes within the complexes via compact, peripheral subunit-binding domains (Mande et al., 1996; Mattevi et al., 1992; Yeaman et al., 1978). However, analysis of rat and human E2-OGDC genes revealed the absence of any E1- or E3-binding motifs, although such sequences were readily located in the E2-OGDC genes from other organisms, notably *E. coli* (Spencer et al., 1984) and *Azotobacter vinelandii* (Westphal and de Kok, 1990).

Studies on mammalian OGDC, employing subunit-specific proteolysis and N-terminal sequence analysis, have identified a proteolytically-sensitive region at the extreme N-terminus of the E1o component with significant sequence similarity to the E3BP and E2 components of mammalian PDC (Rice et al., 1992). These similarities suggested that E1o might perform some functions normally devolved to E2 or E3BP in PDC and E2-BCOADC.

Selective limited tryptic or arg C degradation of OGDC resulted in a single cleavage in E1o, producing an N-terminal fragment (approx. M_r 10,000), abolition of E3 binding and dissociation of an active E1'o species (M_r 100,000). Complete disassembly of OGDC following this proteolytic event indicated that this region of E1o was critical for the maintenance of complex stability and integrity. A putative peripheral subunit-binding domain has been identified at the site of tryptic attack (Rice et al., 1992). To further characterise the N-terminal E1o fragment and to map the precise residues involved in

maintaining critical contact with E2o and E3, N-terminal fragments of human E1o have been cloned, overexpressed and purified and their binding potential tested in this Chapter in order to obtain a better understanding the subunit organisation of this complex. These studies should provide a more comprehensive insight into OGDC subunit interactions contributing to overall complex integrity and enable preliminary mapping of regions of E1o/E3 involved in generation of a stable association with the E2o core. A clear understanding of its overall structural organisation is essential in view of mounting evidence for a role for OGDC in a range of neurodegenerative disorders and its involvement in oxidative stress responses. Moreover, this study should provide initial data on the feasibility of producing a recombinant OGDC model (equivalent to our PDC model) that can be employed for studying its role(s) in disease in future.

5.2 Cloning of full length E1o

Two putative cDNA clones for human E1o were obtained from GeneService, Cambridge. Primers (Materials & Methods section 2.1.4) were designed to amplify the cDNA and to introduce *Nde 1* and *Xho 1* sites at the 5' and 3' termini of the amplicon. For PCR, after initial denaturation at 94 °C for 5 min, reactions were cycled 30 times through 94 °C (30 s), 62 °C (30 s) and 72 °C (40 s) with a final incubation at 72 °C for 5 min. PCR products were resolved on a 1% (w/v) agarose gel and were found to be amplified in 6 individual PCRs from one clone, each yielding a major band of 3 kbp consistent with the predicted size for E1o cDNA (Fig. 5.1 A). Successful amplification confirmed that this plasmid contained a full length copy of the gene. Amplified PCR product was extracted as described in Methods section 2.2.3 and a sample of pET-14b vector was prepared by digestion with *Nde1* and *Xho1* restriction enzymes. Digested vector was also run on an agarose gel and gel extracted. Then, 100 ng of vector was mixed with a 3-fold molar excess of insert. For ligation, a Quick Ligation Kit from New England Biolabs was used. Ligation mix (5 ng) was transformed into competent *E. coli* TOP 10 cells and the bacteria plated onto LB-amp agarose plates. After overnight incubation at 37 °C, clones were screened by colony PCR for the presence of insert. In colony PCR, around 5-6 colonies were picked, individually suspended in 7 μl of sterilized distilled water and streaked onto a master plate for future use. Individual bacterial suspensions were heated at 95 °C for 5 min, chilled on ice and centrifuged to collect 4 μl of supernatant as a crude DNA template

for PCR. Diagnostic colony PCR was carried out with primers as described earlier. Only two clones were found to be positive. Positive clones were further screened by restriction digestion analysis (Fig. 5.1 B) and the correct reading frame and E1o sequence again confirmed by DNA sequencing.
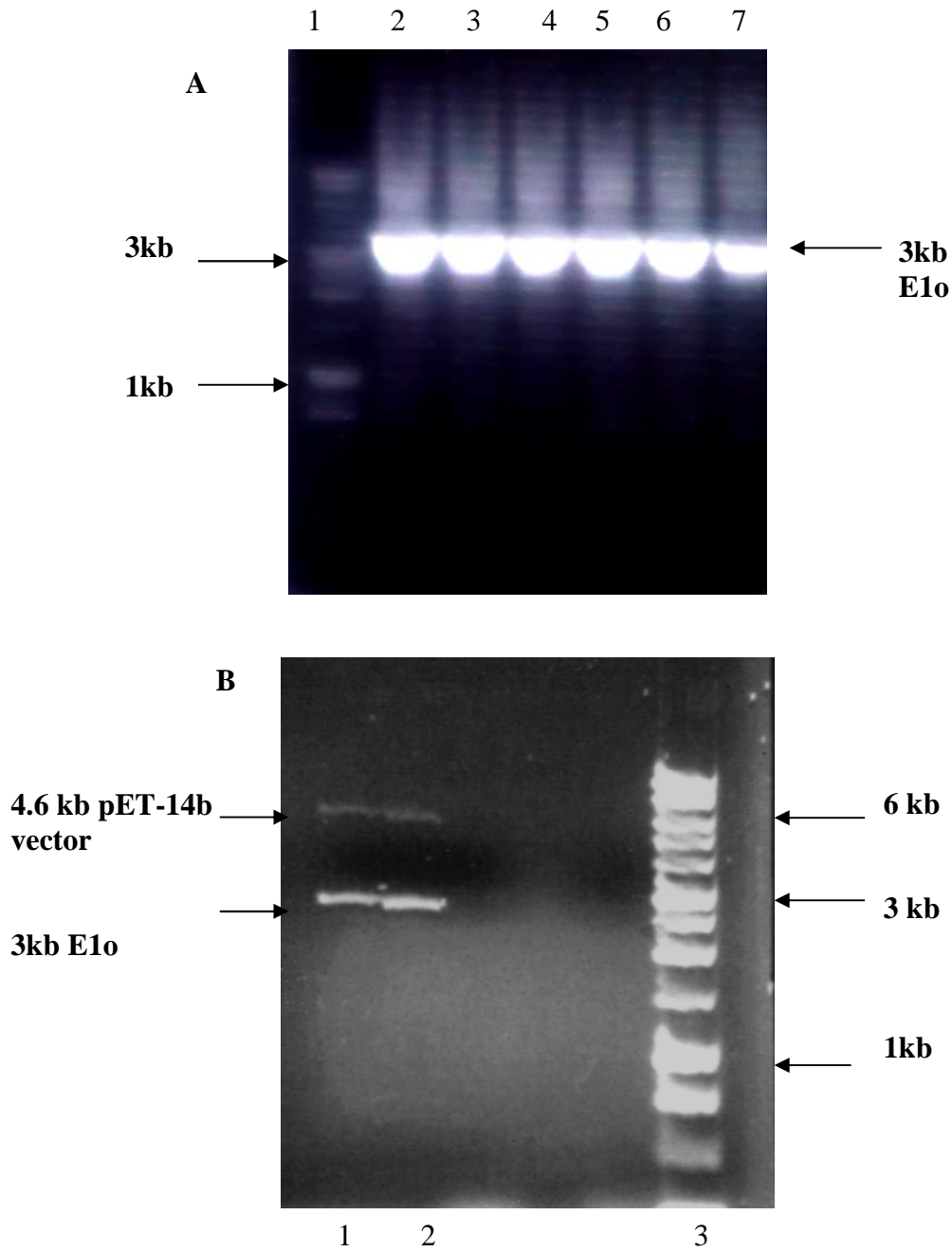
Figure 5.1: Cloning of the E1o cDNA

(A) PCR amplification of the E1o cDNA (lanes 2-7) with *Nde1* and *Xho1*. 10 kb ladder in lane 1. (B) Restriction digestion of the two putative E1o clones using *Nde1* and *Xho1* releasing pET-14b vector and E1o cDNA insert of the predicted size (lanes 1 & 2). 10 kb ladder in lane 3.

5.3 Overexpression of E1o

E1o plasmids were transformed into competent *E. coli* BL21 (DE3) cells to enable E1o expression as His-tagged protein. Overexpression was attempted at 18 °C as well as 30 °C with 1 mM IPTG. No expression was detected on SDS-PAGE analysis as well on Western blotting with anti-His tag antibody (data not shown).

Microbial proteins are relatively easy to express in the *E. coli* host system. Many mammalian proteins have also been overexpressed successfully although these can be more difficult to obtain in active, folded form. *E. coli* is the quickest and most economical expression host of choice, being easy to scale to large volumes and suitable for generation of labelled proteins. However, not all large proteins can be successfully overexpressed in *E. coli.* Moreover, it is often not feasible to perform post-translational modifications that are required for function. E1o is a homodimer of two 100 kDa subunits and, in this case, it proved impossible to achieve detectable expression of this enzyme in the time available. To date, there are no reports in the literature on successful expression of recombinant mammalian E1o. In fact, the native enzyme is also extremely labile and difficult to study because of its tight association with E2o.

5.4 Subcloning of E2o

An E2o construct in pET-14b was already available in the laboratory. As the vector is ampicillin resistant, it is not suitable for carrying out co-expression with other ampicillin resistant vectors. Therefore, E2o cDNA was subcloned from pET-14b into pET-28b, thereby conferring kanamycin resistance as well as incorporating a N-terminal His-tag. Minipreps of E2o pET-14b were prepared and digested with *Xho1* (Fig. 5.2 A). The digested E2o DNA was gel extracted by the standard protocol (Methods section 2.2.3). Minipreps of pET-28b vector were also made and cut with *Xho1* in a suitable buffer. The linearised DNA was treated with 2.5U of calf alkaline phosphatase for 60 min. Alkaline phosphatase removes 5′ phosphates from the DNA and prevents re-circularization of cloning

vectors. The treated DNA was run on a 1% (w/v) agarose gel and was gel extracted using the Promega kit as per manufacturer's instructions. The gel extracted E2o and pET-28b DNAs were ligated as described in Methods section 2.2.5. The ligation mixture was transformed into *E. coli* DH5α cells. A control transformation was also carried out in the absence of ligation mixture. Colonies appeared on the test plate and none in the control. Single colonies were picked, grown overnight in LB medium and minipreps were prepared. The plasmids, thus prepared, were cut with *Xho1* and the digested DNA mixture was run on a 1% (w/v) agarose gel. The expected size of DNA insert was released indicating successful subcloning (Fig. 5.2 B). The correct orientation of the DNA, subcloned in pET-28b vector was checked by overexpression of E2o and subsequent SDS-PAGE analysis (Fig. 5.2 C).

A

4.6 kb pET-14b vector →

1.3kb E2o →

← **5.36 kb pET-28b vector**

1   2   3   4   5   6

B

5.36 kb pET-28b vector →

1.3kb E2o →

← **6kb**

← **3kb**

← **1kb**

1   2   3   4   5   6   7

C

kDa T_0 T_5 T_0 T_5 T_0 T_5 T_0 T_5 T_5

Mw

97.0

66.0
45.0
33.0

20.1

14.4

Overexpressed E2o

1   2   3   4   5   6   7   8   9   10
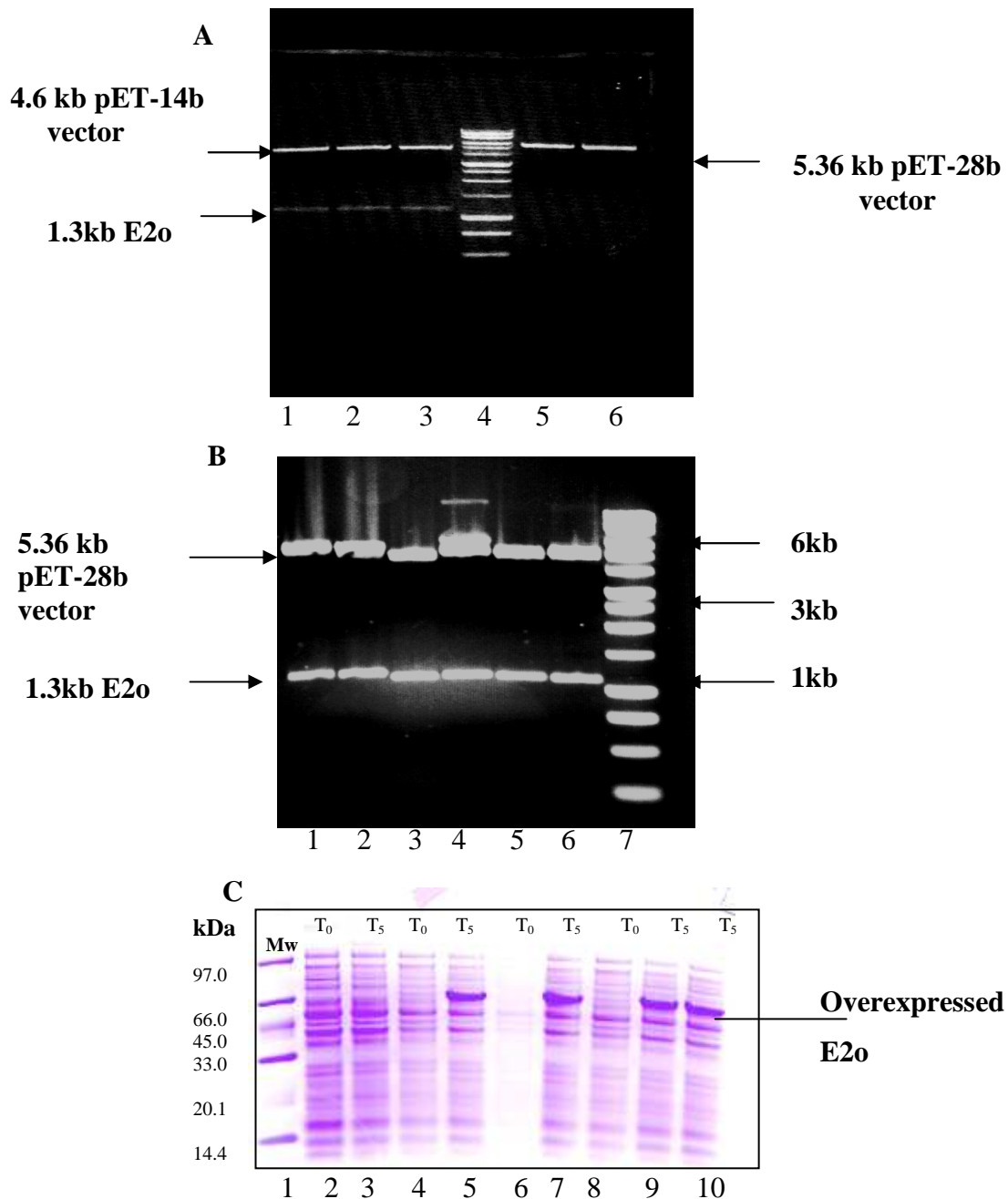
Figure 5.2: Subcloning of the E2o

(A) E2o was released from the pET-14b vector by digestion with *Xho1* (lanes 1, 2 & 3). pET-28b vector was linearised by digesting with *Xho1* (lanes 5 & 6). 10 kb ladder in lane 4. (B) Restriction digestion of six E2o clones of pET-28b with *Xho1* (lanes 1-6). 10 kb ladder in lane 7. (C) Orientation of the E2o cDNA was checked by overexpressing in *E. coli* BL21 (DE3) cells at 30 ºC for 4-5 h. SDS-PAGE analysis shows overexpression at zero time (T_0) and 5 h after induction (T_5). T_0 for the last overexpression is not shown here. Four clones out of five tested were found to be overexpressing (lanes 5, 7, 9 & 10). Molecular weight markers (Mw) are in lane 1.

5.5 To investigate a possible interaction between the E2o and E3 enzymes of OGDC

To check for any potential interaction between the E2o and E3 enzymes of OGDC, both enzymes were overexpressed individually at 30 ºC for 4-5 h. As both enzymes were His-tagged, each was purified using zinc chelate chromatography. Purified enzymes were dialysed against 150 mM NaCl, 50 mM potassium phosphate, pH 7.5. The two enzymes were mixed and passed through a HiPrep 16/60 Sephacryl S-300 High Resolution column attached to a BioCAD 700E workstation equilibrated with 50mM potassium phosphate, 150 mM NaCl, pH 7.5. Two separate peaks of eluted protein were observed. On SDS-PAGE analysis of the individual peaks, it was found that the first peak eluting at the void volume contained only E2o whereas the second peak consisted solely of homodimeric E3 that eluted at the expected position for a 100,000 M_r species (Fig. 5.3). Thus no stable association between E2o and E3 could be detected under these conditions.
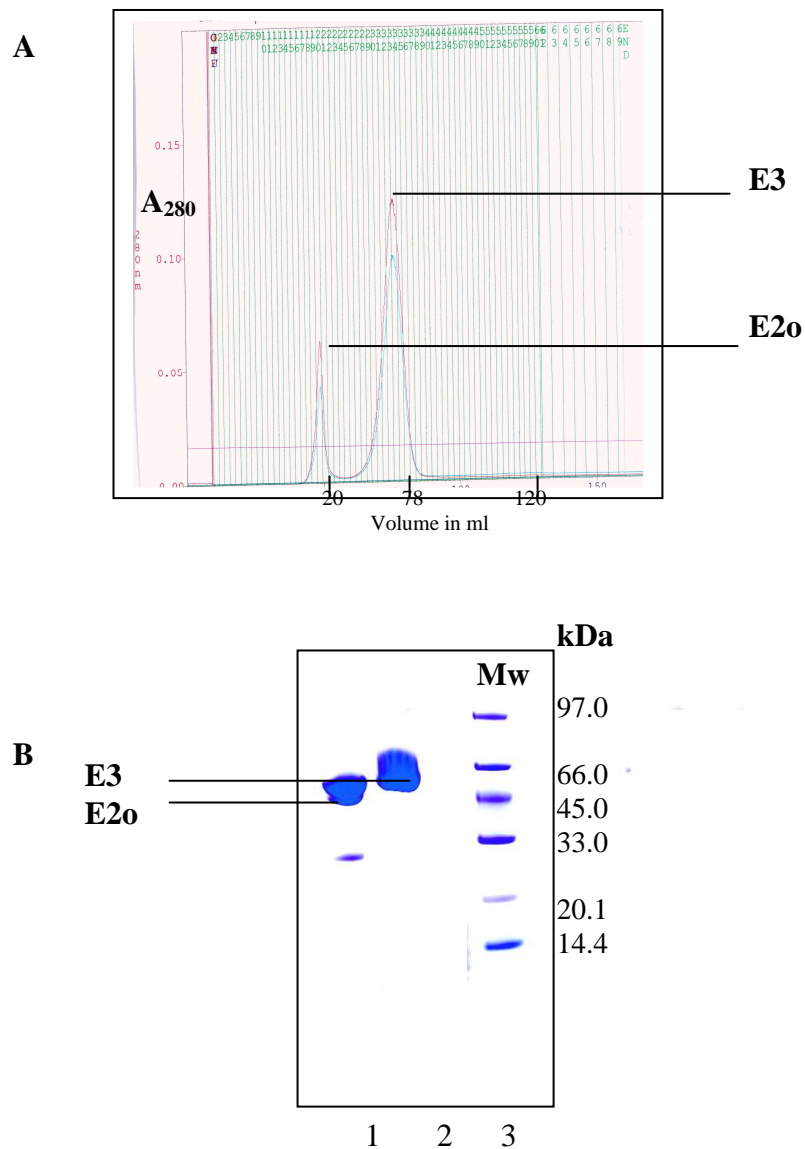
Figure 5.3: Post–translational mixing of E2o and E3 followed by gel filtration

(A) E3 and E2o were overexpressed individually and purified by zinc chelate chromatography as described in Methods section 2.3.6. Purified fractions of each were mixed post–translationally and gel filtered through a Sephacryl HiPrep S-300 High Resolution column attached to a BioCAD 700E workstation. Two eluted peaks were observed, one at the void volume and another where the E3 homodimer elutes routinely. (B) SDS-PAGE analysis of the two peaks showed E2o (lane 1) eluting at the void volume and E3 (lane 2) in the later peak. Molecular weight markers (Mw) are in lane 3.

5.6 Overexpression and solubility check of His-tagged N and C-terminal truncates of E1o

Constructs of the N-terminal (first 579 bases) and C-terminal (next 2313 bases) region of E1o in pET-14b vector were available in the laboratory. The fidelity of the constructs was re-checked by DNA sequencing prior to transforming individually into *E. coli* BL21 (DE3) cells. Overexpression was induced at 18 °C overnight with 1 mM IPTG when cultures attained an A_{600} of 0.5. On SDS-PAGE analysis, it was found that the N-terminal fragment was overexpressed whereas the C-terminal fragment failed to overexpress (Fig. 5.4 A & B) and could not be detected on Western blotting with an anti-His tag antibody (data not shown). Again, possibly owing to its large size, the *E. coli* expression system did not prove suitable for overexpression as was the case for full length E1o. A solubility check of the overexpressed N-terminal fragment was performed as described in the Methods section 2.3.3. and the fragment was found to be insoluble (Fig. 5.4 A).

5.7 Co-expression and interaction study on the His-tagged N-terminal fragment of E1o and E2o

His-tagged N-terminal E1o (comprising the first 193 amino acids) and His-tagged E2o were co-transformed into *E. coli* BL21 (DE3) cells and overexpressed at 22 °C. Co-transformation was possible because the E2o construct was housed in pET-28b, a kanamycin resistant vector whereas the other construct was located in the ampicillin resistant plasmid pET-14b. The identities of co-expressed and His-tagged E2o and N-terminal E1o present in cell extracts were confirmed by Western blotting using anti-His tag antibody (Fig. 5.5 B). This blot also showed that N-terminal E1o overexpression was low

when co-expressed with E2o compared to the levels achieved when overexpressed on its own.

The solubility of the co-expressed proteins was analysed by the standard protocol (Methods section 2.3.3) and resolved by SDS-PAGE. Notably, it was seen that N-terminal E1o fragment that was completely insoluble when expressed alone (Fig. 5.4), now became partially soluble when co-expressed with E2o as shown by SDS-PAGE (Fig. 5.5 A).

This indicated the possibility that the N-terminal E1o truncate may be co-integrated with E2o in a similar fashion to the way in which E3BP is integrated with E2 in PDC. Both the N-termini of E1o as well as E2o were His-tagged and therefore, could be purified on zinc chelate chromatography. However, its stable integration could be observed on gel filtration when the putative purified complex appeared as a single peak at the void volume on a HiPrep 16/60 Sephacryl S-300 High Resolution column and both the proteins could apparently be visualised by SDS-PAGE (Figs. 5.6, A & B). Owing to lack of availability of a suitable E1o antibody for confirming the identity of the putative E1o fragment co-eluting with E2o at the void volume, the binding between the two could not be determined unequivocally as the possibility remained that this band could represent a truncated, His-tagged N-terminal product of E2o. Therefore, this apparent direct interaction was further examined by preparing two glutathione-S-transferase (GST) constructs of N-terminal E1o followed by their co-expression with E2o and purification (see sections 5.10 and 5.13) using 'pull down' assays.
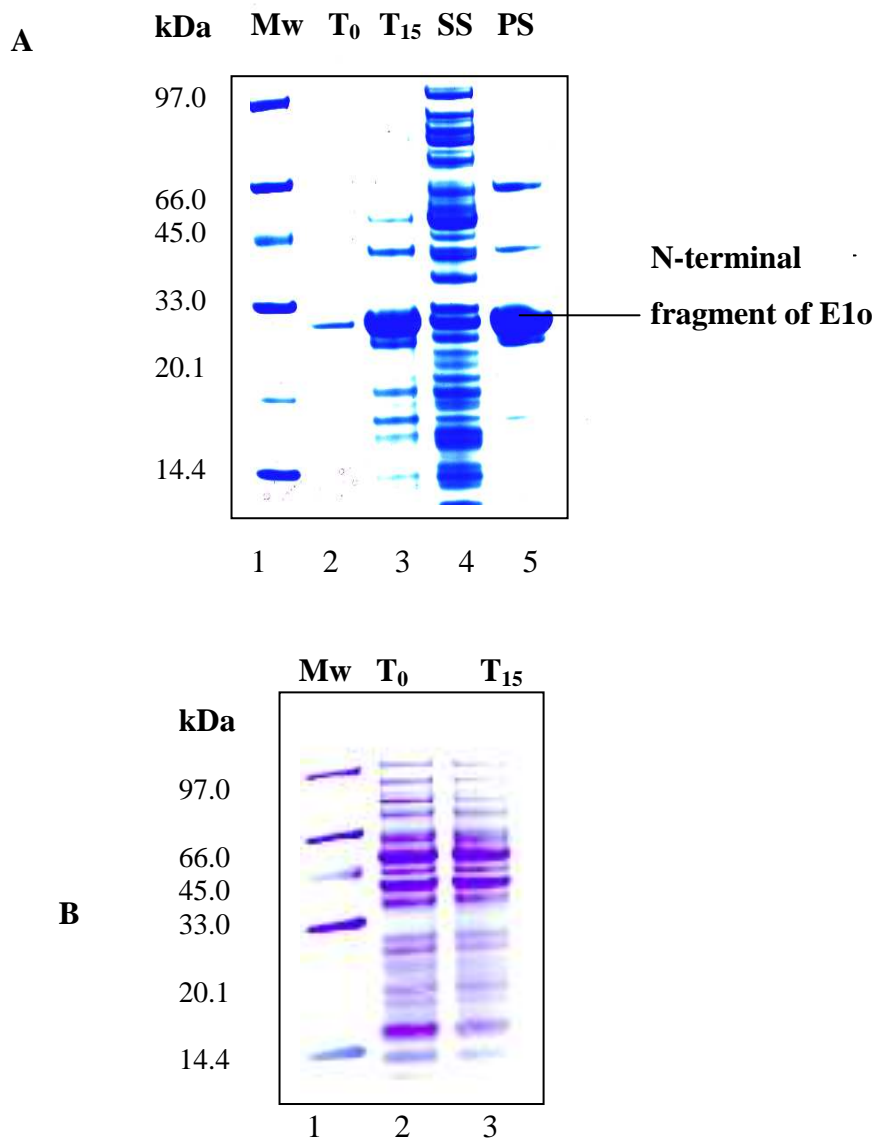
Figure 5.4: Overexpression of the His-tagged N-terminal fragment and C-terminal region of E1o

(A) The N-terminal fragment of E1o was overexpressed at 18 ºC overnight in *E. coli* BL21 (DE3) cells. SDS-PAGE analysis shows expression at zero time (T_0) (lane 2) and 15 h after induction (T_{15}) (lane 3). Solubility checking showed that it was mostly insoluble and present in the pellet sample (PS) (lane 5). Supernatant sample (SS) is in lane 4. Molecular weight markers (Mw) are in lane 1. (B) The C-terminal region of E1o was overexpressed at 18 ºC overnight. SDS-PAGE analysis shows no detectable overexpression of protein corresponding to an anticipated 86 kDa species, 15 h after induction (T_{15}) (lane 3). Molecular weight markers (Mw) are in lane 1.
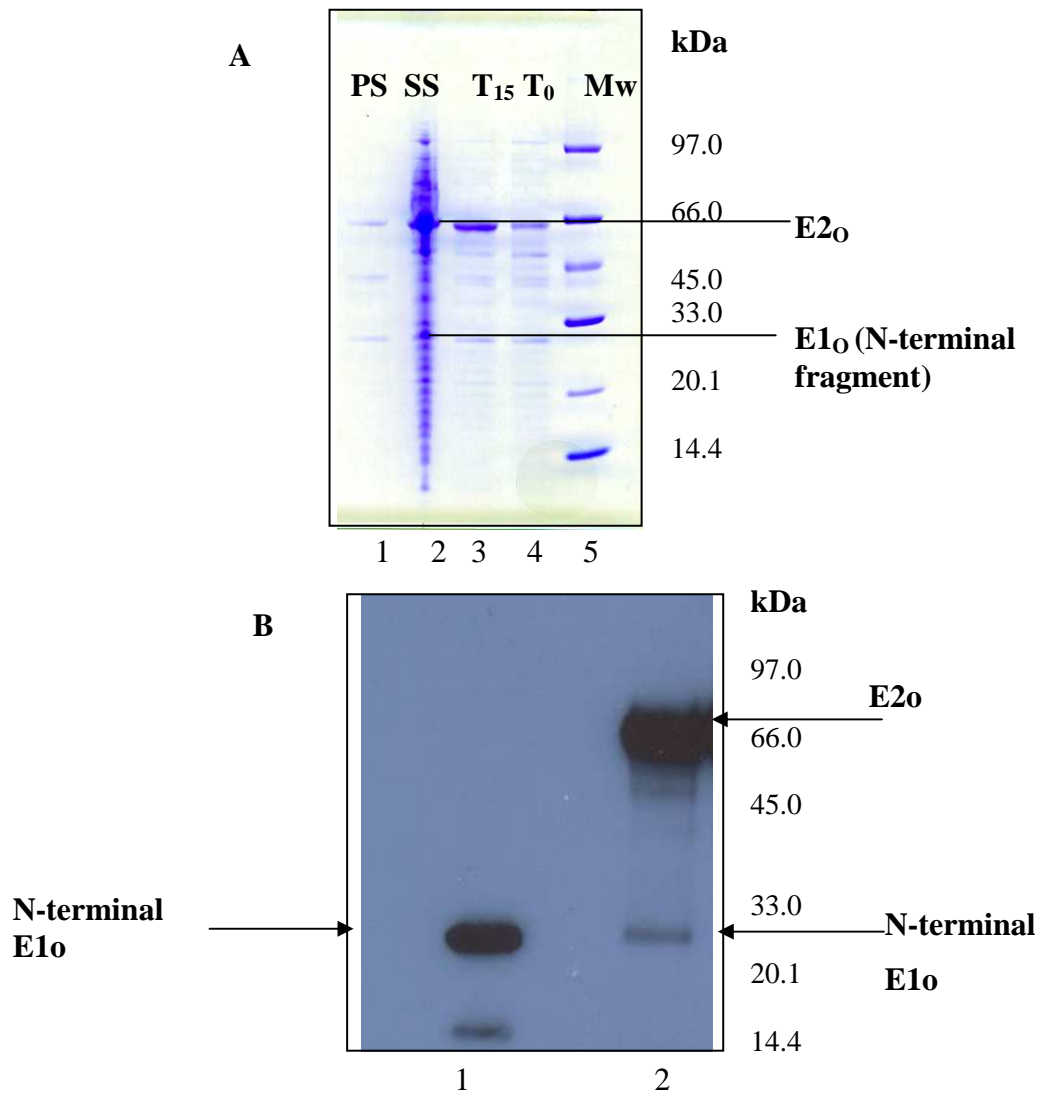
Figure 5.5: Detection of co-expression of N-terminal E1o fragment and E2o

(A) E2o and the N-terminal E1o fragment were co-expressed at 22 ºC overnight. SDS-PAGE analysis on a 4-12% Bis-Tris shows expression at zero time (T_0) and 15 h after induction (T_{15}). Solubility checking showed that both E2o as well as a band corresponding to the expected size of the E1o fragment were soluble and present in the supernatant sample (SS) (lane 2). Pellet sample (PS) in lane 1. Molecular markers are in lane 5. (B) Since the levels of expression were poor, the identities of His-tagged E2o & N-terminal E1o fragment were confirmed by Western blotting with anti-His tag antibody. Blotting analysis shows overexpressed N-terminal E1o (lane 1) as a positive control and co-expressed E2o and N-terminal E1o (lane 2).
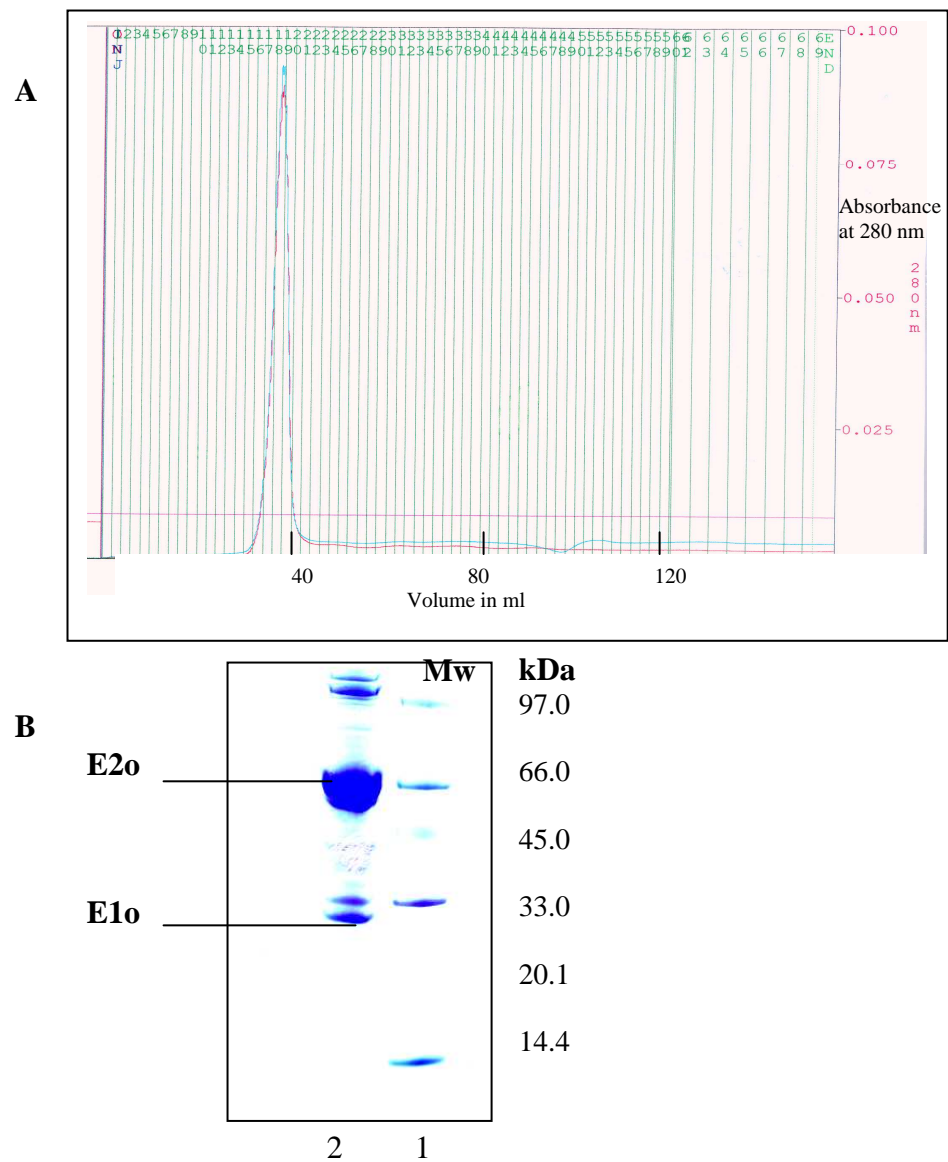
Figure 5.6: Gel filtration of co-expressed and purified E2o and N-terminal E1o

(A) E2o and N-terminal E1o were co-expressed and purified by zinc chelate chromatography. Purified fractions were pooled and gel filtered through a Sephacryl HiPrep S-300 High Resolution column attached to a BioCAD 700E workstation. (B) On SDS-PAGE analysis of the single peak eluting at the void volume, E2o as well as a putative E1o fragment were visualised indicating the possible formation of a high M_r complex between the two species (lane 2). Molecular weight markers (Mw) are in lane 1.

5.8 Subcloning cDNA encoding an N-terminal E1o fragment (166 amino acids) into pGEX-2T

The E1o cDNA sequence encoding the first 166 amino acids of mature E1o was subcloned into pGEX-2T using the previous N-terminal construct housed in pET-14b as a template. This step was carried out in order to facilitate protein-protein interaction studies using 'pull down' assays with a GST-fused E1o fragment and His-tagged E2o. It was also considered that expression of the E1o fragment as a GST fusion may aid solubility when expressed in the absence of E2o, thereby enabling investigations on whether any potential binding to E2o occurred in a co- or post-translational fashion.

For cloning, the first 498 nucleotides were amplified by PCR and *BamH1* and *EcoR1* sites were created at the 5' and 3' termini of the amplicon by designing and employing suitable primers (Materials & Methods section 2.1.4). For PCR, after initial denaturation at 94 °C for 5 min, reactions were cycled 30 times through 94 °C (30 s), 56 °C (30 s) and 72 °C (40 s) with a final incubation at 72 °C for 5 min. PCR products were resolved on a 1% (w/v) agarose gel and were found to be amplified as expected. Amplified PCR product was extracted using a gel extraction kit as described in Methods section 2.2.3. A sample of pGEX-2T vector was prepared by digestion with *BamH1* and *EcoR1* then run on a 1% (w/v) agarose gel and extracted. Digested vector (100 ng) was mixed with a 3-fold molar excess of insert for ligation using the Quick Ligation Kit from New England Biolabs. Ligation mix (5 ng) was transformed into competent *E. coli* TOP 10 cells and the bacteria plated onto LB-amp agarose plates containing ampicillin. After overnight incubation at 37 °C, colonies appearing on the plate were picked and plasmids prepared. Plasmids were screened by restriction digestion with *BamH1* and *EcoR1* (Fig. 5.7). Positive clones were further checked by sequencing.

5.9 Overexpression and purification of the N-terminal E1o GST fusion protein (first 166 amino acids)

The pGEX-2T construct containing N-terminal E1o cDNA (corresponding to the first 166 amino acids) was transformed into E. *coli* BL21 (DE3) cells. Overexpression was carried out at 30 °C for 4-5 h after induction with 1 mM IPTG. Expression was analysed by SDS-PAGE (Fig. 5.8).

Frozen pellet from an overexpressed culture (500 ml) was disrupted by French press treatment as described in Methods section 2.3.2 and the soluble supernatant fraction containing GST-fusion protein purified by glutathione Sepharose 4B chromatography (Methods section 2.3.13). Two protease inhibitor tablets (EDTA free) were added before French press treatment.

SDS-PAGE analysis of the purified fractions showed extensive degradation of the GST-tagged E1o fragment. However, some intact fusion protein (predicted size 45 kDa; 18 kDa E1o fragment coupled to the 27 kDa subunit of GST) could be isolated. Lower M_r degradation products of this fusion protein and a band corresponding to the GST protein (27 kDa) were also observed (Fig. 5.8). Neither addition of 1 mM EDTA and DTT nor expressing at lower temperatures in subsequent experiments helped to limit this degradation.

4.9 kb
PGEX-2T
vector →

→ **5 kb**
→ **3 kb**

1kb

0.50 kb
E1o →

→ **0.50kb**

→ **0.25kb**

1   2   3   4   5
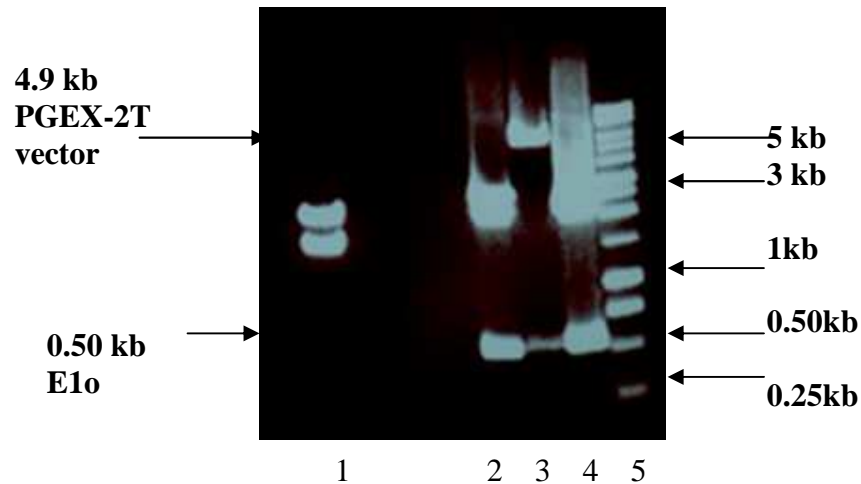
Figure 5.7: Cloning of the N-terminal E1o fragment (corresponding to first 166 amino acids) into pGEX-2T

PCR product corresponding to the N-terminal E1o region (first 166 amino acids) was cloned into pGEX-2T. Diagnostic restriction digestion of putative clones was performed with *BamH1* and *EcoR1*. One clone was positive out of four tested (lane 3) releasing correct-sized insert and vector. Clones in lanes 2 and 4 were discarded as the vector size was incorrect although they appeared to contain appropriate inserts. 10 kb ladder in lane 5.
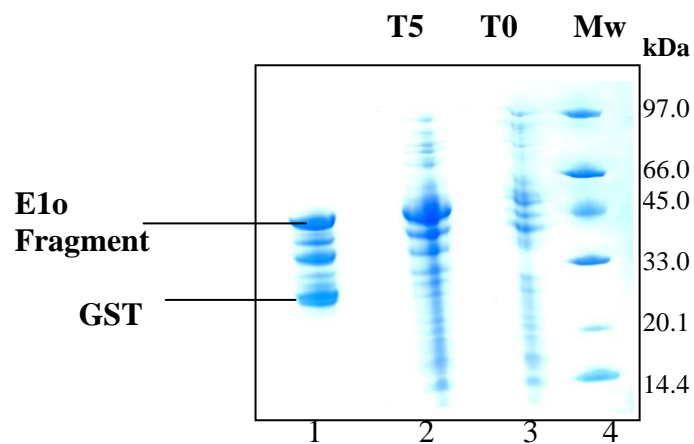
Figure 5.8: Overexpression and purification of the E1o fragment (first 166 amino acids) fused with GST

(A) N-terminal E1o fragment (166 amino acid) fused with GST was overexpressed at 30 ºC for 4-5 h. SDS-PAGE analysis on a 4-12% Bis-Tris shows expression at zero time (T_0) and after 5 h induction (T_5). The protein was purified using a glutathione Sepharose 4B column (lane 1) and shows extensive degradation. Molecular weight markers (Mw) are in lane 4.

5.10 Interaction between E2o and the GST fused E1o N-terminal fragment (first 166 amino acids)

The pGEX-2T construct containing the 5' region of the open reading frame of mature E1o-cDNA (166 amino acids) and E2o cDNA in pET-28b were co-transformed into *E. coli* BL21 (DE3) cells. Overexpression was attempted at 30 °C for 4-5 h after induction with 1 mM IPTG. Protein expression was analysed by SDS-PAGE (Fig. 5.9). Pellet (500 ml culture) was disrupted using French press treatment as described in Methods section 2.3.2 and the soluble supernatant fraction containing GST fusion protein purified by glutathione Sepharose 4B affinity chromatography as described in the Methods section 2.3.13. Two tablets of protease inhibitors (EDTA free) were added before French press treatment.

SDS-PAGE analysis of the purified fractions showed the presence of a band of the predicted size for E2o and therefore a possible integration of E2o with the E1o fragment (Fig. 5.9). In the previous experiment also (section 5.7), the N-terminal E1o fragment was found to be integrating with E2o. No Western blotting was attempted at this point in order to verify the identities of the constituent polypeptides because of extensive degradation of the purified proteins.
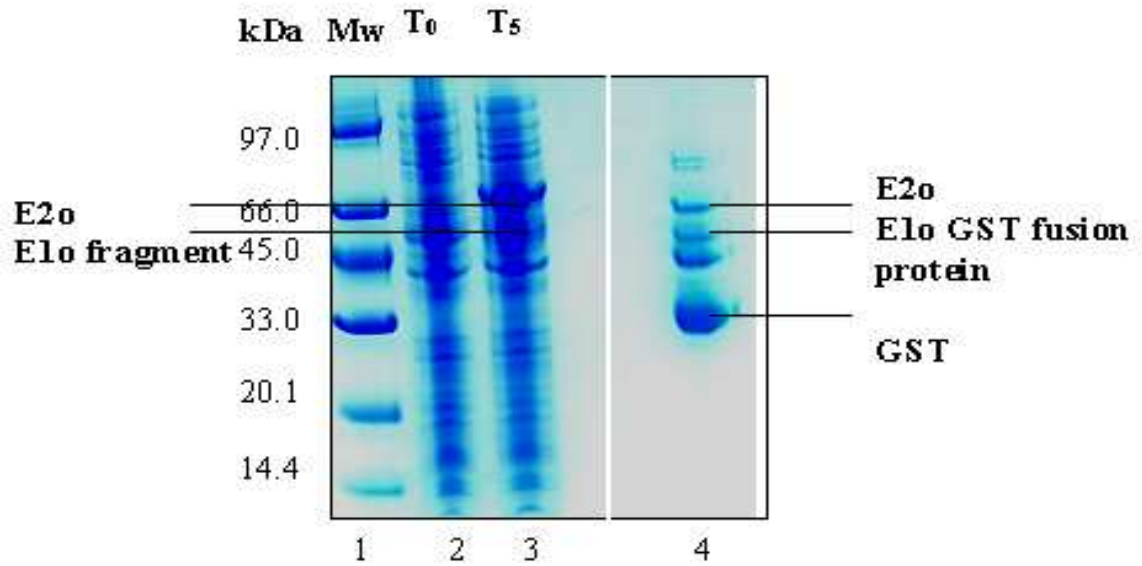
Figure 5.9: Co-expression and purification of the E2o and N terminal E1o GST fusion protein (first 166 amino acids)

SDS-PAGE analysis shows co-expression of E2o and N terminal E1o GST fusion protein at zero time (T_0) and 5 h (T_5) after induction. Soluble fraction obtained from an overexpressed culture (500 ml) after French Press treatment was purified using a glutathione Sepharose 4B column (lane 4) indicating possible E2o co-association with the E1o fragment. Molecular weight markers (Mw) are in lane 1.

5.11 Subcloning cDNA encoding an N-terminal E1o fragment (83 amino acids) into pGEX-2T

The previous experiment (see section 5.10), again suggested a possible integration of E2o with the N-terminal E1o GST fusion protein. However, substantial degradation of the E1o fragment was also observed in several attempts to repeat this study, making it difficult to draw any definitive conclusions. To determine more precisely the putative E2o binding site on E1o and to possibly limit degradation, the first 83 amino acids of mature E1o corresponding to the first 249 nucleotides of mature E1o were subcloned into pGEX-2T.

For this investigation, the first 249 nucleotides were amplified and *BamH1* and *EcoR1* sites created at the 5' and 3' termini of the amplicon by designing and employing the primers as described in Materials & Methods section 2.1.4. For PCR, after initial denaturation at 94 °C for 5 min, reactions were cycled 30 times through 94 °C (30 s), 58 °C (30 s) and 72 °C (40 s) with a final incubation at 72 °C for 5 min. PCR products were resolved on a 1% (w/v) agarose gel and were found to be amplified. Amplified PCR products were extracted using a gel extraction kit as described in Methods section 2.2.3. pGEX-2T vector was prepared by digestion with *BamH1* and *EcoR1* restriction enzymes and digested vector also run on an agarose gel and gel extracted. Then, 100 ng vector was mixed with 3-fold molar excess of insert for ligation employing a Quick Ligation Kit from New England Biolabs. Ligation mix (5 ng) was transformed into competent *E. coli* TOP 10 cells and the bacteria were plated onto LB agarose containing ampicillin. After overnight incubation at 37 °C, clones were prepared and screened by restriction digestion with *BamH1* and *EcoR1* for the presence of the correct-sized insert (Fig. 5.10). Positive clones were further checked by DNA sequencing.
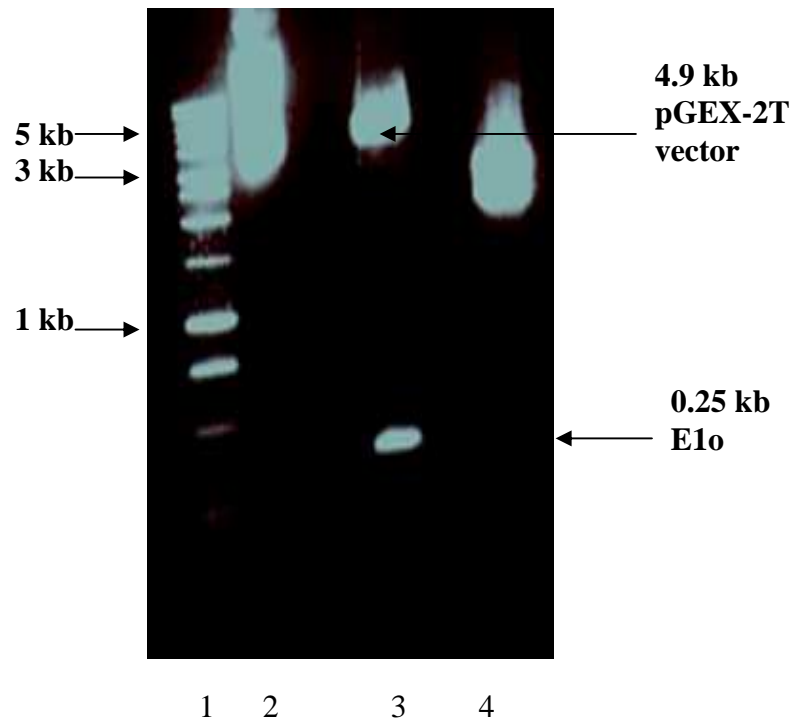
Figure 5.10: Cloning of the E1o cDNA fragment encoding its N-terminal sequence (83 amino acids) into pGEX-2T

PCR product encoding the N-terminal E1o fragment was cloned into pGEX-2T. Restriction digestion of putative recombinant clones treated with *BamH1* and *EcoR1* is shown. One clone was positive, out of three tested (lanes 2-4), containing an insert of the right size (lane 3).

5.12 Overexpression and purification of the N-terminal E1o GST fusion protein (first 83 amino acids)

The N-terminal E1o GST fusion protein (containing the first 83 amino acids) was overexpressed and purified in the same manner as the 166 amino acid E1o-GST fusion protein described in section 5.9. On SDS-PAGE analysis, this fragment was also found to be sensitive to degradation although this was less problematic than for the larger N-terminal truncate (Fig. 5.11). However, significant amounts of intact fusion protein of the predicted size (36 kDa) were present (9 kDa E1o fragment fused with the 27 kDa GST). Free GST (27 kDa) was also observed (Fig. 5.11). The proteolytic degradation did not appear to occur during overexpression *in vivo*, but was apparent after French press treatment or at the end of the purification process. Addition of 1% (v/v) rat serum reduced but did not completely eliminate this degradation. Further addition of more protease inhibitors (2 mM PMSF, 0.15 µM leupeptin, 15 µM aprotinin, 1.5 µM pepstatin) and also ensuring that the purification process was conducted rapidly and efficiently at 4 °C still did not prevent significant degradation.

5.13 Interaction between E2o and N-terminal E1o GST fusion protein (first 83 amino acids)

N-terminal E1o cDNA (corresponding to first 83 amino acids) in pGEX-2T and E2o cDNA in pET-28b were co-transformed into *E. coli* BL21 (DE3) cells. Overexpression was carried out at 30 °C for 4-5 h after induction with 1 mM IPTG. The expression was analysed by SDS-PAGE. Pellet from overexpressed culture (500 ml) was disrupted by French press treatment as described in Methods section 2.3.2 and the soluble supernatant fraction purified by glutathione Sepharose 4B chromatography (Methods section 2.3.13).

Two tablets of protease inhibitors (EDTA free) and 1% (v/v) rat serum were added before French press treatment.

SDS-PAGE analysis of the purified fractions showed the presence of E2o along with E1o GST fusion protein (Fig 5.11). The presence of E2o was further confirmed using an anti-His tag antibody to detect His-tagged E2o (Fig. 5.12 A).

To ensure that E2o was interacting specifically with the E1o fragment and not with free GST, E2o was also co-expressed with free GST in BL21 (DE3) cells at 30 °C for 4-5 h after induction with 1 mM IPTG. The supernatant fraction from a disrupted pellet (500ml culture) was purified by glutathione Sepharose 4B chromatography. On Western blotting of the purified fraction with anti-His tag antibody, His-tagged E2o could not be detected (Fig. 5.12 B) indicating that E2o was not binding adventitiously to the GST tag. These results demonstrated conclusively for the first time that the first 83 amino acids of N-terminal E1o were crucial for integrating with E2o.
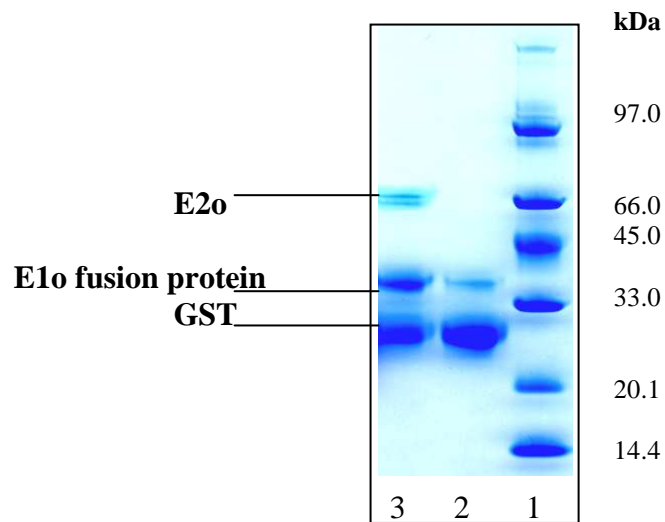
Figure 5.11: Purification of N-terminal E1o GST fusion protein (first 83 amino acids) alone and when co-expressed with E2o

E1o fragment (first 83 amino acids) fused with GST was overexpressed alone and with His-tagged E2o at 30 ºC for 4-5 h in two individual experiments. Soluble fractions obtained from both overexpressed cultures (500 ml) after French Press treatment were purified separately using glutathione Sepharose 4B chromatography. SDS-PAGE analysis of purified fractions on a 4-12% Bis-Tris SDS gel shows the N-terminal E1o GST fusion protein (83 amino acids) (lane 2) and E2o integrated with N-terminal E1o GST fusion protein (lane 3). Molecular weight markers (Mw) are in lane 1.
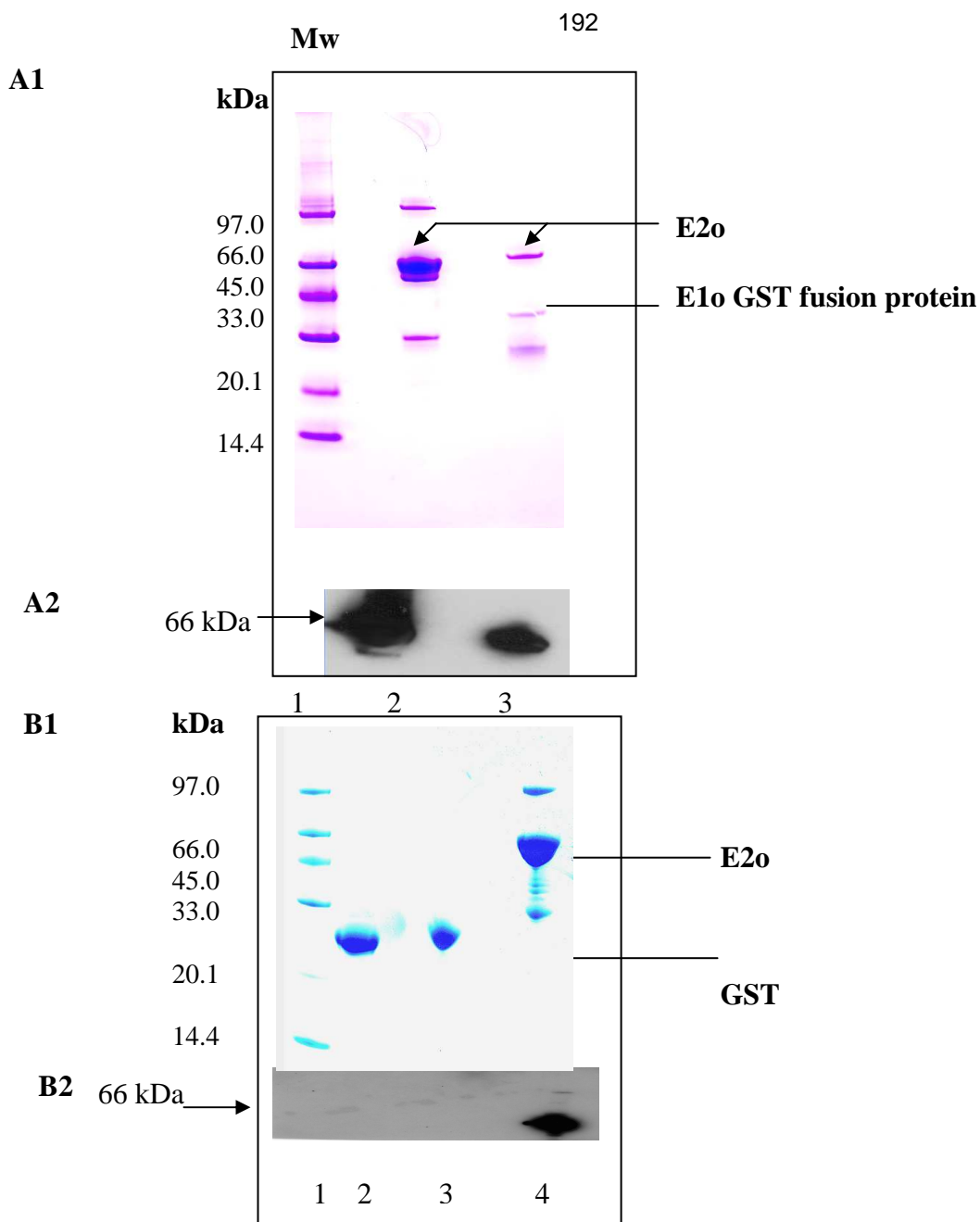
Figure 5.12: Confirming the interaction of E2o with its N-terminal E1o partner

(A1) N-terminal E1o GST fusion protein (83 amino acids) and His-tagged E2o were co-expressed. SDS-PAGE analysis of the fractions purified using glutathione Sepharose 4B chromatography (lane 3) and E2o purified by zinc chelate chromatography as a positive control (lane 2). (A2) Western blotting of the above with anti-His tag antibody shows that E2o was integrated with E1o GST-fusion protein (lane 3). E2o as positive control is in lane 2. (B1) SDS-PAGE analysis of co-expressed E2o and GST purified on glutathione Sepharose 4B (lane 3), E2o as positive control in lane 4 and GST as negative control is in lane 2. Molecular weight markers are in lane 1. (B2) Western blotting of the above with anti-His tag antibody shows that E2o was absent (lane 3) and therefore does not bind non-specifically with the GST tag.

5.14 Discussion of subunit organisation in the OGDC

The structure and subunit organization of mammalian OGDC has not been analysed in depth as compared to other organisms although its E2o core is similarly organised as a 24-meric cube with octahedral (432) symmetry (Reed and Hackert, 1990). In contrast, the structure and catalytic mechanism of the bacterial E2o core, to which the E1o and E3 components are tethered non-covalently, has been elucidated in some detail (Hackert et al., 1983). In mammalian OGDC, an early report also suggested that E1o appears to bind more tightly to E2o than does E3 (Yeaman et al., 1978).

Studies on mammalian OGDC, employing subunit-specific proteolysis and N-terminal sequence analysis, have identified a proteolytically sensitive site in the N-terminal region of E1o that, on cleavage, leads to rapid inactivation of the complex and dissociation of both a large, enzymatically-active, C-terminal E1'o fragment and E3. This region also displays significant sequence similarity to the E3BP and E2 components of mammalian PDC (Rice et al., 1992). These similarities suggested that E1-OGDC may perform some functions normally devolved to E2:E3BP in PDC and E2 in BCOADC. Further indirect evidence, in support of additional roles for E1o, came when the genes for rat and human E2o were cloned (Nakano et al., 1991; Nakano et al., 1994). Analysis of their predicted primary structures failed to locate any E1o or E3-binding motifs, although such sequences were readily located in E2-OGDC genes from other organisms, notably *Escherichia coli* (Spencer et al., 1984) and *Azotobacter vinelandii* (Westphal and de Kok, 1990). Another report suggested that single copies of full length bovine E1o and E3 form a stable 1:1 complex that binds to the E2o core with high affinity via the N-terminal region of E1o (McCartney et al., 1998).

In mammalian OGDC, the E1o enzyme also has high affinity for the E2o core assembly, a property it shares with the E3BP of PDC (Sanderson et al., 1996a). This affinity is so great that attempts to use low (non-denaturing) levels of GdmCl to dissociate E1o from the intact core also proved futile. The successful dissociation of mammalian OGDC into active E2o and E1o/E3 fractions was achieved by employing high levels of $MgCl_2$ and slightly alkaline pH to achieve optimal dissociation with minimal denaturation of the individual

enzymes, yielding functionally active E2o and E1o/E3 fractions (McCartney et al., 1998). These studies provided the first direct biochemical evidence that uniquely, in mammalian OGDC, its constituent E1o enzyme is responsible for binding the E3 component to the core of this multienzyme complex.

As indicated previously, selective proteolysis of bovine OGDC with protease arg C has shown that, with a single cleavage, a 100 kDa E1'o C-terminal fragment and E3 are released from E2o (Rice et al., 1992). The cleavage site of E1'o in bovine OGDC is shown in Fig. 5.13 and this amino acid sequence shows great similarity with the human E1o. However, as the precise arg C cleavage site in bovine E1o is not conserved in human E1o, it is not known whether human E1o can be selectively cleaved in a similar fashion.

Interestingly, there is no direct evidence to show that E3 interacts with E1'o with high affinity (Rice et al., 1992). In previous studies, on gel permeation of an isolated, full-length E1o/E3 fraction under associative conditions, the presence of a higher M_r assembly (303,000 kDa) corresponding to an E1:E3 sub-complex exhibiting 1:1 stoichiometry was detected. Moreover, it was observed that limited proteolysis of OGDC promotes release of both a large C-terminal E1'o fragment and E3, implying that sequences critical for their tight interaction with the E2o core reside in the N-terminal region (McCartney et al., 1998). It was not clear, however, from these two previous publications whether E3 was released directly as a consequence of its binding to E1o or whether E3 association with the core is also dependent on the integrity of the extreme N-terminal region of E1o. A potential interaction between E1'o and E3 could not be evaluated in this study owing to the non-availability of recombinant E1'o.

In this chapter, the main aim was to map the region of E1o that was involved in maintaining high affinity contact with E2o. For this, full length E1o was cloned in pET-14b. Nucleotide sequence corresponding to the first 193, 166 and 83 amino acids of mature E1o were also cloned in pET-14b and pGEX-2T respectively. For studying the co-expression of E1o with E2o, E2o cDNA was subcloned into a kanamycin resistant vector, namely pET-28b. All the cloning strategies employed were successful; however, no detectable expression of full length E1o was achieved in *E. coli*. Difficulties in overexpressing and producing soluble E1-PDC were also observed in the past, but finally solved by cloning into pQE-9, and overexpressing in *E. coli* M15 cells although only limited amounts of active E1 were produced. The available His-tagged, N-terminal E1o fragment (193 amino acids) failed to produce soluble protein (Fig. 5.5). However, when

this N-terminal fragment was co-expressed with E2o, a putative soluble N-terminal E1o: E2o complex was obtained and the two proteins co-eluted on gel filtration (Fig. 5.6 A, B). This was the first indication that indeed the N-terminal region of E1o was capable of forming a stable complex with E2o. However, this was an ambiguous result because the N-terminal fragment was identified only on the basis of SDS-PAGE analysis and Coomassie blue staining. The same result was obtained subsequently by employing two different pGEX-2T constructs harbouring different lengths of N-terminal E1o.

To examine whether the first 80-85 amino acids or a longer N-terminal E1o sequence was required to promote this high affinity interaction, two pGEX-2T constructs of E1o N-terminal truncates were employed. Both E1o GST fusion proteins (83 and 166 amino acids respectively) were relatively soluble as compared to the His-tagged E1o fragment and appeared to bind tightly with E2o in GST 'pull down' assays using glutathione Sepharose 4B chromatography (Figs. 5.9 & 5.11). In addition, interaction of E2o with wild-type GST was excluded in control 'pull down' assays and Western blotting (Fig. 5.12 B). The interaction between E2o and the short (83 amino acid) N-terminal E1o fragment was also confirmed by Western blotting (Fig. 5.12 A) showing that the presence of this extreme N-terminal region was crucial for binding to E2o. These data were consistent with earlier selective proteolysis data in bovine OGDC where a 61 amino acid N-terminal E1o fragment remains attached to E2o upon treatment of OGDC with arg C (McCartney et al., 1998).

In a parallel study, the affinity of E3 for E2o was examined by purifying the two enzymes individually followed by mixing and gel filtration (Fig. 5.3 A, B). The two enzymes did not display any affinity for each other, eluting as individual peaks at their respective elution volumes on gel filtration. Thus E3 is unable to enter into a stable association directly with E2o as anticipated. Therefore, E1o involvement appears crucial for mediating formation of a stable multienzyme assembly that promotes E3 integration with the E2o core.

Although it is possible that the N-terminal residues of E1o may be involved in interacting with E3 directly, nevertheless no co- or post-translational binding studies between N-terminal E1o and E3 were performed as a result of time constraints. However, it was shown that the extreme N-terminal region (first 83 amino acids) of E1o co-integrated with E2o to form a stable complex and moreover, it was conclusively demonstrated that E2o alone does not bind E3 to OGDC.

Most of the earlier research investigating the morphology and subunit organisation of OGDC have employed native complex purified from various organisms. The isolation of individual enzyme components has proved difficult owing to the tight association of the E1o and E2o components. Stringent conditions using chaotrophic agents such as 3 M MgCl$_2$ are required to achieve separation. In this project, recombinant enzymes were employed in an attempt to overcome these difficulties. Recently recombinant homodimeric E1o from *E. coli* has been crystallised and its structure elucidated in detail (Frank et al., 2007). Interestingly, this crystal structure could only be obtained when the first 84 amino acid residues were removed by tryptic digestion. It was suggested by the authors that this distinctive N-terminal region may extend outwards from the core 'fold' and is required to mediate interactions with the other components of OGDC. These observations also show that the N-terminal E1o region is likely to be structurally dynamic, consistent with its presence preventing the crystallisation process. This N-terminal segment displays a high degree of immunogenicity as compared to the large C-terminal E1'o region in mammalian OGDC (McCartney et al., 1998), also indicative of the presence of a flexible and/or extended region of polypeptide.

In our current research, the first 83 and 166 amino acids of human E1o have been cloned, overexpressed and purified as GST fusion proteins. These fragments were very prone to degradation and therefore any possible interactions of E3 with these N-terminal E1o truncates alone or with an equivalent E1o:E2o subcomplex could not be assessed in the time available. Degradation was controlled to some extent by addition of 1% (v/v) rat serum containing serine protease inhibitors that are effective against trypsin, chymotrypsin and elastase (Kuehn et al., 1984). Another reason for rapid degradation could be the intrinsic susceptibility of the N-terminal E1o region to proteolysis, a property that has been noted also with bovine E1o. This again indicates its probable presence as an extended, flexible segment of polypeptide as suggested by Frank et al. (2007).

In this series of experiments, E1o protein production was problematic, in terms of good yields of soluble protein and degradation of GST-tagged protein; however, degradation was reduced to some extent when E1o fragments were co-expressed with E2o when a stable E1o:E2o complex could be purified. It was not possible, however, to determine if a stable interaction between E2o and this N-terminal E1o region could also occur post-translationally owing to the rapid degradation of the various E1o truncates. Assessing if

either these short N-terminal E1o fragments or the large E1'o C-terminal polypeptide can enter into a stable association with E3 is clearly a priority for future work.

E1 OGDC bovine TAPVA- EPFLSGTSSNYVEEMYYAWLENPKSVHKSWDIFFRNTNAGAPPGT

E1 OGDC human SAPVAAEPFLSGTSSNYVEEMYYAWLENPKSVHKSWDIFFRNTNAGAPPGT

E1 OGDC bovine AYQSPLPLSPG- LSAVAR↓ AGPLVEAQPNVDKLV

E1 OGDC human AYQSPLPLSRGSLAAVAH A QSLVEAQPNVDKLV

Figure 5.13: Alignment of first 83 amino acids of mature N-terminal E1o of bovine and human OGDC

The arrow shows the site where E1'o forms as a result of arg C cleavage of bovine heart OGDC. The amino acids in magenta match completely showing high degree of homology between human and bovine E1o. The E1'o sequence in bovine starts from residue G, probably due to loss of A residue due to the presence non-specific amino peptidases.

Chapter 6

Conclusions

In the last 20 years, the 2-oxoacid dehydrogenase complexes have continued to be the subject of intensive investigation. Thus the constituent enzymes have now been cloned, overexpressed and purified from a variety of different organisms. Most of the research on these complexes has so far been based on the analysis of structure, function and interaction of the constituent enzymes, regulated by their associated kinases and phosphatases in the case of mammalian PDC and BCOADC.

In this study, for the first time all the constituent catalytic subunits/enzymes of human PDC were overexpressed, purified to homogeneity and reconstituted to form a fully functional recombinant PDC model. This recombinant multienzyme complex with an overall M_r 9-10 MDa was found to be fully active in enzymatic assays and displayed a similar specific activity (3.5-4 μmol NADH min^{-1} mg protein^{-1}) to PDC extracted from human heart tissue (Palmer et al., 1993). The recombinant model was prepared with a view to studying recently identified novel mutations in the E2 enzyme encountered in three patients diagnosed with PDC deficiency symptoms at Oxford Medical School. Before using this recombinant model to analyse the effect of these mutations on structure, function and assembly, the model was first tested to assess its ability to mimic the effects of combining active and inactive lipoyl domains in the E2:E3BP core. For this, eight mutant recombinant E2:E3BP cores were constructed, overexpressed, purified and reconstituted to form

functional complex by the addition of E1 and E3, in which the lipoyl domains of E2 and the single lipoyl domain of E3BP were mutated in various combinations to prevent lipoylation and thereby render the domains completely inactive (see section 3.14).

In this study, as has been previously observed with *E. coli* PDC, there appears to be a considerable degree of functional redundancy in terms of the presence of multiple lipoyl domains. Thus loss of lipoylation of either outer or inner lipoyl domains of E2 resulted in only a 25-35% decline in overall activity. In addition, the presence of lipoylated or non-lipoylated E3BP had little apparent effect on PDC activity. Interestingly, mutant PDCs in which E2 lipoyl domains were totally inactive still retained approx. 10-15% activity mediated by the 12 remaining lipoyl groups of E3BP. This latter observation is in agreement with a previous study (Sanderson et al., 1996a), in which E2 lipoyl domains were removed by collagenase treatment generating a modified complex that still retained 15% residual activity.

In previous studies assessing a role for the presence of multiple lipoyl domains, the local environment of the remaining lipoyl domain(s) in mutant PDCs was highly perturbed, potentially reducing steric hindrance effects and allowing the remaining domain(s) greater flexibility to visit the active sites of all 3 enzymes during the catalytic cycle. This could have led to overestimation of the activity of the modified complex and the versatility of individual lipoyl domains in serving as effective substrates for all 3 active sites. In this study for the first time, a full complement of correctly folded lipoyl domains was retained, either in active or inactive form in the recombinant PDC, without affecting the native structure of the complex and their redundancy status re-evaluated. However, results were consistent with earlier studies demonstrating the existence of a high degree of functional redundancy and showing that all lipoyl domains on E2 and E3BP appeared to interact effectively with all three partner enzymes.

The validity of the recombinant PDC model for analysing natural mutations was also assessed in another study where the function of the normal recombinant PDC was compared to recombinant PDC without E3BP. PDC devoid of E3BP displayed residual activity of 3-8% in the presence of stoichiometric amounts of E3. About 10-20% activity has been reported in patients lacking the E3BP subunit (Marsac et al., 1993) where E3 is considered to bind weakly to a secondary site on E2. However, the activity of recombinant complex lacking E3BP could be significantly raised by adding a 100-200 fold excess of E3. This result substantiated an important previous finding by Dr. Susan Richards in this

laboratory using surface plasmon resonance (unpublished data) that the E1 binding site on E2 retains a residual affinity for E3. When excess amounts of E3 were added to wild-type recombinant PDC, its activity declined gradually due to partial displacement of E1 from its E2-binding site, again confirming its retention of a residual affinity for E3.

Further analysis of recombinant PDC lacking E3BP was used to study whether E3BP was uniquely involved in the diacetylation reaction i.e. the production of a S^6, S^8 diacetyl-dihydrolipoamide intermediate that is known to be exclusive to mammalian and yeast PDC. The role of diacetylation is unknown but could be of physiological importance, enabling PDC to act as a reservoir of acetyl groups and electrons under conditions of excess acetyl CoA and NADH production e.g. in diabetes, high fat diet or in starvation, providing a buffer against ketone body production. Diacetylated forms of PDC (produced by treatment with AcCoA and NADH or pyruvate in the absence of AcCoA) are protected from inactivation by the specific thiol group inhibitor, NEM (Sanderson et al., 1996b). Recombinant PDC lacking E3BP, but with a 200-fold excess of E3, was similarly treated with AcCoA and NADH. Recombinant PDC in which E3BP was absent, in addition to wild-type control was found to be protected from the inhibitory effect of NEM, indicating that the E3BP component was not responsible for diacetylation. The recombinant model of PDC was found to be an ideal tool to study this phenomenon because it is difficult to obtain native PDC complex lacking E3BP which is tightly integrated into the E2 core and cannot be readily removed without E2 disassembly. To date no enzymatic function has been identified for E3BP and our current analysis also rules out its potential involvement in the diacetylation process that is presumably mediated by E2.

After checking the functional properties of our recombinant PDC model, it was successfully employed to study three natural mutations observed in patients. Two of these mutations were unusual homozygous 'in-frame' 3 base pair deletions in E2. One mutation was in the outer lipoyl domain of E2 leading to the deletion of glutamate 35 whereas the second mutation caused the loss of valine at position 455 that is located in the C-terminal domain. The third mutation was the substitution of a leucine for a phenylalanine at position 490 near the active site of E2. The main objective of this study was to analyse these mutations in order to gain detailed information on the molecular basis of these PDC defects and also ascertain the validity of this model recombinant PDC system for analysing newly-discovered genetic mutations of this type.

All these mutations caused symptoms of PDC deficiency in the relevant patients; however, the exact mechanism of production of clinical symptoms was unclear. Moreover, in the case of the glutamate-35 deletion where the deletion was near to a lipoylatable lysine in the outer lipoyl domain, the clinical symptoms were difficult to explain simply in terms of possible loss of lipoylation of a single lipoyl domain. Inactivation of a single E2 lipoyl domain leads to only about 25-30% reduction in the PDC activity and was not expected to elicit any obvious phenotype. Moreover the patient showed about 70% loss of activity as measured by CO_2 release assay. All mutations were successfully introduced into E2:E3BP cores and a series of experiments conducted to determine changes in structure, enzymatic function and assembly of the mutant complexes. It was demonstrated that the glutamate deletion not only affected lipoylation per se, but led to misfolding of the outer domain or domain instability rendering it 'sticky' and prone to aggregation. In addition, it was observed that the proper folding of this N-terminal region is crucial for the correct folding and assembly of the C-terminal domain of E2 and its integration with E3BP. It is proposed that inappropriate interactions of the N-termini of E2 polypeptide chains disrupt native trimer assembly involving the C-terminal regions of E2 and/or E3BP (Fig. 6.1). Indeed the AUC data suggested that a proper core was not forming in this case, which could be caused by premature and inappropriate aggregation of outer lipoyl domains leading to aberrant core assembly/function. However, in these experimental conditions some core of the correct size was present and indeed the extent of native core formation correlates well with the residual activity in the patient.

The reduced PDC function in the case of F490L mutation appeared to be a relatively straightforward case where no major structural changes were detected, but partial loss of acetyltransferase activity was confirmed due to the presence of this mutation in the vicinity of the catalytic site. Moreover, this phenylalanine has also been reported to be important for the determination of substrate specificity (Mattevi et al., 1993b). It would be of great interest to assess the ability of this mutant E2 to use with other substrates to determine if it had acquired a broader substrate specificity as a result of this mutation.

Analysis of the valine-455 deletion proved to be problematic. This mutation was responsible for the deletion of a highly conserved valine-455 that has the potential to disrupt the catalytic activity or E2 core assembly. A partial loss of catalytic activity (about 50%) was demonstrated in the mutant PDC as well as the E2 enzyme and E2:E3BP core although in all other respects core formation and E3BP integration appeared normal. However, in this case the patient appeared to retain no immunologically detectable levels

of E3BP. Our initial working hypothesis was that the valine-455 deletion on E2 may be responsible for prevention of E3BP integration and that free E3BP was rapidly degraded but no evidence was obtained to support this prediction. A full clinical, genetic and biochemical re-evaluation of this patient is currently in progress.

In this project, a reconstituted model of PDC comprising all three constituent enzymes and the accessory structural protein, E3BP has been used for the first time to uniquely evaluate these rare mutations. From a clinical viewpoint, the *in vitro* approaches employed here can form a basis for providing more comprehensive diagnosis and possibly developing improved treatment regimes in future. Often diagnosis of such mutations leading to PDC deficiency is made from clinical symptoms and CO_2 release assays of cultured fibroblasts which are cumbersome, time-consuming, expensive and require considerable expertise. This type of study employing recombinantly-produced complex should provide important new information on subunit interactions/organisation and mode of assembly. Moreover, the the data obtained will enable clinicians and patients to gain a much clearer picture of the precise biochemical lesions associated with a particular genetic defect. Although PDC has been studied extensively for its structural and functional roles, nevertheless, the development of this novel model system can further provide new insights into the functioning of PDC at a molecular level under normal and disease conditions
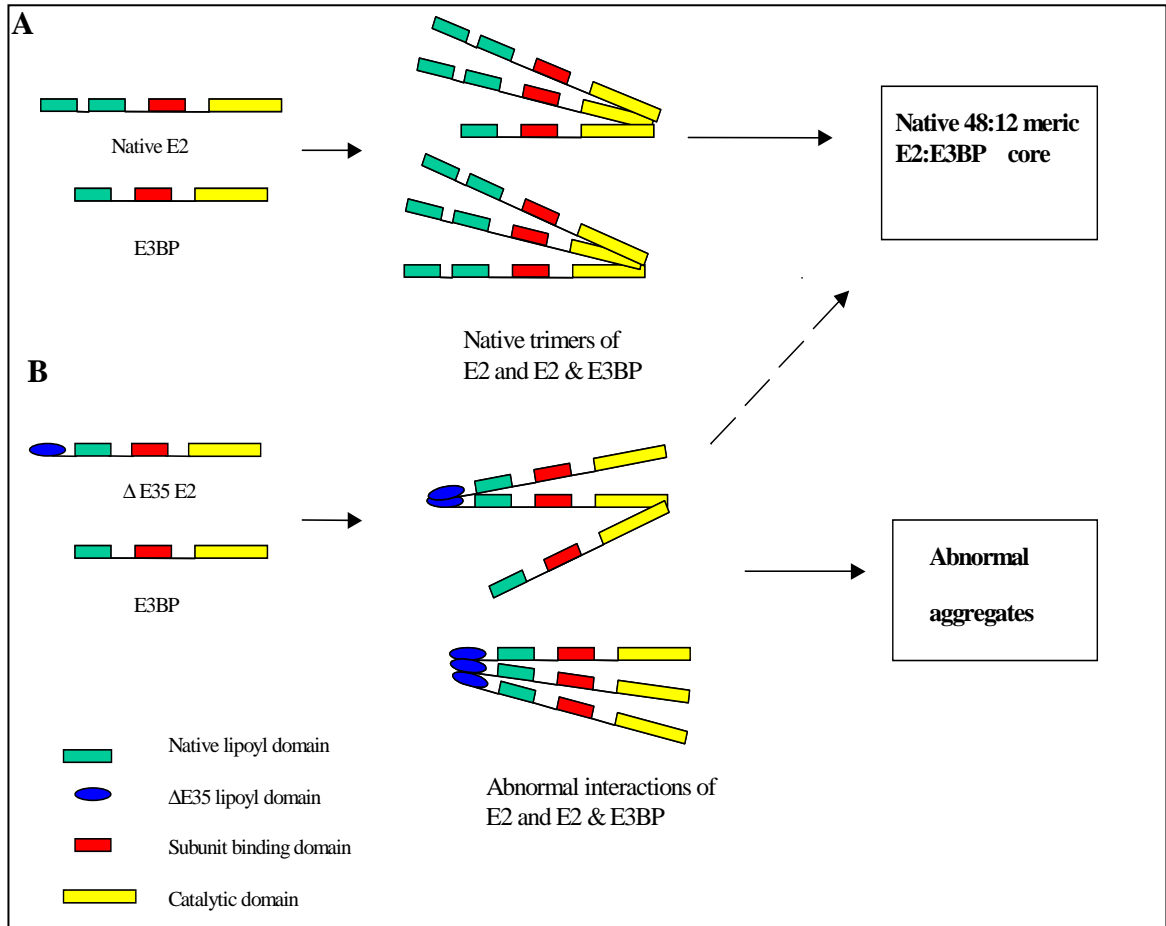
Figure 6.1: Schematic representation depicting formation of normal and abnormal cores of E2:E3BP carrying the ΔE35 E2 mutation

The upper part of the diagram (A) shows formation of normal trimers of E2 and E3BP polypeptides interacting via their C-terminal domains leading to native core assembly. In the case of the ΔE35 mutation in the outer lipoyl domain (B), abnormal oligomers of E2 and E3BP have an increased tendency to aggregate due to inappropriate association of the N-termini of E2 polypeptide disrupting native trimer assembly that involves the C-terminal regions of E2 and/or E3BP. The dotted line indicates that a small amount of native core is also being assembled under these conditions.

The last chapter describes our preliminary attempts to generate a recombinant OGDC model. Human OGDC is less widely studied as compared to PDC. Its constituent enzymes are equivalent to those in PDC i.e. E1, E2 and E3, but without any homologue of E3BP. However, a recombinant model of OGDC on similar lines to PDC is not yet available owing to difficulties in producing soluble full length, high M_r, homodimeric E1o. However, in this study N-terminal fragments of E1o (first 83, 166 and 193 amino acids) have been cloned, overexpressed and purified. Analysis of nucleotide sequence and deduced amino acid sequence of E2o has failed to detect any obvious well defined E3/E1o binding domains although biochemical evidence suggests that N-terminal of E1o seems to carry out some roles assigned to E3BP in PDC.

E2o and E3 were successfully overexpressed and interaction studies showed that E3 did not bind directly to E2o in the OGDC. However, the extreme N-terminal region of E1o (first 83 amino acids) did co-integrate with E2o although it was not demonstrated if this could occur post-translationally as well as co-translationally. Previous studies have also implicated this region of E1o in E3 binding although this was not tested in the current study.

In summary, it has proved feasible to produce a recombinant human PDC that maintained its structural and functional capabilities. It was then successfully utilised to evaluate several natural mutations in considerable detail. For OGDC, which like PDC is also implicated in a number of genetic, metabolic, autoimmune and neurodegenerative diseases, a recombinant model on similar lines should be fully developed and used in future studies to facilitate investigation on its involvement in a number of neurological and degenerative disorders linked to oxidative stress.

Bibliography

Ali, G., W. Wasco, X. Cai, P. Szabo, K.F. Sheu, A.J. Cooper, S.M. Gaston, J.F. Gusella, R.E. Tanzi, and J.P. Blass. 1994. Isolation, characterization, and mapping of gene encoding dihydrolipoyl succinyltransferase (E2k) of human alpha-ketoglutarate dehydrogenase complex. *Somat Cell Mol Genet*. 20:99-105.

Ali, M.S., B.C. Shenoy, D. Eswaran, L.A. Andersson, T.E. Roche, and M.S. Patel. 1995. Identification of the tryptophan residue in the thiamin pyrophosphate binding site of mammalian pyruvate dehydrogenase. *J Biol Chem*. 270:4570-4.

Ali, S.T., A.J. Moir, P.R. Ashton, P.C. Engel, and J.R. Guest. 1990. Octanoylation of the lipoyl domains of the pyruvate dehydrogenase complex in a lipoyl-deficient strain of Escherichia coli. *Mol Microbiol*. 4:943-50.

Allen, A.G., R.N. Perham, N. Allison, J.S. Miles, and J.R. Guest. 1989. Reductive acetylation of tandemly repeated lipoyl domains in the pyruvate dehydrogenase multienzyme complex of Escherichia coli is random order. *J Mol Biol*. 208:623-33.

Andersson, U., B. Leighton, M.E. Young, E. Blomstrand, and E.A. Newsholme. 1998. Inactivation of aconitase and oxoglutarate dehydrogenase in skeletal muscle in vitro by superoxide anions and/or nitric oxide. *Biochem Biophys Res Commun*. 249:512-6.

Aral, B., C. Benelli, G. Ait-Ghezala, M. Amessou, F. Fouque, C. Maunoury, N. Creau, P. Kamoun, and C. Marsac. 1997. Mutations in PDX1, the human lipoyl-containing component X of the pyruvate dehydrogenase-complex gene on chromosome 11p1, in congenital lactic acidosis. *Am J Hum Genet*. 61:1318-26.

Barrera, C.R., G. Namihira, L. Hamilton, P. Munk, M.H. Eley, T.C. Linn, and L.J. Reed. 1972. -Keto acid dehydrogenase complexes. XVI. Studies on the subunit structure of the pyruvate dehydrogenase complexes from bovine kidney and heart. *Arch Biochem Biophys*. 148:343-58.

Behal, R.H., K.S. Browning, T.B. Hall, and L.J. Reed. 1989. Cloning and nucleotide sequence of the gene for protein X from Saccharomyces cerevisiae. *Proc Natl Acad Sci U S A*. 86:8732-6.

Behal, R.H., D.B. Buxton, J.G. Robertson, and M.S. Olson. 1993. Regulation of the pyruvate dehydrogenase multienzyme complex. *Annu Rev Nutr*. 13:497-520.

Behal, R.H., M.S. DeBuysere, B. Demeler, J.C. Hansen, and M.S. Olson. 1994. Pyruvate dehydrogenase multienzyme complex. Characterization of assembly intermediates by sedimentation velocity analysis. *J Biol Chem*. 269:31372-7.

Berendzen, K., D.W. Theriaque, J. Shuster, and P.W. Stacpoole. 2006. Therapeutic potential of dichloroacetate for pyruvate dehydrogenase complex deficiency. *Mitochondrion*. 6:126-35.

Berg, A., J. Vervoort, and A. de Kok. 1996. Solution structure of the lipoyl domain of the 2-oxoglutarate dehydrogenase complex from Azotobacter vinelandii. *J Mol Biol*. 261:432-42.

Bonnefont, J.P., D. Chretien, P. Rustin, B. Robinson, A. Vassault, J. Aupetit, C. Charpentier, D. Rabier, J.M. Saudubray, and A. Munnich. 1992. Alpha-ketoglutarate dehydrogenase deficiency presenting as congenital lactic acidosis. *J Pediatr*. 121:255-8.

Boulatnikov, I., and K.M. Popov. 2003. Formation of functional heterodimers by isozymes 1 and 2 of pyruvate dehydrogenase kinase. *Biochim Biophys Acta*. 1645:183-92.

Brautigam, C.A., J.L. Chuang, D.R. Tomchick, M. Machius, and D.T. Chuang. 2005. Crystal structure of human dihydrolipoamide dehydrogenase: NAD+/NADH binding and the structural basis of disease-causing mutations. *J Mol Biol*. 350:543-52.

Brody, S., C. Oh, U. Hoja, and E. Schweizer. 1997. Mitochondrial acyl carrier protein is involved in lipoic acid synthesis in Saccharomyces cerevisiae. *FEBS Lett*. 408:217-20.

Brown, G.K. 1992. Pyruvate dehydrogenase E1 alpha deficiency. *J Inherit Metab Dis*. 15:625-33.

Brown, J.P., and R.N. Perham. 1976. Selective inactivation of the transacylase components of the 2-oxo acid dehydrogenase multienzyme complexes of Escherichia coli. *Biochem J*. 155:419-27.

Brown, R.M., R.A. Head, Boubriak, II, J.V. Leonard, N.H. Thomas, and G.K. Brown. 2004. Mutations in the gene for the E1beta subunit: a novel cause of pyruvate dehydrogenase deficiency. *Hum Genet*. 115:123-7.

Bukau, B., T. Hesterkamp, and J. Luirink. 1996. Growing up in a dangerous environment: a network of multiple targeting and folding pathways for nascent polypeptides in the cytosol. *Trends Cell Biol*. 6:480-6.

Butterworth, P.J., C.S. Tsai, M.H. Eley, T.E. Roche, and L.J. Reed. 1975. A kinetic study of dihydrolipoyl transacetylase from bovine kidney. *J Biol Chem*. 250:1921-5.

Butterworth, R.F., and A.M. Besnard. 1990. Thiamine-dependent enzyme changes in temporal cortex of patients with Alzheimer's disease. *Metab Brain Dis*. 5:179-84.

Caetano, N.N., A.P. Campello, E.G. Carnieri, M.L. Kluppel, and M.B. Oliveira. 1997. Effect of methotrexate (MTX) on NAD(P)+ dehydrogenases of HeLa cells: malic enzyme, 2-oxoglutarate and isocitrate dehydrogenases. *Cell Biochem Funct*. 15:259-64.

Cao, X., and J.W. Phillis. 1995. The free radical scavenger, alpha-lipoic acid, protects against cerebral ischemia-reperfusion injury in gerbils. *Free Radic Res*. 23:365-70.

Cate, R.L., T.E. Roche, and L.C. Davis. 1980. Rapid intersite transfer of acetyl groups and movement of pyruvate dehydrogenase component in the kidney pyruvate dehydrogenase complex. *J Biol Chem*. 255:7556-62.

Chen, G., L. Wang, S. Liu, C. Chuang, and T.E. Roche. 1996. Activated function of the pyruvate dehydrogenase phosphatase through Ca2+-facilitated binding to the inner lipoyl domain of the dihydrolipoyl acetyltransferase. *J Biol Chem*. 271:28064-70.

Chinopoulos, C., L. Tretter, and V. Adam-Vizi. 1999. Depolarization of in situ mitochondria due to hydrogen peroxide-induced oxidative stress in nerve terminals: inhibition of alpha-ketoglutarate dehydrogenase. *J Neurochem*. 73:220-8.

Chun, K., N. MacKay, R. Petrova-Benedict, and B.H. Robinson. 1991. Pyruvate dehydrogenase deficiency due to a 20-bp deletion in exon II of the pyruvate dehydrogenase (PDH) E1 alpha gene. *Am J Hum Genet*. 49:414-20.

Chun, K., N. MacKay, R. Petrova-Benedict, and B.H. Robinson. 1993. Mutations in the X-linked E1 alpha subunit of pyruvate dehydrogenase leading to deficiency of the pyruvate dehydrogenase complex. *Hum Mol Genet*. 2:449-54.

Ciszak, E.M., L.G. Korotchkina, P.M. Dominiak, S. Sidhu, and M.S. Patel. 2003. Structural basis for flip-flop action of thiamin pyrophosphate-dependent enzymes revealed by human pyruvate dehydrogenase. *J Biol Chem*. 278:21240-6.

Ciszak, E.M., A. Makal, Y.S. Hong, A.K. Vettaikkorumakankauv, L.G. Korotchkina, and M.S. Patel. 2006. How dihydrolipoamide dehydrogenase-binding protein binds dihydrolipoamide dehydrogenase in the human pyruvate dehydrogenase complex. *J Biol Chem*. 281:648-55.

Cooper, R.H., P.J. Randle, and R.M. Denton. 1974. Regulation of heart muscle pyruvate dehydrogenase kinase. *Biochem J*. 143:625-41.

Corder, E.H., A.M. Saunders, W.J. Strittmatter, D.E. Schmechel, P.C. Gaskell, G.W. Small, A.D. Roses, J.L. Haines, and M.A. Pericak-Vance. 1993. Gene dose of apolipoprotein E type 4 allele and the risk of Alzheimer's disease in late onset families. *Science*. 261:921-3.

Dahl, H.H., L.L. Hansen, R.M. Brown, D.M. Danks, J.G. Rogers, and G.K. Brown. 1992. X-linked pyruvate dehydrogenase E1 alpha subunit deficiency in heterozygous females: variable manifestation of the same mutation. *J Inherit Metab Dis*. 15:835-47.

Danson, M.J., and R.N. Perham. 1976. Evidence for two lipoic acid residues per lipoate acetyltransferase chain in the pyruvate dehydrogenase multienzyme complex of Escherichia coli. *Biochem J*. 159:677-82.

Dardel, F., A.L. Davis, E.D. Laue, and R.N. Perham. 1993. Three-dimensional structure of the lipoyl domain from Bacillus stearothermophilus pyruvate dehydrogenase multienzyme complex. *J Mol Biol*. 229:1037-48.

Dardel, F., L.C. Packman, and R.N. Perham. 1990. Expression in Escherichia coli of a sub-gene encoding the lipoyl domain of the pyruvate dehydrogenase complex of Bacillus stearothermophilus. *FEBS Lett*. 264:206-10.

De Marcucci, O., and J.G. Lindsay. 1985. Component X. An immunologically distinct polypeptide associated with mammalian pyruvate dehydrogenase multi-enzyme complex. *Eur J Biochem*. 149:641-8.

De Marcucci, O.G., G.M. Gibb, J. Dick, and J.G. Lindsay. 1988. Biosynthesis, import and processing of precursor polypeptides of mammalian mitochondrial pyruvate dehydrogenase complex. *Biochem J*. 251:817-23.

De Marcucci, O.G., J.A. Hodgson, and J.G. Lindsay. 1986. The Mr-50 000 polypeptide of mammalian pyruvate dehydrogenase complex participates in the acetylation reactions. *Eur J Biochem*. 158:587-94.

Dey, R., B. Aral, M. Abitbol, and C. Marsac. 2002. Pyruvate dehydrogenase deficiency as a result of splice-site mutations in the PDX1 gene. *Mol Genet Metab*. 76:344-7.

Eftink, M.R. 1991. Fluorescence techniques for studying protein structure. *Methods Biochem Anal*. 35:127-205.

Endo, H., S. Miyabayashi, K. Tada, and K. Narisawa. 1991. A four-nucleotide insertion at the E1 alpha gene in a patient with pyruvate dehydrogenase deficiency. *J Inherit Metab Dis*. 14:793-9.

Falk, R.E., S.D. Cederbaum, J.P. Blass, G.E. Gibson, R.A. Kark, and R.E. Carrel. 1976. Ketonic diet in the management of pyruvate dehydrogenase deficiency. *Pediatrics*. 58:713-21.

Farrer, L.A., L.A. Cupples, J.L. Haines, B. Hyman, W.A. Kukull, R. Mayeux, R.H. Myers, M.A. Pericak-Vance, N. Risch, and C.M. van Duijn. 1997. Effects of age, sex, and ethnicity on the association between apolipoprotein E genotype and Alzheimer disease. A meta-analysis. APOE and Alzheimer Disease Meta Analysis Consortium. *Jama*. 278:1349-56.

Feigenbaum, A.S., and B.H. Robinson. 1993. The structure of the human dihydrolipoamide dehydrogenase gene (DLD) and its upstream elements. *Genomics*. 17:376-81.

Frank, R.A., A.J. Price, F.D. Northrop, R.N. Perham, and B.F. Luisi. 2007. Crystal structure of the E1 component of the Escherichia coli 2-oxoglutarate dehydrogenase multienzyme complex. *J Mol Biol*. 368:639-51.

Frank, R.A., C.M. Titman, J.V. Pratap, B.F. Luisi, and R.N. Perham. 2004. A molecular switch and proton wire synchronize the active sites in thiamine enzymes. *Science*. 306:872-6.

Fregeau, D.R., T.E. Roche, P.A. Davis, R. Coppel, and M.E. Gershwin. 1990. Primary biliary cirrhosis. Inhibition of pyruvate dehydrogenase complex activity by autoantibodies specific for E1 alpha, a non-lipoic acid containing mitochondrial enzyme. *J Immunol*. 144:1671-6.

Fujii, T., R.N. Van Coster, S.E. Old, R. Medori, S. Winter, R.M. Gubits, P.M. Matthews, R.M. Brown, G.K. Brown, H.H. Dahl, and et al. 1994. Pyruvate dehydrogenase deficiency: molecular basis for intrafamilial heterogeneity. *Ann Neurol*. 36:83-9.

Fujimoto, M., S. Sato, H. Ihn, K. Kikuchi, K. Tamaki, and K. Takehara. 1995. Autoantibodies to pyruvate dehydrogenase complex in patients with systemic sclerosis. Possible role of anti-E1 alpha antibody as a serologic indicator for development of primary biliary cirrhosis. *Arthritis Rheum*. 38:985-9.

Fujiwara, K., K. Okamura-Ikeda, and Y. Motokawa. 1994. Purification and characterization of lipoyl-AMP:N epsilon-lysine lipoyltransferase from bovine liver mitochondria. *J Biol Chem*. 269:16605-9.

Fujiwara, K., M. Suzuki, Y. Okumachi, K. Okamura-Ikeda, T. Fujiwara, E. Takahashi, and Y. Motokawa. 1999. Molecular cloning, structural characterization and chromosomal localization of human lipoyltransferase gene. *Eur J Biochem*. 260:761-7.

Fussey, S.P., J.R. Guest, O.F. James, M.F. Bassendine, and S.J. Yeaman. 1988. Identification and analysis of the major M2 autoantigens in primary biliary cirrhosis. *Proc Natl Acad Sci U S A*. 85:8654-8.

Fussey, S.P., J.G. Lindsay, C. Fuller, R.N. Perham, S. Dale, O.F. James, M.F. Bassendine, and S.J. Yeaman. 1991. Autoantibodies in primary biliary cirrhosis: analysis of reactivity against eukaryotic and prokaryotic 2-oxo acid dehydrogenase complexes. *Hepatology*. 13:467-74.

Gardberg, A.S., L.T. Dice, S. Ou, R.L. Rich, E. Helmbrecht, J. Ko, R. Wetzel, D.G. Myszka, P.H. Patterson, and C. Dealwis. 2007. Molecular basis for passive immunotherapy of Alzheimer's disease. *Proc Natl Acad Sci U S A*. 104:15659-64.

Geddes, J.W., T.L. Tekirian, N.S. Soultanian, J.W. Ashford, D.G. Davis, and W.R. Markesbery. 1997. Comparison of neuropathologic criteria for the diagnosis of Alzheimer's disease. *Neurobiol Aging*. 18:S99-105.

Geoffroy, V., F. Fouque, C. Benelli, F. Poggi, J.M. Saudubray, W. Lissens, L.D. Meirleir, C. Marsac, J.G. Lindsay, and S.J. Sanderson. 1996. Defect in the X-lipoyl-containing component of the pyruvate dehydrogenase complex in a patient with neonatal lactic acidemia. *Pediatrics*. 97:267-72.

Gershwin, M.E., I.R. Mackay, A. Sturgess, and R.L. Coppel. 1987. Identification and specificity of a cDNA encoding the 70 kd mitochondrial antigen recognized in primary biliary cirrhosis. *J Immunol*. 138:3525-31.

Gibson, G.E., K.F. Sheu, and J.P. Blass. 1998. Abnormalities of mitochondrial enzymes in Alzheimer disease. *J Neural Transm*. 105:855-70.

Gibson, G.E., K.F. Sheu, J.P. Blass, A. Baker, K.C. Carlson, B. Harding, and P. Perrino. 1988. Reduced activities of thiamine-dependent enzymes in the brains and peripheral tissues of patients with Alzheimer's disease. *Arch Neurol*. 45:836-40.

Gong, X., T. Peng, A. Yakhnin, M. Zolkiewski, J. Quinn, S.J. Yeaman, and T.E. Roche. 2000. Specificity determinants for the pyruvate dehydrogenase component reaction mapped with mutated and prosthetic group modified lipoyl domains. *J Biol Chem*. 275:13645-53.

Gopalakrishnan, S., M. Rahmatullah, G.A. Radke, S. Powers-Greenwood, and T.E. Roche. 1989. Role of protein X in the function of the mammalian pyruvate dehydrogenase complex. *Biochem Biophys Res Commun*. 160:715-21.

Greenfield, N., and G.D. Fasman. 1969. Computed circular dichroism spectra for the evaluation of protein conformation. *Biochemistry*. 8:4108-16.

Greenfield, N.J. 1975. Enzyme ligand complexes: spectroscopic studies. *CRC Crit Rev Biochem*. 3:71-110.

Gudi, R., M.M. Bowker-Kinley, N.Y. Kedishvili, Y. Zhao, and K.M. Popov. 1995. Diversity of the pyruvate dehydrogenase kinase gene family in humans. *J Biol Chem*. 270:28989-94.

Guffon, N., C. Lopez-Mediavilla, R. Dumoulin, B. Mousson, C. Godinot, H. Carrier, J.M. Collombet, P. Divry, M. Mathieu, and P. Guibaud. 1993. 2-Ketoglutarate dehydrogenase deficiency, a rare cause of primary hyperlactataemia: report of a new case. *J Inherit Metab Dis*. 16:821-30.

Hackert, M.L., R.M. Oliver, and L.J. Reed. 1983. Evidence for a multiple random coupling mechanism in the alpha-ketoglutarate dehydrogenase multienzyme complex of Escherichia coli: a computer model analysis. *Proc Natl Acad Sci U S A*. 80:2226-30.

Harris, R.A., M.M. Bowker-Kinley, P. Wu, J. Jeng, and K.M. Popov. 1997. Dihydrolipoamide dehydrogenase-binding protein of the human pyruvate dehydrogenase complex. DNA-derived amino acid sequence, expression, and reconstitution of the pyruvate dehydrogenase complex. *J Biol Chem*. 272:19746-51.

Hendle, J., A. Mattevi, A.H. Westphal, J. Spee, A. de Kok, A. Teplyakov, and W.G. Hol. 1995. Crystallographic and enzymatic investigations on the role of Ser558, His610, and Asn614 in the catalytic mechanism of Azotobacter vinelandii dihydrolipoamide acetyltransferase (E2p). *Biochemistry*. 34:4287-98.

Hiromasa, Y., T. Fujisawa, Y. Aso, and T.E. Roche. 2004. Organization of the cores of the mammalian pyruvate dehydrogenase complex formed by E2 and E2 plus the E3-binding protein and their capacities to bind the E1 and E3 components. *J Biol Chem*. 279:6921-33.

Hodgson, J.A., O.G. De Marcucci, and J.G. Lindsay. 1986. Lipoic acid is the site of substrate-dependent acetylation of component X in ox heart pyruvate dehydrogenase multienzyme complex. *Eur J Biochem*. 158:595-600.

Holzwarth, G., and P. Doty. 1965. The Ultraviolet Circular Dichroism of Polypeptides. *J Am Chem Soc*. 87:218-28.

Hong, Y.S., D.S. Kerr, W.J. Craigen, J. Tan, Y. Pan, M. Lusk, and M.S. Patel. 1996. Identification of two mutations in a compound heterozygous child with dihydrolipoamide dehydrogenase deficiency. *Hum Mol Genet*. 5:1925-30.

Howard, M.J., C. Fuller, R.W. Broadhurst, R.N. Perham, J.G. Tang, J. Quinn, A.G. Diamond, and S.J. Yeaman. 1998. Three-dimensional structure of the major autoantigen in primary biliary cirrhosis. *Gastroenterology*. 115:139-46.

Huang, B., R. Gudi, P. Wu, R.A. Harris, J. Hamilton, and K.M. Popov. 1998. Isoenzymes of pyruvate dehydrogenase phosphatase. DNA-derived amino acid sequences, expression, and regulation. *J Biol Chem*. 273:17680-8.

Humphries, K.M., and L.I. Szweda. 1998. Selective inactivation of alpha-ketoglutarate dehydrogenase and pyruvate dehydrogenase: reaction of lipoic acid with 4-hydroxy-2-nonenal. *Biochemistry*. 37:15835-41.

Izard, T., A. Aevarsson, M.D. Allen, A.H. Westphal, R.N. Perham, A. de Kok, and W.G. Hol. 1999. Principles of quasi-equivalence and Euclidean geometry govern the assembly of cubic and dodecahedral cores of pyruvate dehydrogenase complexes. *Proc Natl Acad Sci U S A*. 96:1240-5.

Jilka, J.M., M. Rahmatullah, M. Kazemi, and T.E. Roche. 1986. Properties of a newly characterized protein of the bovine kidney pyruvate dehydrogenase complex. *J Biol Chem*. 261:1858-67.

Jones, D.D., K.M. Stott, P.A. Reche, and R.N. Perham. 2001. Recognition of the lipoyl domain is the ultimate determinant of substrate channelling in the pyruvate dehydrogenase multienzyme complex. *J Mol Biol*. 305:49-60.

Jones, S.M., and S.J. Yeaman. 1986. Phosphorylation of branched-chain 2-oxo acid dehydrogenase complex in isolated adipocytes. Effects of 2-oxo acids. *Biochem J*. 236:209-13.

Kalia, Y.N., S.M. Brocklehurst, D.S. Hipps, E. Appella, K. Sakaguchi, and R.N. Perham. 1993. The high-resolution structure of the peripheral subunit-binding domain of dihydrolipoamide acetyltransferase from the pyruvate dehydrogenase multienzyme complex of Bacillus stearothermophilus. *J Mol Biol*. 230:323-41.

Kaplan, B., and H.P. Lundsgaarde. 1996. Toward an evaluation of an integrated clinical imaging system: identifying clinical benefits. *Methods Inf Med*. 35:221-9.

Kim, H., and M.S. Patel. 1992. Characterization of two site-specifically mutated human dihydrolipoamide dehydrogenases (His-452----Gln and Glu-457----Gln). *J Biol Chem*. 267:5128-32.

Kish, S.J. 1997. Brain energy metabolizing enzymes in Alzheimer's disease: alpha-ketoglutarate dehydrogenase complex and cytochrome oxidase. *Ann N Y Acad Sci*. 826:218-28.

Klingbeil, M.M., D.J. Walker, R. Arnette, E. Sidawy, K. Hayton, P.R. Komuniecki, and R. Komuniecki. 1996. Identification of a novel dihydrolipoyl dehydrogenase-binding protein in the pyruvate dehydrogenase complex of the anaerobic parasitic nematode, Ascaris suum. *J Biol Chem*. 271:5451-7.

Kobayashi, T., H. Matsumine, S. Matuda, and Y. Mizuno. 1998. Association between the gene encoding the E2 subunit of the alpha-ketoglutarate dehydrogenase complex and Parkinson's disease. *Ann Neurol*. 43:120-3.

Koch, M.H., P. Vachette, and D.I. Svergun. 2003. Small-angle scattering: a view on the properties, structures and structural changes of biological macromolecules in solution. *Q Rev Biophys*. 36:147-227.

Koike, K. 1998. Cloning, structure, chromosomal localization and promoter analysis of human 2-oxoglutarate dehydrogenase gene. *Biochimica Et Biophysica Acta-Protein Structure and Molecular Enzymology*. 1385:373-384.

Koike, M., and K. Koike. 1976. Structure, assembly and function of mammalian alpha-keto acid dehydrogenase complexes. *Adv Biophys*:187-227.

Koike, M., and K. Koike. 1982. Biochemical properties of mammalian 2-oxo acid dehydrogenase multienzyme complexes and clinical relevancy with chronic lactic acidosis. *Ann N Y Acad Sci*. 378:225-35.

Korotchkina, L.G., and M.S. Patel. 2001. Site specificity of four pyruvate dehydrogenase kinase isoenzymes toward the three phosphorylation sites of human pyruvate dehydrogenase. *J Biol Chem*. 276:37223-9.

Kuehn, L., M. Rutschmann, B. Dahlmann, and H. Reinauer. 1984. Proteinase inhibitors in rat serum. Purification and partial characterization of three functionally distinct trypsin inhibitors. *Biochem J*. 218:953-9.

Laue, T.M., B.D. Shah, T.M. Ridgeway, and S.L. Pelletier. 1992. Computer-aided interpretation of analytical sedimentation data for proteins. *In Analytical Ultracentrifugation in Biochemistry and Polymer science S. E. Harding, A. J. Rowe and J. C. Horton, eds., Royal Society for Chemistry, London,*:90-125.

Lawlis, V.B., and T.E. Roche. 1981. Regulation of bovine kidney alpha-ketoglutarate dehydrogenase complex by calcium ion and adenine nucleotides. Effects on S0.5 for alpha-ketoglutarate. *Biochemistry*. 20:2512-8.

Lawson, J.E., R.H. Behal, and L.J. Reed. 1991. Disruption and mutagenesis of the Saccharomyces cerevisiae PDX1 gene encoding the protein X component of the pyruvate dehydrogenase complex. *Biochemistry*. 30:2834-9.

Leslie, A.G. 1990. Refined crystal structure of type III chloramphenicol acetyltransferase at 1.75 A resolution. *J Mol Biol*. 213:167-86.

Lessard, I.A., C. Fuller, and R.N. Perham. 1996. Competitive interaction of component enzymes with the peripheral subunit-binding domain of the pyruvate dehydrogenase multienzyme complex of Bacillus stearothermophilus: kinetic analysis using surface plasmon resonance detection. *Biochemistry*. 35:16863-70.

Lessard, I.A., and R.N. Perham. 1995. Interaction of component enzymes with the peripheral subunit-binding domain of the pyruvate dehydrogenase multienzyme complex of Bacillus stearothermophilus: stoichiometry and specificity in self-assembly. *Biochem J*. 306 (Pt 3):727-33.

Ling, M., G. McEachern, A. Seyda, N. MacKay, S.W. Scherer, S. Bratinova, B. Beatty, M.L. Giovannucci-Uzielli, and B.H. Robinson. 1998. Detection of a homozygous four base pair deletion in the protein X gene in a case of pyruvate dehydrogenase complex deficiency. *Hum Mol Genet*. 7:501-5.

Lissens, W., L. De Meirleir, S. Seneca, C. Benelli, C. Marsac, B.T. Poll-The, P. Briones, W. Ruitenbeek, O. van Diggelen, D. Chaigne, V. Ramaekers, and I. Liebaers. 1996. Mutation analysis of the pyruvate dehydrogenase E1 alpha gene in eight patients with a pyruvate dehydrogenase complex deficiency. *Hum Mutat*. 7:46-51.

Lissens, W., L. De Meirleir, S. Seneca, I. Liebaers, G.K. Brown, R.M. Brown, M. Ito, E. Naito, Y. Kuroda, D.S. Kerr, I.D. Wexler, M.S. Patel, B.H. Robinson, and A. Seyda. 2000. Mutations in the X-linked pyruvate dehydrogenase (E1) alpha subunit gene (PDHA1) in patients with a pyruvate dehydrogenase complex deficiency. *Hum Mutat*. 15:209-19.

Liu, T.C., Y.S. Hong, L.G. Korotchkina, N.N. Vettakkorumakankav, and M.S. Patel. 1999. Site-directed mutagenesis of human dihydrolipoamide dehydrogenase: role of lysine-54 and glutamate-192 in stabilizing the thiolate-FAD intermediate. *Protein Expr Purif*. 16:27-39.

Lucas, D.T., and L.I. Szweda. 1999. Declines in mitochondrial respiration during cardiac reperfusion: age-dependent inactivation of alpha-ketoglutarate dehydrogenase. *Proc Natl Acad Sci U S A*. 96:6689-93.

Manavalan, P., and W.C. Johnson, Jr. 1987. Variable selection method improves the prediction of protein secondary structure from circular dichroism spectra. *Anal Biochem*. 167:76-85.

Mande, S.S., S. Sarfaty, M.D. Allen, R.N. Perham, and W.G. Hol. 1996. Protein-protein interactions in the pyruvate dehydrogenase multienzyme complex: dihydrolipoamide dehydrogenase complexed with the binding domain of dihydrolipoamide acetyltransferase. *Structure*. 4:277-86.

Marsac, C., C. Benelli, I. Desguerre, M. Diry, F. Fouque, L. De Meirleir, G. Ponsot, S. Seneca, F. Poggi, J.M. Saudubray, M.T. Zabot, D. Fontan, and W. Lissens. 1997. Biochemical and genetic studies of four patients with pyruvate dehydrogenase E1 alpha deficiency. *Hum Genet*. 99:785-92.

Marsac, C., D. Stansbie, G. Bonne, J. Cousin, P. Jehenson, C. Benelli, J.P. Leroux, and G. Lindsay. 1993. Defect in the lipoyl-bearing protein X subunit of the pyruvate dehydrogenase complex in two patients with encephalomyelopathy. *J Pediatr*. 123:915-20.

Mastrogiacomo, F., C. Bergeron, and S.J. Kish. 1993. Brain alpha-ketoglutarate dehydrogenase complex activity in Alzheimer's disease. *J Neurochem*. 61:2007-14.

Mastrogiacomo, F., J.G. Lindsay, L. Bettendorff, J. Rice, and S.J. Kish. 1996. Brain protein and alpha-ketoglutarate dehydrogenase complex activity in Alzheimer's disease. *Annals of Neurology*. 39:592-598.

Matalon, R., D.A. Stumpf, K. Michals, R.D. Hart, J.K. Parks, and S.I. Goodman. 1984. Lipoamide dehydrogenase deficiency with primary lactic acidosis: favorable response to treatment with oral lipoic acid. *J Pediatr*. 104:65-9.

Matsuda, J., M. Ito, E. Naito, I. Yokota, and Y. Kuroda. 1995. DNA diagnosis of pyruvate dehydrogenase deficiency in female patients with congenital lactic acidaemia. *J Inherit Metab Dis*. 18:534-46.

Mattevi, A., G. Obmolova, K.H. Kalk, A. Teplyakov, and W.G. Hol. 1993a. Crystallographic analysis of substrate binding and catalysis in dihydrolipoyl transacetylase (E2p). *Biochemistry*. 32:3887-901.

Mattevi, A., G. Obmolova, K.H. Kalk, W.J. van Berkel, and W.G. Hol. 1993b. Three-dimensional structure of lipoamide dehydrogenase from Pseudomonas fluorescens at 2.8 A resolution. Analysis of redox and thermostability properties. *J Mol Biol*. 230:1200-15.

Mattevi, A., G. Obmolova, K.H. Kalk, A.H. Westphal, A. de Kok, and W.G. Hol. 1993c. Refined crystal structure of the catalytic domain of dihydrolipoyl transacetylase (E2p) from Azotobacter vinelandii at 2.6 A resolution. *J Mol Biol*. 230:1183-99.

Mattevi, A., G. Obmolova, E. Schulze, K.H. Kalk, A.H. Westphal, A. de Kok, and W.G. Hol. 1992. Atomic structure of the cubic core of the pyruvate dehydrogenase multienzyme complex. *Science*. 255:1544-50.

Matthews, P.M., R.M. Brown, L.J. Otero, D.R. Marchington, M. LeGris, R. Howes, L.S. Meadows, M. Shevell, C.R. Scriver, and G.K. Brown. 1994. Pyruvate dehydrogenase deficiency. Clinical presentation and molecular genetic characterization of five new patients. *Brain*. 117 (Pt 3):435-43.

McCartney, R.G., J.E. Rice, S.J. Sanderson, V. Bunik, H. Lindsay, and J.G. Lindsay. 1998. Subunit interactions in the mammalian alpha-ketoglutarate dehydrogenase complex. Evidence for direct association of the alpha-ketoglutarate dehydrogenase and dihydrolipoamide dehydrogenase components. *J Biol Chem*. 273:24158-64.

McCartney, R.G., S.J. Sanderson, and J.G. Lindsay. 1997. Refolding and reconstitution studies on the transacetylase-protein X (E2/X) subcomplex of the mammalian pyruvate dehydrogenase complex: evidence for specific binding of the dihydrolipoamide dehydrogenase component to sites on reassembled E2. *Biochemistry*. 36:6819-26.

Miles, J.S., J.R. Guest, S.E. Radford, and R.N. Perham. 1988. Investigation of the mechanism of active site coupling in the pyruvate dehydrogenase multienzyme complex of Escherichia coli by protein engineering. *J Mol Biol*. 202:97-106.

Milne, J.L., D. Shi, P.B. Rosenthal, J.S. Sunshine, G.J. Domingo, X. Wu, B.R. Brooks, R.N. Perham, R. Henderson, and S. Subramaniam. 2002. Molecular architecture and mechanism of an icosahedral pyruvate dehydrogenase complex: a multifunctional catalytic machine. *Embo J*. 21:5587-98.

Mizuno, Y., S. Matuda, H. Yoshino, H. Mori, N. Hattori, and S. Ikebe. 1994. An immunohistochemical study on alpha-ketoglutarate dehydrogenase complex in Parkinson's disease. *Ann Neurol*. 35:204-10.

Morris, T.W., K.E. Reed, and J.E. Cronan, Jr. 1994. Identification of the gene encoding lipoate-protein ligase A of Escherichia coli. Molecular cloning and characterization of the lplA gene and gene product. *J Biol Chem*. 269:16091-100.

Munnich, A., J.M. Saudubray, J. Taylor, C. Charpentier, C. Marsac, F. Rocchiccioli, O. Amedee-Manesme, F.X. Coude, J. Frezal, and B.H. Robinson. 1982. Congenital lactic acidosis, alpha-ketoglutaric aciduria and variant form of maple syrup urine disease due to a single enzyme defect: dihydrolipoyl dehydrogenase deficiency. *Acta Paediatr Scand*. 71:167-71.

Nakano, K., S. Matuda, T. Sakamoto, C. Takase, S. Nakagawa, S. Ohta, T. Ariyama, J. Inazawa, T. Abe, and T. Miyata. 1993. Human dihydrolipoamide succinyltransferase: cDNA cloning and localization on chromosome 14q24.2-q24.3. *Biochim Biophys Acta*. 1216:360-8.

Nakano, K., S. Matuda, T. Yamanaka, H. Tsubouchi, S. Nakagawa, K. Titani, S. Ohta, and T. Miyata. 1991. Purification and Molecular-Cloning of Succinyltransferase of the

Rat Alpha-Ketoglutarate Dehydrogenase Complex - Absence of a Sequence Motif of the Putative E3 and or E1 Binding-Site. *Journal of Biological Chemistry*. 266:19013-19017.

Nakano, K., C. Takase, T. Sakamoto, S. Nakagawa, J. Inazawa, S. Ohta, and S. Matuda. 1994. Isolation, characterization and structural organization of the gene and pseudogene for the dihydrolipoamide succinyltransferase component of the human 2-oxoglutarate dehydrogenase complex. *Eur J Biochem*. 224:179-89.

Neagle, J., O. De Marcucci, B. Dunbar, and J.G. Lindsay. 1989. Component X of mammalian pyruvate dehydrogenase complex: structural and functional relationship to the lipoate acetyltransferase (E2) component. *FEBS Lett*. 253:11-5.

Nolan, K.A., M.M. Lino, A.W. Seligmann, and J.P. Blass. 1998. Absence of vascular dementia in an autopsy series from a dementia clinic. *J Am Geriatr Soc*. 46:597-604.

O'Connor, T.P., T.E. Roche, and J.V. Paukstelis. 1982. 13C nuclear magnetic resonance study of the pyruvate dehydrogenase-catalyzed acetylation of dihydrolipoamide. *J Biol Chem*. 257:3110-2.

Old, S.E., and D.C. De Vivo. 1989. Pyruvate dehydrogenase complex deficiency: biochemical and immunoblot analysis of cultured skin fibroblasts. *Ann Neurol*. 26:746-51.

Otero, L.J., R.M. Brown, and G.K. Brown. 1998. Arginine 302 mutations in the pyruvate dehydrogenase E1alpha subunit gene: identification of further patients and in vitro demonstration of pathogenicity. *Hum Mutat*. 12:114-21.

Palmer, J.M., M.F. Bassendine, O.F. James, and S.J. Yeaman. 1993. Human pyruvate dehydrogenase complex as an autoantigen in primary biliary cirrhosis. *Clin Sci (Lond)*. 85:289-93.

Pandolfo, M., and L. Montermini. 1998. Molecular genetics of the hereditary ataxias. *Adv Genet*. 38:31-68.

Panov, A., and A. Scarpa. 1996. Independent modulation of the activity of alpha-ketoglutarate dehydrogenase complex by Ca2+ and Mg2+. *Biochemistry*. 35:427-32.

Park, L.C., H. Zhang, K.F. Sheu, N.Y. Calingasan, B.S. Kristal, J.G. Lindsay, and G.E. Gibson. 1999. Metabolic impairment induces oxidative stress, compromises inflammatory responses, and inactivates a key mitochondrial enzyme in microglia. *J Neurochem*. 72:1948-58.

Patel, J.M., K.M. Sekharam, and E.R. Block. 1992. Oxidant and angiotensin II-induced subcellular translocation of protein kinase C in pulmonary artery endothelial cells. *J Biochem Toxicol*. 7:117-23.

Patel, M.S., and R.A. Harris. 1995. Mammalian alpha-keto acid dehydrogenase complexes: gene regulation and genetic defects. *Faseb J*. 9:1164-72.

Patel, M.S., and T.E. Roche. 1990. Molecular biology and biochemistry of pyruvate dehydrogenase complexes. *Faseb J*. 4:3224-33.

Pekovich, S.R., P.R. Martin, and C.K. Singleton. 1998. Thiamine deficiency decreases steady-state transketolase and pyruvate dehydrogenase but not alpha-ketoglutarate dehydrogenase mRNA levels in three human cell types. *J Nutr*. 128:683-7.

Podda, M., H.J. Tritschler, H. Ulrich, and L. Packer. 1994. Alpha-lipoic acid supplementation prevents symptoms of vitamin E deficiency. *Biochem Biophys Res Commun*. 204:98-104.

Poggi-Travert, F., D. Martin, T. Billette de Villemeur, J.P. Bonnefont, A. Vassault, D. Rabier, C. Charpentier, P. Kamoun, A. Munnich, and J.M. Saudubray. 1996. Metabolic intermediates in lactic acidosis: compounds, samples and interpretation. *J Inherit Metab Dis*. 19:478-88.

Quinn, J., A.G. Diamond, A.K. Masters, D.E. Brookfield, N.G. Wallis, and S.J. Yeaman. 1993. Expression and lipoylation in Escherichia coli of the inner lipoyl domain of

the E2 component of the human pyruvate dehydrogenase complex. *Biochem J*. 289 (Pt 1):81-5.

Radford, S.E., E.D. Laue, R.N. Perham, J.S. Miles, and J.R. Guest. 1987. Segmental structure and protein domains in the pyruvate dehydrogenase multienzyme complex of Escherichia coli. Genetic reconstruction in vitro and 1H-n.m.r. spectroscopy. *Biochem J*. 247:641-9.

Rahmatullah, M., G.A. Radke, P.C. Andrews, and T.E. Roche. 1990. Changes in the core of the mammalian-pyruvate dehydrogenase complex upon selective removal of the lipoyl domain from the transacetylase component but not from the protein X component. *J Biol Chem*. 265:14512-7.

Ramadan, D.G., R.A. Head, A. Al-Tawari, Y. Habeeb, M. Zaki, F. Al-Ruqum, G.T. Besley, J.E. Wraith, R.M. Brown, and G.K. Brown. 2004. Lactic acidosis and developmental delay due to deficiency of E3 binding protein (protein X) of the pyruvate dehydrogenase complex. *J Inherit Metab Dis*. 27:477-85.

Ramassamy, C., D. Averill, U. Beffert, S. Bastianetto, L. Theroux, S. Lussier-Cacan, J.S. Cohn, Y. Christen, J. Davignon, R. Quirion, and J. Poirier. 1999. Oxidative damage and protection by antioxidants in the frontal cortex of Alzheimer's disease is related to the apolipoprotein E genotype. *Free Radic Biol Med*. 27:544-53.

Rice, J.E., B. Dunbar, and J.G. Lindsay. 1992. Sequences directing dihydrolipoamide dehydrogenase (E3) binding are located on the 2-oxoglutarate dehydrogenase (E1) component of the mammalian 2-oxoglutarate dehydrogenase multienzyme complex. *Embo J*. 11:3229-35.

Robinson, B.H., K. Chun, N. Mackay, G. Otulakowski, R. Petrova-Benedict, and H. Willard. 1989. Isolated and combined deficiencies of the alpha-keto acid dehydrogenase complexes. *Ann N Y Acad Sci*. 573:337-46.

Robinson, B.H., N. MacKay, R. Petrova-Benedict, I. Ozalp, T. Coskun, and P.W. Stacpoole. 1990. Defects in the E2 lipoyl transacetylase and the X-lipoyl containing component of the pyruvate dehydrogenase complex in patients with lactic acidemia. *J Clin Invest*. 85:1821-4.

Robinson, B.H., and W.G. Sherwood. 1984. Lactic acidaemia. *J Inherit Metab Dis*. 7 Suppl 1:69-73.

Ross, J.B.A., Laws, W. R., Rousslang, K. W. and Wyssbrod, H.R. 1992. *In Topics in Fluorescence Spectroscopy (ed. Lakowicz, J. R.), Plenum Press, New York,*. 3:1-63.

Rotig, A., P. de Lonlay, D. Chretien, F. Foury, M. Koenig, D. Sidi, A. Munnich, and P. Rustin. 1997. Aconitase and mitochondrial iron-sulphur protein deficiency in Friedreich ataxia. *Nat Genet*. 17:215-7.

Rowles, J., S.W. Scherer, T. Xi, M. Majer, D.C. Nickle, J.M. Rommens, K.M. Popov, R.A. Harris, N.L. Riebow, J. Xia, L.C. Tsui, C. Bogardus, and M. Prochazka. 1996. Cloning and characterization of PDK4 on 7q21.3 encoding a fourth pyruvate dehydrogenase kinase isoenzyme in human. *J Biol Chem*. 271:22376-82.

Ruan, K., J. Li, R. Liang, C. Xu, Y. Yu, R. Lange, and C. Balny. 2002. A rare protein fluorescence behavior where the emission is dominated by tyrosine: case of the 33-kDa protein from spinach photosystem II. *Biochem Biophys Res Commun*. 293:593-7.

Russell, G.C., and J.R. Guest. 1991. Sequence similarities within the family of dihydrolipoamide acyltransferases and discovery of a previously unidentified fungal enzyme. *Biochim Biophys Acta*. 1076:225-32.

Saijo, T., E. Naito, M. Ito, I. Yokota, J. Matsuda, and Y. Kuroda. 1996. Stable restoration of pyruvate dehydrogenase complex in E1-defective human lymphoblastoid cells: evidence that three C-terminal amino acids of E1 alpha are essential for the structural integrity of heterotetrameric E1. *Biochem Biophys Res Commun*. 228:446-51.

Sanderson, S.J., S.S. Khan, R.G. McCartney, C. Miller, and J.G. Lindsay. 1996a. Reconstitution of mammalian pyruvate dehydrogenase and 2-oxoglutarate dehydrogenase complexes: analysis of protein X involvement and interaction of homologous and heterologous dihydrolipoamide dehydrogenases. *Biochem J*. 319 (Pt 1):109-16.

Sanderson, S.J., C. Miller, and J.G. Lindsay. 1996b. Stoichiometry, organisation and catalytic function of protein X of the pyruvate dehydrogenase complex from bovine heart. *Eur J Biochem*. 236:68-77.

Saunders, A.M., W.J. Strittmatter, D. Schmechel, P.H. George-Hyslop, M.A. Pericak-Vance, S.H. Joo, B.L. Rosi, J.F. Gusella, D.R. Crapper-MacLachlan, M.J. Alberts, and et al. 1993. Association of apolipoprotein E allele epsilon 4 with late-onset familial and sporadic Alzheimer's disease. *Neurology*. 43:1467-72.

Schapira, A.H., M. Gu, J.W. Taanman, S.J. Tabrizi, T. Seaton, M. Cleeter, and J.M. Cooper. 1998. Mitochondria in the etiology and pathogenesis of Parkinson's disease. *Ann Neurol*. 44:S89-98.

Schuck, P. 2000. Size-distribution analysis of macromolecules by sedimentation velocity ultracentrifugation and lamm equation modeling. *Biophys J*. 78:1606-19.

Schuck, P., M.A. Perugini, N.R. Gonzales, G.J. Howlett, and D. Schubert. 2002. Size-distribution analysis of proteins by analytical ultracentrifugation: strategies and application to model systems. *Biophys J*. 82:1096-111.

Schulze, E., A.H. Westphal, H. Boumans, and A. Dekok. 1991. Site-Directed Mutagenesis of the Dihydrolipoyl Transacetylase Component (E2p) of the Pyruvate-Dehydrogenase Complex from Azotobacter-Vinelandii - Binding of the Peripheral Component-E1p and Component-E3. *European Journal of Biochemistry*. 202:841-848.

Schwede, T., J. Kopp, N. Guex, and M.C. Peitsch. 2003. SWISS-MODEL: An automated protein homology-modeling server. *Nucleic Acids Res*. 31:3381-5.

Seyda, A., G. McEachern, R. Haas, and B.H. Robinson. 2000. Sequential deletion of C-terminal amino acids of the E(1)alpha component of the pyruvate dehydrogenase (PDH) complex leads to reduced steady-state levels of functional E(1)alpha(2)beta(2) tetramers: implications for patients with PDH deficiency. *Hum Mol Genet*. 9:1041-8.

Shaag, A., A. Saada, I. Berger, H. Mandel, A. Joseph, A. Feigenbaum, and O.N. Elpeleg. 1999. Molecular basis of lipoamide dehydrogenase deficiency in Ashkenazi Jews. *Am J Med Genet*. 82:177-82.

Sheu, K.F., and J.P. Blass. 1999. The alpha-ketoglutarate dehydrogenase complex. *Ann N Y Acad Sci*. 893:61-78.

Shi, Q., H.L. Chen, H. Xu, and G.E. Gibson. 2005. Reduction in the E2k subunit of the alpha-ketoglutarate dehydrogenase complex has effects independent of complex activity. *J Biol Chem*. 280:10888-96.

Shi, Q., S.S. Karuppagounder, H. Xu, D. Pechman, H. Chen, and G.E. Gibson. 2007. Responses of the mitochondrial alpha-ketoglutarate dehydrogenase complex to thiamine deficiency may contribute to regional selective vulnerability. *Neurochem Int*. 50:921-31.

Smolle, M., A.E. Prior, A.E. Brown, A. Cooper, O. Byron, and J.G. Lindsay. 2006. A new level of architectural complexity in the human pyruvate dehydrogenase complex. *Journal of Biological Chemistry*. 281:19772-19780.

Sorbi, S., S. Piacentini, C. Fani, S. Tonini, P. Marini, and L. Amaducci. 1989. Abnormalities of mitochondrial enzymes in hereditary ataxias. *Acta Neurol Scand*. 80:103-10.

Spector, S., B. Kuhlman, R. Fairman, E. Wong, J.A. Boice, and D.P. Raleigh. 1998. Cooperative folding of a protein mini domain: the peripheral subunit-binding

domain of the pyruvate dehydrogenase multienzyme complex. *J Mol Biol*. 276:479-89.

Spencer, M.E., M.G. Darlison, P.E. Stephens, I.K. Duckenfield, and J.R. Guest. 1984. Nucleotide sequence of the sucB gene encoding the dihydrolipoamide succinyltransferase of Escherichia coli K12 and homology with the corresponding acetyltransferase. *Eur J Biochem*. 141:361-74.

Stacpoole, P.W. 1989. The pharmacology of dichloroacetate. *Metabolism*. 38:1124-44.

Stacpoole, P.W., D.S. Kerr, C. Barnes, S.T. Bunch, P.R. Carney, E.M. Fennell, N.M. Felitsyn, R.L. Gilmore, M. Greer, G.N. Henderson, A.D. Hutson, R.E. Neiberger, R.G. O'Brien, L.A. Perkins, R.G. Quisling, A.L. Shroads, J.J. Shuster, J.H. Silverstein, D.W. Theriaque, and E. Valenstein. 2006. Controlled clinical trial of dichloroacetate for treatment of congenital lactic acidosis in children. *Pediatrics*. 117:1519-31.

Stacpoole, P.W., R. Owen, and T.R. Flotte. 2003. The pyruvate dehydrogenase complex as a target for gene therapy. *Curr Gene Ther*. 3:239-45.

Starkov, A.A., C. Chinopoulos, and G. Fiskum. 2004. Mitochondrial calcium and oxidative stress as mediators of ischemic brain injury. *Cell Calcium*. 36:257-64.

Stepp, L.R., F.H. Pettit, S.J. Yeaman, and L.J. Reed. 1983. Purification and properties of pyruvate dehydrogenase kinase from bovine kidney. *J Biol Chem*. 258:9454-8.

Stoops, J.K., T.S. Baker, J.P. Schroeter, S.J. Kolodziej, X.D. Niu, and L.J. Reed. 1992. Three-dimensional structure of the truncated core of the Saccharomyces cerevisiae pyruvate dehydrogenase complex determined from negative stain and cryoelectron microscopy images. *J Biol Chem*. 267:24769-75.

Stoops, J.K., R.H. Cheng, M.A. Yazdi, C.Y. Maeng, J.P. Schroeter, U. Klueppelberg, S.J. Kolodziej, T.S. Baker, and L.J. Reed. 1997. On the unique structural organization of the Saccharomyces cerevisiae pyruvate dehydrogenase complex. *J Biol Chem*. 272:5757-64.

Strittmatter, W.J., A.M. Saunders, D. Schmechel, M. Pericak-Vance, J. Enghild, G.S. Salvesen, and A.D. Roses. 1993. Apolipoprotein E: high-avidity binding to beta-amyloid and increased frequency of type 4 allele in late-onset familial Alzheimer disease. *Proc Natl Acad Sci U S A*. 90:1977-81.

Sugden, M.C., and M.J. Holness. 2003. Recent advances in mechanisms regulating glucose oxidation at the level of the pyruvate dehydrogenase complex by PDKs. *Am J Physiol Endocrinol Metab*. 284:E855-62.

Surh, C.D., T.E. Roche, D.J. Danner, A. Ansari, R.L. Coppel, T. Prindiville, E.R. Dickson, and M.E. Gershwin. 1989. Antimitochondrial autoantibodies in primary biliary cirrhosis recognize cross-reactive epitope(s) on protein X and dihydrolipoamide acetyltransferase of pyruvate dehydrogenase complex. *Hepatology*. 10:127-33.

Szabo, P., K.F. Sheu, R.M. Robinson, K.H. Grzeschik, and J.P. Blass. 1990. The gene for the alpha polypeptide of pyruvate dehydrogenase is X-linked in humans. *Am J Hum Genet*. 46:874-8.

Szutowicz, A., H. Bielarczyk, S. Gul, A. Ronowska, T. Pawelczyk, and A. Jankowska-Kulawy. 2006. Phenotype-dependent susceptibility of cholinergic neuroblastoma cells to neurotoxic inputs. *Metab Brain Dis*. 21:149-61.

Tanaka, N., K. Koike, M. Hamada, K.I. Otsuka, T. Suematsu, and M. Koike. 1972. Mammalian -keto acid dehydrogenase complexes. VII. Resolution and reconstitution of the pig heart 2-oxoglutarate dehydrogenase complex. *J Biol Chem*. 247:4043-9.

Taylor, J.P., J. Hardy, and K.H. Fischbeck. 2002. Toxic proteins in neurodegenerative disease. *Science*. 296:1991-5.

Teague, W.M., F.H. Pettit, T.L. Wu, S.R. Silberman, and L.J. Reed. 1982. Purification and properties of pyruvate dehydrogenase phosphatase from bovine heart and kidney. *Biochemistry*. 21:5585-92.

Terwel, D., J. Bothmer, E. Wolf, F. Meng, and J. Jolles. 1998. Affected enzyme activities in Alzheimer's disease are sensitive to antemortem hypoxia. *J Neurol Sci*. 161:47-56.

Thomson, R.K., Z. Davis, J.M. Palmer, M.J. Arthur, S.J. Yeaman, C.J. Chapman, M.B. Spellerberg, and F.K. Stevenson. 1998. Immunogenetic analysis of a panel of monoclonal IgG and IgM anti-PDC-E2/X antibodies derived from patients with primary biliary cirrhosis. *J Hepatol*. 28:582-94.

Toyoda, T., K. Suzuki, T. Sekiguchi, L.J. Reed, and A. Takenaka. 1998. Crystal structure of eucaryotic E3, lipoamide dehydrogenase from yeast. *J Biochem (Tokyo)*. 123:668-74.

Tsunoda, J.N., and K.T. Yasunobu. 1967. Mammalian lipoic acid activating enzyme. *Arch Biochem Biophys*. 118:395-401.

Tuganova, A., I. Boulatnikov, and K.M. Popov. 2002. Interaction between the individual isoenzymes of pyruvate dehydrogenase kinase and the inner lipoyl-bearing domain of transacetylase component of pyruvate dehydrogenase complex. *Biochem J*. 366:129-36.

Venyaminov, S., I.A. Baikalov, Z.M. Shen, C.S. Wu, and J.T. Yang. 1993. Circular dichroic analysis of denatured proteins: inclusion of denatured proteins in the reference set. *Anal Biochem*. 214:17-24.

Walsh, D.A., R.H. Cooper, R.M. Denton, B.J. Bridges, and P.J. Randle. 1976. The elementary reactions of the pig heart pyruvate dehydrogenase complex. A study of the inhibition by phosphorylation. *Biochem J*. 157:41-67.

Wang, H., P.A. Antinozzi, K.A. Hagenfeldt, P. Maechler, and C.B. Wollheim. 2000. Molecular targets of a human HNF1 alpha mutation responsible for pancreatic beta-cell dysfunction. *Embo J*. 19:4257-64.

Westphal, A.H., and A. de Kok. 1990. The 2-oxoglutarate dehydrogenase complex from Azotobacter vinelandii. 2. Molecular cloning and sequence analysis of the gene encoding the succinyltransferase component. *Eur J Biochem*. 187:235-9.

Wong, A., J. Yang, P. Cavadini, C. Gellera, B. Lonnerdal, F. Taroni, and G. Cortopassi. 1999. The Friedreich's ataxia mutation confers cellular sensitivity to oxidant stress which is rescued by chelators of iron and calcium and inhibitors of apoptosis. *Hum Mol Genet*. 8:425-30.

Xu, D.P., and W.W. Wells. 1996. alpha-Lipoic acid dependent regeneration of ascorbic acid from dehydroascorbic acid in rat liver mitochondria. *J Bioenerg Biomembr*. 28:77-85.

Yang, D., J. Song, T. Wagenknecht, and T.E. Roche. 1997. Assembly and full functionality of recombinantly expressed dihydrolipoyl acetyltransferase component of the human pyruvate dehydrogenase complex. *J Biol Chem*. 272:6361-9.

Yeaman, S.J., E.T. Hutcheson, T.E. Roche, F.H. Pettit, J.R. Brown, L.J. Reed, D.C. Watson, and G.H. Dixon. 1978. Sites of phosphorylation on pyruvate dehydrogenase from bovine kidney and heart. *Biochemistry*. 17:2364-70.

Zhao, X., J.R. Miller, Y. Jiang, M.A. Marletta, and J.E. Cronan. 2003. Assembly of the covalent linkage between lipoic acid and its cognate enzymes. *Chem Biol*. 10:1293-302.

Ziegler, D., H. Schatz, F. Conrad, F.A. Gries, H. Ulrich, and G. Reichel. 1997. Effects of treatment with the antioxidant alpha-lipoic acid on cardiac autonomic neuropathy in NIDDM patients. A 4-month randomized controlled multicenter trial (DEKAN Study). Deutsche Kardiale Autonome Neuropathie. *Diabetes Care*. 20:369-73.